Programa de Doctorado en Bioingeniería

UNIVERSITAS Miguel Hernández

Estudio de los mecanismos fisiológicos y moleculares implicados en la formación y desarrollo de las raíces adventicias en distintas especies vegetales

María Salud Justamante Clemente

Elche, 2019

TESIS DOCTORAL

Estudio de los mecanismos fisiológicos y moleculares implicados en la formación y desarrollo de las raíces adventicias en distintas especies vegetales

María Salud Justamante Clemente

Director: Dr. José Manuel Pérez Pérez

Programa de Doctorado en Bioingeniería

Universidad Miguel Hernández de Elche

Instituto de Bioingeniería

Elche, 2019

Instituto de Bioingeniería

Universidad Miguel Hernández – Campus de Elche

JOSÉ MANUEL PÉREZ PÉREZ, Catedrático de Universidad en el área de conocimiento de Genética de la Universidad Miguel Hernández de Elche,

HAGO CONSTAR

que el presente trabajo ha sido realizado bajo mi dirección y recoge fielmente la labor realizada por la licenciada María Salud Justamante Clemente para optar al grado de Doctor;

que este documento se ha elaborado siguiendo la normativa de la Universidad Miguel Hernández de Elche para la presentación de Tesis por compendio de publicaciones, siendo éstas las siguientes:

1. **María Salud Justamante**, Sergio Ibáñez, Adrián Peidró, **José Manuel Pérez-Pérez** (2019). A genome-wide association study identifies new loci required for wound-induced lateral root formation in *Arabidopsis thaliana*. *Frontiers in Plant Science* **10**: 311. doi: 10.3389/fpls.2019.00311. Artículo. Factor de impacto (FI [2018]): 4,106 (D1; 20 de 228).
2. Antonio Cano, Ana Belén Sánchez-García, Alfonso Albacete, Rebeca González-Bayón, **María Salud Justamante**, Sergio Ibáñez, Manuel Acosta, **José Manuel Pérez-Pérez** (2018). Enhanced conjugation of auxin by GH3 enzymes leads to poor adventitious rooting in carnation stem cuttings. *Frontiers in Plant Science* **9**: 566. doi: 10.3389/fpls.2018.00566. Artículo. FI (2018): 4,106 (D1; 20 de 228).
3. **María Salud Justamante**, José Ramón Acosta-Motos, Antonio Cano, Joan Villanova, Virginia Birlanga, Alfonso Albacete, Emilio A. Cano, Manuel Acosta, **José Manuel Pérez-Pérez** (2019). Integration of phenotypic and hormone data during adventitious rooting in carnation (*Dianthus caryophyllus* L.) stem cuttings. *Plants* **8**: 226. doi: 10.3390/plants8070226. Artículo. FI (2018): 2,623 (Q2; 59 de 228).
4. **María Salud Justamante**, Sergio Ibáñez, Joan Villanova, **José Manuel Pérez-Pérez** (2017). Vegetative propagation of argan tree (*Argania spinosa* (L.) Skeels) using *in vitro* germinated seeds and stem cuttings. *Scientia Horticulturae* **225**: 81 doi: 10.1016/j.scienta.2017.06.066. Artículo. FI (2017): 1,760 (Q1; 8 de 37).

Elche, 3 de octubre de 2019

JOSÉ MANUEL PÉREZ PÉREZ, Coordinador del Programa de Doctorado en Bioingeniería de la Universidad Miguel Hernández de Elche por Resolución Rectoral 0169/17, de 1 de febrero de 2017:

CERTIFICA

Que la Tesis Doctoral por compendio de publicaciones titulada *"Estudio de los mecanismos fisiológicos y moleculares implicados en la formación y desarrollo de las raíces adventicias en distintas especies vegetales"*, ha sido realizada por Dña. María Salud Justamante Clemente, bajo la dirección del Profesor José Manuel Pérez Pérez, y da su conformidad para que sea presentada a la Comisión de Estudios de Doctorado de la Universidad Miguel Hernández de Elche.

Instituto de Bioingeniería
Universidad Miguel Hernández

Elche, 3 de octubre de 2019

AGRADECIMIENTOS

En primer lugar, agradecer a mi director de tesis José Manuel Pérez, por haber sido mi primer contacto con el mundo de la investigación y haberme permitido realizar este trabajo con el que tanto he aprendido y disfrutado. Gracias a su ayuda, confianza y valiosas enseñanzas no sólo he podido crecer como investigadora sino también como persona, transmitiéndome la motivación necesaria para seguir mejorando cada día.

A Joan Villanova y Ana Belén Sánchez, por su inestimable compañía durante los primeros meses de laboratorio. Por haberme escuchado siempre con paciencia y una sonrisa a la hora de resolver mis dudas de principiante, así como por su atenta ayuda y por sus sabios consejos.

A Sergio Ibáñez, por haber sido mi gran apoyo desde el primer día que entré en el laboratorio y haberme enseñado pacientemente todo cuanto necesitaba saber, desde el cultivo *in vitro* de Arabidopsis hasta la recolección de semillas. Por haberme ayudado cada día a mejorar en muchos aspectos, desde biología molecular o bioinformática hasta mi relación con los demás. Gracias por haberme hecho sentir siempre como en casa, como una más del equipo.

A Aurora Alaguero, por su ayuda constante e incondicional, por haber estado siempre a mi lado en los mejores y peores momentos, y sobre todo por darle un valor añadido al concepto de trabajo en equipo. Por todas las raíces de clavel que limpiamos y fotografiamos a lo largo del verano, por empezar siendo compañera y acabar siendo amiga. Sin ella, estos últimos años no habrían sido lo mismo, gracias por todo lo que hemos compartido.

A José Ramón Acosta, por su continua dedicación y sus valiosas aportaciones a una parte muy importante de este trabajo, sin las cuales no habría sido posible su realización. Gracias por haber confiado en mi trabajo y hacerme saber que podía contar con tu apoyo en todo momento.

A Emilio Á. Cano, Manuel Acosta, Antonio Cano y Alfonso Albacete, por su amable atención y colaboración en todos los experimentos de clavel y análisis realizados, por haber construido la base fundamental de este trabajo desde mucho antes de que yo comenzara en él.

Al resto de mis compañeros de laboratorio y de Tesis; Francisco Javier Gran, Alfonso Azorín, Joan Sánchez, José David Celdrán, Eva María Rodríguez, Ricardo Parreño, Gema Martínez, Diana Navarro, Mª Ángeles Fernández, Virginia Birlanga y Paula Jadczak, por vuestra valiosa compañía y apoyo. A todos ellos, gracias por tantos buenos momentos y enseñarme siempre algo nuevo.

A mis amigas de toda la vida, Laura Moreno y Verónica Mancheño, dos personas maravillosas que a pesar de la distancia me han acompañado a cada paso durante este largo camino. Gracias por estar siempre ahí.

A Adrián Peidró, una de las personas más brillantes que he conocido a lo largo de mi vida y que me ha dedicado parte de la suya. Por todos los días y semanas que dejamos el descanso a un lado para concentrarnos en programar, en debatir y en sacar adelante este trabajo. Por haberle entregado una parte importante de su tiempo al procesado de todos estos datos, y por ofrecerme en todo momento su apoyo y afecto incondicional. Gracias por creer en mí.

A mi familia, que aun siendo pequeña es lo más grande que tengo en el mundo. Por su paciencia y cariño, por apoyarme y animarme en los momentos más difíciles. Sin su ayuda y su motivación constante nada de esto habría sido posible.

ÍNDICE DE CONTENIDOS

ÍNDICE DE FIGURAS

Abstract

The adventitious root formation is critical for the plant survival during its vegetative propagation through cuttings, hence the study and understanding of this process is strategic during mass propagation of the new elite varieties obtained by genetic breeding. This Thesis pursues genetic, morphological and hormonal studies of *de novo* root formation in the *Arabidopsis thaliana* (L.) Heynh. model, and in two other plant species of agronomic interest in the Mediterranean region, such as the cultivated carnation (*Dianthus caryophyllus* L.) and the argan tree (*Argania spinosa* [L.] Skeels).

To identify some genetic determinants involved in wound–induced root formation process, we carried out a genome–wide association (GWA) study in a collection of 174 *Arabidopsis thaliana* natural accessions. We found statistically significant associations between wound–induced root system architectural traits and 19 genomic loci. We then studied three candidate loci associated with wound–induced lateral root formation. Loss–of–function mutants in one of these genes, At4g01090, which encodes a protein of unknown function, were affected in wound–induced lateral root development. We identified null alleles in the At5g19710 gene, which encodes a histidine phosphotransfer protein putatively involved in cytokinin signalling, with a reduced number of lateral roots after root tip excision. In addition, we found an epistatic interaction between several non–synonymous single nucleotide polymorphisms in the coding region of K^+ *UPTAKE TRANSPORTER 5* (*KUP5*), which encodes a potassium uptake transporter; and At5g19710, which would point to a functional relationship between both processes and wound–induced root formation.

We studied morphological changes occurring in the basal region of stem cuttings during rooting in a collection of 159 F_1 lines derived from a cross between two carnation hybrid cultivars, *2101–02 MFR* and *2003 R 8*, with contrasting rooting performances. We provided molecular evidence

that the bad–rooting behaviour of *2003 R 8* cuttings was caused by an early inactivation of active auxin, indole–3–acetic acid, through its conjugation with aspartic acid by GRETCHEN HAGEN 3 proteins. Our analyses further elucidated the relationship between the physiological state of carnation cuttings, estimated by the proportion of salicylic acid and jasmonate, and the formation of adventitious roots.

In addition, we developed an effective method for argan micropropagation from *in vitro* germinated seeds and we considerably increased the adventitious rooting from lignified cuttings obtained from adult plants. When combined with a suitable genetic selection, our procedure will allow the efficient production of elite varieties of argan trees for intensive cultivation.

Resumen

La formación de raíces adventicias supone un paso crítico y de vital importancia para la supervivencia de las plantas que se propagan vegetativamente mediante esquejes, por lo que el estudio y la comprensión de este proceso es clave para optimizar la propagación vegetativa de las nuevas variedades élite obtenidas por métodos convencionales de mejora genética. En esta Tesis se propone el estudio a nivel genético, morfológico y hormonal de la formación de raíces *de novo* en la crucífera modelo *Arabidopsis thaliana* (L.) Heynh., y en dos especies de interés agronómico en la región mediterránea: el clavel cultivado (*Dianthus caryophyllus* L.) y el argán (*Argania spinosa* [L.] Skeels).

Para identificar algunos de los determinantes genéticos implicados en la formación de raíces en respuesta a herida, hemos llevado a cabo un estudio de asociación a genoma completo o GWA (*genome–wide association study*) en una colección de 174 estirpes silvestres de *Arabidopsis thaliana*. Nuestros resultados indican que existen asociaciones estadísticamente significativas entre los cambios en la arquitectura radicular en respuesta a herida y 19 regiones genómicas concretas. Nos hemos centrado en el análisis genético de 6 polimorfismos de un solo nucleótido o SNPs (*single nucleotide polymorphisms*) que generan cambios no conservados de residuos aminoacídicos en la región codificante de tres genes. Los mutantes de pérdida de función en At4g01090, que codifica una proteína de función desconocida, muestran un menor número de raíces laterales en respuesta a herida. Hemos identificado alelos nulos en el gen At5g19710, que codifica una proteína con un dominio de histidina para la fosfotransferencia implicado en la señalización de las citoquininas, con un número reducido de raíces laterales en respuesta a herida. Además, hemos encontrado una interacción epistática entre los SNPs de la región codificante de *K^+ UPTAKE TRANSPORTER 5* (*KUP5*), cuyo producto participa en la asimilación del potasio, y At5g19710, lo que apuntaría a una relación

funcional entre ambos procesos y con la formación de raíces en respuesta a herida.

Por otra parte, hemos llevado a cabo un análisis detallado de la formación de raíces adventicias a partir de esquejes de clavel cultivado en una colección de 159 líneas F_1 derivadas del cruzamiento entre dos variedades comerciales, *2101–02 MFR* y *2003 R 8*, que difieren de forma significativa en su capacidad de enraizamiento adventicio. Hemos proporcionado evidencias moleculares de que la baja capacidad de enraizamiento adventicio de los esquejes en la estirpe *2003 R 8* se debe a una inactivación temprana de la auxina activa, el ácido indolacético, en la base del esqueje mediante su conjugación con ácido aspártico por enzimas de la familia GRETCHEN HAGEN 3. Nuestros análisis han permitido dilucidar, además, la relación existente entre el estado fisiológico de los esquejes de clavel, estimada por la proporción de ácidos salicílico y jasmónico, y la formación de raíces adventicias.

Adicionalmente, hemos desarrollado un método eficaz para la micropropagación del argán a partir de semillas germinadas *in vitro*, además de un protocolo que ha permitido incrementar considerablemente la formación de raíces adventicias a partir de esquejes lignificados obtenidos de plantas adultas. Combinado con una selección genética adecuada, nuestro procedimiento permitirá la producción eficiente de variedades élite de argán para su uso en cultivo intensivo.

Capítulo 1

Introducción general

1. INTRODUCCIÓN GENERAL

1.1 Especies vegetales que se han estudiado en esta Tesis

1.1.1 *Arabidopsis thaliana* como sistema modelo

Arabidopsis thaliana (L.) Heynh., en adelante Arabidopsis, es una planta vascular de la familia de las Crucíferas que se ha convertido en el organismo modelo más adecuado para el estudio de la Biología vegetal [1, 2]. Como muestra de su importancia, más de 33.000 artículos en Pubmed contienen la palabra "Arabidopsis" en su título (septiembre de 2019). En las condiciones adecuadas, Arabidopsis completa su ciclo vital en tan sólo seis semanas (figura 1), y su pequeño tamaño permite el cultivo de cientos de plántulas en una sola placa de Petri, facilitando así su manipulación experimental en condiciones controladas [1].

Otra de sus características diferenciales es el pequeño tamaño de su genoma haploide (de unas 125 Mpb), que contiene 38.194 genes, 27.655 de los cuales codifican proteínas [3]. Puesto que tres de cada cuatro familias génicas de Arabidopsis se encuentran presentes en los genomas de otras fanerógamas, se facilita el análisis genético de los procesos de desarrollo que son comunes a distintas especies vegetales; como la morfogénesis de las raíces o de las hojas [1]. Aunque Arabidopsis es una planta autógama, es capaz de tolerar la fecundación cruzada, permitiendo de esta manera los abordajes genéticos clásicos [2]. La transformación genética en Arabidopsis se lleva a cabo de forma sencilla mediante la inmersión de las inflorescencias jóvenes en un cultivo líquido de *Agrobacterium tumefaciens* que contiene la construcción deseada [4]. Esta metodología de transformación facilita la obtención de mutantes y el estudio de las funciones biológicas de genes concretos mediante abordajes de la Genética inversa. Además, respecto a las colecciones de mutantes disponibles, es posible encontrar líneas homocigotas para el ADN–T en prácticamente todos sus genes [5], así como otros producidos por

mutagénesis química con metanosulfonato de etilo [6], o mediante edición génica con CRISPR/Cas9 [7, 8].

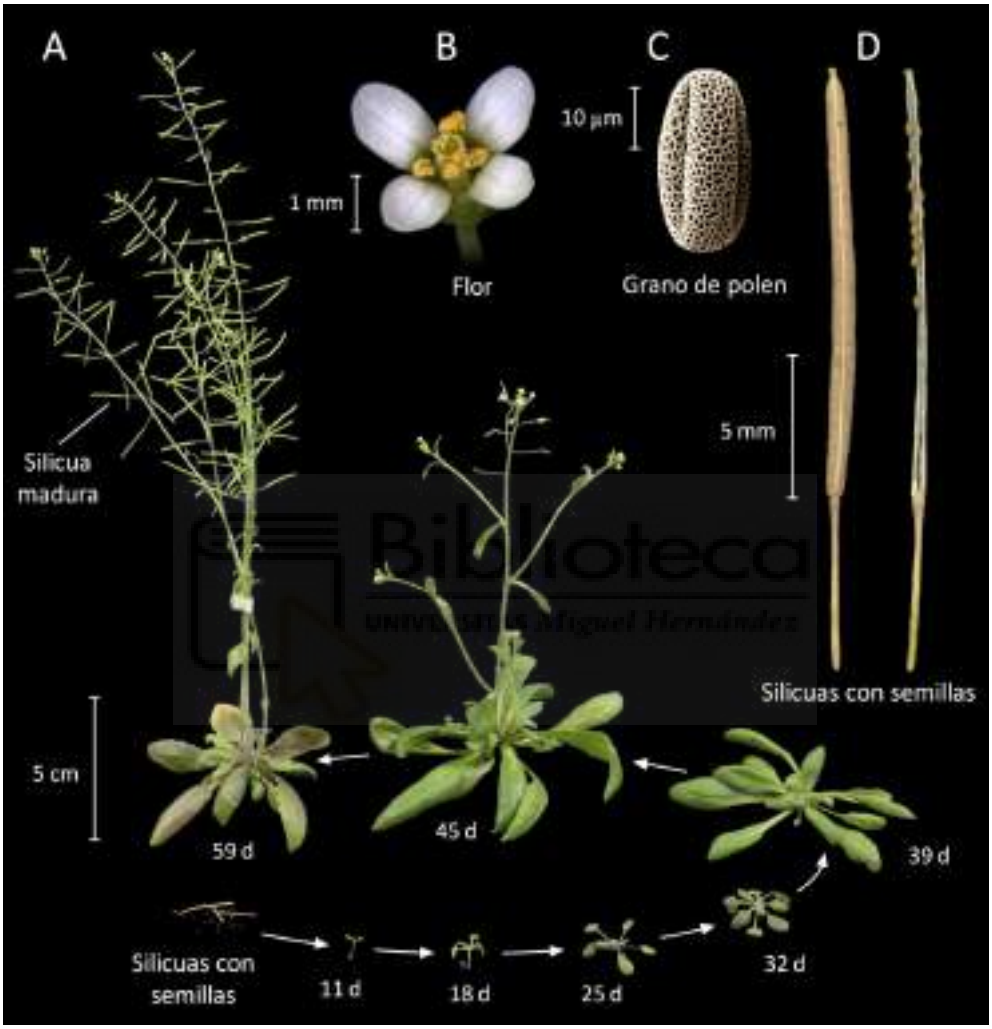

Figura 1.- Características morfológicas y ciclo vital de *Arabidopsis thaliana*. Imagen tomada de Krämer (2015) [12], con algunas modificaciones.

El estudio de la variación natural en Arabidopsis se ha utilizado para dilucidar algunas de las bases moleculares responsables de las diferencias fenotípicas relacionadas con la adaptación a distintos ambientes, así como de los procesos ecológicos y evolutivos que mantienen dicha variación [9].

Las colecciones de estirpes silvestres de Arabidopsis, muchas de las cuales se han caracterizado a nivel molecular, recogen la enorme diversidad fenotípica existente como resultado de la adaptación a las condiciones climáticas locales [10]. Tradicionalmente, la disección genética de la variación natural en Arabidopsis se ha realizado mediante el mapeo de genes de caracteres cuantitativos o QTL (*quantitative trait loci*). El mapeo de QTL consiste en realizar estudios de asociación entre la variación fenotípica observada y la variación alélica en la secuencia nucleotídica de las líneas analizadas [10]. Inicialmente, se identifican algunas de las regiones genómicas que contienen los QTL que explicarían la variación fenotípica en los rasgos de interés. Estas regiones deberán analizarse posteriormente de forma detallada para identificar los polimorfismos moleculares que alteran la función de genes concretos localizados en dichas regiones [10]. Una desventaja de las poblaciones de mapeo biparental es que sólo permiten el análisis de las diferencias genéticas existentes entre ambos parentales. Además, los resultados obtenidos para la localización física de los genes concretos suelen ser inexactos [11].

Las metodologías basadas en los estudios de asociación a genoma completo o GWA (*genome–wide association*) surgieron inicialmente como un abordaje a gran escala para encontrar la base genética de varias enfermedades en el ser humano [13], y en la actualidad suponen una herramienta de especial interés para el estudio de la variación natural y rasgos genéticos de importancia agrícola en organismos vegetales [14]. El elevado nivel de homocigosidad de las estirpes naturales de Arabidopsis, junto con la alta densidad de marcadores moleculares disponibles, la convierten en la especie vegetal idónea para la aplicación de este enfoque experimental [10, 11, 15]. El enfoque básico de este método consiste en evaluar la asociación estadística existente entre cada marcador genotípico y el rasgo fenotípico de interés, previamente cuantificado en un número elevado de individuos de una población cuyas relaciones de parentesco se

desconocen [16]. Gracias al avance en las tecnologías de secuenciación y genotipado masivo se ha recopilado gran cantidad de información sobre las características genéticas de muchas especies vegetales, sobre todo en Arabidopsis [14], donde se ha comprobado que 90 estirpes naturales son suficientes para la identificación de algunos alelos de interés asociados a rasgos genéticamente simples mediante un enfoque de GWA [17].

1.1.2 Algunas peculiaridades del clavel cultivado

El clavel (*Dianthus caryophyllus* L.) es una planta herbácea de la familia de las Cariofiláceas, con tallos de hasta 80 cm de altura e inflorescencias simples, con una única flor terminal formada por cinco pétalos insertados en un cáliz estrecho y alargado, con dos o tres pares de brácteas en la base, diez estambres y un pistilo súpero (figura 2A). La mayoría de las más de trescientas especies que constituyen el género *Dianthus* presenta una amplia distribución mediterránea, donde las variaciones extremas en las temperaturas a lo largo del año y la falta de lluvias durante el verano han favorecido su rápida diversificación como consecuencia de la adaptación local de los genotipos más resilientes [18, 19]. Los claveles que se cultivan comercialmente son en su mayoría híbridos interespecíficos, obtenidos de cruces entre variedades ancestrales y especies silvestres. Mediante estos cruces se incorporan características de interés, y tras un largo proceso de selección se van obteniendo variedades con flores de mayor tamaño y una gran diversidad de colores, así como con tallos más largos y robustos que sus antecesores silvestres [20]. La Comunidad Europea es, con 980 hectáreas de cultivo, el tercer mayor productor de flor cortada de clavel, después de Asia y Sudamérica [21]. España contribuye con una producción de 480 millones de claveles anuales en unas 340 hectáreas de cultivo. En la Región de Murcia el cultivo de clavel cuenta con unas 175 hectáreas, suponiendo el 50% de la producción total en nuestro país [22].

Figura 2.- Ilustraciones y fotografías del clavel cultivado. (A) Imagen tomada del catálogo ilustrado de plantas cultivadas de Blackwell (1737) [23], con algunas modificaciones. (B) Esquejes de clavel cultivado en maceta en el invernadero. (C) Detalle de un esqueje de clavel enraizado en sustrato. Barra de escala: 35 mm. (D) Esquejes de clavel en cultivo *in vitro*.

Los métodos de propagación de clavel cultivado que se utilizan durante su producción comercial son el cultivo *in vitro* y la propagación vegetativa por esquejes (figuras 2B–D). El procedimiento habitual para la propagación de clavel en la empresa Dümmen Orange, proveedora del material vegetal empleado en esta Tesis, consta de una serie de etapas bien definidas que permiten mantener la estabilidad genética de los híbridos comerciales seleccionados previamente por los mejoradores. De estos genotipos seleccionados se establecen dos bancos de material vegetal: el banco *in vitro* (conservado en el laboratorio) y el banco *in vivo* (conservado en el invernadero). El material del banco *in vitro* se mantiene como reserva, mientras que los esquejes obtenidos de los genotipos seleccionados del banco *in vivo* son plantados en una reserva nuclear, a partir de la que se recolectan y plantan nuevos esquejes en una reserva de propagación. Desde la reserva de propagación, se obtienen las plantas madre a partir de las cuales crecerán los esquejes comerciales [24]. Este sistema evita la aparición de enfermedades gracias a los controles de calidad periódicos y a la renovación anual de las plantas madre.

El clavel cultivado presenta un genoma nuclear haploide de unas 670 Mpb, y actualmente se dispone de varios mapas genéticos de clavel [25, 26]. Utilizando técnicas de secuenciación masiva se obtuvo por primera vez en 2012 el transcriptoma en la variedad de referencia “Francesco” [27], y en 2014 se publicó el primer borrador del genoma de clavel que, con unas 569 Mpb de secuencia anotada, contiene algo más de 43.000 genes que codifican proteínas [28]. Estos avances han permitido la realización de nuevos estudios genómicos en esta especie relacionados con distintos procesos, como la identificación de marcadores moleculares de las distintas etapas del enraizamiento adventicio en esquejes [29], la caracterización de familias génicas de acuaporinas relacionadas con la apertura floral [30] o la caracterización de genes relacionados con la homeostasis de las auxinas [31].

1.1.3 Cultivo e importancia del argán

El árbol de argán (*Argania spinosa* [L.] Skeels) (véanse las figuras 1A–B del cuarto artículo en la pág. 163) es endémico del sudoeste de Marruecos, donde la escasez de agua y las altas temperaturas son los principales factores que determinan la supervivencia de las especies vegetales. Tradicionalmente, el argán se ha empleado en la cultura bereber para la alimentación del ganado y la producción de aceite que se utiliza en cosmética o alimentación [32]. La pulpa de los frutos contiene numerosos compuestos polifenólicos que pueden resultar útiles para incorporarlos a productos nutracéuticos y de cuidado corporal [33]. En sus frutos se han identificado y caracterizado también otros compuestos bioactivos, con potencial antioxidante y efectos tanto antiinflamatorios como analgésicos o antimicrobianos [33]. Además, los árboles de argán protegen los suelos de la erosión, proporcionan sombra a diferentes tipos de cultivos y ayudan a mantener la fertilidad del suelo [34]. La tolerancia de esta especie a los ambientes desfavorables, junto con el interés creciente de sus derivados, sugieren una interesante funcionalidad del argán como reemplazo ecológico de otros árboles productores de aceite menos tolerantes a la sequía, en caso de que las temperaturas continúen incrementándose por efecto del cambio climático. A diferencia de Arabidopsis o clavel, no se dispone de información alguna sobre el genoma del argán. En 2016 se llevó a cabo un análisis preliminar sobre la diversidad genética de las poblaciones naturales de argán empleando polimorfismos en la longitud de fragmentos amplificados o AFLP (*amplified fragment length polymorphism*) [35]. En base a estos resultados se ha propuesto un tamaño de su genoma de unas 500 Mpb [35].

1.2 Formación de raíces adventicias

Las raíces son órganos de vital importancia para el crecimiento vegetal; participan en funciones básicas como la absorción de agua y

nutrientes, el soporte mecánico de la planta y actúan como barrera frente a patógenos, regulando numerosas respuestas de adaptación a los cambios en el ambiente [36]. Aunque existe una amplia variedad de sistemas radiculares en las angiospermas, todos ellos se componen de una raíz primaria, derivada de un meristemo radicular formado durante la embriogénesis, y diferentes tipos de raíces laterales o secundarias, que a su vez pueden ramificarse [37, 38] (figura 3A). Por otra parte, las raíces adventicias, aunque muestran la misma funcionalidad que las raíces secundarias, se desarrollan siempre de tejidos vegetales no radiculares como el tallo o las hojas, de forma natural o como respuesta adaptativa a situaciones adversas del entorno [38, 39, 40] (figura 3B). Las raíces adventicias proporcionan a las plantas funciones adicionales como el incremento de la superficie de absorción en suelos pobres, el aporte de un anclaje adecuado para las estructuras aéreas o el suministro de una vía radicular alternativa cuando existe daño en el sistema radicular principal [39, 41, 42]. Además, el desarrollo de las raíces adventicias resulta fundamental para la propagación vegetativa de muchas especies forestales y hortícolas [43, 44] (figuras 3C–E).

La formación de raíces adventicias a partir de esquejes de tallo comprende tres etapas sucesivas denominadas inducción, iniciación y expresión [45]. En muchas especies, las células precursoras de las raíces adventicias no están preformadas, y se originan por la desdiferenciación de una población muy definida de células vasculares, como las células del periciclo en el hipocótilo de Arabidopsis [46] o del cambium vascular en los tallos de clavel y petunia [47, 48]. Durante la fase de inducción, las células precursoras de las raíces adventicias sufren una reprogramación celular que conduce a su especificación como células iniciadoras de los nuevos órganos. Durante la iniciación, se activa la proliferación celular y se forman los primordios radiculares. Finalmente, en la fase de expresión, el crecimiento de los primordios se acentúa, estableciéndose su conexión

vascular con el tallo y culminando el proceso con la emergencia de las raíces funcionales [45].

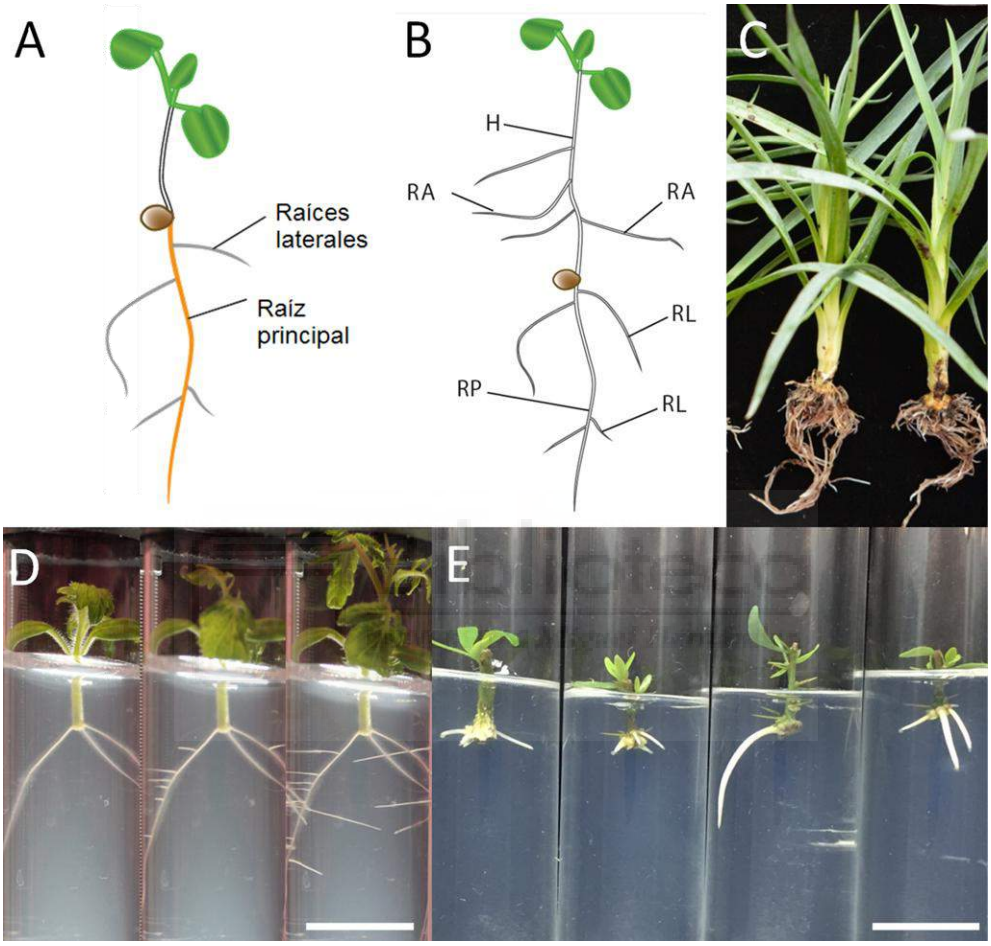

Figura 3.- Arquitectura radicular de *Arabidopsis thaliana* y enraizamiento adventicio en otras especies vegetales. (A) Esquema de la raíz principal y las raíces laterales. (B) Esquema que muestra la diferencia entre raíces laterales (RL) y raíces adventicias (RA); H: hipocótilo, RP: raíz principal. Esquemas tomados de Bellini *et al*. (2014) [38], con algunas modificaciones. (C) Esquejes de clavel (*Dianthus caryophyllus* L.) con raíces adventicias desarrolladas. (D) Formación de raíces adventicias *in vitro* en hipocótilos de tomate (*Solanum lycopersicum* L.). (E) Ejemplo de enraizamiento adventicio en microesquejes de argán (*Argania spinosa* [L.] Skeels). Barras de escala: 15 mm.

1.2.1 Regulación molecular y hormonal del enraizamiento adventicio

La formación de raíces adventicias es un proceso regulado a nivel hormonal, determinado por factores endógenos y ambientales, y que implica distintos mecanismos genéticos, algunos de los cuales se encuentran compartidos con el desarrollo de las raíces laterales [38, 43]. De entre estos mecanismos, el balance interno de las auxinas y las citoquininas desempeña una función relevante durante todo el proceso [38, 39] (figura 4). En el modelo de los explantes foliares aislados de Arabidopsis [49, 50] se ha constatado que la señal local de las auxinas en la región cercana a la herida activa la expresión de varios factores de transcripción de la familia *WUSCHEL–RELATED HOMEOBOX* (*WOX*) que se requieren para la formación de los primordios de raíces adventicias a partir de algunas células del cambium [51]. En una primera etapa, la expresión de *WOX11* y *WOX12* activa la reprogramación de las células fundadoras de las raíces adventicias [51]. Posteriormente, *WOX5* junto con *WOX7* activan transcripcionalmente a los genes *LATERAL ORGAN BOUNDARIES DOMAIN 16* (*LBD16*) y *LBD29*, requeridos a su vez para la proliferación celular de los primordios radiculares adventicios [49, 50, 51].

Las auxinas derivan del triptófano y actúan como morfógenos, regulando distintos aspectos del crecimiento vegetal [52]. Las auxinas son las principales inductoras del desarrollo radicular [53, 54]. El ácido indol–3–acético (AIA) es la auxina natural más abundante, aunque se han descrito otras que, como el ácido indol–3–butírico (AIB), presentan funciones específicas [55, 56]. Existen auxinas sintéticas, como el ácido 1–naftalenacético, que se utilizan habitualmente para la inducción de raíces adventicias en especies recalcitrantes [39]. Las mutaciones de pérdida de función en los genes *SUPERROOT 1* (*SUR1*) y *SUR2*, implicados en la biosíntesis de glucosinolatos indólicos, producen como efecto indirecto una acumulación del AIA endógeno y, en consecuencia, la

formación espontánea de raíces adventicias en distintos tipos de explantos [57]. En los mutantes *sur1* y *sur2* es posible restaurar el fenotipo silvestre mediante las mutaciones en los genes *ANTHRANILATE SYNTHASE ALPHA SUBUNIT 1* (*ASA1*) y *ASB1*, los cuales limitan la cantidad de triptófano disponible para la posterior síntesis de AIA a través de esta vía [57].

Figura 4.- Esquema global de la regulación del enraizamiento adventicio. Los cuadros violetas y las flechas negras describen la regulación de las señales endógenas, y los cuadros amarillos y las flechas rosas describen los reguladores externos de la formación de raíces adventicias. CK: citoquinina; ET: etileno; JA: ácido jasmónico; ABA: ácido abscísico; SL: estrigolactonas; H_2O_2: peróxido de hidrógeno. Las deficiencias incluyen nutrientes como nitratos, fosfatos o hierro. Imagen tomada de Gonin *et al*. (2019) [39], con algunas modificaciones.

En las etapas iniciales de la formación de raíces adventicias se requieren niveles elevados de auxinas endógenas (AIA) y su acumulación en células específicas en forma de un gradiente de concentración [48, 58]. Este gradiente endógeno depende, fundamentalmente, del transporte polar de auxinas o PAT (*polar auxin transport*) desde las regiones de biosíntesis, habitualmente en las hojas, y de su coordinación con las vías de conjugación y degradación de las auxinas [37]. El PAT requiere la

movilización activa de auxinas mediante la participación de varias familias de transportadores de membrana encargados de introducir las auxinas en el citoplasma celular, como AUXIN 1/LIKE–AUX 1 (AUX/LAX), o de los transportadores que controlan el transporte de salida de las auxinas del citoplasma, como PIN–FORMED (PIN) y ATP–BINDING–CASSETTE B (ABCB) [43]. La localización polar de estos transportadores a nivel celular y su actuación conjunta permiten establecer una direccionalidad en el flujo de auxinas. En Arabidopsis, las mutaciones de pérdida de función en el gen *ABCB19* causan una reducción en el número de raíces adventicias que se generan en el hipocótilo tras la escisión del sistema radicular, mientras que la expresión constitutiva de *ABCB19* las aumenta. Paralelamente, se ha demostrado que la expresión de *ABCB19* aumenta en respuesta a herida, lo que contribuye a un aumento en el transporte de AIA desde las hojas [46].

A nivel celular, las auxinas son reconocidas por los receptores nucleares de la familia F–BOX PROTEIN TRANSPORT INHIBITOR RESPONSE 1/AUXIN SIGNALING F–BOXES (TIR1/AFB) y promueven la degradación de los correpresores de la familia AUXIN/INDOLE–3–ACETIC ACID (Aux/IAA); liberándose de esta manera la función reguladora de la transcripción de los AUXIN RESPONSE FACTORS (ARF) sobre sus genes diana [43]. A partir de los estudios con varios mutantes de pérdida de función en algunos genes *ARF* de Arabidopsis se ha determinado que existe una red de regulación génica, aguas abajo de la auxina, en la que participan *ARF6* y *ARF8* como reguladores positivos y *ARF17* como regulador negativo de la formación de raíces adventicias en el hipocótilo [59].

Las citoquininas participan en la modulación del ciclo celular y el mantenimiento de los meristemos, actuando como antagonistas de las auxinas en muchas respuestas fisiológicas como el enraizamiento adventicio [37]. Mientras que los tratamientos con auxinas exógenas mejoran el enraizamiento adventicio, el tratamiento de esquejes con citoquininas exógenas suprime la formación de raíces [38, 39, 43]. Sin

embargo, las citoquininas también pueden tener una influencia promotora del enraizamiento durante las primeras horas después del corte de los esquejes a través de la estimulación de las divisiones celulares [43]. En explantos foliares de Arabidopsis, se ha determinado que la biosíntesis local de citoquininas junto con el máximo de señalización de auxinas en la región de la herida induce la proliferación de algunas células vasculares, de manera previa a la especificación de las células fundadoras de las raíces adventicias [43, 60]. A nivel intracelular, la señal de citoquininas modula la actividad de los factores de transcripción ARABIDOPSIS RESPONSE REGULATORS (ARR) [61]. Los análisis transcriptómicos para las distintas etapas de la producción de raíces adventicias en esquejes de álamo han mostrado una reducción en la expresión de varios genes *ARR* y de sus genes diana durante el enraizamiento, observándose que un nivel elevado del balance de auxinas y citoquininas en el esqueje produce la inactivación de un ortólogo de *ARR1* de Arabidopsis, activando la ruta de síntesis de las auxinas que contribuye directamente a la formación de los nuevos primordios radiculares adventicios [62]. Las proteínas ARABIDOPSIS HISTIDINE–CONTAINING PHOSPHOTRANSFER PROTEINS (AHP) son elementos clave en la vía de señalización de las citoquininas, ya que transfieren la señal de fosfato desde los receptores transmembrana de las citoquininas a los ARR nucleares. Los análisis de mutantes con pérdida de función para varias AHP muestran su mecanismo como reguladores positivos redundantes de la señalización de citoquininas [61]. Se ha determinado, además, que las citoquininas afectan negativamente a la expresión de los transportadores de auxinas PIN1 y LAX3, lo que reduce el flujo de auxina durante el enraizamiento adventicio [63].

La formación de raíces adventicias en esquejes está muy influenciada por el efecto del estrés causado por la ausencia de un sistema radicular funcional [47]. En esquejes de petunia, los niveles de ácido jasmónico son muy elevados a tiempos muy cortos tras la escisión de la planta madre,

aunque se restauran rápidamente [64]. A partir de los resultados obtenidos en distintas especies, se ha propuesto una función reguladora para el metil–jasmónico (MeJA) durante el enraizamiento adventicio a través de su interacción con otras hormonas, como las auxinas [37] o el etileno [65]. Puesto que el MeJA se acumula de forma rápida y transitoria en la base de los tallos tras el corte, y las plantas de petunia deficientes en la síntesis de jasmonatos muestran un menor número de raíces adventicias [66], se ha propuesto una función para el jasmónico como regulador positivo de la formación de raíces adventicias. Sin embargo, su aplicación exógena a los esquejes de petunia se traduce en una menor producción de raíces adventicias [66], indicando una regulación más compleja de este proceso. En los hipocótilos de Arabidopsis se ha observado que los genes *GRETCHEN HAGEN 3.3* (*GH3.3*), *GH3.5* y *GH3.6*, cuya expresión se induce por las auxinas, son necesarios para la formación de raíces adventicias, a través de la modulación de los niveles del ácido jasmónico activo [67], lo que confirmaría una interacción directa entre ambas hormonas en este proceso. De hecho, tanto ARF6 como ARF8 actúan como reguladores transcripcionales de la expresión de estos genes *GH3* durante la formación de raíces adventicias en el hipocótilo de Arabidopsis [67].

El ácido abscísico o ABA (*abscisic acid*) y las estrigolactonas son dos fitohormonas derivadas del β–caroteno de funciones diversas. El ABA es una fitohormona clave como reguladora del crecimiento en situaciones de estrés abiótico, fundamentalmente estrés hídrico [68]. En arroz, se ha observado que la aplicación exógena de ABA disminuye la formación de raíces adventicias hasta en un 50% [69]. Por su parte, las estrigolactonas son fitorreguladores inicialmente relacionados con la interacción entre plantas parásitas y microorganismos beneficiosos del suelo [70], pero que también participan en la regulación de otros procesos de adaptación a distintos estreses abióticos [71]. En este contexto, los mutantes de tomate s*itiens* (*sit*) y *flacca* (*flc*), deficientes en ABA, presentan un mayor número

de raíces adventicias en tallos que la estirpe silvestre. El genotipo s*it* tiene una mutación en el gen que codifica la enzima ABA ALDEHIDO OXIDASA (AAO), mientras que *flc* tiene una mutación en el cofactor de molibdeno requerido para la actividad de la AAO [72]. Por su parte, el mutante *notabilis* (*not*), también afectado en la biosíntesis del ABA y con mayor número de raíces adventicias producidas en el tallo, recupera el fenotipo silvestre mediante la expresión del gen *9–CIS–EPOXYCAROTENOID DIOXYGENASE 1* (*NCED1*) que se encuentra dañado en este mutante [57, 73]. Los mutantes *sit*, *flc* y *not* tienen, además, un menor contenido endógeno en estrigolactonas, lo que sugiere una interacción positiva entre ambas fitohormonas a través de un mecanismo de acción desconocido [72]. Por otro lado, se ha observado una mayor capacidad de formación de raíces adventicias en las líneas transgénicas de tomate que presentan niveles reducidos del gen de biosíntesis de estrigolactonas *CAROTENOID CLEAVAGE DIOXYGENASE 8* (*CCD8*) [74]. Los mutantes de Arabidopsis y de guisante deficientes en la síntesis de estrigolactonas o en su señalización también muestran una mayor producción de raíces adventicias [75]. Se ha propuesto que las estrigolactonas limitan la producción de raíces adventicias al inhibir las divisiones celulares en los primordios [75]. Curiosamente, también se ha observado que las estrigolactonas regulan negativamente el PAT a través del tallo en estas especies, probablemente mediante la internalización de PIN2, limitando así la cantidad de auxinas disponibles en la región de enraizamiento [76, 77].

El etileno es una hormona gaseosa que se sintetiza rápidamente en respuesta a distintos estreses, como heridas o inundaciones. En esquejes de petunia, se ha comprobado que la incorporación exógena del ácido 1–aminociclopropano–1–carboxílico, el precursor del etileno, incrementó la tasa de formación de raíces adventicias [78]. Los mutantes de tomate insensibles al etileno *Never ripe* (*Nr*) desarrollan un menor número de raíces adventicias que su genotipo silvestre [79, 80]. En otro trabajo [81] se

encontró que los mutantes de Arabidopsis deficientes en la síntesis o en la señalización del etileno presentaron un menor número de raíces adventicias en el hipocótilo. Estos resultados indican una función positiva del etileno sobre la formación de raíces adventicias. A partir de los resultados obtenidos en Arabidopsis se ha propuesto que existe una regulación positiva del etileno sobre la tasa de conversión del AIB a AIA, que también es dependiente de los transportadores AUX1 y LAX3 [82]. En *Solanum dulcamara* se ha estudiado con detalle la formación de raíces adventicias en respuesta a la inundación, un proceso que depende de la reactivación de los primordios preformados en la base del tallo de las plantas jóvenes [83, 84]. Mediante un análisis transcriptómico, se ha determinado que se produce un reajuste metabólico global en esta región, lo que permite la adaptación a la falta de oxígeno. Este reajuste depende de la señal positiva del etileno y estaría regulado negativamente por el ABA [83]. En cualquier caso, la reactivación de los primordios de las raíces adventicias requiere de la señalización funcional de las auxinas [85]. Por su parte, los estudios realizados en condiciones de inundación en trigo también confieren una función relevante al etileno en este proceso, en cooperación con las auxinas [86, 87].

En arroz, el ortólogo de *WOX11* se expresa de manera específica en los primordios de las raíces adventicias, y la proteína WOX11 interacciona con ETHYLENE RESPONSE FACTOR 3 (ERF3) para la regulación de sus genes diana implicados en la regulación hormonal de la formación de raíces adventicias en esta especie [88, 89]. En el álamo, la expresión constitutiva de uno de los dos genes *WOX11* que hay en su genoma no solo incrementó el número de raíces adventicias en esquejes de tallo, sino que indujo la producción ectópica de raíces en las partes aéreas [90]. En Arabidopsis, WOX11 y WOX12 activan junto con las auxinas la expresión de *WOX5*, *WOX7* y *LBD16* para iniciar la formación de primordios adventicios [91, 92], aunque se desconoce la regulación del etileno en este proceso.

1.3 Objetivos

La formación de raíces adventicias es clave durante la propagación vegetativa de numerosas especies vegetales, por lo que conocer las bases genéticas y hormonales que regulan este proceso en especies agronómicas permitirá optimizar los procesos de producción de nuevas variedades con características genéticas mejoradas.

En este contexto se enmarcan los trabajos científicos presentados en esta memoria y que constituyen esta Tesis Doctoral, encaminada a:

- Determinar algunos de los factores genéticos que contribuyen a las diferencias observadas en la arquitectura radicular en respuesta a herida en una colección de estirpes silvestres de *Arabidopsis thaliana* (L.) Heynh.
- Caracterizar la variabilidad morfológica observada durante la formación de raíces adventicias a partir de esquejes en una población derivada del cruzamiento entre dos variedades comerciales de clavel cultivado (*Dianthus caryophyllus* L.), que difieren de forma significativa en su capacidad de enraizamiento adventicio.
- Obtener herramientas para la identificación de marcadores asociados a la capacidad de enraizamiento adventicio en esquejes de clavel cultivado.
- Diseñar y optimizar un protocolo adecuado para la micropropagación de plantas de argán (*Argania spinosa* [L.] Skeels) para su uso en cultivo intensivo.

1.4 Bibliografía

1. **Woodward, A. W., Bartel, B.** (2018). Biology in bloom: A primer on the *Arabidopsis thaliana* model system. *Genetics* **208**: 1337–1349
2. **Provart, N. J., Alonso, J., Assmann, S. M., Bergmann, D., Brady, S. M., Brkljacic, J., Browse, J., Chapple, C., Colot, V., Cutler, S., Dangl, J., Ehrhardt, D., Friesner, J.D., Frommer, W.B., Grotewold, E., Meyerowitz, E., Nemhauser, J., Nordborg, M., Pikaard, C., Shanklin, J., Somerville, C., Stitt, M., Torii, K.U., Waese, J., Wagner, D., McCourt, P.** (2016). 50 years of Arabidopsis research: highlights and future directions. *New Phytol* **209**: 921–944
3. **Cheng, C.Y., Krishnakumar, V., Chan, A.P., Thibaud-Nissen, F., Schobel, S., Town, C.D.** (2017). Araport11: a complete reannotation of the *Arabidopsis thaliana* reference genome. *Plant J* **89**: 789–804
4. **Clough, S.J., Bent, A.F.** (1998). Floral dip: a simplified method for Agrobacterium-mediated transformation of *Arabidopsis thaliana*. *Plant J* **16**: 735–743
5. **O'Malley, R.C., Ecker, J.R.** (2010). Linking genotype to phenotype using the Arabidopsis unimutant collection. *Plant J* **61**: 928–940
6. **Martín, B., Ramiro, M., Martínez-Zapater, J.M., Alonso-Blanco, C.** (2009). A high-density collection of EMS-induced mutations for TILLING in *Landsberg erecta* genetic background of Arabidopsis. *BMC Plant Biol* **9**: 147
7. **Yamaguchi, Y.L., Ishida, T., Yoshimura, M., Imamura, Y., Shimaoka, C., Sawa, S.** (2017). A collection of mutants for CLE-peptide-encoding genes in Arabidopsis generated by CRISPR/Cas9-mediated gene targeting. *Plant Cell Physiol* **58**: 1848–1856
8. **Li, J. F., Norville, J. E., Aach, J., McCormack, M., Zhang, D., Bush, J., Church, G.M., Sheen, J.** (2013). Multiplex and homologous recombination–mediated genome editing in Arabidopsis and *Nicotiana benthamiana* using guide RNA and Cas9. *Nat Biotechnol* **31**: 688
9. **Mitchell-Olds, T., Schmitt, J.** (2006). Genetic mechanisms and evolutionary significance of natural variation in Arabidopsis. *Nature* **441**: 947
10. **Alonso-Blanco, C., Aarts, M.G., Bentsink, L., Keurentjes, J.J., Reymond, M., Vreugdenhil, D., Koornneef, M.** (2009). What has natural variation taught us about plant development, physiology, and adaptation? *Plant Ce*ll **21**: 1877–1896
11. **Koornneef, M., Meinke, D.** (2010). The development of Arabidopsis as a model plant. *Plant J* **61**: 909–921
12. **Krämer, U.** (2015). Planting molecular functions in an ecological context with *Arabidopsis thaliana*. *Elife* **4**
13. **Hirschhorn, J.N., Daly, M.J.** (2005). Genome-wide association studies for common diseases and complex traits. *Nat Rev Genet* **6**: 95

14. **Atwell, S., Huang, Y.S., Vilhjálmsson, B.J., Willems, G., Horton, M., Li, Y., Meng, D., Platt, A., Tareno, A.M., Hu, T.T., Jiang, R., Muliyati, N.W., Zhang, X., Amer, M.A., Baxter, I., Brachi, B., Chory, J., Dean, C., Debieu, M., de Meaux, J., Ecker, J.R., Faure, N., Kniskern, J.M., Jones, J.D.G., Michael, T., Nemri, A., Roux, F., Salt, D.E., Tang, C., Todesco, M., Traw, M.B., Weigel, D., Marjoram, P., Borevitz, J.O., Bergelson, J., Nordborg, M.** (2010). Genome-wide association study of 107 phenotypes in *Arabidopsis thaliana* inbred lines. *Nature* **465**: 627

15. **Nordborg, M., Weigel, D.** (2008). Next-generation genetics in plants. *Nature* **456**: 720

16. **Korte, A., Farlow, A.** (2013). The advantages and limitations of trait analysis with GWAS: a review. *Plant methods* **9**: 29

17. **Cao, J., Schneeberger, K., Ossowski, S., Günther, T., Bender, S., Fitz, J., Koening, D., Lanz, C., Stegle, O., Lipper, C., Wang, X., Ott, F., Müller, J., Alonso-Blanco, C., Borgwardt, K., Schmid, K.J., Weigel, D.** (2011). Whole-genome sequencing of multiple *Arabidopsis thaliana* populations. *Nature Gen* **43**: 956

18. **Balao, F., Herrera, J., Talavera, S.** (2011). Phenotypic consequences of polyploidy and genome size at the microevolutionary scale: a multivariate morphological approach. *New Phytol* **192**: 256–265

19. **Valente, L.M., Savolainen, V., Vargas, P.** (2010). Unparalleled rates of species diversification in Europe. *Proc R Soc Biol Sci* **277**: 1489–1496

20. **Sheela, V.L.** (2008) Carnation. *Flowers for trade*. New Delhi, New India Publishing, 95–112

21. **Ahmadian, M., Babaei, A., Shokri, S., Hessami, S.** (2017). Micropropagation of carnation (*Dianthus caryophyllus* L.) in liquid medium by temporary immersion bioreactor in comparison with solid culture. *J Genet Eng Biotech* **15**: 309–315

22. **Ministerio de Agricultura, Pesca y Alimentación** (2013). https://www.mapa.gob.es/es/agricultura/temas/producciones-agricolas/flores-plantas-ornamentales/

23. **Blackwell, E.** (1737). A Curious Herbal containing five hundred cuts of the most useful plants, which are now used in the practice of physick. Vol. 1: Londres.

24. **Villanova, J.** (2017). Desarrollo de herramientas para la mejora genética del enraizamiento de esquejes en clavel cultivado (*Dianthus caryophyllus* L.). Tesis Doctoral. Universidad Miguel Hernández de Elche.

25. **Yagi, M., Yamamoto, T., Isobe, S., Hirakawa, H., Tabata, S., Tanase, K., Yamaguchi, H., Onozaki, T.** (2013). Construction of a reference genetic linkage map for carnation (*Dianthus caryophyllus* L.). *BMC Genomics* **14**: 734

26. **Yagi, M., Onozaki, T., Taneya, M., Watanabe, H., Yoshimura, T., Yoshinari, T., Ochiai, Y., Shibata, M.** (2006). Construction of a genetic linkage map for the carnation by using RAPD and SSR markers and mapping quantitative trait loci (QTL) for resistance to bacterial wilt caused by *Burkholderia caryophylli*. *J Japan Soc Hort Sci* **75**: 166–172

27. **Tanase, K., Nishitani, C., Hirakawa, H., Isobe, S., Tabata, S., Ohmiya, A., Onozaki, T.** (2012). Transcriptome analysis of carnation (*Dianthus caryophyllus* L.) based on next-generation sequencing technology. *BMC Genomics* **13**: 292

28. **Yagi, M., Kosugi, S., Hirakawa, H., Ohmiya, A., Tanase, K., Harada, T., Kishimoto, K., Nakayama, M., Ichimura, K., Onozaki, T., Yamaguchi, H., Sasaki, N., Miyahara, T., Nishizaki, Y., Ozeki, Y., Nakamura, N., Suzuki, T., Tanaka, Y., Sato, S., Shirasawa, N., Isobe, S., Miyamura, Y., Watanabe, A., Nakayama, S., Kishida, Y., Kohara, M., Tabata, S.** (2014). Sequence analysis of the genome of carnation (*Dianthus caryophyllus* L.). *DNA Res* **21**: 231–241

29. **Villacorta-Martín, C., Sánchez-García, A. B., Villanova, J., Cano, A., van de Rhee, M., de Haan, J., Acosta, M., Passarinho, P., Pérez-Pérez, J.M.** (2015). Gene expression profiling during adventitious root formation in carnation stem cuttings. *BMC Genomics* **16**: 789

30. **Kong, W., Bendahmane, M., Fu, X.** (2018). Genome-wide identification and characterization of aquaporins and their role in the flower opening processes in carnation (*Dianthus caryophyllus*). *Molecules* **23**: 1895

31. **Sánchez-García, A.B., Ibáñez, S., Cano, A., Acosta, M., Pérez-Pérez, J.M.** (2018). A comprehensive phylogeny of auxin homeostasis genes involved in adventitious root formation in carnation stem cuttings. *PloS one* **13**: e0196663

32. **Charrouf, Z., Guillaume, D.** (2009). Sustainable development in Northern Africa: The argan forest case. *Sustainability* **1**: 1012–1022

33. **Khallouki, F., Voggel, J., Breuer, A., Klika, K.D., Ulrich, C.M., Owen, R.W.** (2017). Comparison of the major polyphenols in mature argan fruits from two regions of Morocco. *Food Chem* **221**: 1034–1040

34. **Zunzunegui, M., Boutaleb, S., Díaz Barradas, M. C., Esquivias, M. P., Valera, J., Jáuregui, J., Tagma, T., Ain-Lhout, F.** (2017). Reliance on deep soil water in the tree species *Argania spinosa*. *Tree physiology* **38**: 678–689

35. **Pakhrou, O., Medraoui, L., Yatrib, C., Alami, M., Souda-kouraichi, S.I., Ferradous, A., Msanda, F., El modafar, C., Filai-maltouf, A., Belkadi, B.** (2016). Study of genetic diversity and differentiation of argan tree population (*Argania spinosa* L.) using AFLP markers. *Aust J Crop Sci* **10**: 990

36. **Rogers, E.D., Benfey, P.N.** (2015). Regulation of plant root system architecture: implications for crop advancement. *Curr Opin Biotech* **32**: 93–98

37. **Lakehal, A., Bellini, C.** (2019). Control of adventitious root formation: insights into synergistic and antagonistic hormonal interactions. *Physiol Plant* **165**: 90–100

38. **Bellini, C., Pacurar, D. I., Perrone, I.** (2014). Adventitious roots and lateral roots: similarities and differences. *Annu Rev Plant Biol* **65**: 639–666

39. **Gonin, M., Bergougnoux, V., Nguyen, T.D., Gantet, P., Champion, A.** (2019). What Makes Adventitious Roots? *Plants* **8**: 240

40. **Steffens, B., Rasmussen, A.** (2016). The physiology of adventitious roots. *Plant Physiol* **170**: 603–617

41. **Coudert, P., van Anh, T., Gantet, P.** (2013). Rice: a model plant to decipher the hidden origin of adventitious roots. *Plant roots: the hidden half.* CRC Press, Third edition, Taylor and Francis, Beeckman T. and Eshel A. (Ed.)

42. **Lynch, J.P.** (2013). Steep, cheap and deep: an ideotype to optimize water and N acquisition by maize root systems. *Ann Bot* **112**: 347–357

43. **Druege, U., Hilo, A., Pérez-Pérez, J.M., Klopotek, Y., Acosta, M., Shahinnia, F., Zerche, S., Franken, P., Hajirezaei, M.R.** (2019). Molecular and physiological control of adventitious rooting in cuttings: phytohormone action meets resource allocation. *Ann Bot* **123**: 929–949

44. **Druege, U., Franken, P., Hajirezaei, M.R**. (2016). Plant hormone homeostasis, signaling, and function during adventitious root formation in cuttings. *Front Plant Sci* **7**: 381

45. **de Klerk, G.J., van der Krieken, W., de Jong, J.C.** (1999). Review the formation of adventitious roots: new concepts, new possibilities. *In Vitro Cell Dev Biol Plant* **35**: 189–199

46. **Sukumar, P., Maloney, G.S., Muday, G.K.** (2013). Localized induction of the ATP-binding cassette B19 auxin transporter enhances adventitious root formation in Arabidopsis. *Plant Physiol* **162**: 1392–1405

47. **Agulló-Antón, M. Á., Ferrández-Ayela, A., Fernández-García, N., Nicolás, C., Albacete, A., Pérez-Alfocea, F., Sánchez-Bravo, J., Pérez-Pérez, J.M., Acosta, M.** (2013). Early steps of adventitious rooting: morphology, hormonal profiling and carbohydrate turnover in carnation stem cuttings. *Physiol Plant* **150**: 446–462

48. **Ahkami, A. H., Melzer, M., Ghaffari, M.R., Pollmann, S., Javid, M.G., Shahinnia, F., Hajirezaei, M.R., Druege, U.** (2013). Distribution of indole-3-acetic acid in *Petunia hybrida* shoot tip cuttings and relationship between auxin transport, carbohydrate metabolism and adventitious root formation. *Planta* **238**: 499–517

49. **Ibáñez, S., Ruiz-Cano, H., Fernández, M.Á., Sánchez-García, A.B., Villanova, J., Micol, J.L., Pérez-Pérez, J.M.** (2019). A network-guided genetic approach to identify novel regulators of adventitious root formation in *Arabidopsis thaliana*. *Front Plant Sci* **10**: 461

50. **Liu, J., Sheng, L., Xu, Y., Li, J., Yang, Z., Huang, H., Xu, L.** (2014). WOX11 and 12 are involved in the first-step cell fate transition during de novo root organogenesis in Arabidopsis. *Plant Cell* **26**: 1081–1093

51. **Li, J., Zhang, J., Jia, H., Liu, B., Sun, P., Hu, J., Wang, L., Lu, M.** (2018). The WUSCHEL-related homeobox 5a (PtoWOX5a) is involved in adventitious root development in poplar. *Tree physiology* **38**:139–153

52. **Casanova-Sáez, R., Voß, U.** (2019). Auxin metabolism controls developmental decisions in land plants. *Trends Plant Sci* **24**: 741–754

53. **Lavenus, J., Goh, T., Roberts, I., Guyomarc'h, S., Lucas, M., De Smet, I., Fukaki, H., Beeckman, T., Bennett, M., Laplaze, L.** (2013). Lateral root development in Arabidopsis: fifty shades of auxin. *Trends Plant Sci* **18**: 450–458

54. **Lee, S., I. Sergeeva, L., Vreugdenhil, D.** (2018). Natural variation of hormone levels in Arabidopsis roots and correlations with complex root architecture. *J Integr Plant Biol* **60**: 292–309

55. **Frick, E.M., Strader, L.C.** (2018). Roles for IBA-derived auxin in plant development. *J Exp Bot* **69**: 169–177

56. **Xuan, W., Audenaert, D., Parizot, B., Möller, B.K., Njo, M.F., De Rybel, B., De Rop, G., Van Isterdael, G., Mähönen, A.P., Vanneste, S., Beeckman, T.** (2015). Root cap-derived auxin pre-patterns the longitudinal axis of the Arabidopsis root. *Curr Biol* **25**: 1381–1388

57. **Pacurar, D.I., Perrone, I., Bellini, C.** (2014). Auxin is a central player in the hormone cross-talks that control adventitious rooting. *Physiol Plant* **151**: 83–96

58. **Acosta, M., Oliveros-Valenzuela, M.R., Nicolás, C., Sánchez-Bravo, J.** (2009) Rooting of carnation cuttings: the auxin signal. *Plant Signal Behav* **4**: 234–236

59. **Gutierrez, L., Bussell, J.D., Pacurar, D.I., Schwambach, J., Pacurar, M., Bellini, C.** (2009). Phenotypic plasticity of adventitious rooting in Arabidopsis is controlled by complex regulation of *AUXIN RESPONSE FACTOR* transcripts and microRNA abundance. *Plant Cell* 21: 3119–3132

60. **Bustillo-Avendaño, E., Ibáñez, S., Sanz, O., Barros, J.A S., Gude, I., Perianez-Rodriguez, J., Micol, J.L., del Pozo, J.C., Moreno-Risueño, M.A., Pérez-Pérez, J.M.** (2018). Regulation of hormonal control, cell reprogramming, and patterning during de novo root organogenesis. *Plant Physiol* **176**: 1709–1727

61. **Kieber, J.J., Schaller, G.E.** (2014). Cytokinins. *TAB Society of Plant Biologists* **12**

62. **Ramírez-Carvajal, G.A., Morse, A.M., Dervinis, C., Davis, J.M.** (2009). The cytokinin type-B response regulator PtRR13 is a negative regulator of adventitious root development in *Populus*. *Plant physiol* **150**: 759–771

63. **Della Rovere, F., Fattorini, L., D'angeli, S., Veloccia, A., Falasca, G., Altamura, M.M.** (2013). Auxin and cytokinin control formation of the quiescent centre in the adventitious root apex of Arabidopsis. *Ann Bot* **112**: 1395–1407

64. **Ahkami, A.H., Lischewski, S., Haensch, K.T., Porfirova, S., Hofmann, J., Rolletschek, H., Melzer, M., Franken, P., Hause, B., Druege, U., Hajirezaei, M.R.** (2009). Molecular physiology of adventitious root formation in *Petunia hybrida* cuttings: involvement of wound response and primary metabolism. *New Phytol* **181**: 613–625

65. **Fattorini, L., Hause, B., Gutierrez, L., Veloccia, A., Della Rovere, F., Piacentini, D., Falasca, G., Altamura, M.M.** (2018). Jasmonate promotes auxin-induced adventitious rooting in dark-grown Arabidopsis thaliana seedlings and stem thin cell layers by a cross-talk with ethylene signalling and a modulation of xylogenesis. *BMC Plant Biol* **18**: 182

66. **Lischweski, S., Muchow, A., Guthörl, D., Hause, B.** (2015). Jasmonates act positively in adventitious root formation in petunia cuttings. *BMC Plant Biol* **15**: 229

67. **Gutierrez, L., Mongelard, G., Floková, K., Păcurar, D.I., Novák, O., Staswick, P., Kowalczyk, M., Pacurar, M., Demailly, H., Geiss, G., Bellini, C.** (2012). Auxin controls Arabidopsis adventitious root initiation by regulating jasmonic acid homeostasis. *Plant Cell* **24**: 2515–2527

68. **Vishwakarma, K., Upadhyay, N., Kumar, N., Yadav, G., Singh, J., Mishra, R.K., Kumar, V., Verma, R., Upadhyay, R.G., Pandey, M., Sharma, S.** (2017). Abscisic acid signaling and abiotic stress tolerance in plants: a review on current knowledge and future prospects. *Front Plant Sci* **8**: 161

69. **Ma, B., Yin, C.C., He, S.J., Lu, X., Zhang, W.K., Lu, T.G., Chen, S.Y., Zhang, J.S.** (2014). Ethylene-induced inhibition of root growth requires abscisic acid function in rice (*Oryza sativa* L.) seedlings. *PLoS genetic*s **10**: e1004701

70. **Al-Babili, S., Bouwmeester, H.J.** (2015). Strigolactones, a novel carotenoid-derived plant hormone. *Annu Rev Plant Biol* **66**: 161–186

71. **Li, W., Nguyen, K.H., Chu, H.D., Van Ha, C., Watanabe, Y., Osakabe, Y., Leyva-González, M.A., Sato, M., Toyooka, K., Voges, L., Tanaka, M., Mostofa, M.G., Seki, M., Seo, M., Yamaguchi, S., Nelson, D.C., Tian, C., Herrera-Estrella, L., Tran, L.S.P.** (2017). The karrikin receptor KAI2 promotes drought resistance in *Arabidopsis thaliana*. *PLoS Genet* **13**: e1007076

72. **López-Ráez, J.A., Kohlen, W., Charnikhova, T., Mulder, P., Undas, A. K., Sergeant, M.J., Verstappen, F., Bugg, T.D.H., Thompson, A.J., Ruyter-Spira, C., Bouwmeester, H.** (2010). Does abscisic acid affect strigolactone biosynthesis?. *New Phytol* **187**: 343–354

73. **Thompson, A.J., Thorne, E.T., Burbidge, A., Jackson, A.C., Sharp, R.E., Taylor, I.B.** (2004). Complementation of *notabilis*, an abscisic acid-deficient mutant of tomato: importance of sequence context and utility of partial complementation. *Plant Cell Environ 27*: 459–471

74. **Kohlen, W., Charnikhova, T., Lammers, M., Pollina, T., Tóth, P., Haider, I., Pozo., M.J., de Maagd, R.A., Ruyter-Spira, C., Bouwmeester, H.J., López-Ráez, J.A.** (2012). The tomato CAROTENOID CLEAVAGE DIOXYGENASE 8 (SlCCD8) regulates rhizosphere signaling, plant architecture and affects reproductive development through strigolactone biosynthesis. *New Phytol* **196**: 535–547

75. **Rasmussen, A., Mason, M. G., De Cuyper, C., Brewer, P. B., Herold, S., Agusti, J., Geelen, D., Greb, T., Goormachtig, S., Beeckman, T., Beveridge, C.A.** (2012). Strigolactones suppress adventitious rooting in Arabidopsis and pea. *Plant physiol* **158**: 1976–1987

76. **Pandya-Kumar, N., Shema, R., Kumar, M., Mayzlish-Gati, E., Levy, D., Zemach, H., Belausov, E., Wininger, S., Abu-Abied, M., Kapulnik, Y., Koltai, H.** (2014). Strigolactone analog GR 24 triggers changes in PIN2 polarity, vesicle trafficking and actin filament architecture. *New Phytol* **202**: 1184–1196

77. **Rasmussen, A., Beveridge, C. A., Geelen, D.** (2012). Inhibition of strigolactones promotes adventitious root formation. *Plant Signal Behav* **7**: 694–697

78. **Druege, U., Franken, P., Lischewski, S., Ahkami, A.H., Zerche, S., Hause, B., Hajirezaei, M.R.** (2014). Transcriptomic analysis reveals ethylene as stimulator and auxin as regulator of adventitious root formation in petunia cuttings. *Front Plant Sci* **5**: 494

79. **Negi, S., Sukumar, P., Liu, X., Cohen, J.D., Muday, G.K**. (2010). Genetic dissection of the role of ethylene in regulating auxin-dependent lateral and adventitious root formation in tomato. *Plant J* **61**: 3–15

80. **Vidoz, M. L., Loreti, E., Mensuali, A., Alpi, A., Perata, P.** (2010). Hormonal interplay during adventitious root formation in flooded tomato plants. *Plant J* **63**: 551–562

81. **Rasmussen, A., Hu, Y., Depaepe, T., Vandenbussche, F., Boyer, F.D., Van Der Straeten, D., Geelen, D.** (2017). Ethylene controls adventitious root initiation sites in Arabidopsis hypocotyls independently of strigolactones. *J Plant Growth Regul* **36**: 897–911

82. **Veloccia, A., Fattorini, L., Della Rovere, F., Sofo, A., D'angeli, S., Betti, C., Falasca, G., Altamura, M.M.** (2016). Ethylene and auxin interaction in the control of adventitious rooting in *Arabidopsis thaliana*. *J Exp Bot* **67**: 6445–6458

83. **Dawood, T., Yang, X., Visser, E.J., Te Beek, T.A., Kensche, P.R., Cristescu, S.M., Lee, S., Flokova, K., Nguyen, D., Mariani, C., Rieu, I.** (2016). A co-opted hormonal cascade activates dormant adventitious root primordia upon flooding in *Solanum dulcamara*. *Plant Physiol* **170**: 2351–2364

84. **Zhang, Q., Visser, E.J., de Kroon, H., Huber, H.** (2015). Life cycle stage and water depth affect flooding-induced adventitious root formation in the terrestrial species *Solanum dulcamara*. *Ann Bot* **116**: 279–290

85. **Yang, X., Jansen, M.J., Zhang, Q., Sergeeva, L., Ligterink, W., Mariani, C., Rieu, I., Visser, E. J.** (2018). A disturbed auxin signaling affects adventitious root outgrowth in *Solanum dulcamara* under complete submergence. *J Plant Physiol* **224**: 11–18

86. **Nguyen, T.N., Tuan, P.A., Mukherjee, S., Son, S., Ayele, B.T.** (2018). Hormonal regulation in adventitious roots and during their emergence under waterlogged conditions in wheat. *J Exp Bot* **69**: 4065–4082

87. **Yamauchi, T., Watanabe, K., Fukazawa, A., Mori, H., Abe, F., Kawaguchi, K., Oyanagi A., Nakazono, M.** (2013). Ethylene and reactive oxygen species are involved in root aerenchyma formation and adaptation of wheat seedlings to oxygen-deficient conditions. *J Exp Bot* **65**: 261–273

88. **Jiang, W., Zhou, S., Zhang, Q., Song, H., Zhou, D.X., Zhao, Y.** (2017). Transcriptional regulatory network of WOX11 is involved in the control of crown root development, cytokinin signals, and redox in rice. *J Exp Bot* **68**: 2787–2798

89. **Zhao, Y., Cheng, S., Song, Y., Huang, Y., Zhou, S., Liu, X., Zhou, D.X.** (2015). The interaction between rice ERF3 and WOX11 promotes crown root development by regulating gene expression involved in cytokinin signaling. *Plant Cell* **27**: 2469–2483

90. Xu, M., Xie, W., Huang, M. (2015). Two WUSCHEL-related HOMEOBOX genes, *PeWOX11a* and *PeWOX11b*, are involved in adventitious root formation of poplar. *Physiol Plant* **155**: 446–456

91. Xu, L. (2018). De novo root regeneration from leaf explants: wounding, auxin, and cell fate transition. *Curr Opin Plant Biol* **41**: 39–45

92. Hu, X., Xu, L. (2016). Transcription factors WOX11/12 directly activate WOX5/7 to promote root primordia initiation and organogenesis. *Plant Physiol* **172**: 2363–2373

Capítulo 2

Resumen global

2. RESUMEN GLOBAL

2.1 Materiales y métodos

2.1.1 Estudio de GWA en *Arabidopsis thaliana*

Nuestra población inicial a estudio consta de 174 estirpes silvestres seleccionadas del proyecto 1001 Genomes [93, 94] en función de la información disponible en la base de datos GWA–Portal [95]. Todas las semillas utilizadas en este trabajo se obtuvieron del Nottingham Arabidopsis Stock Centre. Una vez estériles, las semillas se sembraron en las condiciones de cultivo *in vitro* habituales establecidas en el laboratorio, y se indujo la formación de raíces tras la eliminación quirúrgica del ápice de la raíz principal. A continuación, se estudiaron algunos parámetros relevantes de su arquitectura radicular (véanse los materiales y métodos del primer artículo en las págs. 52–54).

Se determinó la estructura poblacional de nuestra colección utilizando una muestra aleatoria de marcadores SNP bialélicos neutrales y se utilizó la información fenotípica recopilada en nuestro trabajo para realizar un estudio de asociación a genoma completo o GWA (*genome–wide association*) con los parámetros que se definen en los materiales y métodos del primer artículo (págs. 52–54). Las líneas insercionales de ADN–T de *Agrobacterium tumefaciens* en cada uno de los tres genes seleccionados se genotiparon siguiendo los procedimientos habituales de trabajo en el laboratorio. La cuantificación de la expresión génica se realizó mediante retrotranscripción de ARN, seguida de PCR cuantitativa en tiempo real (véanse los materiales y métodos del primer artículo en la pág. 54).

2.1.2 Análisis de la formación de raíces adventicias en clavel

El material vegetal para nuestros estudios fue proporcionado por la empresa Dümmen Orange (Puerto Lumbreras, Murcia). Las extracciones y los análisis de fitohormonas correspondientes a los experimentos

realizados en clavel fueron realizados siguiendo el protocolo que se indica en los materiales y métodos del segundo (págs. 80–81) y tercer artículo (págs. 120–123). Los metabolitos estudiados se identificaron según su masa molecular y el tiempo de retención en los cromatogramas obtenidos. Para inhibir la actividad de las enzimas GRETCHEN HAGEN 3 en la base de los esquejes (véanse los materiales y métodos del segundo artículo en la pág. 80), se hizo uso del inhibidor competitivo adenosina–5–[2–(1H–indol–3–il)etil]fosfato proporcionado desinteresadamente por la profesora Christine Böttcher (CSIRO Plant Industry, Glen Osmond, Australia).

Para el análisis del enraizamiento adventicio en esquejes de clavel en la colección F_1 derivada del cruzamiento entre las estirpes *2101–02 MFR* y *2003 R 8*, se llevaron a cabo tres experimentos consecutivos, siguiendo el diseño experimental que se define en los materiales y métodos del tercer artículo (págs. 120–122).

El procesamiento de las imágenes de clavel obtenidas, el análisis estadístico de los datos y su representación gráfica se llevó a cabo según los procedimientos habituales utilizados en el laboratorio, y que se describen detalladamente en los materiales y métodos del segundo (págs. 80–81) y tercer artículo (págs. 120–122).

2.1.3 Micropropagación de argán

Para los ensayos con argán hemos utilizado frutos y esquejes obtenidos de tres árboles distintos de un campo abandonado en San Vicente del Raspeig (Alicante). Las semillas de argán utilizadas se obtuvieron de frutos seleccionados por su tamaño, y se desinfectaron por inmersión transitoria en lejía diluida (véanse los materiales y métodos del cuarto artículo en la pág. 147). A continuación, las plántulas derivadas de estas semillas se incubaron en tubos de ensayo individuales con medio nutritivo suplementado con diferentes concentraciones de reguladores del crecimiento, en particular con ácido giberélico o GA_3, thidiazurón, ácido

indol−3−butírico y ácido 1−naftalenacético. Las plántulas se mantuvieron en estos medios en una cámara de crecimiento con las condiciones de temperatura, humedad y fotoperiodo adecuadas, realizando las transferencias a nuevos medios de cultivo de manera periódica y siguiendo el diseño experimental propuesto (véanse los materiales y métodos del cuarto artículo en las págs. 147–149). Una vez se produjo el enraizamiento adecuado de los microesquejes, éstos se transfirieron a macetas pequeñas y se aclimataron en la cámara de crecimiento de manera previa a su traslado a condiciones de invernadero, donde se mantuvieron hasta la finalización de los experimentos (véanse los materiales y métodos del cuarto artículo en las págs. 148–149).

Además de los ensayos de propagación a partir de semillas, se obtuvieron esquejes nodales lignificados partir de varias ramas jóvenes recolectadas en primavera procedentes de árboles de argán maduros. Estos esquejes se utilizaron para llevar a cabo distintos ensayos de enraizamiento en presencia de reguladores del crecimiento de tipo auxínico, tal y como se describe en los materiales y métodos del cuarto artículo (págs. 149–150). Los análisis y contrastes estadísticos se han llevado a cabo con el programa StatGraphics Centurion XV (StatPoint Technologies, Inc.).

2.2 Resultados y discusión

2.2.1 Estudio de GWA en *Arabidopsis thaliana*

Para identificar nuevos factores genéticos implicados en la modulación de la arquitectura radicular en respuesta a heridas, hemos llevado a cabo un estudio GWA utilizando una amplia colección de estirpes silvestres de *Arabidopsis thaliana* que había sido caracterizada a nivel genético de manera previa [94]. Aunque nuestra población de estudio original contenía 174 líneas, hemos seleccionado 120 para llevar a cabo los estudios de GWA en función de los resultados fenotípicos obtenidos y de la

información genética depositada en la base de datos del GWA–Portal sobre estas estirpes [95]. Hemos estimado la heredabilidad en sentido amplio (H^2) para los distintos caracteres analizados del sistema radicular tras la escisión del ápice de la raíz principal, con valores de H^2 comprendidos entre 0,90 para el tiempo de iniciación de las raíces laterales (*LR emergence onset*) y 0,95 para el número de raíces laterales (*LR number*). Hemos encontrado una correlación positiva estadísticamente significativa (r = 0,83; valor de P < 0,05) entre el número de raíces laterales que se forman en respuesta a heridas (*LR number*) y la longitud de la raíz principal en el momento de la escisión del ápice radicular (*PR length*) (véase la figura 2A del primer artículo en la pág. 55). Además, algunas de las estirpes estudiadas, como Leo−1 y Voeran−1, con una longitud similar de su raíz principal, presentaron diferencias significativas (valor de P < 0,05) en el número de raíces laterales en respuesta a heridas; 7,1 ± 1,4 y 3,1 ± 1,5 respectivamente (véase la figura 2C del primer artículo en la pág. 55). Se ha determinado que la fluctuación periódica de la respuesta a las auxinas en la región vascular próxima al meristemo de la raíz principal determina la especificación temprana de las raíces laterales [96]. Esta respuesta es consecuencia directa del transporte facilitado de la auxina activa, el ácido indol−3−acético, hacia esta región vascular, desde su síntesis en la cofia que protege al meristemo radicular [56]. Dado que los resultados de un estudio reciente sugieren que para la formación de las raíces laterales en la raíz primaria tras la escisión del ápice radicular se requiere el gen *WUSCHEL–RELATED HOMEOBOX 11* (*WOX11*) [97], sería interesante caracterizar la expresión de *WOX11* durante la formación de raíces en respuesta a heridas en aquellas estirpes naturales con valores fenotípicos más extremos.

Basándonos en la información obtenida de marcadores neutrales bialélicos, hemos determinado que nuestra población a estudio incluye dos subpoblaciones genéticamente distintas, con 101 y 19 estirpes cada una

respectivamente (véase la figura 3A del primer artículo en la pág. 56), que se corresponden con las áreas geográficas de distribución natural de *Arabidopsis thaliana* (véase la figura 3B del primer artículo en la pág. 56). A pesar de esta estructura poblacional subyacente, hemos encontrado suficiente variabilidad fenotípica dentro de cada una de estas subpoblaciones para iniciar los estudios de GWA. Dado que la arquitectura radicular en *Arabidopsis thaliana* es un proceso muy plástico y regulado por las condiciones ambientales [98, 99], las diferencias fenotípicas observadas entre estirpes genéticamente próximas podrían utilizarse para la construcción de nuevas poblaciones cartográficas para la identificación de genes de caracteres cuantitativos o QTL (*quantitative trait loci*).

Hemos encontrado asociaciones estadísticamente significativas entre alguno de los cuatro parámetros estudiados (*PR length*, *LR emergence onset*, *LR number* y *LR density*) con 162 polimorfismos de un solo nucleótido o SNPs (*single nucleotide polymorphisms*). El 53,2% de estos SNPs se localizan en regiones intergénicas o suponen cambios no conservados de aminoácidos en regiones codificantes (véase la figura suplementaria S4B del primer artículo en la pág. 70). Para iniciar la validación funcional de algunos de estos marcadores, se establecieron 19 regiones genómicas que se estudiaron con más detalle (véase la figura 5 del primer artículo en la pág. 58). Catorce de estas regiones incluían SNPs no sinónimos asociados con la variación en el número de raíces laterales en respuesta a heridas (véase la figura 5C del primer artículo en la pág. 58). Curiosamente, los SNPs no sinónimos localizados en tres de estas regiones, y que afectan a los genes At1g04470, At4g01090 y At4g22940, solapan también con las regiones genómicas asociadas con la variación en la longitud de la raíz principal en el momento de la escisión, lo que confirma la relación funcional entre ambos parámetros.

Mediante distintas aproximaciones analíticas hemos seleccionado cinco SNPs no sinónimos que afectan a tres genes (At4g01090, At4g33530 y

At5g19710), para llevar a cabo estudios adicionales. Para ello hemos identificado y caracterizado fenotípicamente alelos de pérdida de función en cada uno de ellos. Encontramos que una línea insercional de ADN–T que interrumpe el gen At4g01090, que codifica una proteína de función desconocida, presenta una raíz principal corta y un número reducido de raíces laterales en respuesta a heridas (véanse las figuras suplementarias S6D–S6E del primer artículo en la pág. 72). De los tres SNPs presentes en la región codificante de este gen, uno de ellos, el que genera un cambio del residuo de glicina por serina en la posición 175 de la proteína, presenta una asociación estadísticamente significativa con la reducción en el número de raíces laterales en respuesta a heridas en la población analizada (véanse las figuras suplementarias S6B–S6C del primer artículo en la pág. 72). Se sabe que la proteína codificada por el gen At4g01090 interacciona con una proteína que regula el tráfico vesicular y la endocitosis durante las infecciones fúngicas [100]. Tenemos previsto realizar experimentos adicionales para confirmar la hipótesis de que la proteína codificada por At4g01090 participa en la localización subcelular de los transportadores de auxina de la familia PIN–FORMED durante la formación de raíces laterales en respuesta a heridas. Ninguna de las dos líneas insercionales del ADN–T que interrumpen el gen At4g33530, que codifica el transportador de potasio K^+ UPTAKE TRANSPORTER 5 (KUP5), presentaron diferencias con el silvestre en la formación de raíces laterales en respuesta a heridas (véanse las figuras suplementarias S7A, S7D y S7E del primer artículo en la pág. 73). Dado que existen numerosos ortólogos en el genoma de *Arabidopsis thaliana*, se requerirá la inactivación múltiple de varios de estos genes para observar un fenotipo aparente. De hecho, los triples mutantes *kup2 kup6 kup8* presentan una mayor formación de raíces laterales en respuesta a la adición exógena de auxinas [101]. Se ha propuesto que un exceso de iones K^+ en las células del periciclo en estos mutantes causaría una aceleración del ciclo celular y, en consecuencia, la iniciación temprana de los nuevos

primordios de raíces laterales [101]. El gen At5g19710 codifica una proteína con un dominio de histidina para la transferencia de fosfato implicada en la señalización de las citoquininas, que no había sido caracterizado previamente. Hemos identificado una línea que contiene una inserción de ADN–T en el segundo intrón de este gen y que incrementa sus niveles de expresión (véanse las figuras 6A y 6G del primer artículo en la pág. 60). Los individuos homocigotos para esta inserción presentan un menor número de raíces laterales en respuesta a herida, de manera similar a lo que ocurre con los triples mutantes *ahp1 ahp2 ahp3*, deficientes en la señalización intracelular de las citoquininas (véanse las figuras 6E–6F del primer artículo en la pág. 60).

Nuestros resultados indican que se requiere una regulación fina de la señalización de las citoquininas durante la formación de raíces laterales en respuesta a heridas. La expresión de At5g19710 se induce de manera específica en la cofia radicular en condiciones de déficit de nitrógeno, unas condiciones que reprimen la formación de raíces laterales [102]. Nuestra hipótesis de trabajo es que la proteína codificada por At5g19710 actuaría como un regulador negativo local de la formación de raíces laterales en condiciones de deficiencia nutricional severa, interfiriendo con la señal de las auxinas que procede de la cofia de la raíz principal. Hemos encontrado una interacción epistática entre los SNPs de los genes At4g33530 y At5g19710 (véase la figura suplementaria S8A del primer artículo en la pág. 74), lo que sugiere una relación funcional entre la absorción del potasio y la señalización de las citoquinas. De hecho, se ha descrito el papel regulador de las citoquininas en la absorción de varios nutrientes [103], aunque su papel en la asimilación del potasio apenas se conoce [104].

2.2.2 Análisis de la formación de raíces adventicias en clavel

En trabajos previos realizados en el laboratorio del profesor José Manuel Pérez Pérez se llevó a cabo un análisis de los cambios morfológicos

y fisiológicos que se producían en la base de los esquejes durante el enraizamiento de dos variedades de clavel cultivado, *2101–02 MFR y 2003 R 8*, que diferían significativamente en su capacidad de enraizamiento adventicio [29, 105, 106]. En estos trabajos se determinó que las diferencias en su capacidad de enraizamiento adventicio se debían a un retardo en la activación de las divisiones celulares en el cambium de la variedad *2003 R 8*, que además presentó unos niveles de la auxina activa, el ácido indol–3–acético (AIA), más bajos que en la variedad *2101–02 MFR* [29]. Hemos determinado que las auxinas se producen mayoritariamente en la región distal de las hojas maduras (véase la figura 3 del segundo artículo en la pág. 85) y se transportan de forma activa hasta la base de los esquejes, en la región próxima a la escisión. De esta manera y tras la separación de los esquejes de la planta madre, se produce un máximo local de auxinas en la región vascular cercana al corte, que activa la formación de los primordios radiculares adventicios. Hemos caracterizado la dinámica de este gradiente de auxinas en la base del esqueje, observándose una ausencia del mismo en la variedad *2003 R 8* con respecto a los de la variedad *2101–02 MFR*, así como con los de la variedad de referencia *Master*. Una de las vías principales de inactivación endógena del AIA es por su conjugación con el ácido aspártico, mediada por las enzimas GRETCHEN HAGEN 3 (GH3) [107] o por su oxidación por dioxigenasas de la familia DIOXYGENASE FOR AUXIN OXIDATION 1 [108]. Tras estudiar estas vías de inactivación, hemos encontrado diferencias significativas (valor de $P < 0,05$) en los niveles de expresión del gen *DcGH3.1* entre las variedades *2101–02 MFR* y *2003 R 8*, que se correlacionan con unos mayores niveles de AIA conjugado con ácido aspártico en la región basal de los esquejes en la variedad *2003 R 8* tras la escisión y durante el enraizamiento (véanse las figuras 4B y 4E del segundo artículo en la pág. 87). Estos resultados sugieren que la menor capacidad de enraizamiento adventicio que muestran los esquejes de la variedad *2003 R 8* podría deberse a una

inactivación rápida del AIA en la base del esqueje debido a una mayor actividad de las enzimas GH3 en este tejido. Para demostrar experimentalmente nuestra hipótesis, hemos llevado a cabo experimentos de inhibición competitiva de las enzimas GH3 utilizando 10 µM de adenosina–5'–[2–(1H–indol–3–il)etil] fosfato [109]. Con ello, nuestros resultados indican que la inactivación de las enzimas GH3 en la variedad *2003 R 8* incrementa de manera significativa (valor de $P < 0,05$) la formación de raíces adventicias en la base del esqueje (véase la figura 5 del segundo artículo en la pág. 88). Se había observado previamente que los niveles de las formas conjugadas de AIA en la base de los esquejes de guisante se incrementan con la edad de la planta madre [110], lo que podría explicar la disminución observada en la formación de raíces adventicias en esquejes obtenidos de plantas más viejas. De forma paralela, también hemos confirmado que la inactivación de la actividad GH3 igualmente mejora el enraizamiento en otras variedades de clavel, como la *2441–7 R*.

Tal como se había determinado previamente en el laboratorio [105], existe una variabilidad morfológica sustancial en los esquejes recolectados de las plantas madre de *2101–02 MFR* y *2003 R 8* durante la temporada de producción debido a las fluctuaciones en las condiciones ambientales en el invernadero (véase la figura 1A del tercer artículo en la pág. 109). Por otro lado, la capacidad de enraizamiento de los esquejes en la variedad *2003 R 8* es muy heterogénea y está influenciada negativamente por las altas temperaturas que se alcanzan durante la época estival. Los esquejes de la variedad *2101–02 MFR*, con una estructura más compacta de los esquejes y un rápido desarrollo de su sistema radicular adventicio, responden de manera más eficiente al estrés hídrico causado por las elevadas temperaturas estivales (véanse las figuras 1B–1D del tercer artículo en la pág. 109). Con objeto de determinar las bases genéticas de la variación observada en la capacidad de enraizamiento entre distintas variedades de

clavel cultivado [106] y aprovechando la existencia de herramientas moleculares en algunas de estas variedades [29], hemos llevado a cabo un cruzamiento entre plantas *2101–02 MFR* y *2003 R 8*. De las 159 líneas F_1 que se establecieron finalmente, 33 procedían de la autofecundación de plantas *2101–02 MFR* (que se utilizaron como receptoras de polen tras su emasculación) y 126 eran híbridos entre ambos parentales. Estos resultados son consistentes con el efecto deletéreo de la consanguinidad en las variedades comerciales de clavel cultivado [111]. Hemos cuantificado la variabilidad morfológica en los esquejes durante el enraizamiento para cinco parámetros de la parte vegetativa y otros siete de la arquitectura radicular (véase la tabla 1 del tercer artículo en la pág. 110). Tres de las líneas F_1 estudiadas (*L107*, *L240* y *L245*) presentaron una respuesta de enraizamiento adventicio (RR_20) muy baja (<10%). Hemos determinado que tres componentes principales o PC (*principal components*) explicarían alrededor del 97% de la varianza observada, siendo dependientes del grosor radicular y del número de raíces (PC1) o del área del sistema radicular (PC2), entre otros parámetros (véase la figura suplementaria S2B del tercer artículo en la pág. 130). Además, en nuestro estudio, el diámetro promedio medido en las raíces adventicias contribuye sustancialmente (~10%) a la variación fenotípica observada (PC3). Hemos llevado a cabo estudios comparativos entre dos subpoblaciones F_1, la resultante de la autofecundación de *2101–02 MFR* y la población híbrida, respectivamente. En ambos casos se observó la presencia de fenotipos transgresivos, lo que indica la combinación de alelos favorables o desfavorables en la F_1 debido a la segregación de alelos (véase la figura 3 del tercer artículo en la pág. 111). De hecho, todas las variedades comerciales de clavel son híbridas [111], por lo que su autofecundación incrementa la variabilidad genotípica de sus descendientes. Como era esperable, la población F_1 híbrida, la derivada del cruzamiento entre los parentales *2101–02 MFR* y *2003 R 8*, presentó un mayor rango de variación

en parámetros relevantes como el área del sistema radicular adventicio (RA_20) o el diámetro medio de las raíces adventicias (ARD_20).

En un segundo experimento estudiamos las 26 líneas de la subpoblación F_1 híbrida que presentaron los valores extremos en los parámetros de enraizamiento adventicio más relevantes, observando una enorme influencia de los factores ambientales sobre estos parámetros en alguno de estos genotipos. A continuación, se seleccionaron para análisis posteriores las ocho líneas F_1 que mostraron los valores extremos con una menor influencia ambiental (véase la figura suplementaria S3A del tercer artículo en la pág. 131). Hemos estimado la heredabilidad en sentido amplio (H^2) para los distintos caracteres analizados, con valores de H^2 comprendidos entre 0,53 para ARD_20 y 0,88 para el estadio radicular (RS_20) (véase la figura suplementaria S3B del tercer artículo en la pág. 131). En un tercer experimento se analizaron cinco parámetros relevantes de la parte vegetativa y nueve del sistema radicular adventicio durante el enraizamiento (véase la tabla 2 del tercer artículo en las págs. 113–114). Dos de estas líneas, *L192* y *L245*, presentaron valores inferiores a los de la variedad *2003 R 8* en todos los descriptores de la capacidad de enraizamiento adventicio. Otras tres líneas, *L162*, *L214*, y *L216*, mostraron valores superiores a los de la variedad *2101–02 MFR* en el área del sistema radicular adventicio. De todas las líneas analizadas, la *L062* presentó los valores más elevados en todos los descriptores de la capacidad de enraizamiento adventicio (véase la figura 6B del tercer artículo en la pág. 116). Hemos estudiado también algunos parámetros ecofisiológicos de los esquejes durante su enraizamiento. Los parámetros relevantes de la arquitectura del sistema radicular adventicio, como la longitud, el diámetro y el área, determinan la capacidad de las plantas para adquirir agua y nutrientes, y son clave para limitar la pérdida de agua en condiciones de estrés hídrico [112, 113]. Hemos identificado una correlación clave entre el desarrollo de un sistema radicular adventicio funcional, estimado por el

parámetro RA_40, y el equilibrio hídrico adecuado en la parte vegetativa del esqueje, que determina su potencial de crecimiento. En un estudio reciente realizado en trigo se ha determinado que el diámetro radicular contribuye de manera directa a la tolerancia en condiciones de déficit de fosfato, ya que incrementa el volumen efectivo de suelo en contacto con las raíces [114]. Nuestros resultados previos con un número limitado de genotipos, sugerían que el diámetro medio de las raíces adventicias estaba correlacionado negativamente con la capacidad de enraizamiento [106], mientras que nuestros resultados actuales apuntarían en la dirección contraria. Se requieren, por tanto, experimentos adicionales para determinar si el diámetro medio de las raíces adventicias debe incluirse como un factor positivo o negativo del enraizamiento adventicio durante la selección genética de las nuevas variedades de clavel cultivado.

Por otra parte, hemos caracterizado el perfil hormonal en la base de los esquejes durante el enraizamiento en estas ocho líneas F_1 y en sus parentales, *2101–02 MFR* y *2003 R 8* (véase la figura 7 del tercer artículo en la pág. 117). Se observó que los niveles de la citoquinina *trans*–zeatina se incrementaron considerablemente durante el almacenamiento de los esquejes en condiciones de baja temperatura, aunque no se encontró ninguna correlación evidente de este parámetro con la capacidad de enraizamiento adventicio de las líneas F_1 analizadas. En línea con nuestros resultados previos [115], hemos encontrado niveles bajos de AIA conjugado con ácido aspártico en el momento de la recolección de los esquejes y un aumento significativo tras el periodo de almacenamiento en frío. Cabe destacar que los valores extremos y opuestos de este metabolito encontrados en las líneas *L062* y *L245* confirman la importancia de la inactivación del AIA mediada por las enzimas GH3 en la regulación de la actividad auxínica durante el enraizamiento de esquejes de clavel [115]. En el futuro se tiene previsto llevar a cabo experimentos adicionales con el inhibidor de la actividad GH3 en la línea *L245* para confirmar nuestras

observaciones. A nivel global, observamos que los niveles del precursor de etileno, el 1−aminociclopropano−1−carboxílico (ACC), fueron más elevados en la base de los esquejes tras el almacenamiento en frío en aquellas variedades que presentaron posteriormente una mayor capacidad de enraizamiento, como *L062*, *L162* y *L216*. Estos resultados podrían ser consistentes con una mayor producción de etileno tras el trasplante de los esquejes y durante el enraizamiento. En esquejes de *Vigna radiata*, la aplicación exógena de etileno promovió la formación de raíces adventicias [116]. Además, existen evidencias adicionales de la interacción directa y positiva entre el etileno y el transporte de auxinas durante la formación de raíces adventicias en otras especies vegetales como el tomate [79] o *Arabidopsis thaliana* [82].

2.2.3 Micropropagación de argán

En este trabajo hemos desarrollado un procedimiento para la germinación *in vitro* de semillas de argán en un medio suplementado con 0,1 mg/L de ácido giberélico GA_3, que redujo considerablemente la dormancia de las semillas, a la vez que incrementó su porcentaje de germinación hasta un 90% a los 30 días. En condiciones naturales, las semillas de argán se encuentran protegidas por una cáscara muy gruesa para evitar su deshidratación (véase la figura 1D del cuarto artículo en la pág. 163), y para su germinación necesitan pasar por un cierto tiempo a temperaturas elevadas o atravesar el tracto digestivo de rumiantes [117]. Para inducir la formación de raíces laterales en plántulas germinadas *in vitro* se eliminó quirúrgicamente el ápice de la raíz principal, y las plántulas se mantuvieron en cultivo controlado durante tres semanas adicionales. A continuación, se transfirieron éstas a un medio suplementado con 0,5 mg/L de la citoquinina sintética thidiazurón para inducir la formación de yemas adicionales tras el corte de la yema principal del tallo. Después de otras tres semanas de incubación en este medio, se observó un incremento

significativo (valor de $P < 0,05$) del número medio de yemas que habían elongado. Es factible en este punto, tras la separación quirúrgica de estas yemas elongadas de la plántula madre, mantener las plántulas en el medio con thidiazurón para la producción continua de yemas axilares y su uso como microesquejes para su propagación vegetativa. Los microesquejes se incubaron en un medio suplementado con 1,0 mg/L de dos auxinas sintéticas, el ácido 1–naftalenacético y el ácido indol–3–butírico, para inducir la formación de raíces adventicias. A los 20 días de incubación en este medio, se observó la formación de tejido calloso en la base de los microesquejes como consecuencia de la proliferación de los tejidos vasculares internos en respuesta a las auxinas presentes en el medio. A continuación, se transfirieron los microesquejes de entre 20 y 25 mm de longitud a un medio suplementado con 1,0 mg/L de GA_3, lo que indujo la elongación de los primordios radiculares que ya estaban preformados en el callo. Después de 15 días en este medio, el 100% de los explantes presentaron 4,9 ± 3,6 raíces adventicias. La aclimatación de las plántulas de argán producidas *in vitro* en una cámara de crecimiento con condiciones ambientales controladas durante cuatro semanas contribuyo a la elevada tasa de supervivencia en condiciones de invernadero. Con este nuevo protocolo para la micropropagación de argán que hemos desarrollado en nuestro laboratorio (véase el resumen gráfico del cuarto artículo en la pág. 143), estimamos que en un período de unos cinco o seis meses, sería posible obtener entre 40 y 50 microesquejes enraizados a partir de una única semilla. A su vez, cada uno de estos microesquejes primarios podría usarse como una plántula madre inicial para producir microesquejes secundarios. De esta manera, en un año se podrían producir entre 1.600 y 2.000 plántulas clonales de argán por cultivo *in vitro* y libres de patógenos a partir de un genotipo único.

El enraizamiento de esquejes lignificados de argán es un proceso muy complejo que depende de factores tanto endógenos como ambientales, lo

que dificulta su aplicación práctica para la producción comercial de cultivares élite en esta especie [118]. En un trabajo reciente se caracterizó la recuperación de plantas de argán tras un período de sequía, concluyendo que el crecimiento radicular se mantiene activo durante el período de estrés y se mejora la conductividad hidráulica tras una corta rehidratación tras la sequía, lo que sugiere una respuesta fisiológica radicular adaptativa relacionada con una estrategia de tolerancia a la falta de agua en esta especie [119]. Este mecanismo adaptativo sería susceptible de posteriores investigaciones dirigidas a la mejora del enraizamiento en esquejes leñosos de argán.

Nuestros resultados indican que la adición, en la base del esqueje, de una mezcla en polvo al 0,4% peso/peso de ácido 1–naftalenacético y ácido indol–3–butírico sin tratamiento líquido previo con auxinas incrementó significativamente (valor de $P < 0,05$) el porcentaje de enraizamiento a los tres meses hasta un 43% (véase la figura 6 del cuarto artículo en la pág. 168). En su área de distribución nativa, el argán desempeña una importante función por su contribución a la economía local y al mantenimiento de las condiciones edáficas favorables en las zonas semiáridas. La propagación natural del argán está limitada por una producción reducida de semillas y por ser árboles de crecimiento lento [32]. Se ha propuesto que el cultivo *in vitro* es una técnica útil para la producción en masa de especies oleaginosas [120] y representa un paso fundamental hacia la conservación *ex situ* de los genotipos de interés. En su conjunto, nuestros resultados establecen nuevos procedimientos eficientes para la propagación clonal de individuos altamente productivos, lo que contribuirá a reducir la brecha en los métodos de propagación vegetativa en esta especie.

2.3 Bibliografía

93. **Togninalli, M., Seren, Ü., Meng, D., Fitz, J., Nordborg, M., Weigel, D., Borgwardt, K., Korte, A., Grimm, D.G.** (2017). The AraGWAS Catalog: a curated and standardized *Arabidopsis thaliana* GWAS catalog. *Nucleic Acids Res* **46**: D1150–D1156

94. **The 1001 Genomes Consortium** (2016). 1,135 genomes reveal the global pattern of polymorphism in *Arabidopsis thaliana*. *Cell* **166**: 481–491

95. **Seren, Ü.** (2018). GWA-Portal: Genome-Wide Association Studies made easy. *Root Development, Humana Press, NY* 303–319

96. **Moreno-Risueno, M.A., Van Norman, J.M., Moreno, A., Zhang, J., Ahnert, S.E., Benfey, P.N.** (2010). Oscillating gene expression determines competence for periodic Arabidopsis root branching. *Science* **329**: 1306–311

97. **Sheng, L., Hu, X., Du, Y., Zhang, G., Huang, H., Scheres, B., Xu, L.** (2017). Non-canonical WOX11-mediated root branching contributes to plasticity in Arabidopsis root system architecture. *Development* **144**: 3126–3133

98. **Koevoets, I.T., Venema, J.H., Elzenga, J.T., Testerink, C.** (2016). Roots withstanding their environment: exploiting root system architecture responses to abiotic stress to improve crop tolerance. *Front Plant Sci* **7**: 1335

99. **Bao, Y., Aggarwal, P., Robbins, N.E., Sturrock, C.J., Thompson, M.C., Tan, H.Q., Tham, C., Duan, L., Rodríguez, P.L., Vernoux, T., Mooney, S.J., Bennet, M.J., Dinneny, J.R.** (2014). Plant roots use a patterning mechanism to position lateral root branches toward available water. *Proc Natl Acad Sci USA* **111**: 9319–9324

100. **Mukhtar, M.S., Carvunis, A.R., Dreze, M., Epple, P., Steinbrenner, J., Moore, J., Tasan, M., Galli, M., Hao, T., Nishimura, M.T., Pevzner , S.J., Donovan, S.E., Ghamsari, L., Santhanam, B., Romero, V., Poulin, M.M., Gebreab, F., Gutiérrez, B.J., Tam, S., Monachello, D., Boxem, M., Harbort, C.J., McDonald, N., Gai, L., Chen, H., He, Y., Vandenhaute, J., Roth, F.P., Hill, D.E, Ecker, J.R., Vidal, M., Beynon, J., Braun, P., Dangl, J.L.** (2011). Independently evolved virulence effectors converge onto hubs in a plant immune system network. *Science* **333**: 596–601

101. **Osakabe, Y., Arinaga, N., Umezawa, T., Katsura, S., Nagamachi, K., Tanaka, H., Ohiraki, H., Yamada, K., Seo, S.U., Abo, M., Yoshimura, E., Shinozaki, K., Yamaguchi-Shinozaki, K.** (2013). Osmotic stress responses and plant growth controlled by potassium transporters in Arabidopsis. *Plant Cell* **25**: 609–624

102. **Ruffel, S., Poitout, A., Krouk, G., Coruzzi, G.M., Lacombe, B.** (2016). Long-distance nitrate signaling displays cytokinin dependent and independent branches. *J Integr Plant Biol* **58**: 226–229

103. **Brenner, W.G., Ramireddy, E., Heyl, A., Schmülling, T.** (2012). Gene regulation by cytokinin in Arabidopsis. *Front Plant Sci* **3**: 8

104. **Nam, Y.J., Tran, L.S.P., Kojima, M., Sakakibara, H., Nishiyama, R., Shin, R.** (2012). Regulatory roles of cytokinins and cytokinin signaling in response to potassium deficiency in Arabidopsis. *PLoS One* **7**: e47797

105. **Villanova, J., Cano, A., Albacete, A., López, A., Cano, E.Á., Acosta, M., Pérez-Pérez, J.M.** (2017). Multiple factors influence adventitious rooting in carnation (*Dianthus caryophyllus* L.) stem cuttings. *Plant Growth Regul* **81**: 511–521

106. **Birlanga, V., Villanova, J., Cano, A., Cano, E.A., Acosta, M., Pérez-Pérez, J.M.** (2015). Quantitative analysis of adventitious root growth phenotypes in carnation stem cuttings. *PLoS One* **10**: e0133123

107. **Ludwig-Müller, J.** (2011). Auxin conjugates: their role for plant development and in the evolution of land plants. *J Exp Bot* **62**: 1757–1773

108. **Porco, S., Pěnčík, A., Rashed, A., Voß, U., Casanova-Sáez, R., Bishopp, A., Golebiowska, A., Bhosale, R., Swarup, R., Swarup, K., Peňáková, P., Novák, O., Staswick, P., Hedden, P., Phillips, A.L., Vissenberg, K., Bennett, M.J., Ljung, K.** (2016). Dioxygenase-encoding AtDAO1 gene controls IAA oxidation and homeostasis in Arabidopsis. *Proc Natl Acad Sci USA* **113**: 11016–11021

109. **Böttcher, C., Dennis, E.G., Booker, G.W., Polyak, S.W., Boss, P.K., Davies, C.** (2012). A novel tool for studying auxin-metabolism: the inhibition of grapevine indole-3-acetic acid-amido synthetases by a reaction intermediate analogue. *PloS One* **7**: e37632

110. **Rasmussen, A., Hosseini, S.A., Hajirezaei, M.R., Druege, U., Geelen, D.** (2015). Adventitious rooting declines with the vegetative to reproductive switch and involves a changed auxin homeostasis. *J Exp Bot* **66**: 1437–1452

111. **Onozaki, T.** (2018). Breeding of carnations (*Dianthus caryophyllus* L.) for long vase life. *Breeding science* **68**: 3–13

112. **Dodd, I.C., Puértolas, J., Huber, K., Pérez-Pérez, J.G., Wright, H.R., & Blackwell, M.S.** (2015). The importance of soil drying and re-wetting in crop phytohormonal and nutritional responses to deficit irrigation. *J Exp Bot* **66**: 2239–2252

113. **Franco, J.A., Bañón, S., Vicente, M.J., Miralles, J., Martínez-Sánchez, J.J.** (2011). Root development in horticultural plants grown under abiotic stress conditions–a review. *J Hortic Sci Biotech* **86**: 543–556

114. **Wu, F., Yang, X., Wang, Z., Deng, M., Ma, J., Chen, G., Wei, Y., Liu, Y.** (2017). Identification of major quantitative trait loci for root diameter in synthetic hexaploid wheat under phosphorus-deficient conditions. *J Appl Genet* **58**: 437–447

115. **Cano, A., Sánchez-García, A.B., Albacete, A., González-Bayón, R., Justamante, M.S., Ibáñez, S., Acosta, M., Pérez-Pérez, J.M.** (2018). Enhanced conjugation of auxin by GH3 enzymes leads to poor adventitious rooting in carnation stem cuttings. *Front Plant Sci* **9**: 566

116. **de Klerk, G.J., Hanecakova, J.** (2008). Ethylene and rooting of mung bean cuttings. The role of auxin induced ethylene synthesis and phase-dependent effects. *Plant Growth Regul* **56**: 203

117. **Al-Menaie, H.S., Bhat, N.R., El-Nil, M.A., Al-Dosery, S.M., Al-Shatti, A.A., Gamalin, P., Suresh, N.** (2007). Seed germination of argan (*Argania spinosa* L.). *Amer-Eurasian J Sci Res* **2**: 1–4

118. Ferradous, A., Alifriqui, M., Bellefontaine, R. (2013). Optimisation des techniques de bouturage sous mist chez l'arganier. *AGRIS*

119. Chakhchar, A., Chaguer, N., Ferradous, A., Filali-Maltouf, A., El Modafar, C. (2018). Root system response in *Argania spinosa* plants under drought stress and recovery. *Plant Signal Behav* **13**: e1489669

120. Mangal, M., Sharma, D., Sharma, M., Kumar, S. (2014). *In vitro* regeneration in olive (*Olea europaea* L.) cv,'Frontio'from nodal segments. *Indian J Exp Biol* **52**: 912–916

Capítulo 3

Conclusiones y proyección futura

3. CONCLUSIONES Y PROYECCIÓN FUTURA

3.1 Conclusiones

- Hemos caracterizado cuatro parámetros de la arquitectura radicular tras la eliminación del ápice de la raíz primaria en una colección de 174 estirpes silvestres de *Arabidopsis thaliana*.
- Hemos llevado a cabo un estudio de asociación a genoma completo con 120 de estas estirpes que nos ha permitido localizar 162 SNPs bialélicos asociados de manera estadísticamente significativa con la variación fenotípica observada.
- Se ha confirmado que el producto del gen At4g01090, que codifica una proteína de función desconocida y que interacciona con proteínas reguladoras del tráfico vesicular, se requiere para la formación de raíces laterales en respuesta a heridas.
- Nuestros resultados sugieren que la proteína codificada por At5g19710, presuntamente implicada en la señalización de las citoquininas, actuaría como un regulador negativo local de la formación de raíces laterales en respuesta a heridas, interfiriendo con la señal auxínica procedente de la cofia de la raíz principal.
- Hemos encontrado una interacción epistática entre los SNPs de la región codificante de K^+ *UPTAKE TRANSPORTER 5* (*KUP5*), cuyo producto participa en la asimilación del potasio, y At5g19710, lo que apuntaría a una relación funcional entre ambos procesos y con la formación de raíces laterales en respuesta a heridas.
- Hemos proporcionado evidencias moleculares de que la baja capacidad de enraizamiento adventicio de los esquejes en la estirpe *2003 R 8* se debe a una inactivación temprana de la auxina activa, el ácido indol–3–acético, en la base del esqueje mediante su conjugación con

ácido aspártico, por enzimas de la familia GRETCHEN HAGEN 3 (GH3).

- Hemos llevado a cabo un análisis detallado de la formación de raíces adventicias a partir de esquejes en una colección de 159 líneas F_1 de clavel cultivado derivadas del cruzamiento entre dos variedades comerciales, *2101–02 MFR* y *2003 R 8*, que difieren de forma significativa en su capacidad de enraizamiento adventicio.
- En un segundo experimento estudiamos las 26 líneas de la subpoblación F_1 híbrida que presentaron los valores extremos en los parámetros de enraizamiento más relevantes, observando una gran influencia de los factores ambientales sobre estos parámetros en algunos genotipos.
- Hemos caracterizado el perfil hormonal en la base de los esquejes durante el enraizamiento de ocho líneas F_1 y en sus parentales, *2101–02 MFR* y *2003 R 8*. Los valores extremos y opuestos de AIA conjugado con ácido aspártico encontrados en las líneas *L062* y *L245* confirman la importancia de la inactivación del AIA por enzimas GH3 en la regulación de la actividad de las auxinas durante el enraizamiento en clavel.
- Los niveles del precursor de etileno, el 1–aminociclopropano–1–carboxílico, fueron más elevados en la base de los esquejes tras el almacenamiento en frío en aquellas variedades que presentaron una mayor capacidad de enraizamiento.
- Hemos desarrollado un nuevo procedimiento para la propagación vegetativa del argán a partir de semillas germinadas *in vitro* que permitiría la producción anual de entre 1.600 y 2.000 plántulas clonales de argán libres de patógenos a partir de un genotipo único.
- Hemos desarrollado un protocolo para el enraizamiento adventicio de esquejes lignificados obtenidos de plantas adultas de argán que podría aplicarse para la propagación clonal de individuos altamente productivos.

3.2 Proyección futura

En relación al estudio de GWA sobre la arquitectura radicular tras la eliminación del ápice de la raíz primaria en *Arabidopsis thaliana*, tenemos prevista la caracterización funcional de los SNPs adicionales localizados en dos genes que hasta ahora no habíamos estudiado, mediante la caracterización fenotípica y molecular de alelos mutantes de pérdida y de ganancia de función en estos genes. Adicionalmente, se llevarán a cabo experimentos que permitan confirmar nuestra hipótesis de que la proteína codificada por el gen At4g01090 se requiere para el posicionamiento subcelular adecuado de los transportadores de auxina de la familia PIN–FORMED durante la formación de raíces laterales en respuesta a heridas. Por último, se podrían utilizar las estirpes naturales que mostraron fenotipos antagónicos y extremos en su arquitectura radicular en respuesta a heridas como fundadoras de una nueva población de líneas MAGIC (*multiparent advanced generation inter–cross*) que podrá permitir la cartografía fina de los QTL que participan en la regulación de esta respuesta. Sin embargo, actualmente no disponemos de recursos humanos y económicos suficientes para mantener abierta esta línea de investigación.

La propagación vegetativa de las nuevas variedades de clavel cultivado que se están obteniendo en la empresa Dümmen Orange (Puerto Lumbreras, Murcia), dependen del adecuado desarrollo de un sistema radicular adventicio. Nuestros trabajos han contribuido a desentrañar algunos de los mecanismos fisiológicos que regulan la diversidad fenotípica observada entre los distintos cultivares de clavel, así como la modulación de estas respuestas por algunos factores ambientales, como el estrés hídrico causado por las altas temperaturas estivales en la zona de producción de los esquejes enraizados. Proponemos que la monitorización del contenido foliar de agua mediante técnicas de espectroscopía no invasiva podría utilizarse para predecir la capacidad de enraizamiento adventicio de los diferentes genotipos de clavel que se utilizan en los

programas de mejora genética de la empresa. Alternativamente, la disección molecular de los determinantes genéticos sería factible mediante la caracterización de los perfiles de expresión génica en aquellas líneas F_1 que mostraron una respuesta de enraizamiento extrema y opuesta, como *L192/L245* y *L214/L162/L062*. Desafortunadamente, la nueva dirección científica de la empresa Dümmen Orange ha congelado la colaboración existente con el laboratorio del profesor José Manuel Pérez Pérez, por lo que carecemos de acceso al material vegetal adecuado para continuar esta línea de investigación.

En su área de distribución nativa en Marruecos, el argán contribuye de manera significativa a la economía local y a la conservación del suelo de las regiones semiáridas donde se cultiva. A pesar de su importancia, se ha constatado un declive sustancial de las poblaciones nativas de esta especie, al tratarse de árboles con una tasa de reposición muy elevada. Los protocolos de trabajo que hemos desarrollado en este trabajo permiten llevar a cabo una propagación vegetativa eficiente, lo que permitirá, por un lado, la conservación *ex situ* de genotipos de argán con características agronómicas mejoradas (mayor producción, tolerancia a estreses ambientales, etc.) y, por otro, iniciar el cultivo intensivo de genotipos élite de argán en las regiones semiáridas del sureste español. Es nuestra intención buscar una colaboración empresarial para continuar el desarrollo experimental de esta línea de investigación.

Capítulo 4

Compendio de publicaciones

Artículo 1

A genome-wide association study identifies new loci required for wound-induced lateral root formation in *Arabidopsis thaliana*

María Salud Justamante[1], Sergio Ibáñez[1], Adrián Peidró[2], José Manuel Pérez-Pérez[1]

[1] Instituto de Bioingeniería, Universidad Miguel Hernández, 03202 Elche, Spain

[2] Departamento de Ingeniería de Sistemas y Automatización, Universidad Miguel Hernández de Elche, Elche, Spain

Frontiers in Plant Science 2019; 10: 311

Published online 15 Mar 2019. doi: 10.3389/fpls.2019.00311

FI (2018): 4,106 (D1; 20 de 228)

frontiers in Plant Science

ORIGINAL RESEARCH
published: 15 March 2019
doi: 10.3389/fpls.2019.00311

A Genome-Wide Association Study Identifies New Loci Involved in Wound-Induced Lateral Root Formation in *Arabidopsis thaliana*

*María Salud Justamante[1], Sergio Ibáñez[1], Adrián Peidró[2] and José Manuel Pérez-Pérez[1]**

[1] Instituto de Bioingeniería, Universidad Miguel Hernández de Elche, Elche, Spain, [2] Departamento de Ingeniería de Sistemas y Automatización, Universidad Miguel Hernández de Elche, Elche, Spain

Root systems can display variable architectures that contribute to nutrient foraging or to increase the tolerance of abiotic stress conditions. Root tip excision promotes the developmental progression of previously specified lateral root (LR) founder cells, which allows to easily measuring the branching capacity of a given root as regards its genotype and/or growth conditions. Here, we describe the natural variation among 120 *Arabidopsis thaliana* accessions in root system architecture (RSA) after root tip excision. Wound-induced changes in RSA were associated with 19 genomic loci using genome-wide association mapping. Three candidate loci associated with wound-induced LR formation were investigated. Sequence variation in the hypothetical protein encoded by the At4g01090 gene affected wound-induced LR development and its loss-of-function mutants displayed a reduced number of LRs after root tip excision. Changes in a histidine phosphotransfer protein putatively involved in cytokinin signaling were significantly associated with LR number variation after root tip excision. Our results provide a better understanding of some of the genetic components involved in LR capacity variation among accessions.

Keywords: wound-induced lateral root formation, root system architecture, genome-wide association mapping, single nucleotide polymorphism, natural variation, histidine phosphotransfer protein

OPEN ACCESS

Edited by:
Laurent Laplaze, Institut de Recherche pour le Développement (IRD), France

Reviewed by:
Magdalena Maria Julkowska, King Abdullah University of Science and Technology, Saudi Arabia
Boris Parizot, VIB-UGent Center for Plant Systems Biology, Belgium

****Correspondence:***
José Manuel Pérez-Pérez
jmperez@umh.es; arolab.edu.umh.es

Specialty section:
This article was submitted to Plant Development and EvoDevo, a section of the journal Frontiers in Plant Science

Received: *05 November 2018*
Accepted: *26 February 2019*
Published: *15 March 2019*

Citation:
Justamante MS, Ibáñez S, Peidró A and Pérez-Pérez JM (2019) A Genome-Wide Association Study Identifies New Loci Involved in Wound-Induced Lateral Root Formation in Arabidopsis thaliana. Front. Plant Sci. 10:311. doi: 10.3389/fpls.2019.00311

INTRODUCTION

Strong modulation of root system architecture (RSA) by environmental cues, such as nutrient and water availability has been a well-documented process in *Arabidopsis thaliana* (Giehl and von Wirén, 2014; Giehl et al., 2014; Robbins and Dinneny, 2015). In primary roots (PRs) (PRs), a regular pre-branching pattern of lateral roots (LRs) is established by an endogenous periodic oscillation in gene expression near the root tip (Moreno-Risueno et al., 2010). A subset of xylem pole pericycle cells within the pre-branch sites becomes specified as LR founder cells. Subsequently, LR founder cells undergo a self-organizing and non-deterministic cell division patterning (Lucas et al., 2013; von Wangenheim et al., 2016) to initiate a LR primordium that eventually emerges through the PR tissues (Peret et al., 2009; Du and Scheres, 2018). However, the developmental progression of individual LR primordia is dependent on environmental cues, such as water distribution within the soil (Bao et al., 2014). In addition, a local auxin source from the LR cap of the PR, which is

derived from the auxin precursor indole-3-butyric acid (IBA), determines whether a pre-branch site is specified or not (Xuan et al., 2015). The spatial distribution of LRs is not fixed, yet the total number of LR competent sites was stable with time. Root tip excision promotes the developmental progression of nearly all pre-branch sites toward LR emergence, providing an accurate measure for LR branching capacity. This later approach will allow assessing whether changes in LR pre-patterning have occurred in different genotypes and/or growth conditions (Van Norman et al., 2014). These results are in agreement with the current view that cells at the root tip are capable of integrating information about the local soil environment, tailoring the RSA for optimal nutrient and water uptake or after PR damage (Robbins and Dinneny, 2015).

Genome-wide association (GWA) studies have contributed to the identification of natural variation in key genes controlling PR growth under control and abiotic stress conditions (Meijon et al., 2014; Slovak et al., 2014; Satbhai et al., 2017; Bouain et al., 2018). Natural variation in RSA has also been reported (Rosas et al., 2013). Salt-induced changes in RSA were associated with more than 100 genetic loci identified by GWA mapping, some of which are involved in ethylene and abscisic acid (ABA) signaling (Julkowska et al., 2017). In addition, strong additive effects of phosphate starvation on LR density and salt stress on LR length were found in a recent study with a large number of Arabidopsis accessions (Kawa et al., 2016). Their results suggested that the integration of signals from phosphate starvation and salt stress might partially rely on endogenous ABA signaling. One of the candidate genes identified in these studies was *HIGH-AFFINITY K^+ TRANSPORTER1* (*HKT1*), previously identified for its role in salinity tolerance by modulating sodium/potassium homeostasis (Munns et al., 2012). The targeted HKT1 expression to pericycle cells reduced LR formation under salt stress (Julkowska et al., 2017). Recently, Ristova et al. (2018) reported a comprehensive atlas of RSA variation upon treatment with auxin, cytokinin (CK) and ABA in a large number of *A. thaliana* accessions. In that study, hierarchical clustering analyses identified groups of accessions sharing similar or diverse responses to a particular hormone perturbation that can be very useful to identify accessions that behave differently than the bulk and to use them as parents for QTL mapping.

To explore the natural variation of LR branching capacity in Arabidopsis (Van Norman et al., 2014), we performed a wound-induced LR formation assay in 174 accessions from the Haplotype Map (HapMap) collection (Weigel and Mott, 2009). GWA mapping using data from 120 accessions revealed 162 SNP associations with several RSA traits measured after root tip excision. SNPs affecting six genes were found significantly associated with LR number variation.

MATERIALS AND METHODS

Plant Materials and Growth Conditions

Our population for GWA mapping consisted of 174 natural inbred lines (i.e., accessions) of *A. thaliana* (L.) Heyhn. selected from the 1001 Genomes Project (Weigel and Mott, 2009) based on marker information and seed availability (**Supplementary Table S1**). The laboratory strain Columbia-0 (Col-0) was chosen as the reference. The following lines (in the Col-0 background) were used to isolate T-DNA homozygous mutants of the studied genes: N572850, N586312, N616200, and N620707 (**Supplementary Table S2**). The *ahp1 ahp2 ahp3* (Hutchison et al., 2006) mutants were also used. All lines used were obtained from the Nottingham Arabidopsis Stock Centre (NASC[1]). Seeds were stored at 4°C for several weeks (>12) to break dormancy.

Seeds were surface-sterilized in 2% (w/v) NaClO and rinsed with sterile water before being transferred to 120 mm × 120 mm × 10 mm Petri dishes containing 75 mL of one-half-Murashige & Skoog (MS) medium with 2% sucrose, 8 g/L plant agar (Duchefa Biochemie, Netherlands) and 1× Gamborg B5 vitamin mixture (Duchefa Biochemie). After 4 days of stratification at 4°C in darkness, plates were wrapped in aluminum foil and were transferred (0 days after sowing) to an MLR-352-PE growth chamber (Panasonic, Japan) at 22 ± 1°C during 3 days in a nearly vertical position. Plates were unwrapped (3 days after sowing) and grew during another 3 days with continuous light (50 $\mu mol \cdot m^{-2} \cdot s^{-1}$). For each accession, 12 seeds were sown per petri dish in triplicate (36 samples/line). Sixteen consecutive sowings including 11 accessions each were established. Additionally, Col-0 was also included in all the sowings to be used as the growth reference accession and for normalization purposes (**Supplementary Figure S1A**). Lines with germination percentage lower than 80% and with ambiguous marker information were discarded for further analysis (**Supplementary Table S1**).

Induction of Lateral Root Formation

To induce LR development during early seedling growth (Van Norman et al., 2014), we excised about 2 mm of the root tip using a sterile scalpel on a laminar flow hood at 6 days after sowing (**Figure 1A**). Next, samples were transferred back to the growth chamber and followed during 4 days for the analysis of several root traits as described below.

Image Processing and Parameter Measurement

Petri dishes were daily imaged from 6 to 10 days after sowing using an Epson Perfection V330 Photo scanner (Seiko Epson Corporation, Nagano, Japan), at a resolution of 600 dpi, and saved as RGB color images in JPEG file format. Scanned images were processed using EZ-Rhizo (Armengaud et al., 2009) with available plug-in macros to convert them into binary images, remove noise, gap-filling, and skeletonize them prior to automated root detection (**Supplementary Figures S1B–S1E**). PR length was directly obtained from the EZ-Rhizo output files from scanned images of 6 days after sowing. A highly significant and positive correlation was found for PR length estimated by EZ-Rhizo and directly measured by ImageJ software[2] from hand-drawn roots (**Supplementary Figure S1F**). LR number was visually counted from the scanned images between 6 and 10 days after sowing.

[1] http://arabidopsis.info/

[2] http://rsb.info.nih.gov/ij/

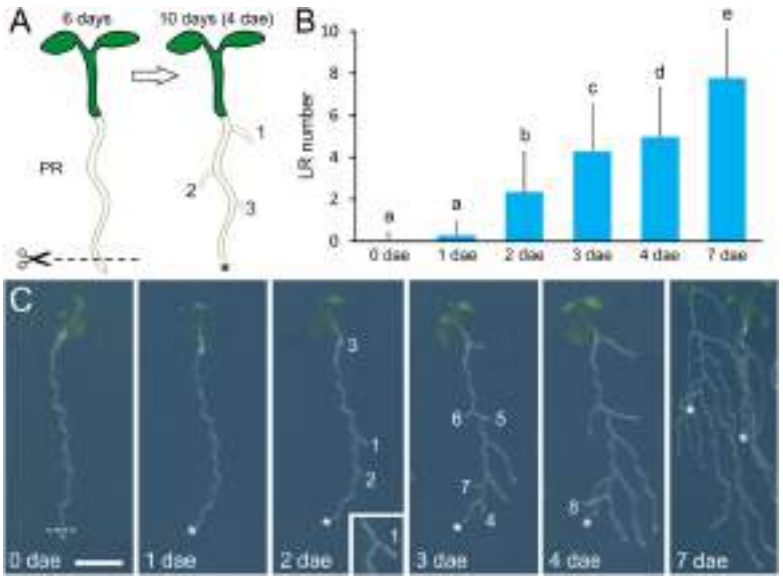

FIGURE 1 | Wound-induced lateral root (LR) development. **(A)** Schematic representation of LR induction by root tip excision (the excision site is indicated by the scissors). dae, days after excision; PR, primary root. **(B)** Average LR number observed in the Columbia-0 (Col-0) reference accession after root tip excision. Different letters indicate significant differences (LSD, *P*-value < 0.01). **(C)** Time course of LR development in Col-0 after root tip excision. Scale bar: 5 mm. Numbers in **(A,C)** indicate order of LR emergence (1, first; 2, second; etc.). Asterisks mark the PR tips after excision.

LR emergence onset corresponds to the day when the first newly emerged LR was visible. LR density was estimated at 8 and 10 days after sowing by the LR number/PR length ratio. Data values were normalized relative to Col-0 values in each sowing dividing each individual value by the Col-0 average (**Supplementary Table S3**).

Statistical Analyses and Heritability Estimation

Statistical analyses of the data was performed by using StatGraphics Centurion XV (StatPoint Technologies, United States) and SPSS 21.0.0 (SPSS Inc., United States) software packages. Data outliers were identified based on aberrant standard deviation values and were excluded for posterior analyses as described elsewhere (Aguinis et al., 2013). One-sample Kolmogorov–Smirnov tests were performed to analyze the goodness-of-fit between the distribution of the data and a theoretical normal distribution. Non-parametric tests and data transformation were applied when needed. To compare the data for a given variable, we performed multiple testing analyses with the ANOVA F-test or the Fisher's LSD (Least Significant Differences) methods. Significant differences were collected with 5% level of significance (*P*-value < 0.05) unless otherwise indicated.

The broad-sense heritability (H^2) for the studied dataset was calculated as $H^2 = \sigma_G{}^2/(\sigma_G{}^2 + \sigma_{GE}{}^2/e + \sigma^2{}_e 2/re)$, in which $\sigma_G{}^2$, $\sigma_{GE}{}^2$, $\sigma_e{}^2$, r, and e represent the estimated variances for the genetic effects, genotype-environment interactions, random errors, number of replications (12) and number of environments (three), respectively. The estimated variances for $\sigma_G{}^2$, $\sigma_{GE}{}^2$, and $\sigma_e{}^2$ were obtained by ANOVA using normalized data values as regards to the Col-0 reference accession from 106 of the studied lines.

Population Structure Analysis

The population structure of the selected accessions was estimated using the Bayesian model-based clustering algorithm (Porras-Hurtado et al., 2013) implemented in Structure v2.3.4 software[3] (Falush et al., 2003). To this end, we used a collection of 319 randomly selected bi-allelic synonymous (likely evolutionary-neutral) SNP markers from available sequence data (Atwell et al., 2010; Cao et al., 2011; Seren et al., 2012). An in-house Matlab script (**Supplementary Table S4**) was used for single nucleotide polymorphism (SNP) data selection and file formatting. Structure analysis was performed for $K = 1$ to $K = 10$ clusters with 20 replicates and 50,000 burn-in period iterations, followed by 50,000 Markov chain Monte Carlo iterations while using a population admixture ancestry model. To determine the most likely number of subpopulations (K) we applied the ΔK method, as described elsewhere (Evanno et al., 2005).

[3]https://web.stanford.edu/group/pritchardlab/structure.html

Genome-Wide Association Studies

Genome-wide association mapping was performed using the GWAPP web interface[4], which contains genotypic information for up to 250,000 bi-allelic SNP markers (Seren et al., 2012). GWAS was conducted for the studied traits using the linear regression model (LM) to identify associations between the phenotype of 120 studied accessions and the 205,978 SNPs available in the database. Relative LR numbers were transformed using the $y = \sqrt{x}$ function to fit the theoretical normal distribution. Association mapping was obtained excluding from the analyses all SNPs with a frequency <0.12. SNPs with a $-\log_{10}(P\text{-value}) > 6.5$ were considered significantly associated to the studied trait (**Supplementary Table S5**). Manhattan plots, representing the genomic position of each SNP and its association $[-\log_{10}(P\text{-value})]$ with the studied trait, were downloaded from the GWAPP web interface. We analyzed the sampling bias on GWAS by systematically removing one or several geographically isolated accessions and found that it did not make any difference to the detected SNP associations (**Supplementary Table S6**). We selected non-synonymous SNPs with a $-\log_{10}(P\text{-value}) > 6.5$ (P-value = 3.16×10^{-7}) for further studies.

Genotyping

Seedlings with T-DNA homozygous insertions in the annotated genes were identified by PCR verification with T-DNA specific primers and a pair of gene-specific primers (**Supplementary Table S2**). Genomic DNA isolation and genotyping of T-DNA insertion loci PCR were performed as described elsewhere (Pérez-Pérez et al., 2004).

Gene Expression Analysis by Real-Time Quantitative PCR

Primers amplified 81–178 bp of the cDNA sequences (**Supplementary Table S2**). To avoid amplifying genomic DNA, forward and reverse primers bound different exons and hybridized across consecutive exons.

RNA extraction and cDNA synthesis were performed as described elsewhere (Villacorta-Martín et al., 2015). For real-time quantitative PCR, 14 μl reactions were prepared with 7 μl of the SsoAdvanced Universal SYBR Green Supermix (Bio-Rad, United States), 4 μM of specific primer pairs, and 1 μl of cDNA- and DNase-free water (up to 14 μl of total volume reaction). PCR amplifications were carried out in 96-well optical reaction plates on a Step One Plus Real-Time PCR System (Applied Biosystems, United States). Three biological and two technical replicates were performed for each gene. The thermal cycling program started with a step of 10 s at 95°C, followed by 40 cycles (15 s at 95°C and 60 s at 60°C), and the melt curve (from 60 to 95°C, with increments of 0.3°C every 5 s). Dissociation kinetics of the amplified products confirmed their specificity.

Primer validation and gene expression analyses were performed by the absolute quantification method (Lu et al., 2012) by using a standard curve that comprised equal amounts from each cDNA sample. The housekeeping At4g26410 gene (*RGS1-HXK1 INTERACTING PROTEIN 1*, *RHIP1*) (Czechowski et al., 2005) was chosen as an internal control and to ensure reproducibility. In each gene, the mean of fold-change values relative to the Col-0 reference genotype was used for graphic representation. Relative expression values were analyzed using SPSS 21.0.0 (SPSS Inc., United States) by applying the Mann–Whitney U-test for statistical differences between cDNA samples (P-value < 0.05).

[4]http://gwas.gmi.oeaw.ac.at

RESULTS

Natural Variation of Wound-Induced Lateral Root Formation

To validate our experimental approach (**Figure 1A**), we studied wound-induced LR formation in Columbia-0 (Col-0) during 7 days. PR length remained almost invariable after root tip excision during the whole experiment (**Supplementary Figure S1G**). The new LRs were already visible at 1 day after PR tip excision (1 dae) and reached 4.97 ± 2.36 (n = 467) LRs at 4 dae (**Figure 1B**). At 7 dae, the number of LRs slightly increased but it was not possible to measure it unambiguously due to overlap between the LRs of adjacent seedlings (**Figures 1B,C**). We did not observe a clear spatial pattern of LR emergence from the PRs except that, in all cases, the new LRs emerged from its convex side (**Figure 1C**, inset). We found a slight variation in PR length and LR number between the different sowings (**Supplementary Figures S2A,B**), which might be caused by subtle environmental differences at the growth chamber.

We studied wound-induced LR formation in a collection of 173 additional accessions selected from the 1001 Genomes Project (Weigel and Mott, 2009; **Supplementary Table S1**). In 34 of the studied accessions, the germination percentage at 6 days after sowing was lower than 80% and were discarded for further analysis; other 20 accessions were also discarded because of ambiguous genotypes at the GWAPP web interface (Seren et al., 2012) (**Supplementary Table S1**). We found variation in all the studied traits (**Supplementary Figure S2B**). Exceptionally, one or two LRs were observed before root tip excision (0 dae) in some samples, but these were not considered. The broad-sense heritability (H^2) was calculated for each of the studied traits (see section "Materials and Methods"). Heritability estimates ranged between 0.90 (LR emergence onset and LR density) and 0.95 (LR number). Broad-sense heritability for PR length was 0.93. Interestingly, we found a positive and significant correlation between LR number and PR length at 4 dae (r = 0.83; **Figure 2A**), as well as a negative and significant correlation between LR number at 4 dae and LR emergence onset (r = −0.69; **Figure 2B**). LR number ranged from 1.38 ± 0.82 in Ru3.1-31 (PR length: 0.28 ± 0.07 cm; n = 24) and 9.42 ± 4.84 in Kidr-1 (PR length: 1.90 ± 0.50 cm; n = 24). Hence, reduced LR number in Ru3.1-31 compared to Kidr-1 was likely caused by its reduced PR length. Some accessions, such as Leo-1 and Voeran-1 displayed contrasting phenotypes as regards their LR number (7.07 ± 1.41 and 3.14 ± 1.48 LRs, respectively; n = 29) although they displayed similar PR lengths (**Figures 2A,C**). On the other hand, Leo-1 and Aitba-2 displayed similar LR number which were larger in Leo-1

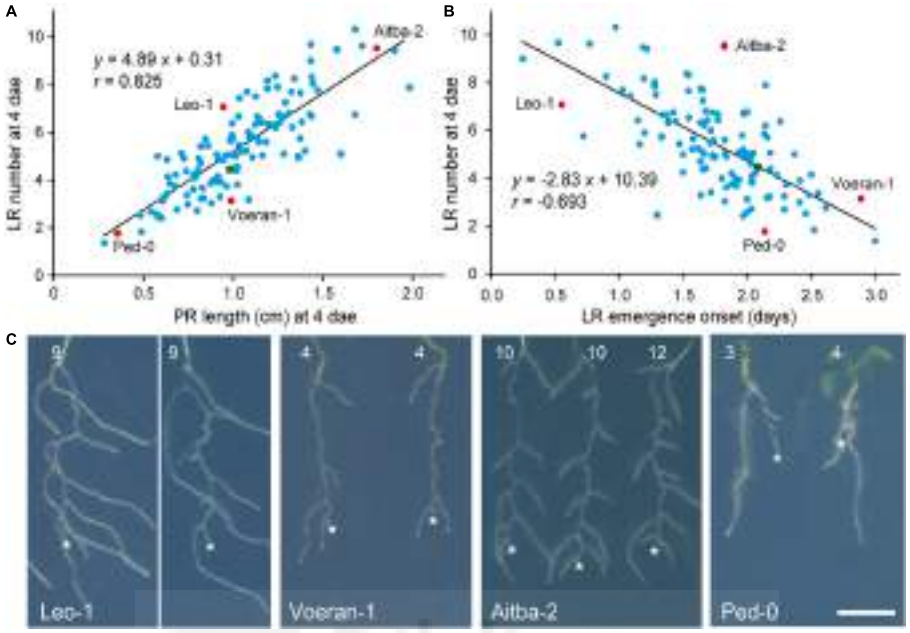

FIGURE 2 | Phenotypic variation of LR architecture after root tip excision. **(A,B)** Scatter plots of average values for LR number and PR length, or LR number and LR emergence onset among the studied accessions. **(C)** Some accessions with extreme LR architecture phenotypes after root tip excision. Asterisk marks the PR tip after excision and numbers refer to LR number at 4 dae. Scale bar: 5 mm. Red dots indicate the accessions with contrasting phenotypes shown in **(C)** and green dots correspond to Col-0.

likely due to its earlier LR emergence onset (0.55 ± 0.57 days in Leo-1 and 1.82 ± 0.50 days in Aitba-2; n = 29; **Figures 2B,C**). Ped-0 displayed very short PRs while their wound-induced LRs were much longer (**Figure 2C**). As regards LR density, Castelfed4.2 and Leo-1 displayed extreme phenotypes, with 2.98 ± 1.35 and 8.05 ± 2.37 roots/cm (n = 29), respectively.

Assessment of Population Structure

The observed phenotypic distribution for the studied traits (PR length, LR emergence onset, LR number and LR density) suggested that these traits were controlled by multiple genes, that some of the causal alleles are pleiotropic (i.e., affect several of these traits), and that the studied population (n = 120 accessions) was polymorphic for those causal alleles. We determined the genetic relationship among the studied accessions using a Structure analysis with 319 genome-wide randomly selected and synonymous (likely evolutionary neutral) SNP markers already available (see section "Materials and Methods"). Structure analysis of these accessions identified two distinct genetic groups (**Figure 3A**) that closely correspond to their geographic regions of origin (**Figure 3B**): The so-called "West" subpopulation including 101 accessions, and the "East" subpopulation with the remaining 19 accessions. However, a detailed analysis of these results indicated a continuous genetic shift from "East" to "West" accessions that follow *A. thaliana* geographical distribution and that likely arose by local haplotypes, as it has been previously proposed (Platt et al., 2010).

We found a significant variation range for the studied traits between these two genetically distinct subpopulations (**Figure 3C**). Altogether, accessions belonging to the "East" subpopulation displayed longer PRs and an increasing number of LRs as regards the "West" subpopulation. However, some accessions of the "East" subpopulation, such as Shigu-1, displayed lower phenotypic values for the studied traits than most of their relatives (**Figure 4**). On the other hand, accessions of the "West" subpopulation and highly genetically divergent from those in the "East" subpopulation (i.e., Aitba-2, HKT2-4, Leo-1, Mrk-0, and Pra-6) displayed higher number of LRs compared with their closest relatives (**Figure 4**). Despite some population structure among the studied lines and due to high heritability estimates, there is potential for the identification of natural alleles affecting wound-induced LR formation responses through GWA mapping with our dataset.

Genome-Wide Association Mapping of Wound-Induced LR Formation

To obtain insight into the genetic basis of the observed variation in wound-induced responses in young *A. thaliana*

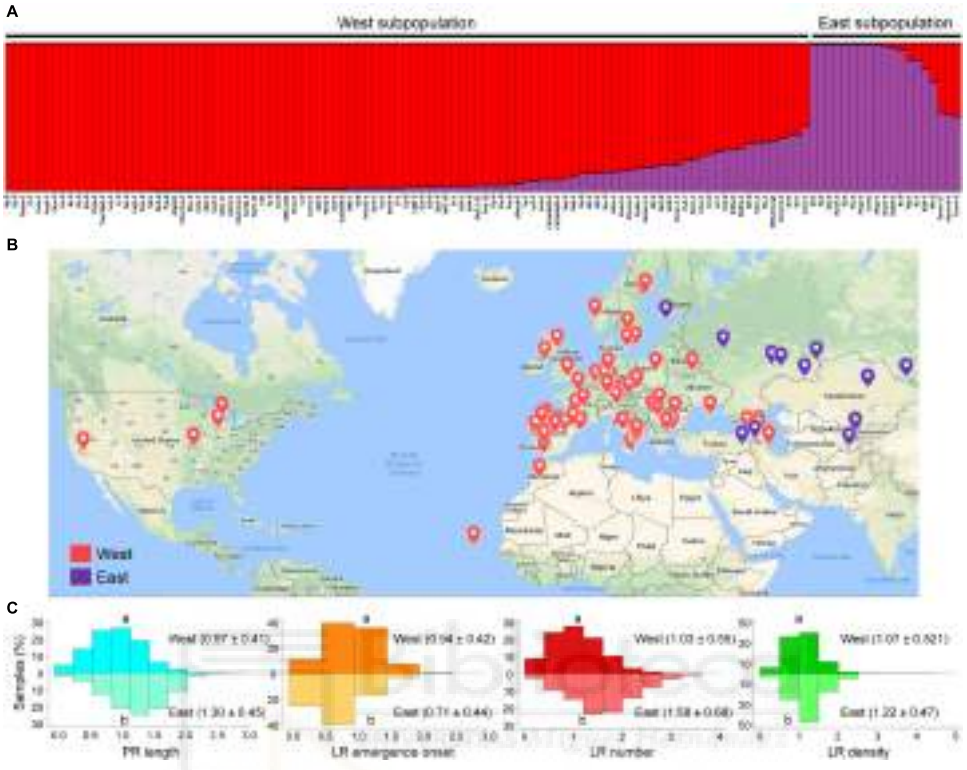

FIGURE 3 | Population structure of the studied accessions. **(A)** Population structure for the studied accessions using a collection of 319 whole-genome distributed and randomly selected synonymous single nucleotide polymorphism (SNP) markers. **(B)** Geographical localization of the studied accessions. Accessions from the "West" subpopulation are labeled in red; those from the "East" subpopulation are labeled in purple. **(C)** Histograms for the studied parameters. Relative data values at 4 dae as compared with the Col-0 reference accession from the "West" subpopulation are represented in the top histograms, while those from the "East" subpopulation are represented in the bottom histograms. Different letters indicate significant differences (LSD, P-value < 0.05).

roots, we performed GWA mapping (see section "Materials and Methods"). The significance of association was first evaluated with three different statistical models (LM, KW and AMM; **Supplementary Figures S3A–C**) and no significant SNP associations were identified by randomization of the phenotypic values within the studied lines (**Supplementary Figure S3D**). Although LM, and KW usually include more false positives than AMM, they do not present any risk of overcorrection in P-value when applied to traits correlated with population structure (Filiault and Maloof, 2012). We used a conservative threshold of $-\log_{10}(P\text{-value}) > 6.5$ and minor allele frequency (MAF) $> 12\%$ to select the SNPs being associated with a given trait. A total of 162 SNP associations were found with the LM method for the studied parameters (**Supplementary Table S5**). We found 32 SNPs associated with PR length with P-values ranging from 1.41×10^{-10} to 3.04×10^{-7}. Thirty-two SNPs were significantly associated with LR emergence onset (P-values ranging from 1.22×10^{-8} to 3.09×10^{-7}) and only one SNP was found associated with LR density. The larger number of significantly associated SNPs was found for LR number ($n = 114$), with P-values ranging from 8.27×10^{-11} to 3.15×10^{-7}. Consistently with our previous observation that PR length and LR number are significantly correlated, 11 SNPs were significantly associated with both traits; similarly, six significantly associated SNPs were shared between LR emergence onset and LR number (**Supplementary Figure S4A**).

Next, we classified the selected SNPs based on its molecular effect (**Supplementary Figure S4B**). About 36% of the significantly associated SNPs were located in intergenic regions and 17.2% of the SNPs laid in the coding region of the annotated gene causing amino acid changes in the protein (**Supplementary Figure S4B**). Previous reports have shown that, due to linkage disequilibrium, multiple significantly associated SNPs should be found within a small chromosome region for true associations (Rajarammohan et al., 2018). To reduce the number of selected loci for further studies, we focused

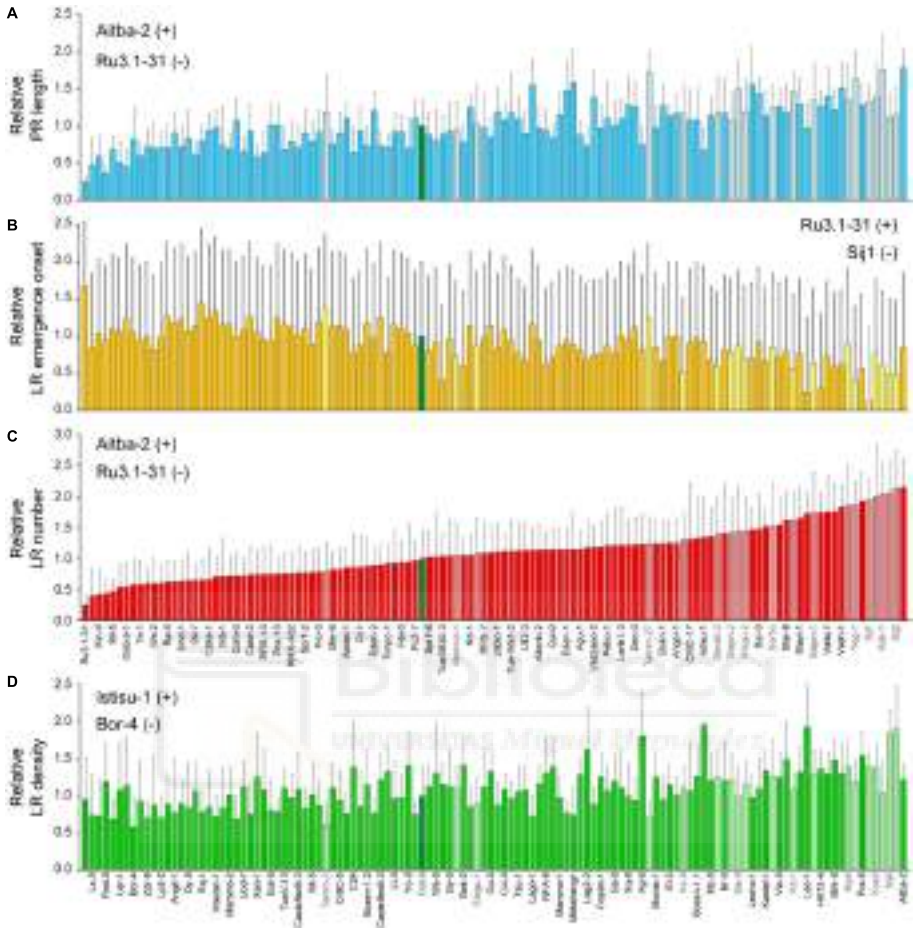

FIGURE 4 | Natural variation of LR architecture after root tip excision in 120 accessions of *Arabidopsis thaliana*. Average ± standard deviation (SD) values of **(A)** relative PR length, **(B)** relative LR emergence onset, **(C)** relative LR number, and **(D)** relative LR density at 4 dae as compared with the Col-0 reference accession. Light-colored bars indicate accessions belonging to the "East" subpopulation (names indicated in gray). The Col-0 reference is shown in green. Accessions are sorted based on their relative LR numbers. Those accessions with extreme phenotypes (+, maximum; –, minimum) are also indicated.

on 19 candidate genomic regions based on the following criteria (**Supplementary Figure S4C**): (1) *P*-value of associated SNPs $< 3.16 \times 10^{-7}$ (which corresponded to a LOD score > 6.5), (2) presence of multiple significantly associated SNPs within an average of 10 Kpb genomic window, and (3) presence of, at least, one non-synonymous SNP within the selected region. We found five genomic regions putatively contributing to PR length variation in the studied population (**Figure 5A**), with one (At1g04260), two (At1g04470), three (At2g22660), one (At4g01090), and two (At4g22920, At4g22940) non-synonymous SNPs each (**Supplementary Table S5**). Three genomic regions were identified as regards their effect on variation in LR emergence onset (**Figure 5B**), each with one non-synonymous SNP (At1g72250, At1g72300 and At5g20980, respectively; **Supplementary Table S5**). We found 14 genomic regions putatively involved in the observed variation in LR number among the studied accessions (**Figure 5C**). Interestingly, the non-synonymous SNPs of three of these regions (dubbed as 2′, 4′, and 5′) overlapped with three genomic regions also selected as being involved in PR length variation (**Supplementary Table S5**). Hence, the affected genes in these cases, At1g04470, At4g01090, and At4g22940, might indirectly contribute to the LR number differences likely due to their direct effect on PR length before root tip excision. The remaining regions identified in the

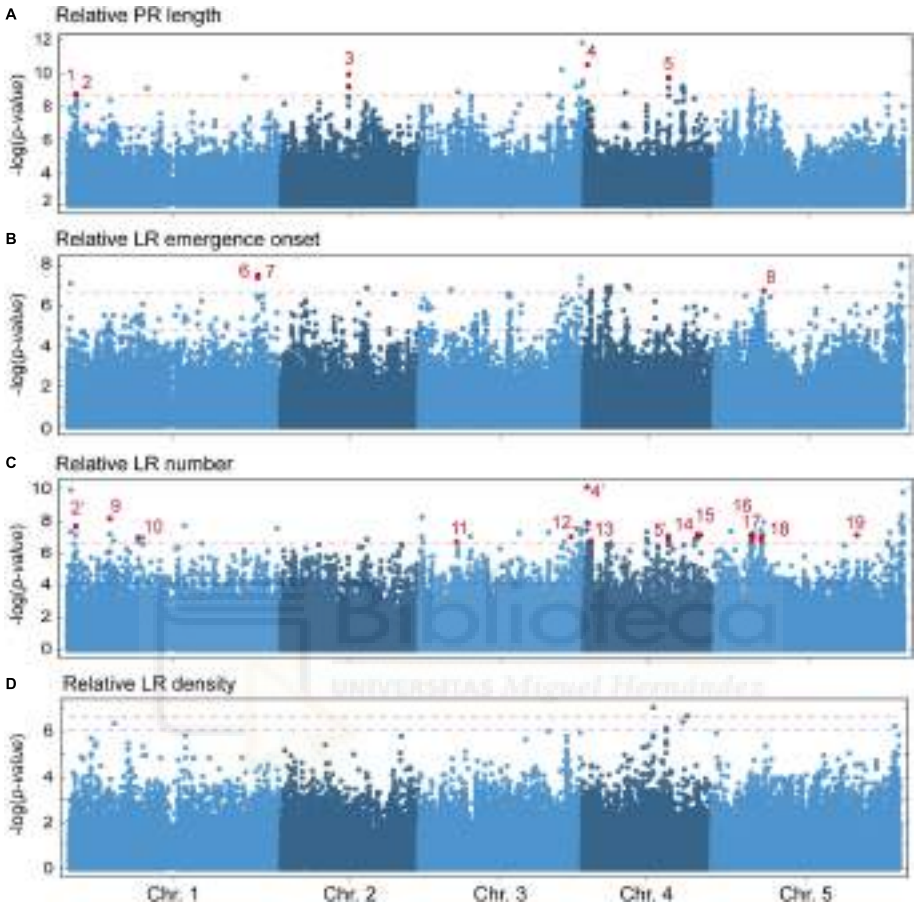

FIGURE 5 | Manhattan plots of associations between SNPs and the studied parameters using a linear regression model (LM). **(A)** Relative PR length, **(B)** relative LR emergence onset, **(C)** relative LR number, and **(D)** relative LR density at 4 dae as compared with the Col-0 reference accession. Dashed horizontal red lines indicate threshold for significance in genome-wide association (GWA) mapping set at $-\log_{10}(P\text{-value}) > 6.5$. Red dots indicate the position of non-synonymous significantly associated SNPs. Numbers 1–19 indicate the genomic regions considered for further studies. Some statistically significant SNP were found both in PR length and LR number (2 and 2′, 4 and 4′, 5 and 5′).

GWA analysis for LR number might include genes that directly contribute to wound-induced LR formation (**Supplementary Table S5**) and therefore deserve further studies. On the contrary, no other genomic region fulfilled our selection criteria as regards LR density and this trait was not considered (**Figure 5D**).

Selection of Candidate Genes Involved in Wound-Induced LR Formation

To identify allelic variation in genes contributing to the observed differences in LR number after root tip excision, we selected 20 non-synonymous SNPs for further studies (**Supplementary Table S6**). Although SNPs in intergenic regions could also be causative, we decided to focus on non-synonymous polymorphisms as their later characterization can be performed on an easier way using reverse genetics tools. Based on both geographic distribution and genotype (**Figure 3**), we hypothesized that Nemrut-1 and Yeg-1 might represent atypical accessions due to ancient migration and genetic isolation. To discard the false-positive SNPs of this spurious association, we repeated the GWA mapping by removing either one or both accessions, which allowed us to reduce to 11 the number of significantly associated SNPs contributing to LR number

(**Supplementary Table S6**). Due to the genetic structure of the studied accessions, we performed ANOVA analyses as regards the "East" and "West" subpopulations independently. Polymorphisms at eight SNPs affecting six genes (At1g17700, At3g58220, At4g01090, At4g33530, At5g16220, and At5g19710; **Table 1**) were found significantly associated with LR number variation (**Supplementary Table S6**). Four haplotypes were detected for selected SNPs within the At4g01090 gene (CAA, CAT, CTA, and TAT). The accessions containing the TAT haplotype displayed a significant increase in LR number, irrespectively of their subpopulation of origin (**Supplementary Figure S5A**). Indeed, the T to A polymorphism at Chr4:472726 accounted for the quantitative differences in LR number by its own. In addition, we observed a haplotype-dependent relationship between SNPs at At5g16220, and At5g19710, which are separated by 1.4 Mb and were previously assigned to two different candidate genomic regions (**Figure 5C**). The GA haplotype for these two genes corresponded to the higher phenotypic values for LR number (**Supplementary Figure S5B**). To our knowledge, this is the first example of two-linked quantitative trait nucleotides (QTNs) detected through GWA mapping and further experiments will account for the functional relationship between the two genes and wound-induced LR number.

Experimental Validation of Candidate Genes

To validate the identification of novel genes involved in wound-induced LR formation in *A. thaliana* seedlings, we chose At4g01090, At4g33530, and At5g19710 for further studies. We searched for available T-DNA insertions in those three genes and identified homozygous mutants by means of PCR and sequencing (**Supplementary Table S1**). Based on haplotype studies, we found that the Chr4:472726 C/T polymorphism at the At4g01090 gene (**Supplementary Figure S6A**) was significantly associated with LR number variation, even in those accessions belonging to the same subpopulation such as Fei-0 (5.19 ± 1.88; $n = 36$) and Star-8 (8.36 ± 2.33; $n = 36$; **Supplementary Figures S6B,C**). Additionally, T-DNA homozygotes from the Salk_086312 segregating line displayed a reduced number of wound-induced LR at 4 dae (2.82 ± 1.27; $n = 34$) in comparison to their wild-type siblings (6.68 ± 1.87; $n = 63$; **Supplementary Figures 6D,E**). The homozygous seedlings were also characterized by their longer hypocotyl and shorter PRs (**Supplementary Figure 6D**). Our results confirmed that the hypothetical protein encoded by the At4g01090 gene participates in wound-induced LR development and that the observed natural variation in their protein sequence might affect their biochemical activity.

At4g33530 (**Supplementary Figure S7A**) encodes a potassium (K^+) uptake transporter which is highly expressed in root hairs (Ahn et al., 2004). We found a statistically significant and non-synonymous SNP (Chr4:16128906) correlated with wound-induced LR phenotype variation (**Supplementary Figure S7B**). The accessions Pu2-7 and Aitba-2 differed in their LR number (6.44 ± 1.95; $n = 32$ and 9.53 ± 1.94; $n = 34$, respectively) and carried alternative alleles of the Chr4:16128906 marker (**Supplementary Figure S7C**). We identified T-DNA homozygotes from two Salk insertion lines interrupting the coding region of this gene (**Supplementary Figure S7A**). None of the studied homozygous mutants from Salk_120707 and Salk_072850 lines displayed significant differences in wound-induced LR number as regards their wild-type siblings (**Supplementary Figures S7D,E**).

The At5g19710 gene (**Figure 6A**) encodes a histidine phosphotransfer protein (AHP) whose function on the CK

TABLE 1 | Candidate genes for LR number identified in the genome-wide association (GWA) mapping.

Gene	SNP coordinate	-log(*P*-value)	Description (domain/name)	Root expression[a]	Reference
At1g04470	Chr1:1214221	7.660	Hypothetical protein (DUF810)	N/A	Hanada et al., 2011
	Chr1:1214425	7.660			
At1g17700	Chr1:6089805	8.130	Prenylated RAB acceptor 1.F1	Elongation zone (EZ) and mature endodermis	Alvim Kamei et al., 2008
At3g58220	Chr3:21566092	6.980	TRAF-like family protein/ MATH domain RTM3-like protein	N/A	N/A
At4g01090	Chr4:472438	7.876	Hypothetical protein (DUF3133)	EZ and LR primordium	Ascencio-Ibáñez et al., 2008
	Chr4:472726	10.082			
	Chr4:473027	7.889			
At4g33530	Chr4:16128906	7.143	Potassium transporter (KUP5)	EZ and mature cortex	Ahn et al., 2004
At5g16220	Chr5:5299807	7.080	Octicosapeptide/Phox/Bem1p family protein	Columella stem cells	N/A
At5g19710	Chr5:6665363	7.000	Histidine containing phosphotransfer protein	Lateral root cap	Nishizawa et al., 2006
At5g49880	Chr5:20286041	7.129	Spindle assembly checkpoint protein (MAD1)	Meristem and LR primordium	Du and Scheres, 2018

[a]*Gene expression was obtained from the eFP browser (Winter et al., 2007). N/A: not available.*

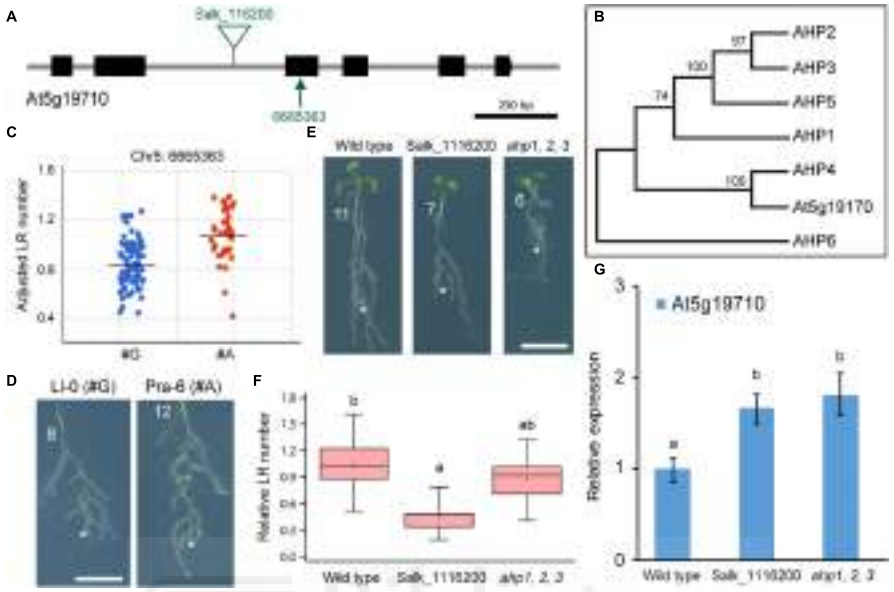

FIGURE 6 | Functional analysis of At5g19710 variation concerning LR number. **(A)** Gene structure of At5g19710. Exons are represented by black boxes and introns are depicted as gray lines. The studied non-synonymous SNP markers (arrows) and annotated T-DNA insertions (triangles) are indicated. **(B)** Phylogenetic analyses of the AHP gene family. Trees were drawn to scale, with branch lengths representing the number of substitutions per site. These analyses were conducted in MEGA7 as described elsewhere (Sánchez-García et al., 2018). **(C)** Scatterplot of average LR number values used for GWA mapping, sorted by the alleles, G and A, at Chr5:6665363 position. **(D)** Some accessions of the studied haplotypes with contrasting LR number values. **(E)** Representative images of wild-type and homozygous seedlings of indicated Salk and mutant lines at 4 dae. Asterisk marks the PR tip after excision and numbers refer to LR number at 4 dae. Scale bars: 5 mm. **(F)** Boxplot showing relative LR number values of wild type and homozygous T-DNA mutants of the indicated Salk lines. Different letters indicate significant differences (LSD, *P*-value < 0.01). (G) RT-qPCR of the expression of At5g19710 in wild-type and mutant seedlings at 7 dae. Bars indicate normalized expression levels ± standard deviation relative to the wild type. Asterisks indicate significant differences between the assayed genotypes and the reference (LSD; *P*-value < 0.05).

transduction pathway has not yet been elucidated. There are six other known AHPs involved in CK responses (Hutchison et al., 2006). Phylogenetic tree reconstruction of AHPs including At5g19710 (**Figure 6A**), suggested that the annotated AHP protein encoded by this gene was incorrectly predicted due to an exon skipping, and clustered together with the AHP4 negative regulator of CK signaling (**Figure 6B**; Moreira et al., 2013). We found that the Chr5:6665363 G/A polymorphism at the third exon of this gene (**Figure 6A**) was significantly associated with LR number variation (**Figure 6C**), even in those accessions belonging to the same subpopulation such as Ll-0 (3.91 ± 2.20; n = 32) and Pra-6 (7.91 ± 1.91; n = 33; **Figure 6D**). We identified a homozygous T-DNA insertion line for the At5g19710 gene whose seedlings showed a reduced number of wound-induced LRs (**Figures 6E,F**) due to a significant miss-regulation of At5g19710 gene expression (**Figure 6G**). We also confirmed that the triple *ahp1 ahp2 ahp3* mutants, which was defective in CK root responses (Hutchison et al., 2006), displayed a significant reduction in wound-induced LRs at 4 dae compared to their wild-type background (**Figures 6E,F**). Taken together, our results seem to indicate that altered homeostasis of AHP proteins required for CK signaling interferes with wound-induced LR formation, a statement that requires further investigation.

Finally, we wondered whether there was an epistatic interaction between the allelic variants for some of the studied non-synonymous SNP markers (Chr4:472726, Chr4:16128906 and Chr5:6665363, respectively) that contributed to the observed variation in wound-induced LR formation in the studied population. Accessions sharing the CCG haplotype for these three markers displayed the smallest number of wound-induced LRs (**Supplementary Figure S8A**), while only the accessions with the haplotype containing a single polymorphism in the At4g01090 gene showed a significant increase (LSD; *P*-value < 0.01) in LR numbers (**Supplementary Figure S8A**). The individual contribution of the SNP polymorphisms in the other two genes considered, At4g33530 and At5g19710, hardly increased wound-induced LR numbers alone but in combination (CGA haplotype) their effects on wound-induced LR formation were enhanced (**Supplementary Figure S8A**). Similar interactions were found between the other SNP pairs (TGG and TCA haplotypes).

Interestingly, we identified several accessions in the "West" subpopulation of all the haplotypes correlated with an increase in wound-induced LR numbers, such as Mrk-0 (8.17 ± 2.12; $n = 36$) and Vie-0 (6.33 ± 1.80; $n = 33$) (**Supplementary Figure S8B**). However, all accessions with the TGA haplotype combining the allelic variants that contribute to an increase of wound-induced LR formation belonged to the "East" subpopulation, which suggested that this trait might be ancestral.

DISCUSSION

The spatial configuration of the RSA allows the plant to dynamically respond to changing soil conditions (Koevoets et al., 2016). Root plasticity relies on the integration of systemic and local signals of nutrient and water availability into the core developmental program of the root (Araya et al., 2014; Bao et al., 2014). Periodic fluctuations in auxin response within the vascular region of the PR near the meristem control the patterning of LR founder cell specification (Moreno-Risueno et al., 2010). A novel IBA-to-IAA conversion pathway in the outer LR cap cells creates a local auxin source that contributes to these periodic auxin fluctuations, which in turn are essential for LR pre-patterning (Xuan et al., 2015). Our wound-induced RSA assay is simple and provides an accurate measure of LR capacity, defined as the total number of competent sites for LR formation on a given root (Van Norman et al., 2014). Interestingly, a recent study has demonstrated that *A. thaliana* PRs might use a specific pathway to activate LR formation when the PR is damaged (Sheng et al., 2017). The authors found that *WUSCHEL-related homeobox11* (*WOX11*), which is involved in *de novo* regeneration of adventitious roots from leaf explants (Liu et al., 2014), was also required for LR formation in soil conditions, likely upstream of the LATERAL ORGAN BOUNDARIES DOMAIN (LBD) genes required for LR initiation (Goh et al., 2012).

We found a wide variation for the studied wound-induced RSA traits in our GWA mapping population. There was a clear correlation between the number of wound-induced LRs (i.e., LR branching capacity) with PR length at the excision day and with the time of LR emergence after excision. Some accessions, such as Leo-1 and Voeran-1, significantly differed in their LR number because of an earlier initiation of wound-induced LRs in Leo-1, which were also longer. Hence, Leo-1 contained alleles for higher LR branching capacity that positively contributed to an enhanced root system, which might allow survival in harsh environments. It will be interesting to evaluate whether differences in *WOX11* expression between these accessions might account for the observed differences in RSA after root tip excision.

A population analysis of the studied accessions inferred two distinct genetic groups that closely corresponded to the geographic regions of *A. thaliana* native distribution and the proposed postglacial colonization routes in this species (Platt et al., 2010; Cao et al., 2011). Interestingly, the "East" subpopulation included accessions, mainly from Central Asia, with enhanced wound-induced RSA traits. In this case, genetic polymorphism may be strongly correlated with RSA traits because of demographic history, challenging the identification of the causal polymorphisms. Within the "West" subpopulation however, there was a clear longitudinal gradient of genetic polymorphisms, such as the accessions in Central Europe were also genetically close to those in the "East" subpopulation. Additionally, Nemrut-1 and Yeg-1 were included in the "East" subpopulation in our study, which is in agreement with a recently proposed migration route connecting Asia and Africa from the south (Brennan et al., 2014). Although it is well-known that population structure, among other effects, can complicate GWA studies in Arabidopsis (Filiault and Maloof, 2012), we reasoned that the studied traits showed broad phenotypic variation, globally as well as within the two subpopulations, that also exhibited continuous isolation by distance as observed earlier in this species (Platt et al., 2010). For example, some accessions from the "West" subpopulation, like Leo-1 and Pra-6, showed an enhanced root system after wounding, while other genetically and geographically close accessions (Cdm-0 and Qui-0, respectively) displayed a less complex RSA. It is well known that nutrients and other environmental signals in the soil might alter the RSA (Kellermeier et al., 2014). We thus speculate that the observed differences in wound-induced RSA traits might represent local adaptations to distinct ecological niches, and one of the environmental signals that might be involved is osmotic stress. Some accessions from the "East" subpopulation, such as Shigu-1 and Tamm-2, displayed lower RSA values than their close relatives. Hence, these contrasting accessions might be used as parents for QTL identification through conventional linkage association mapping in different soil stress conditions.

Through GWA mapping, we identified 162 SNP associations that significantly accounted for variation in wound-induced RSA traits located at 19 genomic regions, which were defined based primarily by non-synonymous SNPs. As expected by our trait correlation analyses, we found a clear overlap between three genomic regions associated for PR length and LR number (2/2′, 4/4′, and 5/5′). In all these cases, the causal polymorphism(s) might affect genes with pleiotropic effects on RSA. GWA mapping has facilitated the identification of the molecular variants underlying complex traits in crops, such as heterosis (Huang et al., 2016), grain size (Si et al., 2016), or drought resistance (Wang et al., 2016). In all these examples, hundreds of genetic variants were identified and candidate genes were assigned based on prior knowledge. In most cases, the genetic variation affected regulatory regions of candidate genes and functional validation using transgenic approaches were required for the functional validation of these genes.

Our results suggest that non-synonymous variation in the coding region of At4g01090 was significantly associated with wound-induced LR variation. At4g01090 encodes a hypothetical protein (DUF3133) of unknown function, which is expressed at higher levels in the endodermis of the elongation zone of the root and the mature xylem (Winter et al., 2007). Other ortholog genes encoding proteins with the DUF3133 domain are At4g01410, which has been annotated as a late embryogenesis abundant (LEA) protein, and *enhanced disease resistance 4* (*EDR4*), which modulates plant immunity by regulating clathrin heavy chain 2 (CHC2)-mediated vesicle trafficking (Wu et al., 2015). The protein encoded by At4g01410 has been found to interact with

EDR4 (Mukhtar et al., 2011). One intriguing possibility is that these DUF3133-containing proteins might also interact with clathrin-coated vesicles during PIN-FORMED (PIN) endocytosis (Dhonukshe et al., 2007; Kitakura et al., 2011), which could then be directly linked to LR initiation (Ditengou et al., 2008). Additional experiments will be performed in our lab to confirm the involvement of DUF3133-containing proteins in clathrin-mediated PIN endocytosis during wound-induced LR formation.

At5g19710 encodes a histidine phosphotransfer protein belonging to the AHP bridge components of the His-Asp phosphorelay transduction pathway of CK signaling (Hwang et al., 2012). Five AHPs (AHP1-5) mediate the cytoplasmic-to-nuclear transduction of the CK signal by transferring the phosphoryl group from the CK receptors to nuclear type-B (positive) and type-A (negative) Arabidopsis response regulators (ARRs). AHP6 lacks the conserved His residue and negatively interferes with CK response (Moreira et al., 2013), most likely by competing with AHP1–5 for interaction with CK-activated receptors (Mahonen et al., 2006). The AHP protein encoded by the At5g19710 gene resembled AHP4. Based on loss-of-function analysis (Hutchison et al., 2006), a negative role of AHP4 for a subset of CK responses (i.e., LR formation) has also been proposed. Interestingly, At5g19710 is specifically expressed in LR cap cells in a low nitrogen environment while it was significantly downregulated by a short nitrate treatment (Gifford et al., 2007). Despite the local inhibitory role of CKs on LR initiation (Laplaze et al., 2007), CKs are essential components of the systemic signaling network leading to the enhancement of LR formation where nitrate is available (Ruffel et al., 2016). In Arabidopsis, the adaptive root response to nitrate depends on the NRT1.1/NPF6.3 transporter/sensor system (Bouguyon et al., 2016). NRT1.1 represses LR emergence at low nitrate concentration through its auxin transport activity that lowers auxin accumulation in the LR primordia (Bouguyon et al., 2016). An additional layer of regulation of systemic N signaling involves TCP20 (Guan et al., 2014). TCP20 is a transcription factor from the TEOSINTE BRANCHED1, CYCLOIDEA, and PCF (TCP) family that binds the promoters of type-A ARR5 and ARR7 at high nitrate levels and of NRT1.1 at low nitrate only (Guan et al., 2014). We speculate that the AHP protein encoded by At5g19710 might function as a negative regulator of a subset of CK responses in LR cap cells at low nitrate, leading to a net reduction of the number of competent sites for LR formation. Interestingly, cell-specific regulation of a transcriptional circuit including ARF8 and miR167 mediates LR outgrowth in response to nitrogen (Gifford et al., 2007). Additional experiments will be required to establishing a functional link between At5g19710-encoding AHP and the ARF8/miR167 circuit.

We found a statistically significant association between a non-synonymous SNP in the coding region of *K^+ UPTAKE TRANSPORTER5 (KUP5)* that changes a Gln to His residue in a conserved transmembrane domain of the protein. Potassium is an essential element in plant growth as it affects osmotic regulation and cell water potential (Lebaudy et al., 2007). The Arabidopsis genome contains multigene families of potassium channels with distinct or redundant functions (Lebaudy et al., 2007), which might explain why the loss-of-function of kUP5 alone did not produce any effect on wound-induced RSA (this work). Consistently, loss-of-function mutations in three KUP family potassium efflux transporters, KUP6, 8 and 2, showed increased auxin responses and enhanced LR formation (Osakabe et al., 2013). As proposed earlier, these KUP transporters might coordinately control potassium homeostasis across root tissues, and the enhanced LR formation in the triple mutants might be caused by a local excess of potassium in the pericycle cells, resulting in enhanced LR formation due to its effect on cell cycle progression (Osakabe et al., 2013). We found an interesting epistatic interaction between the SNP polymorphisms in At4g33530 and At5g19710, which suggest a functional link between potassium uptake and CK signaling. CKs are fairly known to regulate uptake and metabolism of different nutrients: nitrogen, sulfate, phosphate, and iron (Brenner et al., 2012), but the roles of CKs in potassium signaling are poorly understood (Nam et al., 2012).

Through GWA mapping we have identified a number of significant non-synonymous polymorphisms that accounted for some of the variation found in wound-induced RSA. Our results highlighted new regulators of LR formation in Arabidopsis and the further dissection of the developmental mechanisms involved might help to understand the genetic basis of the natural variation of root plasticity.

AUTHOR CONTRIBUTIONS

JP-P was responsible for conceptualization and supervision and provided the funding acquisition. MJ and JP-P were responsible for methodology and performed the formal analysis. MJ, SI, and JP-P were involved in the investigation, writing of the original draft, and review and editing of the manuscript. AP was responsible for software development.

FUNDING

This work was supported by the Ministerio de Economía, Industria y Competitividad (MINECO) of Spain (Grant Nos. AGL2012-33610 and BIO2015-64255-R) and by European Regional Development Fund (ERDF) of the European Commission.

ACKNOWLEDGMENTS

We are especially indebted to Ümit Seren (Gregor Mendel Institute of Molecular Plant Biology, Austria) for sharing relevant data for this project and the two reviewers for their useful suggestions.

SUPPLEMENTARY MATERIAL

The Supplementary Material for this article can be found online at: https://www.frontiersin.org/articles/10.3389/fpls.2019.00311/full#supplementary-material

REFERENCES

Aguinis, H., Gottfredson, R. K., and Joo, H. (2013). 'Best-practice recommendations for defining, identifying, and handling outliers'. *Organ. Res. Methods* 16, 270–301. doi: 10.1177/1094428112470848

Ahn, S. J., Shin, R., and Schachtman, D. P. (2004). 'Expression of KT/KUP genes in *Arabidopsis* and the role of root hairs in K+ uptake'. *Plant Physiol.* 134, 1135–1145. doi: 10.1104/pp.103.034660

Alvim Kamei, C. L., Boruc, J., Vandepoele, K., Van den Daele, H., Maes, S., Russinova, E., et al. (2008). 'The PRA1 gene family in *Arabidopsis*'. *Plant Physiol.* 147, 1735–1749. doi: 10.1104/pp.108.122226

Araya, T., Miyamoto, M., Wibowo, J., Suzuki, A., Kojima, S., Tsuchiya, Y. N., et al. (2014). 'CLE-CLAVATA1 peptide-receptor signaling module regulates the expansion of plant root systems in a nitrogen-dependent manner'. *Proc. Natl. Acad. Sci. U.S.A.* 111, 2029–2034. doi: 10.1073/pnas.1319953111

Armengaud, P., Zambaux, K., Hills, A., Sulpice, R., Pattison, R. J., Blatt, M. R., et al. (2009). 'EZ-Rhizo: integrated software for the fast and accurate measurement of root system architecture'. *Plant J.* 57, 945–956. doi: 10.1111/j.1365-313X.2008.03739.x

Ascencio-Ibáñez, J. T., Sozzani, R., Lee, T. J., Chu, T. M., Wolfinger, R. D., Cella, R., et al. (2008). 'Global analysis of *Arabidopsis* gene expression uncovers a complex array of changes impacting pathogen response and cell cycle during geminivirus infection'. *Plant Physiol.* 148, 436–454. doi: 10.1104/pp.108.121038

Atwell, S., Huang, Y. S., Vilhjálmsson, B. J., Willems, G., Horton, M., Li, Y., et al. (2010). 'Genome-wide association study of 107 phenotypes in a common set of *Arabidopsis thaliana* inbred lines'. *Nature* 465, 627–631. doi: 10.1038/nature08800

Bao, Y., Aggarwal, P., Robbins, N. E., Sturrock, C. J., Thompson, M. C., Tan, H. Q., et al. (2014). 'Plant roots use a patterning mechanism to position lateral root branches toward available water'. *Proc. Natl. Acad. Sci. U.S.A.* 111, 9319–9324. doi: 10.1073/pnas.1400966111

Bouain, N., Satbhai, S. B., Korte, A., Saenchai, C., Desbrosses, G., Berthomieu, P., et al. (2018). 'Natural allelic variation of the AZI1 gene controls root growth under zinc-limiting condition'. *PLoS Genet.* 14:e1007304. doi: 10.1371/journal.pgen.1007304

Bouguyon, E., Perrine-Walker, F., Pervent, M., Rochette, J., Cuesta, C., Benkova, E., et al. (2016). 'Nitrate controls root development through posttranscriptional regulation of the NRT1.1/NPF6.3 transporter/sensor'. *Plant Physiol.* 172, 1237–1248.

Brennan, A. C., Méndez-Vigo, B., Haddioui, A., Martínez-Zapater, J. M., Picó, F. X., and Alonso-Blanco, C. (2014). 'The genetic structure of *Arabidopsis thaliana* in the south-western mediterranean range reveals a shared history between north africa and southern europe'. *BMC Plant Biol.* 14:17. doi: 10.1186/1471-2229-14-17

Brenner, W. G., Ramireddy, E., Heyl, A., and Schmülling, T. (2012). 'Gene regulation by cytokinin in *Arabidopsis*'. *Front. Plant Sci.* 3:8. doi: 10.3389/fpls.2012.00008

Cao, J., Schneeberger, K., Ossowski, S., Gunther, T., Bender, S., Fitz, J., et al. (2011). 'Whole-genome sequencing of multiple *Arabidopsis thaliana* populations'. *Nat. Genet.* 43, 956–963. doi: 10.1038/ng.911

Czechowski, T., Stitt, M., Altmann, T., Udvardi, M. K., and Scheible, W. R. (2005). 'Genome-wide identification and testing of superior reference genes for transcript normalization in *Arabidopsis*'. *Plant Physiol.* 139, 5–17. doi: 10.1104/pp.105.063743

Dhonukshe, P., Aniento, F., Hwang, I., Robinson, D. G., Mravec, J., Stierhof, Y. D., et al. (2007). 'Clathrin-mediated constitutive endocytosis of PIN auxin efflux carriers in *Arabidopsis*'. *Curr. Biol.* 17, 520–527. doi: 10.1016/j.cub.2007.01.052

Ditengou, F. A., Teale, W. D., Kochersperger, P., Flittner, K. A., Kneuper, I., van der Graaff, E., et al. (2008). 'Mechanical induction of lateral root initiation in *Arabidopsis thaliana*'. *Proc. Natl. Acad. Sci. U.S.A.* 105, 18818–18823. doi: 10.1073/pnas.0807814105

Du, Y., and Scheres, B. (2018). 'Lateral root formation and the multiple roles of auxin'. *J. Exp. Bot.* 69, 155–167. doi: 10.1093/jxb/erx223

Evanno, G., Regnaut, S., and Goudet, J. (2005). 'Detecting the number of clusters of individuals using the software STRUCTURE: a simulation study'. *Mol. Ecol.* 14, 2611–2620. doi: 10.1111/j.1365-294X.2005.02553.x

Falush, D., Stephens, M., and Pritchard, J. K. (2003). 'Inference of population structure using multilocus genotype data: linked loci and correlated allele frequencies'. *Genetics* 164, 1567–1587.

Filiault, D. L., and Maloof, J. N. (2012). 'A genome-wide association study identifies variants underlying the *Arabidopsis thaliana* shade avoidance response'. *PLoS Genet.* 8:e1002589. doi: 10.1371/journal.pgen.1002589

Giehl, R. F., Gruber, B. D., and von Wiren, N. (2014). 'It's time to make changes: modulation of root system architecture by nutrient signals'. *J. Exp. Bot.* 65, 769–778. doi: 10.1093/jxb/ert421

Giehl, R. F., and von Wirén, N. (2014). 'Root nutrient foraging'. *Plant Physiol.* 166, 509–517. doi: 10.1104/pp.114.245225

Gifford, M. L., Dean, A., Gutierrez, R. A., Coruzzi, G. M., and Birnbaum, K. D. (2007). 'Cell-specific nitrogen responses mediate developmental plasticity'. *Proc. Natl. Acad. Sci. U.S.A.* 105, 803–808. doi: 10.1073/pnas.0709559105

Goh, T., Joi, S., Mimura, T., and Fukaki, H. (2012). ' The establishment of asymmetry in *Arabidopsis* lateral root founder cells is regulated by LBD16/ASL18 and related LBD/ASL proteins'. *Development* 139, 883–893. doi: 10.1242/dev.071928

Guan, P., Wang, R., Nacry, P., Breton, G., Kay, S. A., Pruneda-Paz, J. L., et al. (2014). 'Nitrate foraging by *Arabidopsis* roots is mediated by the transcription factor TCP20 through the systemic signaling pathway'. *Proc. Natl. Acad. Sci. U.S.A.* 111, 15267–15272. doi: 10.1073/pnas.1411375111

Hanada, K., Sawada, Y., Kuromori, T., Klausnitzer, R., Saito, K., Toyoda, T., et al. (2011). 'Functional compensation of primary and secondary metabolites by duplicate genes in *Arabidopsis thaliana*'. *Mol. Biol. Evol.* 28, 377–382. doi: 10.1093/molbev/msq204

Huang, X., Yang, S., Gong, J., Zhao, Q., Feng, Q., Zhang, Q., et al. (2016). 'Genomic architecture of heterosis for yield traits in rice'. *Nature* 537, 629–633. doi: 10.1038/nature19760

Hutchison, C. E., Li, J., Argueso, C., Gonzalez, M., Lee, E., Lewis, M. W., et al. (2006). 'The *Arabidopsis* histidine phosphotransfer proteins are redundant positive regulators of cytokinin signaling'. *Plant Cell* 18, 3073–3087. doi: 10.1105/tpc.106.045674

Hwang, I., Sheen, J., and Muller, B. (2012). 'Cytokinin signaling networks'. *Annu. Rev. Plant Biol.* 63, 353–380. doi: 10.1146/annurev-arplant-042811-105503

Julkowska, M. M., Koevoets, I. T., Mol, S., Hoefsloot, H., Feron, R., Tester, M. A., et al. (2017). 'Genetic components of root architecture remodeling in response to salt stress'. *Plant Cell* 29, 3198–3213. doi: 10.1105/tpc.16.00680

Kawa, D., Julkowska, M. M., Sommerfeld, H. M., ter Horst, A., Haring, M. A., and Testerink, C. (2016). 'Phosphate-dependent root system architecture responses to salt stress. *Plant Physiol.* 172, 690–706. doi: 10.1104/pp.16.00712

Kellermeier, F., Armengaud, P., Seditas, T. J., Danku, J., Salt, D. E., and Amtmann, A. (2014). 'Analysis of the root system architecture of *Arabidopsis* provides a quantitative readout of crosstalk between nutritional signals'. *Plant Cell* 26, 1480–1496. doi: 10.1105/tpc.113.122101

Kitakura, S., Vanneste, S., Robert, S., Löfke, C., Teichmann, T., Tanaka, H., et al. (2011). 'Clathrin mediates endocytosis and polar distribution of PIN auxin transporters in *Arabidopsis*'. *Plant Cell* 23, 1920–1931. doi: 10.1105/tpc.111.083030

Koevoets, I. T., Venema, J. H., Elzenga, J. T. M., and Testerink, C. (2016). 'Roots withstanding their environment: exploiting root system architecture responses to abiotic stress to improve crop tolerance'. *Front. Plant Sci.* 7:1335. doi: 10.3389/fpls.2016.01335

Laplaze, L., Benkova, E., Casimiro, I., Maes, L., Vanneste, S., Swarup, R., et al. (2007). 'Cytokinins act directly on lateral root founder cells to inhibit root initiation'. *Plant Cell* 19, 3889–3900. doi: 10.1105/tpc.107.055863

Lebaudy, A., Very, A. A., and Sentenac, H. (2007). 'K+ channel activity in plants: genes, regulations and functions'. *FEBS Lett.* 581, 2357–2366. doi: 10.1016/j.febslet.2007.03.058

Liu, J., Sheng, L., Xu, Y., Li, J., Yang, Z., Huang, H., et al. (2014). 'WOX11 and 12 are involved in the first-step cell fate transition during de novo root organogenesis in *Arabidopsis*'. *Plant Cell* 26, 1081–1093. doi: 10.1105/tpc.114.122887

Lu, Y., Xie, L., and Chen, J. (2012). 'A novel procedure for absolute real-time quantification of gene expression patterns'. *Plant Methods* 8, 9–19. doi: 10.1186/1746-4811-8-9

Lucas, M., Kenobi, K., von Wangenheim, D., Vobeta, U., Swarup, K., De Smet, I., et al. (2013). 'Lateral root morphogenesis is dependent on the mechanical

properties of the overlaying tissues'. *Proc. Natl. Acad. Sci. U.S.A.* 110, 5229–5234. doi: 10.1073/pnas.1210807110

Mahonen, A. P., Bishopp, A., Higuchi, M., Nieminen, K. M., Kinoshita, K., Tormakangas, K., et al. (2006). 'Cytokinin signaling and its inhibitor AHP6 regulate cell fate during vascular development'. *Science* 311, 94–98. doi: 10.1126/science.1118875

Meijon, M., Satbhai, S. B., Tsuchimatsu, T., and Busch, W. (2014). 'Genome-wide association study using cellular traits identifies a new regulator of root development in *Arabidopsis*'. *Nat. Genet.* 46, 77–81. doi: 10.1038/ng.2824

Moreira, S., Bishopp, A., Carvalho, H., and Campilho, A. (2013). 'AHP6 inhibits cytokinin signaling to regulate the orientation of pericycle cell division during lateral root initiation'. *PLoS One* 8:e56370. doi: 10.1371/journal.pone.0056370

Moreno-Risueno, M. A., Van Norman, J. M., Moreno, A., Zhang, J., Ahnert, S. E., and Benfey, P. N. (2010). 'Oscillating gene expression determines competence for periodic *Arabidopsis* root branching'. *Science* 329, 1306–1311. doi: 10.1126/science.1191937

Mukhtar, M. S., Carvunis, A. R., Dreze, M., Epple, P., Steinbrenner, J., Moore, J., et al. (2011). 'Independently evolved virulence effectors converge onto hubs in a plant immune system network'. *Science* 333, 596–601. doi: 10.1126/science.1203659

Munns, R., James, R. A., Xu, B., Athman, A., Conn, S. J., Jordans, C., et al. (2012). 'Wheat grain yield on saline soils is improved by an ancestral Na(+) transporter gene'. *Nat. Biotechnol.* 30, 360–364. doi: 10.1038/nbt.2120

Nam, Y. J., Tran, L. S. P., Kojima, M., Sakakibara, H., Nishiyama, R., and Shin, R. (2012). 'Regulatory roles of cytokinins and cytokinin signaling in response to potassium deficiency in *Arabidopsis*'. *PLoS One* 7:e47797. doi: 10.1371/journal.pone.0047797

Nishizawa, A., Yabuta, Y., Yoshida, E., Maruta, T., Yoshimura, K., and Shigeoka, S. (2006). '*Arabidopsis* heat shock transcription factor A2 as a key regulator in response to several types of environmental stress'. *Plant J.* 48, 535–547. doi: 10.1111/j.1365-313X.2006.02889.x

Osakabe, Y., Arinaga, N., Umezawa, T., Katsura, S., Nagamachi, K., Tanaka, H., et al. (2013). 'Osmotic stress responses and plant growth controlled by potassium transporters in *Arabidopsis*'. *Plant Cell* 25, 609–624. doi: 10.1105/tpc.112.105700

Peret, B., De Rybel, B., Casimiro, I., Benkova, E., Swarup, R., Laplaze, L., et al. (2009). '*Arabidopsis* lateral root development: an emerging story'. *Trends Plant Sci.* 14, 399–408. doi: 10.1016/j.tplants.2009.05.002

Pérez-Pérez, J. M., Ponce, M. R., and Micol, J. L. (2004). 'The ULTRACURVATA2 gene of *Arabidopsis* encodes an FK506-binding protein involved in auxin and brassinosteroid signaling'. *Plant Physiol.* 134, 101–117. doi: 10.1104/pp.103.032524

Platt, A., Horton, M., Huang, Y. S., Li, Y., Anastasio, A. E., Mulyati, N. W., et al. (2010). 'The scale of population structure in *Arabidopsis thaliana*'. *PLoS Genet.* 6:e1000843. doi: 10.1371/journal.pgen.1000843

Porras-Hurtado, L., Ruiz, Y., Santos, C., Phillips, C., Carracedo, Á., and Lareu, M. V. (2013). 'An overview of STRUCTURE: applications, parameter settings, and supporting software'. *Front. Genet.* 4:98. doi: 10.3389/fgene.2013.00098

Rajarammohan, S., Pradhan, A. K., Pental, D., and Kaur, J. (2018). 'Genome-wide association mapping in *Arabidopsis* identifies novel genes underlying quantitative disease resistance to *Alternaria brassicae*'. *Mol. Plant Pathol.* 19, 1719–1732. doi: 10.1111/mpp.12654

Ristova, D., Giovannetti, M., Metesch, K., and Busch, W. (2018). 'Natural genetic variation shapes root system responses to phytohormones in *Arabidopsis*'. *Plant J.* 96, 468–481. doi: 10.1111/tpj.14034

Robbins, N. E., and Dinneny, J. R. (2015). 'The divining root: moisture-driven responses of roots at the micro- and macro-scale'. *J. Exp. Bot.* 66, 2145–2154. doi: 10.1093/jxb/eru496

Rosas, U., Cibrian-Jaramillo, A., Ristova, D., Banta, J. A., Gifford, M. L., Fan, A. H., et al. (2013). 'Integration of responses within and across *Arabidopsis* natural accessions uncovers loci controlling root systems architecture'. *Proc. Natl. Acad. Sci. U.S.A.* 110, 15133–15138. doi: 10.1073/pnas.1305883110

Ruffel, S., Poitout, A., Krouk, G., Coruzzi, G. M., and Lacombe, B. (2016). 'Long-distance nitrate signaling displays cytokinin dependent and independent branches'. *J. Integr. Plant Biol.* 58, 226–229. doi: 10.1111/jipb.12453

Sánchez-García, A. B., Ibáñez, S., Cano, A., Acosta, M., and Pérez-Pérez, J. M. (2018). 'A comprehensive phylogeny of auxin homeostasis genes involved in adventitious root formation in carnation stem cuttings'. *PLoS One* 13:e0196663. doi: 10.1371/journal.pone.0196663

Satbhai, S. B., Setzer, C., Freynschlag, F., Slovak, R., Kerdaffrec, E., and Busch, W. (2017). 'Natural allelic variation of FRO2 modulates *Arabidopsis* root growth under iron deficiency'. *Nat. Commun.* 8, 15603–15612. doi: 10.1038/ncomms15603

Seren, Ü., Vilhjálmsson, B. J., Horton, M. W., Meng, D., Forai, P., Huang, Y. S., et al. (2012). 'GWAPP: A web application for genome-wide association mapping in *Arabidopsis*. *Plant Cell* 24, 4793–4805. doi: 10.1105/tpc.112.108068

Sheng, L., Hu, X., Du, Y., Zhang, G., Huang, H., Scheres, B., et al. (2017). 'Non-canonical WOX11-mediated root branching contributes to plasticity in *Arabidopsis* root system architecture'. *Development* 144, 3126–3133. doi: 10.1242/dev.152132

Si, L., Chen, J., Huang, X., Gong, H., Luo, J., Hou, Q., et al. (2016). 'OsSPL13 controls grain size in cultivated rice. *Nat. Genet.* 48, 447–456. doi: 10.1038/ng.3518

Slovak, R., Göschl, C., Su, X., Shimotani, K., Shiina, T., and Busch, W. (2014). 'A scalable open-source pipeline for large-scale root phenotyping of *Arabidopsis*'. *Plant Cell* 26, 2390–2403. doi: 10.1105/tpc.114.124032

Van Norman, J., Zhang, J., Cazzonelli, C., Pogson, B., Harrison, P., Bugg, T., et al. (2014). 'Periodic root branching in *Arabidopsis* requires synthesis of an uncharacterized carotenoid derivative'. *Proc. Natl. Acad. Sci. U.S.A.* 111, E1300–E1309. doi: 10.1073/pnas.1403016111

Villacorta-Martín, C., Sánchez-García, A. B., Villanova, J., Cano, A., van de Rhee, M., de Haan, J., et al. (2015). 'Gene expression profiling during adventitious root formation in carnation stem cuttings'. *BMC Genomics* 16:789. doi: 10.1186/s12864-015-2003-5

von Wangenheim, D., Fangerau, J., Schmitz, A., Smith, R. S., Leitte, H., Stelzer, E. H., et al. (2016). 'Rules and self-organizing properties of post-embryonic plant organ cell division patterns'. *Curr. Biol.* 26, 439–449. doi: 10.1016/j.cub.2015.12.047

Wang, X., Wang, H., Liu, S., Ferjani, A., Li, J., Tan, J., et al. (2016). 'Genetic variation in ZmVPP1 contributes to drought tolerance in maize seedlings'. *Nat. Genet.* 48, 1233–1244. doi: 10.1038/ng.3636

Weigel, D., and Mott, R. (2009). 'The 1001 Genomes project for *Arabidopsis thaliana*'. *Genome Biol.* 10, 107–111. doi: 10.1186/gb-2009-10-5-107

Winter, D., Vinegar, B., Nahal, H., Ammar, R., Wilson, G. V., and Provart, N. J. (2007). 'An "electronic fluorescent pictograph" browser for exploring and analyzing large-scale biological data sets'. *PLoS One* 2:e718. doi: 10.1371/journal.pone.0000718

Wu, G., Liu, S., Zhao, Y., Wang, W., Kong, Z., and Tang, D. (2015). 'Enhanced disease resistance4 associates with clathrin heavy chain2 and modulates plant immunity by regulating relocation of EDR1 in *Arabidopsis*'. *Plant Cell* 27, 857–873. doi: 10.1105/tpc.114.134668

Xuan, W., Audenaert, D., Parizot, B., Moller, B. K., Njo, M. F., De Rybel, B., et al. (2015). 'Root cap-derived auxin pre-patterns the longitudinal axis of the *Arabidopsis* root'. *Curr. Biol.* 25, 1381–1388. doi: 10.1016/j.cub.2015.03.046

Conflict of Interest Statement: The authors declare that the research was conducted in the absence of any commercial or financial relationships that could be construed as a potential conflict of interest.

Supplementary Figures:

Supplementary Figure S1. Experimental procedure used for root analysis using EZRhizo.

Supplementary Figure S2. Quantitative variation of the studied parameters.

Supplementary Figure S3. Manhattan plots of associations between SNPs and relative LR number using different models.

Supplementary Figure S4. Candidate gene selection.

Supplementary Figure S5. Haplotype analysis for markers involved in LR number variation.

Supplementary Figure S6. Functional analysis of At4g01090 variation concerning LR number.

Supplementary Figure S7. Functional analysis of At4g33530 variation concerning LR number.

Supplementary Figure S8. Haplotype analysis for selected SNP markers in candidate genes involved in LR number variation.

Supplementary Tables:

Supplementary Table S1. *Arabidopsis thaliana* accessions used in this study. The accessions used for genome-wide association (GWA) mapping displayed high germination percentage (>80%) and unambiguous marker information (unique ID at the GWAPP web interface). N/A: not available at the time of experiment.

Supplementary Table S2. Oligonucleotides used in this study.

Supplementary Table S3. Individual data values obtained in this work.

Supplementary Table S4. MATLAB script used for data selection and formatting.

Supplementary Table S5. Statistically significant SNP markers identified in this work. Detailed information for each marker was obtained from the GWAPP web interface. GVE, genetic variance explained; MAC, minor allele count; MAF, minor allele frequency. We defined putative QTL (from 1 to 19) as indicated in the Results section.

Supplementary Table S6. Haplotype diversity for statistically significant non-synonymous SNPs accounting for LR number. See Supplementary Table S5 for legends.

Supplementary Figure S1

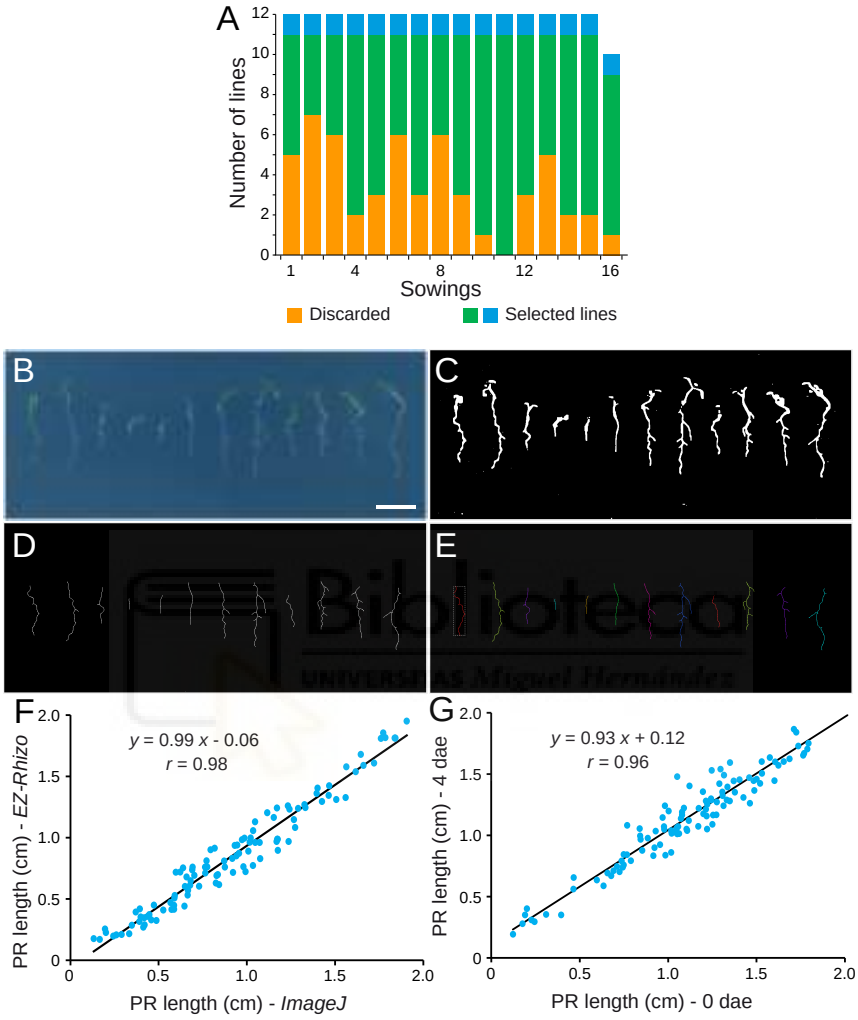

Supplementary Figure S1. Experimental procedure used for root analysis using EZ-Rhizo. (A) Number of accessions studied in each sowing. Those accessions with germination lower than 80% or with ambiguous marker information (orange bars) were discarded for further studies. Col–0 is shown in blue. (B) Petri dishes were individually scanned and cropped. Scale bar: 10 mm (C) Scans were converted into monochrome images using a default threshold and gaps were filled by using the 'Dilate' option. (D) Monochrome images were skeletonized and (E) roots within each image were semi-automatically detected as individual objects and the selected parameters were measured. (F) Scatter plot of PR lengths measured with EZ-Rhizo and ImageJ software. (G) Scatter plot of PR lengths measured at 0 and 4 dae.

Supplementary Figure S2

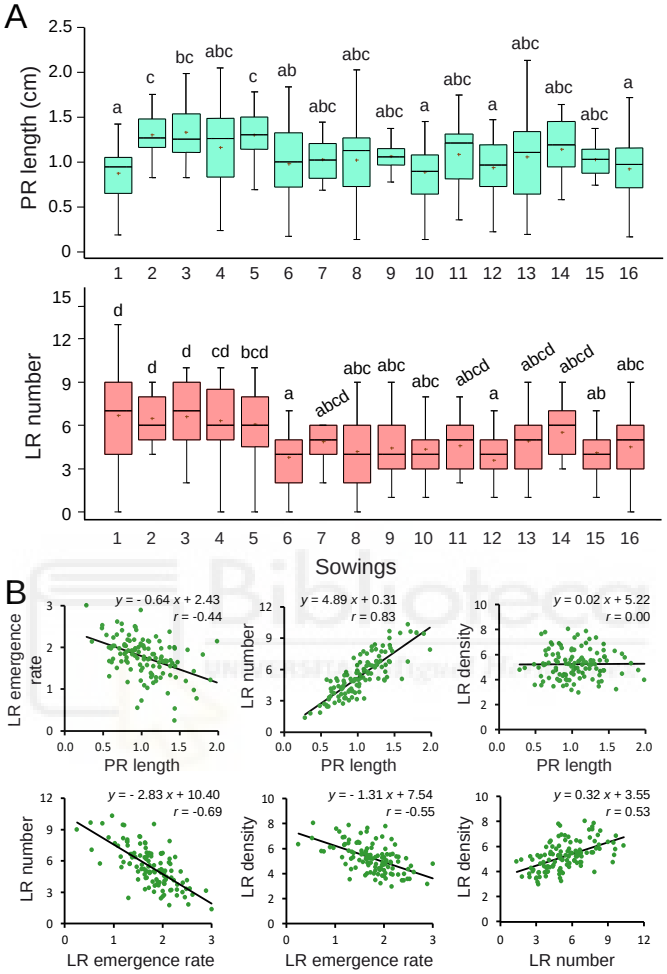

Supplementary Figure S2. Quantitative variation of the studied parameters. (A) Box-plots of PR length and LR number in Col–0 at 4 dae according to the different sowings. Letters indicate statistically significant differences (LSD; P-value < 0.05) between sowings. (B) Scatter plots of average values for the studied parameters in the different accessions.

Supplementary Figure S3

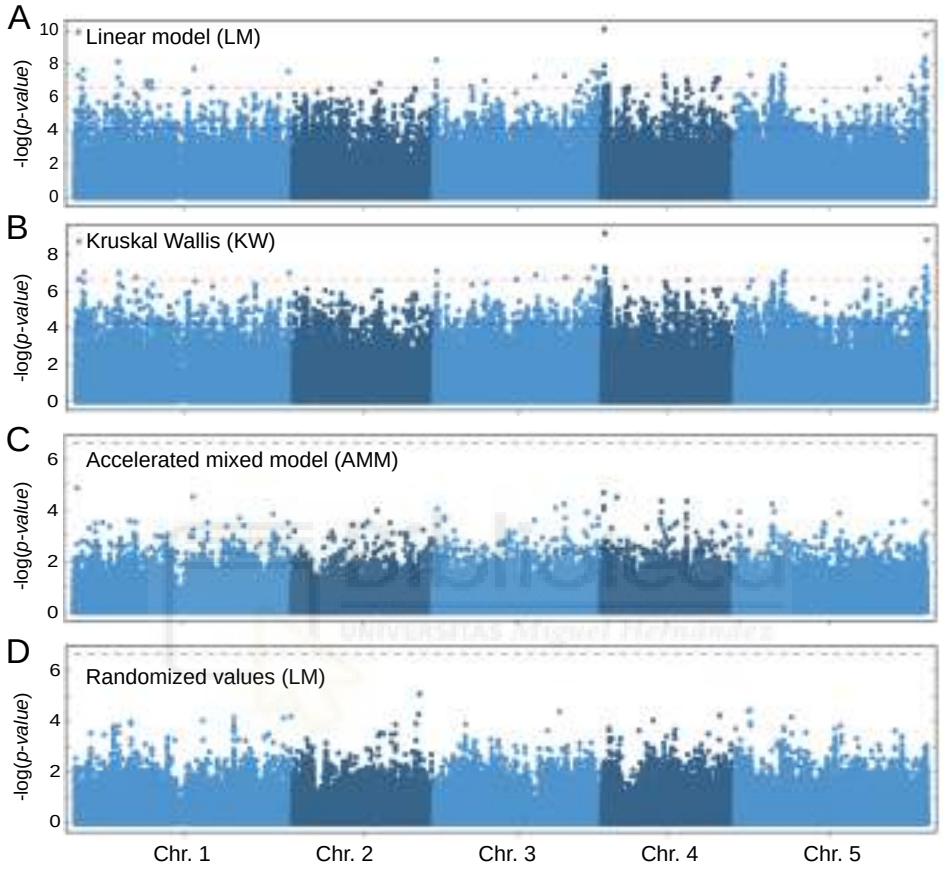

Supplementary Figure S3. Manhattan plots of associations between SNPs and relative LR number using different models. (A) Linear regression model (LM), (B) Kruskal-Wallis (KW) model and (C) accelerated mixed model (AMM). (D) Manhattan plot of association between SNPs and a randomized set of relative LR number values using a linear regression model. Dashed horizontal lines indicate threshold for significance in genome-wide association (GWA) mapping set at $-\log_{10}$(P-value)>6.5.

Supplementary Figure S4

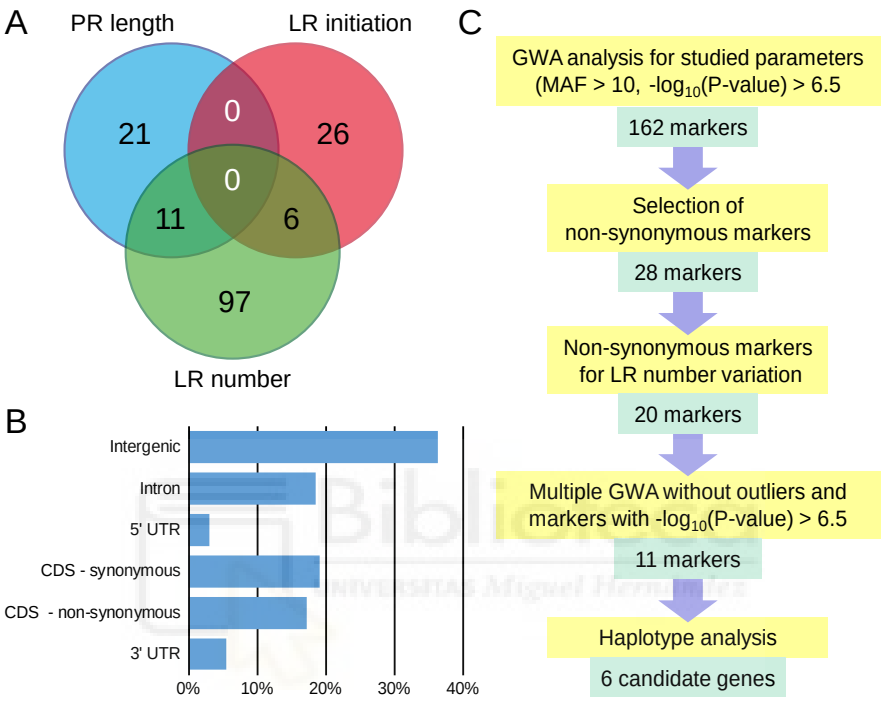

Supplementary Figure S4. Candidate gene selection. (A) Venn-diagram showing the number of statistically significant SNP markers identified from the studied parameters. The single SNP marker found for LR density is not included. (B) Frequency distribution of statistically significant SNP markers grouped according to the gene structural element they interrupt. CDS, coding sequence; UTR, upstream transcription start site. (C) Workflow chart followed for candidate SNP selection involved in LR number variation.

Supplementary Figure S5

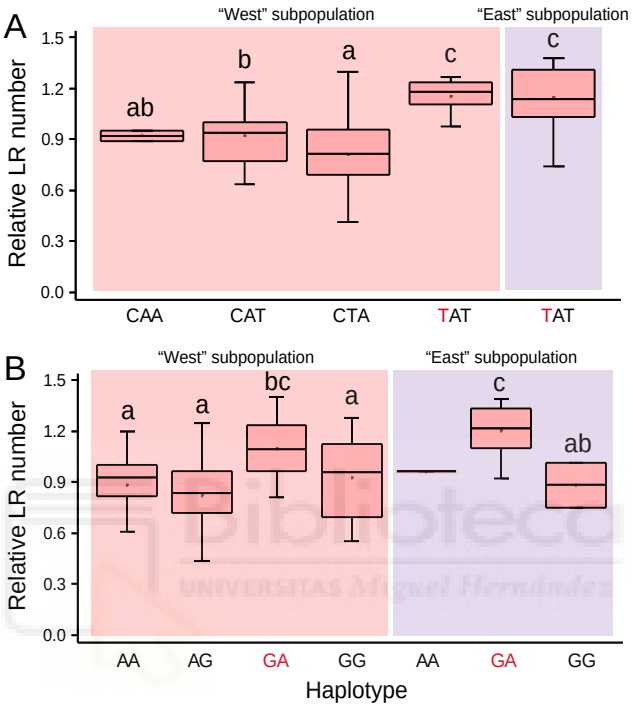

Supplementary Figure S5. Haplotype analysis for markers involved in LR number variation. In each subpopulation, accessions with the same haplotype for selected markers were grouped. Different letters indicate statistically significant differences (LSD; P-value < 0.05). (A) Non-synonymous SNP haplotypes for At4g01090. (B) Non-synonymous SNP haplotypes for At5g16220 and At5g19710. SNP positions associated with higher LR number values are depicted in red.

Supplementary Figure S6

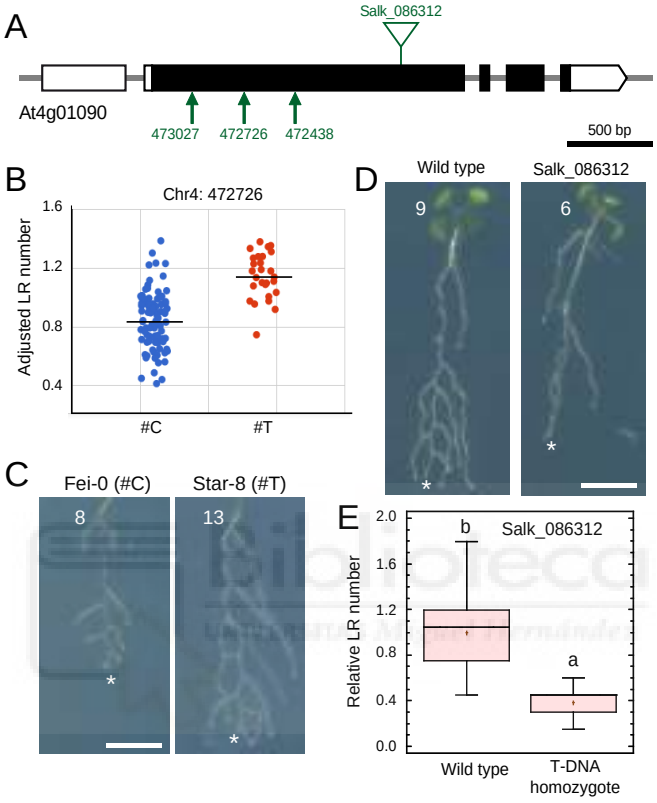

Supplementary Figure S6. Functional analysis of At4g01090 variation concerning LR number. (A) Gene structure of At4g01090. UTR regions and coding exons are represented by white and black boxes, respectively; introns are depicted as grey lines. The studied non-synonymous SNP markers (arrows) and annotated T-DNA insertions (triangles) are indicated in green. (B) Scatterplot of average LR number values used for GWA mapping, sorted by the alleles, C and T, at the Chr4:472726 position. (C) Some accessions of the studied haplotypes with contrasting LR number values. (D) Representative images of wild-type (left) and mutant (right) seedlings of indicated Salk lines at 4 dae. Asterisk marks the PR tip after excision and numbers refer to LR number at 4 dae. Scale bars: 5 mm. (E) Boxplot showing relative LR number values of wild type and homozygous T-DNA mutant plants from the Salk_086312 line. Different letters indicate significant differences (LSD, P-value<0.05).

Supplementary Figure S7

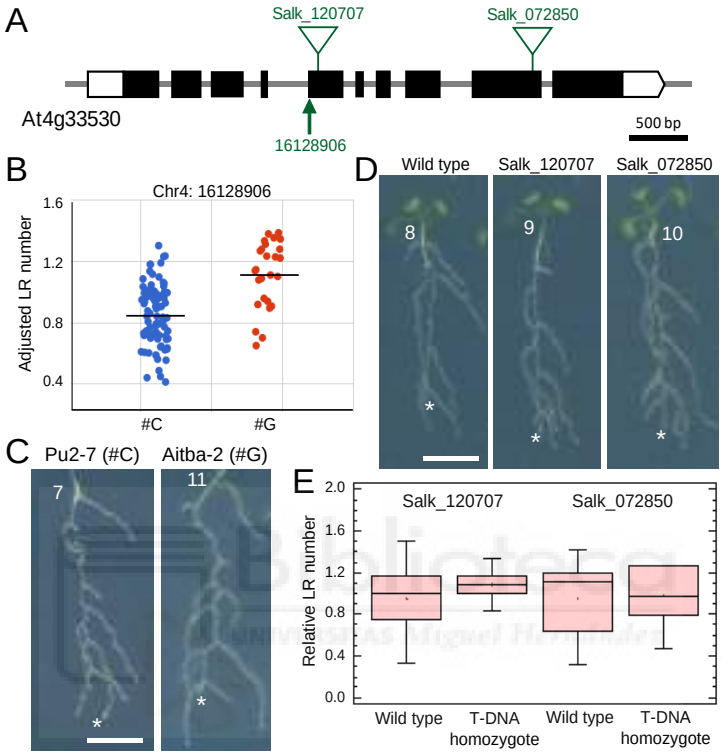

Supplementary Figure S7. Functional analysis of At4g33530 variation concerning LR number. (A) Gene structure of At4g33530. UTR regions and coding exons are represented by white and black boxes, respectively; introns are depicted as grey lines. The studied non-synonymous SNP markers (arrows) and annotated T-DNA insertions (triangles) are indicated in green. (B) Scatterplot of average LR number values used for GWA mapping, sorted by the alleles, C and G, at Chr4:16128906 position. (C) Some accessions of the studied haplotypes with contrasting LR number values. (D) Representative images of wild-type and T-DNA homozygous seedlings of indicated Salk lines at 4 dae. Asterisk marks the PR tip after excision and numbers refer to LR number at 4 dae. Scale bars: 5 mm. (E) Boxplot showing relative LR number values of wild type and homozygous T-DNA mutants of the indicated Salk lines.

Supplementary Figure S8

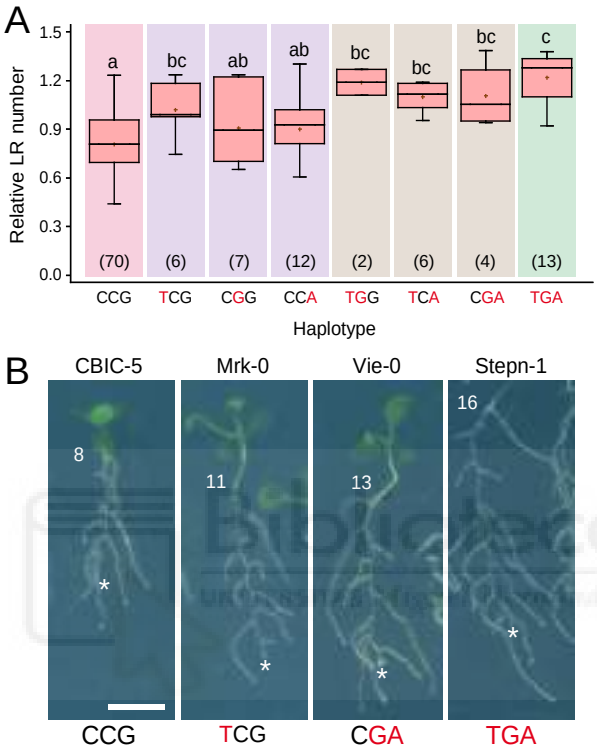

Supplementary Figure S8. Haplotype analysis for selected SNP markers in candidate genes involved in LR number variation. In each subpopulation, accessions with the same haplotype for selected markers were grouped. (A) Haplotypes for Chr4:472726, Chr4:16128906 and Chr5:6665363 markers. Different letters indicate statistically significant differences (LSD; P-value < 0.01). Numbers between parentheses refer to the number of accessions studied. Background colors refer to the number of allelic changes as regards the reference haplotype (CCG, red): one (purple), two (brown), three (green). (B) Some accessions with contrasting haplotypes correlated with wound-induced LR variation. Asterisk marks the PR tip after excision and numbers refer to LR number at 4 dae. Scale bars: 5 mm.

Supplementary Table S2.- Oligonucleotides used in this study

Gene	NASC ID	T-DNA stock / Primer	Oligonucleotide sequences (5'→3')	
At4g01090	N586312	Salk_086312	GCTTATCAAGATCCTTATG	TTATGTAACCTTTCCTGAG
At4g33530	N572850	Salk_072850	TGACCCTTATCATGCTTC	TTATTACCAGCTTCTTCAG
	N620707	Salk_120707	TAATCTTATCTTGATGAGTG	GAAGCTAGTGGATCTTAC
At5g19710	N616200	Salk_116200c	ACATATCAATCCGGTTGAT	TTGAAGAAGCTAGAATCAG
T-DNA		LBb1.3	ATTTTGCCGATTTCGGAAC	
At4g26410		qPCR	GAGCTGAAGTGGCTTCCATGAC	GGTCCGACATACCCATGATCC
At5g19710		qPCR	GTGCTATCAAAGTTGTTAAG	TCTGTTGGACCAGCTTG

Supplementary Table S4.- Matlab script used in this work

```
% Read desired accessions and positions from input xls file
desired_accessions =
xlsread('00_Dataset_Structure.xlsx','posADVRootNumber4DAC','B2:B121');
desired_positions =
xlsread('00_Dataset_Structure.xlsx','posADVRootNumber4DAC','C2:C205979');

% Read hdf5 file
snp = hdf5read('all_chromosomes_binary_gzip.hdf5','snps');
all_positions = hdf5read('all_chromosomes_binary_gzip.hdf5','positions');
all_accessions_struct =
hdf5read('all_chromosomes_binary_gzip.hdf5','accessions');
all_accessions = zeros(all_accessions_struct.length,1);
for i=1:all_accessions_struct.length
    all_accessions(i,1) = str2num(all_accessions_struct(i).Data);
end

number_of_desired_accessions = length(desired_accessions);
number_of_desired_positions = length(desired_positions);

result = zeros(number_of_desired_accessions,number_of_desired_positions);

tic
stored_positions = zeros(number_of_desired_positions,1);
for i=1:number_of_desired_accessions
    disp(100*(i-1)/number_of_desired_accessions);
    current_desired_accession = desired_accessions(i);
    row_of_desired_accession = find(all_accessions ==
current_desired_accession);
    k = 1;
    for j=1:length(all_positions)
        current_position = all_positions(j);
        is_desired_position = find(desired_positions ==
current_position);
        if isempty(is_desired_position)
            % Do nothing
        else
            result(i,k) = snp(row_of_desired_accession,j);
            stored_positions(k,1) = current_position;
            k = k + 1;
        end
    end
end
elapsed_time = toc
```

Artículo 2

Enhanced conjugation of auxin by GH3 enzymes leads to poor adventitious rooting in carnation stem cuttings

Antonio Cano[1], Ana Belén Sánchez-García[2], Alfonso Albacete[3], Rebeca González-Bayón[2], **María Salud Justamante**[2], Sergio Ibáñez[2], Manuel Acosta[1], José Manuel Pérez-Pérez[2]

[1] Departamento de Biología Vegetal (Fisiología Vegetal), Universidad de Murcia, Murcia, Spain

[2] Instituto de Bioingeniería, Universidad Miguel Hernández, Elche, Spain

[3] Departamento de Nutrición Vegetal, Centro de Edafología y Biología Aplicada del Segura-Consejo Superior de Investigaciones Científicas, Murcia, Spain

Frontiers in Plant Science 2018; 9: 566

Published online 26 April 2018 Mar 15. doi: 10.3389/fpls.2018.00566

FI (2018): 4,106 (D1; 20 de 228)

frontiers in Plant Science

published: 26 April 2018
doi: 10.3389/fpls.2018.00566

Enhanced Conjugation of Auxin by GH3 Enzymes Leads to Poor Adventitious Rooting in Carnation Stem Cuttings

*Antonio Cano[1], Ana Belén Sánchez-García[2], Alfonso Albacete[3], Rebeca González-Bayón[2], María Salud Justamante[2], Sergio Ibáñez[2], Manuel Acosta[1] and José Manuel Pérez-Pérez[2]**

[1] Departamento de Biología Vegetal (Fisiología Vegetal), Universidad de Murcia, Murcia, Spain, [2] Instituto de Bioingeniería, Universidad Miguel Hernández, Elche, Spain, [3] Departamento de Nutrición Vegetal, Centro de Edafología y Biología Aplicada del Segura-Consejo Superior de Investigaciones Científicas, Murcia, Spain

OPEN ACCESS

Edited by:
Michael James Considine, The University of Western Australia, Australia

Reviewed by:
Elison B. Blancaflor, Noble Research Institute, United States
Amanda Rasmussen, University of Nottingham, United Kingdom

***Correspondence:**
José Manuel Pérez-Pérez
arolab.edu.umh.es; jmperez@umh.es

Specialty section:
This article was submitted to Plant Physiology, a section of the journal Frontiers in Plant Science

Received: *24 January 2018*
Accepted: *10 April 2018*
Published: *26 April 2018*

Citation:
Cano A, Sánchez-García AB, Albacete A, González-Bayón R, Justamante MS, Ibáñez S, Acosta M and Pérez-Pérez JM (2018) Enhanced Conjugation of Auxin by GH3 Enzymes Leads to Poor Adventitious Rooting in Carnation Stem Cuttings. Front. Plant Sci. 9:566. doi: 10.3389/fpls.2018.00566

Commercial carnation (*Dianthus caryophyllus*) cultivars are vegetatively propagated from axillary stem cuttings through adventitious rooting; a process which is affected by complex interactions between nutrient and hormone levels and is strongly genotype-dependent. To deepen our understanding of the regulatory events controlling this process, we performed a comparative study of adventitious root (AR) formation in two carnation cultivars with contrasting rooting performance, "2101–02 MFR" and "2003 R 8", as well as in the reference cultivar "Master". We provided molecular evidence that localized auxin response in the stem cutting base was required for efficient adventitious rooting in this species, which was dynamically established by polar auxin transport from the leaves. In turn, the bad-rooting behavior of the "2003 R 8" cultivar was correlated with enhanced synthesis of indole-3-acetic acid conjugated to aspartic acid by GH3 proteins in the stem cutting base. Treatment of stem cuttings with a competitive inhibitor of GH3 enzyme activity significantly improved rooting of "2003 R 8". Our results allowed us to propose a working model where endogenous auxin homeostasis regulated by GH3 proteins accounts for the cultivar dependency of AR formation in carnation stem cuttings.

Keywords: adventitious rooting, auxin homeostasis, auxin-conjugating enzymes, *Dianthus caryophyllus*, IAA degradation, polar auxin transport, stem cuttings

INTRODUCTION

New carnation (*Dianthus caryophyllus*) cultivars are mainly bred for traits affecting flower morphology, such as flower size, petal shape, petal number, flower color, and flower vase-life among others, as well as for traits improving plant production and pathogen resistance (Sheela, 2008). However, less attention is usually paid to breed the hidden-part of the plant, its root system, which is very important to warrant water and mineral nutrient supply. Commercial carnation cultivars are vegetatively propagated from axillary stem cuttings that undergo controlled rooting and acclimation (Garrido et al., 1996, 1998), which are high energy-demanding processes that lead to severe losses in certain cultivars (Agulló-Antón et al., 2011; Birlanga et al., 2015). Effective rooting of stem cuttings in several species strongly depends on the production of a functional

adventitious root (AR) system, which is in turn affected by complex interactions between nutrient and hormone levels (Agulló-Antón et al., 2011; Díaz-Sala, 2014; Druege et al., 2016).

We previously performed a detailed analysis of the morphological and physiological changes occurring in the basal region of stem cuttings during rooting in a reference cultivar "Master", and we reported how these were modified in response to exogenous auxin application (Agulló-Antón et al., 2014). We found significant crosstalk between auxin levels, stress hormone homeostasis, and sugar availability in the stem cutting base of "Master" during the initial steps of adventitious rooting (Agulló-Antón et al., 2014). To further characterize these interactions, we made use of a large collection of commercial carnation cultivars selecting two additional cultivars because of their contrasting rooting performance (Birlanga et al., 2015). The "2101–02 MFR" cultivar showed higher number of roots and faster growth than other spray cultivars, while the "2003 R 8" standard cultivar displayed a smaller root system because of a delay in root emergence and further slow root growth (Birlanga et al., 2015). We characterized gene expression and functional changes in the stem cutting base during the early stages of adventitious rooting in these two cultivars, which provided a number of molecular, histological, and physiological markers to initiate the genetic dissection of AR formation in this species (Villacorta-Martín et al., 2015).

In the current work, we performed a comparative study of AR formation in "2101–02 MFR", "Master", and "2003 R 8" grown *in vitro* and in soil plugs. We found that local auxin response in the stem cutting base was required for adventitious rooting, and that this local auxin maximum was dynamically established by active polar auxin transport (PAT) from the leaves. In turn, the bad-rooting behavior of the "2003 R 8" cultivar correlated with enhanced auxin inactivation in the root-formative region. Taking together, our results provide a detailed view of the major pathways triggering AR formation and how differential auxin homeostasis in the stem cutting base might account for cultivar-dependent adventitious rooting in carnation stem cuttings.

MATERIALS AND METHODS

Plant Materials and Growth Conditions

Stem cuttings from the cultivars used in this work ("Master", "2101–02 MFR", and "2003 R 8") are available upon request. All the mother plants had been grown in the same glasshouse under environmental conditions at 37°34'50″ N, 1°46'35″ W, and 395 m altitude within the rooting station of Barberet & Blanc, S.A. (Puerto Lumbreras, Murcia, Spain). Water, fertilizers, and adequate phytosanitary treatments were periodically applied, as described previously (Jawaharlal et al., 2009; Birlanga et al., 2015).

Auxin Transport Inhibition

Terminal stem cuttings of about 10–15 cm with four to five pairs of leaves were manually harvested from several mother plants by skilled operators at the rooting station at noon on 26 April 2016, wrapped in plastic bags just after pinching and stored in a cold chamber at 5 ± 2°C for about 24 h, as described previously (Jawaharlal et al., 2009; Birlanga et al., 2015). A ring of lanolin paste (Sigma–Aldrich, United States) was individually set at about 6–8 mm of the basal end of each stem cutting using a syringe. Previously, warm lanolin was thoroughly mixed with 1% (w/w) of 1-naphthoxyacetic acid (1-NOA; Sigma–Aldrich, United States), 1% (w/w) of 1-*N*-naphthylphthalamic acid (NPA; Sigma–Aldrich, United States), or an equimolar mixture (0.8% w/w) of α-naphthalene acetic acid (NAA; Duchefa, Netherlands) and indole-3-butyric acid (IBA; Duchefa, Netherlands) for the different treatments. Non-supplemented lanolin paste was used as a mock treatment. After the treatments, the cuttings were individually planted in 104-well trays containing moistened peat/perlite (90/10 v/v) plugs (3.5 cm diameter × 3.5 cm length; ∼26 cm^3) in a Gothic Arch Greenhouse at 38°16'43″ N, 0°41'15″ W, and 96 m altitude (Elche, Spain). Stem cuttings were grown from 27 April to 2 June 2016 under the environmental conditions of the greenhouse, with periodic sprinkler irrigation (5 min every 4 h).

For scoring adventitious rooting, the soil plug was carefully removed by washing it with high pressure tap water and the entire root system was imaged using a Nikon D3200 camera with an AF-S DX NIKKOR 18–55 mm f/3.5-5.6G VR objective. We visually defined seven rooting stages representing the different AR phenotypes observed (Birlanga et al., 2015).

Auxin Transport Analysis

Three-to-five stem cutting basal sections (50 mm) from each carnation cultivar were used to estimate the basipetal indole-3-acetic acid (IAA) transport, as previously described (Garrido et al., 2002; Nicolás et al., 2007). The isolated stem sections were placed on top of an agar block keeping their endogenous apical–basal orientation and a 5 μl drop of a 200 μM labeled IAA ($[^{13}C]_6C_4H_9NO_2$) was added to the top of each stem section. Every 30 min, the agar block was replaced by a new agar block and the experiment was carried out for 240 min. The amount of labeled IAA present in the agar blocks was analyzed by U-HPLC–MS Orbitrap (ThermoFisher Scientific, United States) using negative electrospray mode (ESI). Detection was made using the *m*/*z* ratio for labeled IAA (*m*/*z* 180.0761) and retention time to unequivocally identify transported labeled IAA. The linear traces of the cumulative labeled IAA transported per time unit were used to estimate different transport parameters according to Van der Weij (1932).

Chemical Inhibition of Auxin Degradation

Terminal stem cuttings were collected from several mother plants at noon on 28 September 2017 and immediately placed on Erlenmeyer flasks filled with 50 mL of Murashige and Skoog salt media with Gamborg's vitamins, pH 5.0 supplemented with 10 μM adenosine-5'-[2-(1H-indol-3-yl)ethyl]phosphate (AIEP) or with distilled water as a mock treatment. After 15 h in the dark, the cuttings were individually planted in 104-well trays and kept in a Gothic Arch Greenhouse as described above. Adventitious rooting stage and total root area were scored 29 days after planting as indicated elsewhere (Birlanga et al., 2015).

Phytohormone Extraction and Analysis

Phytohormones were extracted and analyzed according to Großkinsky et al. (2014) and Villacorta-Martín et al. (2015). Auxin homeostasis metabolites were identified according to molecular mass and retention time from Total Ion Chromatograms obtained in the phytohormone analysis.

RNA Isolation and First-Strand cDNA Synthesis

Sample collection and RNA extractions were performed as described elsewhere (Villacorta-Martín et al., 2015). Briefly, total RNA from ∼120 mg of powdered carnation stem tissue from 10 to 15 individuals was extracted in triplicate using Spectrum Plant Total RNA Kit (Sigma–Aldrich, United States) as previously described (Villacorta-Martín et al., 2015), and cDNA samples were synthesized from purified RNA using the iScript Reverse Transcription Supermix (Bio-Rad, United States). RNA extraction and cDNA synthesis were preformed according to the manufacturer's instructions.

Gene Expression Analysis by Real-Time Quantitative PCR

Primers were designed to amplify 87–178 bp of the cDNA sequences (**Supplementary Table S1**). To avoid amplifying genomic DNA, forward and reverse primers were designed to bind different exons and to hybridize across consecutive exons.

For real-time quantitative PCR, 14 μl reactions were prepared with 7 μl of the SsoAdvanced Universal SYBR Green Supermix (Bio-Rad, United States), 4 μM of specific primer pairs, and 1 μl of cDNA- and DNase-free water (up to 14 μl of total volume reaction). PCR amplifications were carried out in 96-well optical reaction plates on a Step One Plus Real-Time PCR System (Applied Biosystems, United States). Three biological and two technical replicates were performed for each gene. The thermal cycling program started with a step of 10 s at 95°C, followed by 40 cycles (15 s at 95°C and 60 s at 60°C), and the melt curve (from 60 to 95°C, with increments of 0.3°C every 5 s). Dissociation kinetics of the amplified products confirmed their specificity.

Primer pair validation was performed by using the $2^{-\Delta\Delta CT}$ method (Livak and Schmittgen, 2001). Gene expression was measured by the absolute quantification method (Lu et al., 2012) by using a standard curve which comprised equal amounts from each cDNA sample. The *Dca3524* gene (homolog of the *Arabidopsis thaliana* housekeeping gene *EF1α*; AT5G60390) was chosen for normalization of the assayed genes, when needed. In each gene, mean of fold-change values relative to the distal region of the leaf in the "Master" cultivar (for the leaf data) and to the −23 h dataset in "2101–02 MFR" (for stem cutting base data) was used for graphic representation. ΔC_T values were analyzed using SPSS 21.0.0 (SPSS Inc., United States) by applying the Mann–Whitney *U*-test for statistical differences between cDNA samples (P-value ≤ 0.05).

In Silico Identification of Candidate Genes From RNA-Sequencing Data and Heat Map Drawing

Sixty-nine differentially expressed genes (DEGs) identified from previous RNA sequencing (RNA-seq) data using the Short Time-Series Expression Miner (STEM) program (Villacorta-Martín et al., 2015) and annotated as GO:0009734 "auxin-activated signaling pathway" were initially selected; this list was further completed by including 35 genes from CarnationDB (Yagi et al., 2014) using keyword search (**Supplementary Table S2**). Sixty-six of these carnation genes were confirmed as putative auxin-responsive genes based on their highest homology with the *A. thaliana* annotation (Berardini et al., 2015). Following a similar approach, 49 genes were selected as cytokinin (CK)-related genes (GO:0009736 and GO:0009690) (**Supplementary Table S2**). Gene expression data from previous experiments (Villacorta-Martín et al., 2015) were processed using the heatmap.plus package of R[1]. Neighbor-joining distance matrixes between genes (rows) and between samples (columns) were calculated to build the dendrograms.

Statistical Analyses

Statistical analyses were performed using the StatGraphics Centurion XV software (StatPoint Technologies, Inc., Warrenton, VA, United States). Data outliers were identified based on aberrant standard deviation values and excluded for posterior analyses. One-sample Kolmogorov–Smirnov tests were performed to analyze the goodness-of-fit between the distribution of the data and a given theoretical distribution as previously described (Chacón et al., 2013). Average ± standard deviation values were represented, except for those cases that did not exhibit a normal distribution and for which the median was used instead. The differences between the data groups were analyzed by *t*-test ($P \leq 0.05$) when only two groups were compared. To compare the data for a given variable, we performed multiple testing analyses with a two-way ANOVA (cultivar × day after planting or cultivar × treatment) and the Tukey's honestly significant difference (HSD) tests ($P \leq 0.05$). Nonparametric tests were used when necessary.

RESULTS

Adventitious Rooting in Carnation Stem Cuttings Is Genotype-Dependent

Using an environmentally controlled hydroponic system developed previously (Birlanga et al., 2015), we characterized the root system architecture during rooting of stem cuttings of two standard cultivars, "Master" and "2003 R 8", and one spray cultivar, "2101–02 MFR" (**Figure 1**). In the "2101–02 MFR" and the "Master" cultivars, ARs emerged between 13 and 15 days after planting while there was a significant delay in AR emergence in the "2003 R 8" cultivar (**Figure 1A**). Although the three cultivars showed a well-developed and functional root system at

[1]http://www.r-project.org/

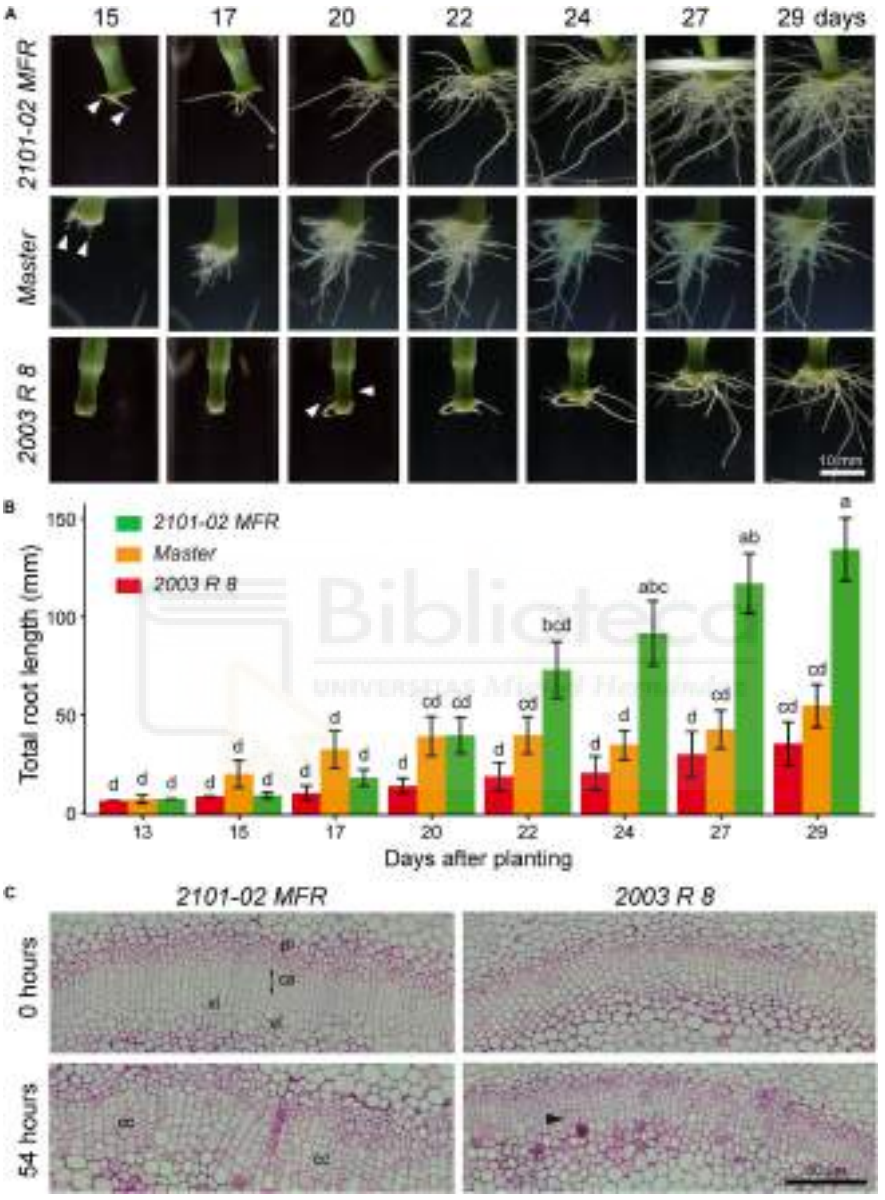

FIGURE 1 | Cultivar-dependent adventitious rooting in carnation stem cuttings. **(A)** Time series of adventitious rooting in carnation stem cuttings grown *in vitro*. A representative sample in each cultivar was imaged between 15 and 29 days after planting. **(B)** The average lengths ± standard deviations of scanned root systems between 13 and 29 days are shown for the studied cultivars. Letters indicate significant differences ($P < 0.05$) between data points ($n = 20$). **(C)** Light micrographs from cross-sections of stem cutting basal regions at 0 and 54 h after planting. Black arrowhead indicates periclinal cell divisions in the cambium (ca). cc, cell clusters; pl: phloem; xl, xylem.

29 days, the "2101–02 MFR" cultivar showed a larger root system than the other two (**Figure 1A**). Considering total root length as an indicator of rooting performance (Birlanga et al., 2015), exponential root growth in "Master" initiated earlier (15 days) than in the two other cultivars: "2101–02 MFR" at 17 days and "2003 R 8" at 22 days (**Figure 1B**). The bad-rooting performance of "2003 R 8" was mostly caused by the severe growth delay of its root system compared to the other studied cultivars (**Figure 1B**). Conversely, the "2101–02 MFR" cultivar showed continuous root growth along the experiment with higher root growth rates (mm/day) than the two other cultivars (**Figure 1B**).

Periclinal cell divisions within the cambial ring were among the first morphological markers for the AR induction phase (de Klerk et al., 1999) observed in this species (Agulló-Antón et al., 2014). Discrete clusters of meristematic cells appeared along the cambial ring shortly afterward (Agulló-Antón et al., 2014), which correspond to AR initiation phase (de Klerk et al., 1999). Consistently with early AR initiation in "Master" and "2101–02 MFR", cell clusters were observed within the vascular cambium at 54 h after planting (**Figure 1C**), while only sporadic periclinal divisions at the cambial ring were observed in "2003 R 8" growing in the hydroponic system (**Figure 1C**).

Based on a previously defined qualitative scale for rooting performance (**Figure 2A**; Birlanga et al., 2015), we confirmed the AR phenotypes of these three cultivars grown in soil plugs at the rooting station of our commercial provider. At 20 days, most stem cuttings in "Master" and "2101–02 MFR" were on stages 3 and 4, while only 60% of them reached stage 2 in "2003 R 8" (**Supplementary Figure S1A**). One week later, "Master" and "2003 R 8" cuttings reached similar rooting performances (**Supplementary Figure S1A**), but the root density in "2101–02 MFR" cuttings increased significantly (**Supplementary Figures S1A,B**). These results confirmed that the rooting behavior of "2003 R 8" (bad-rooting), "Master" (intermediate-rooting), and "2101–02 MFR" (good-rooting), despite it might be influenced by the environment and by the physiological status of the mother plants (Villanova et al., 2017), was under strict genetic control.

Auxin Is Required for AR Initiation and AR Growth in Stem Cuttings

After stem cutting harvest, basipetal transport of auxin from mature leaves contributes to auxin accumulation in the stem cutting base and hence to AR formation (Garrido et al., 2002). In agreement with these results, exogenous auxin application improved AR formation in stem cuttings of "Master" (**Figures 2A–C**), likely by accelerating the formative divisions that lead to the establishment of the new root primordia (Agulló-Antón et al., 2014). The bad-rooting behavior of "2003 R 8" was rescued by exogenous auxin application, while a slightly negative effect of exogenously applied auxin was observed for adventitious rooting of "2101–02 MFR" cuttings (**Figures 2A–C**), leading to enhanced formation of callus-like tissue. However, the effect of the auxin treatment seems to be stronger at 29 days, because then the three cultivars showed similar root phenotypes (**Figure 2C**).

To confirm the relevance of a functional auxin transport through the stem for rooting, we chemically inhibited PAT either by NPA (Guerrero et al., 1999), which disrupts membrane trafficking (Geldner et al., 2001), or by 1-NOA, which blocked the activities of both auxin influx and efflux carriers (Parry et al., 2001; Lanková et al., 2010). Chemical disruption of PAT strongly inhibited AR formation in the stem cutting base in all three cultivars (**Figure 2B**). The inhibitory effect of NPA was stronger than that of 1-NOA, which also caused subtle cultivar-specific differences in AR development and growth, with incomplete inhibition of AR formation in "2101–02 MFR" (**Figure 2C**).

We next measured endogenous IAA transport through the stem using labeled IAA. The IAA transport rate was higher in "2003 R 8" than in the two other cultivars, while "Master" showed the highest IAA transport intensity (i.e., IAA mobilization) of the three (**Figure 2D**). In addition, we gathered the expression data of several genes putatively encoding auxin influx (*AUX/LAX*) and auxin efflux (*PIN* and *ABCB*) transporters (Oliveros-Valenzuela et al., 2008; Villacorta-Martín et al., 2015; Sánchez-García et al., 2018).

We validated these results by quantitative reverse transcription PCR (RT-qPCR) and extended them to additional time-points at −23 and −15 h. On the one hand, the expression of *DcAUX1* (*Dca32369*) and *DcLAX3* (*Dca6786*) auxin influx genes was not considerably changed over the rooting experiment in these two contrasting cultivars, although it was slightly higher in "2003 R 8" (**Supplementary Figures S2A,B**). On the other hand, the expression of auxin efflux genes, *DcABCB1* (*Dca43405*), *DcABCB19* (*Dca25164*), and *DcPIN1* (*Dca20927*), was higher in the stem cutting base at harvest time (−23 h) and diminished after planting in "2101–02 MFR" and specially in "2003 R 8" (**Supplementary Figures S2C–E**). In addition, the expression levels of *DcABCB1*, *DcABCB19*, and *DcPIN1*, were significantly higher in "2003 R 8" than in "2101–02 MFR" (**Supplementary Figures S2C–E**). These results indicated that the differences in PAT through the stem between "2101–02 MFR" and "2003 R 8" are likely caused by differential expression of auxin transporters, although these differences did not explain the contrasting rooting performance between "2003 R 8" and "2101–02 MFR".

Auxin Is Produced in Mature Leaves and Is Actively Transported to the Stem

The differences in AR formation between cultivars might arise by differential auxin production from mature leaves, as these are the main source of endogenous auxin required for rooting stem cuttings (Garrido et al., 2002). Carnation leaves are linear, display parallel venation, and are directly attached to the stem by a proximal sheath-like tissue, resembling monocot leaves (**Figure 3A**; Agulló-Antón et al., 2013). We measured endogenous auxin levels in proximal and distal regions of the leaf blade (**Figures 3A,B**). IAA was found at similar, albeit low levels, at the proximal region of the leaves in the three studied cultivars and it was below detection in their distal region (**Figure 3C**). In most plants, such as Arabidopsis and rice, the major IAA biosynthesis pathway occurs through indole-3-pyruvic acid (IPyA) (Zhao, 2010).

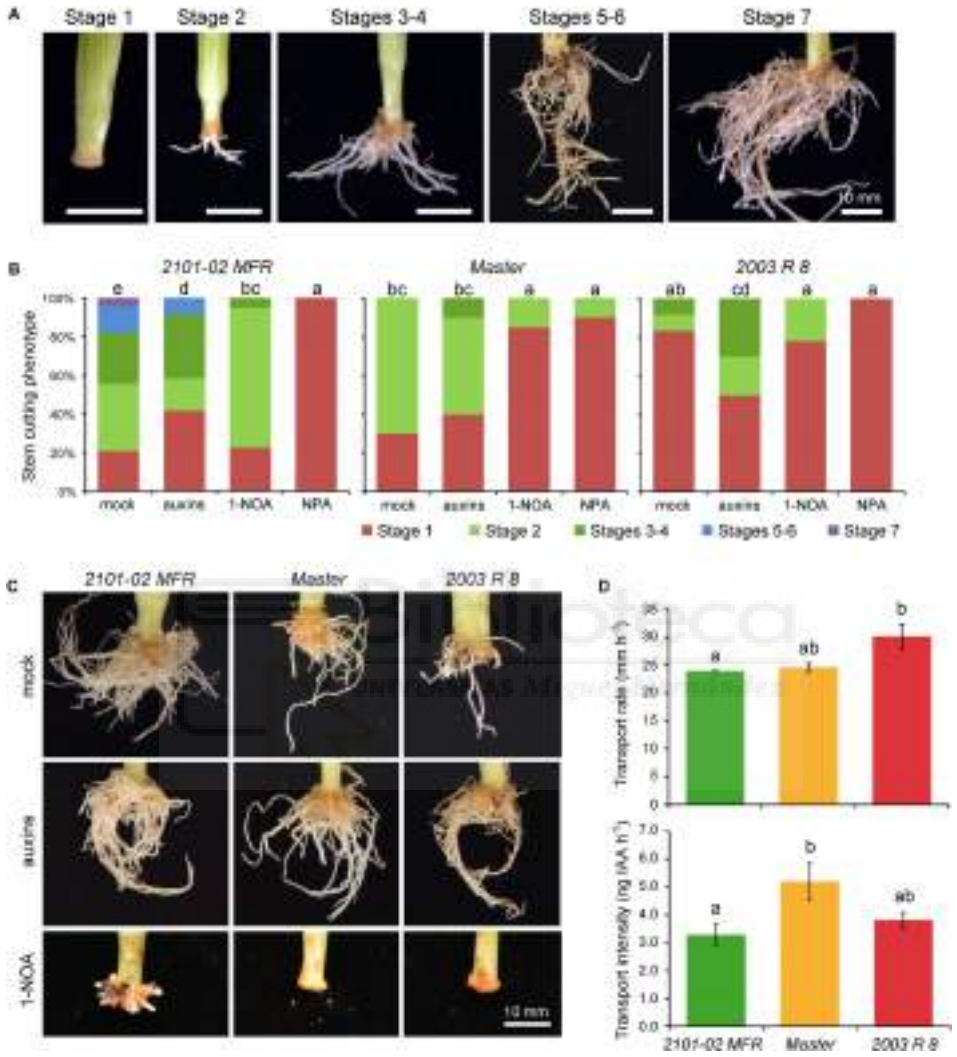

FIGURE 2 | Auxin transport through the stem cutting base is required for adventitious root (AR) formation. **(A)** Representative images of adventitious rooting stages in carnation stem cuttings growing in soil plugs as defined previously (Birlanga et al., 2015). To visualize the entire root system, the soil substrate was carefully removed with pressurized water. **(B)** Graphic representations of rooting stage values in different carnation cultivars and treatments at 29 days, as described in Birlanga et al. (2015). Different letters indicate significant differences ($P < 0.05$) over sample means (cultivar × treatment). **(C)** Representative images of adventitious rooting in the studied carnation cultivars at 29 days treated with exogenous auxins or a polar auxin transport inhibitor (1-NOA). **(D)** Basipetal auxin transport parameters, transport rate (mm h^{-1}), and transport intensity (ng IAA h^{-1}) measured in stem cutting basal sections of the studied cultivars. Average ± standard deviation values are shown. Letters indicate significant differences ($P < 0.05$) over samples.

The tryptophan aminotransferase (TAA/TAR) family produces IPyA and the YUCCA (YUC) family functions downstream in the conversion of IPyA to IAA (Mashiguchi et al., 2011; Won et al., 2011; Mano and Nemoto, 2012; Tivendale et al., 2014). Putative carnation orthologs *DcTAR2a* (*Dca35926*) and *DcYUC1* (*Dca37589*) were differentially expressed in proximal

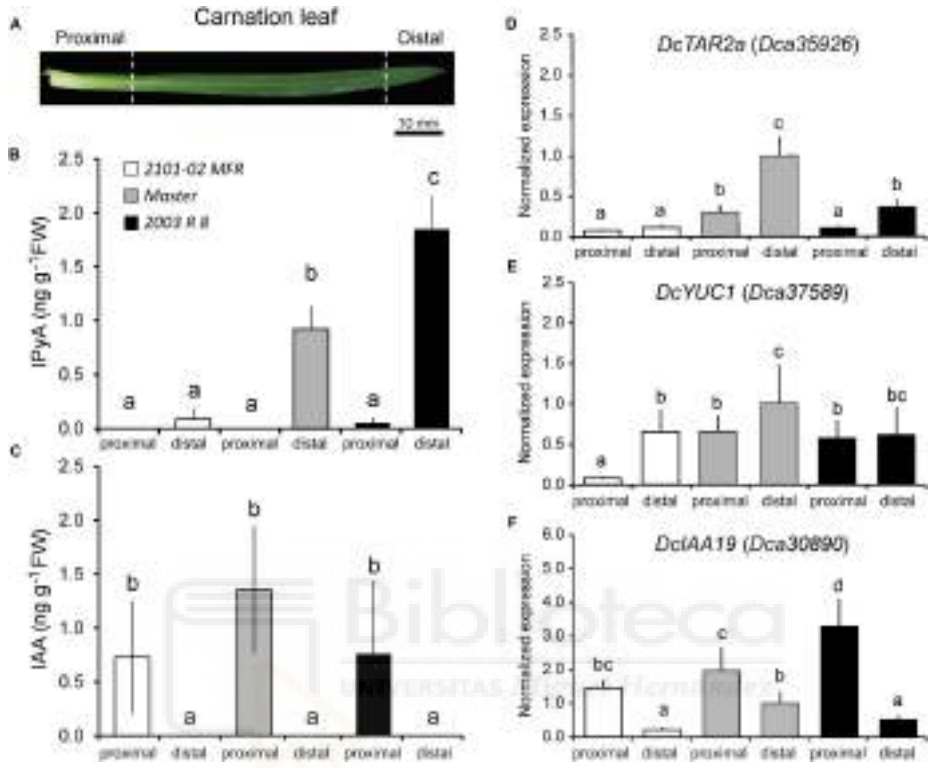

FIGURE 3 | Differential auxin biosynthesis and auxin signaling in mature leaves at harvest. **(A)** Scheme of a carnation stem cutting leaf with indication of the two regions studied. **(B)** Indole-3-pyruvic acid (IPyA) and **(C)** indole-3-acetic acid (IAA) were measured in mature leaves of carnation stem cuttings at severance time. Average ± standard deviation values are shown. **(D,F)** RT-qPCR of the expression of selected transcripts related to **(D,E)** auxin biosynthesis or **(F)** auxin signaling in mature leaves of carnation stem cuttings at harvesting time. Bars indicate normalized expression levels ± standard deviation relative to the distal region of the leaf in the "Master" cultivar. Letters indicate significant differences between samples ($P < 0.05$).

regions of mature leaves in all the three cultivars (**Figures 3D,E**). In addition, the expression of *DcTAR2a* and *DcYUC1* was significantly lower in "2101–02 MFR" than in "Master", which was in agreement with the higher IAA levels found in the leaves of "Master" (**Figure 3C**). Consistent with local auxin biosynthesis occurring preferentially in the tip of the leaf, as it occurs in rice (Yamamoto et al., 2007), we confirmed that IPyA accumulated in the distal region of mature leaves, with significantly lower levels in "2101–02 MFR" leaves (**Figure 3B**). Auxin influx genes *DcAUX1* and *DcLAX3* were significantly expressed at higher levels in the proximal leaf region (**Supplementary Figures S3A,B**). The expression of genes involved in auxin efflux, such as *DcPIN1*, *DcABCB1*, and *DcABCB19*, was significantly higher in the proximal region of the leaves in the three cultivars (**Supplementary Figures S3C,E,F**). On the other hand, the carnation ortholog of *PIN3*, *Dca17139*, did not showed significant changes along the studied leaf regions (**Supplementary Figure S3D**). Similarly to that found for the stem (see above), combined expression levels of these auxin transporter genes were lower in "2101–02 MFR" than in the other two cultivars (**Supplementary Figure S3**), suggesting lower auxin transport rates also in the leaves of "2101–02 MFR". To confirm the establishment of a gradient of IAA concentration within the leaf blade, we studied the expression of the auxin-induced *DcIAA19* gene (Villacorta-Martín et al., 2015) as a signaling read-out for the endogenous auxin gradient in the leaves (**Figure 3F**).

Differential Accumulation of Active IAA in the Stem Cutting Base Between Cultivars Affects Rooting

Auxin flooding in the vascular region above the wounding has been proposed to trigger de-differentiation and cell cycle reactivation of cambial cells in this region (Acosta et al., 2009).

Endogenous IAA levels in the stem cutting base of "Master" transiently increased after harvesting and before planting from 8 to 65 ng g^{-1} FW (**Figure 4A**), similarly to as previously reported (Agulló-Antón et al., 2014). In "2101–02 MFR", the IAA levels increased fivefold from steady-state levels up to 42 ng g^{-1} FW at planting time (**Figure 4A**). *DcYUC1* transcript levels were significantly downregulated in the stem cutting base of "2003 R 8" and "2101–02 MFR" after harvesting (**Supplementary Figure S2F**), and negligible IPyA concentrations were detected in these tissues. These results allowed us to discard the hypothesis that local auxin biosynthesis had contributed to the endogenous IAA accumulation found in the stem cutting base of these two cultivars after harvesting them from the mother plants.

Despite the highest PAT rate in the stem cutting base of "2003 R 8" (**Figure 2D**), its endogenous IAA level did not significantly increase after harvesting and during rooting (**Figure 4A**). These results suggested that the auxin maximum in the stem cutting base of "2003 R 8" was not properly formed. In *A. thaliana*, the main IAA degradation pathways (Ludwig-Müller, 2011) include oxidation by DIOXYGENASE FOR AUXIN OXIDATION 1 (DAO1) (Porco et al., 2016) and conjugation by GRETCHEN HAGEN 3 (GH3) amide synthetases (Staswick et al., 2005), which played highly redundant roles to regulate endogenous auxin levels (Mellor et al., 2016). To account for IAA degradation in the stem cutting base of the studied cultivars, we measured IAA conjugated to aspartic acid (IAA-Asp) and 2-oxoindole-3-acetic acid (oxIAA), which are metabolically inactive forms unable to be transported through the PAT system (Pencík et al., 2013). At harvest time (−23 h) and before rooting (−15 h), the levels of IAA-Asp in the stem cutting base of the three cultivars were low, but significantly increased at planting time and during rooting in "2003 R 8" (**Figure 4B**). On the other hand, oxIAA levels were low in the stem cutting base of these cultivars up to 54 h (**Figure 4C**). Remarkably, IAA-Asp levels in the stem cutting base of the bad-rooting cultivar, "2003 R 8", increased threefold between planting time and 24 h (161.4 ± 14.1 ng g^{-1} FW) and returned to initial levels at 54 h (**Figure 4B**), which suggest further modification of the IAA-Asp pool by additional conjugations or oxidative reactions. OxIAA levels were not significantly different in the stem cutting base of "2003 R 8" during rooting, although some variation was found in oxIAA levels in "2101–02 MFR" during early rooting (**Figure 4C**).

We wondered whether the differences in endogenous IAA levels in the stem cutting base shortly after harvesting and before rooting might have a functional relevance for the rooting differences observed between cultivars. As described above, we used *DcIAA19* expression as a read-out for endogenous IAA levels. Interestingly, *DcIAA19* expression in the stem cutting base of the good-rooting cultivar ("2101–02 MFR") matched its endogenous IAA levels (**Figure 4D**), while in the bad-rooting cultivar ("2003 R 8"), *DcIAA19* expression significantly decreased after planting (**Figure 4D**).

We previously identified five carnation genes encoding GH3-like proteins whose orthologs synthesize IAA–amino acid conjugates, such as IAA-Asp (Staswick et al., 2005), two of which are known to be differentially expressed during rooting (Sánchez-García et al., 2018). The expression of *DcGH3.1* (*Dca37575*) was significantly higher in "2003 R 8" than in "2101–02 MFR", with the strongest differences in expression after severance and before rooting (**Figure 4E**). In line with the endogenous oxIAA levels found in "2101–02 MFR" and "2003 R 8", differences in gene expression levels were observed for the *DAO1* ortholog, *DcDAO1* (*Dca2789*) (**Figure 4F**). To confirm whether the differential accumulation of IAA-Asp in the studied cultivars contributed to rooting performance, we incubated freshly harvested stem cuttings of "2101–02 MFR", "Master", and "2003 R 8" with AIEP, a known chemical inhibitor of GH3 activities (Böttcher et al., 2012). Treatment with 10 μM AIEP did not significantly improve rooting performance either in the good-rooting cultivar "2101–02 MFR" or in "Master" (**Figure 5A**). In contrast, AIEP significantly improved the rooting performance of the bad-rooting cultivar "2003 R 8" (**Figure 5A**), which now produced more roots than in "Master" (**Figure 5B**). We found that the AIEP treatment increased both the percentage of cuttings with visible roots (**Figure 5C**) and the total root area (**Figure 5D**) in "2003 R 8", with hardly any effect in the two other cultivars. Our results confirmed that GH3-mediated IAA-Asp accumulation in "2003 R 8" reduced IAA accumulation in the stem cutting base, which in turn negatively affects its rooting performance.

Cytokinins and Stress-Related Hormone Levels in Cultivars With Contrasting Rooting Performance

Cytokinins are negative regulators of AR formation (de Klerk et al., 2001; Werner et al., 2003; Konieczny et al., 2009). We previously found that *trans*-zeatin (*t*Z) levels were high in the stem cutting base of "Master" after excision and they dropped abruptly after planting (Agulló-Antón et al., 2014). Consistently with these results, we found high *t*Z levels in the stem cutting base of "2101–02 MFR" and "2003 R 8" after excision (43.9 ± 15.8 and 34.8 ± 16.1 ng g^{-1} FW, respectively) that were quickly reduced in both cultivars before planting (**Supplementary Figure S4A**). From 24 h, *t*Z levels significantly increased in "2003 R 8" compared with those in "2101–02 MFR", and remained at low levels during the experiment in this later cultivar (**Supplementary Figure S4A**).

Stem cutting excision from the mother plant alters the endogenous levels of the hormones regulating stress responses, particularly jasmonate (JA), abscisic acid (ABA), and ethylene (Agulló-Antón et al., 2014). In the stem cutting base of "Master", endogenous levels of the metabolic precursor of ethylene, 1-aminocyclopropane-1-carboxylic acid (ACC), were low after excision and slightly increased during rooting (Agulló-Antón et al., 2014). While we found similar results regarding the ACC levels in the stem cutting base of "2101–02 MFR", those in "2003 R 8" were constitutively and significantly lower during rooting (**Supplementary Figure S4B**). The increasing levels of ACC in "Master" and "2101–02 MFR" might reflect the decrease in endogenous ethylene production during adventitious rooting. The highest levels of endogenous ABA were found after cutting excision and during cold storage, with significant higher levels of ABA in "2101–02 MFR" than in "2003 R 8" (**Supplementary Figure S4C**). ABA levels diminished at planting time in both

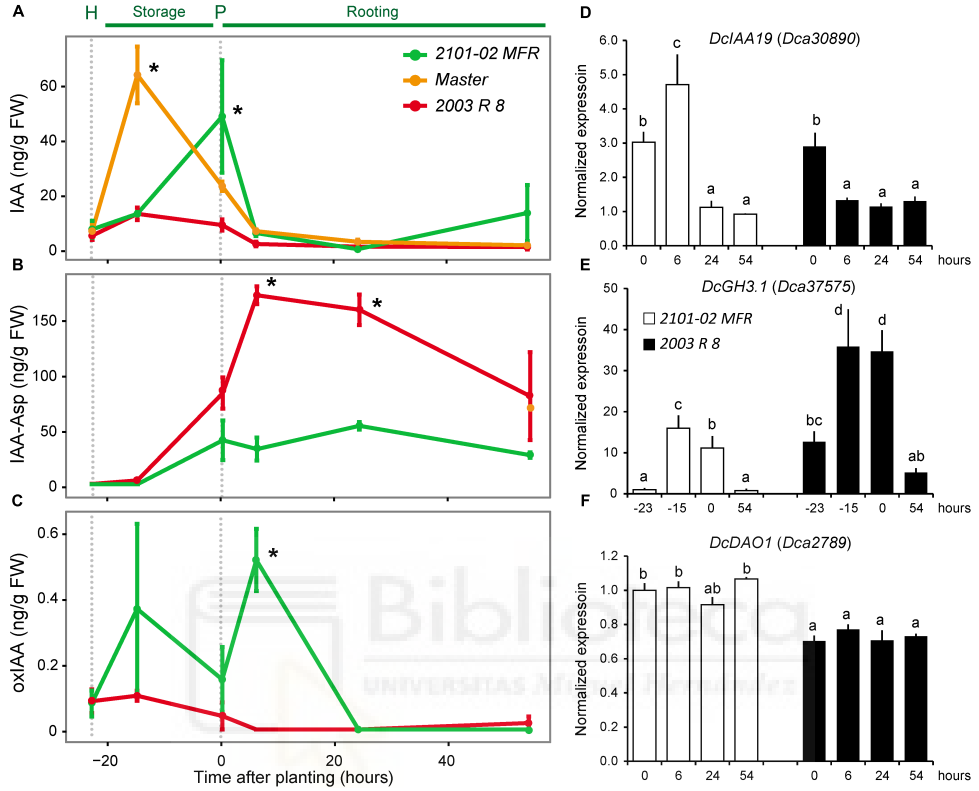

FIGURE 4 | Endogenous levels of several auxin derivatives in the stem cutting base during adventitious rooting and expression of selected genes. **(A)** IAA, **(B)** indole-3-acetyl-L-aspartic acid (IAA-Asp), and **(C)** 2-oxo-indole-3-acetic acid (oxIAA). Average ± standard deviation values are shown at selected time-points: at harvesting time (H; –23 h), during storage at low temperature (–15 h), at planting time (P; 0 h), and during rooting (6, 24, and 54 h). Asterisks indicate significant differences between samples ($P < 0.05$). **(D–F)** Real-time PCR quantification of the expression of **(D)** *DcIAA19*, **(E)** *DcGH3.1*, and **(F)** *DcDAO1* relative to the –23 h dataset in the "2101–02 MFR" cultivar (not shown in the graph). Bars indicate normalized expression levels ± standard deviation. Letters indicate significant differences between samples ($P < 0.05$).

cultivars due to stem cutting rehydration and slightly increased during rooting (**Supplementary Figure S4C**).

Auxin- and Cytokinin-Responsive Gene Expression Are Correlated With Rooting Performance

Auxin signaling is mediated through the interaction of active auxin (e.g., IAA) with the TRANSPORT INHIBITOR RESPONSE 1/AUXIN SIGNALING F-BOX PROTEIN (TIR1/AFB) co-receptor and the Auxin/INDOLE-3-ACETIC ACID (Aux/IAA) transcriptional repressors, resulting in degradation of the Aux/IAAs and the release of AUXIN RESPONSE FACTOR (ARF) transcriptional partners (Lavy and Estelle, 2016). Some genes putatively encoding Aux/IAA repressors of auxin signaling, such as SUPPRESSOR OF HY2 MUTATION (SHY2), also named IAA3 (Tian et al., 2002) (*Dca3109*), IAA4 (*Dca29160*), or MASSUGU 2 (MSG2, also named IAA19; Tatematsu et al., 2004) (*Dca30890*), were expressed at higher levels in "2101–02 MFR" than in "2003 R 8" at 6 h (**Figure 6A**). In addition, other early auxin-responsive genes, such as *DcIAA13* (Weijers et al., 2005) (*Dca43286*), and *DcSAUR66* (*Dca30062*), were expressed at higher levels in "2101–02 MFR" across the experiment (**Supplementary Table S2**). Conversely, carnation genes putatively encoding *DcAFB5* (*Dca28499*), *DcARF4* (*Dca49318*), and *DcARF16* (*Dca57896*) were also expressed at higher levels in the stem cutting base of "2003 R 8" than in "2101–02 MFR" (**Supplementary Table S2**). Interestingly, the putative ortholog of the root-specific gene *LATERAL*

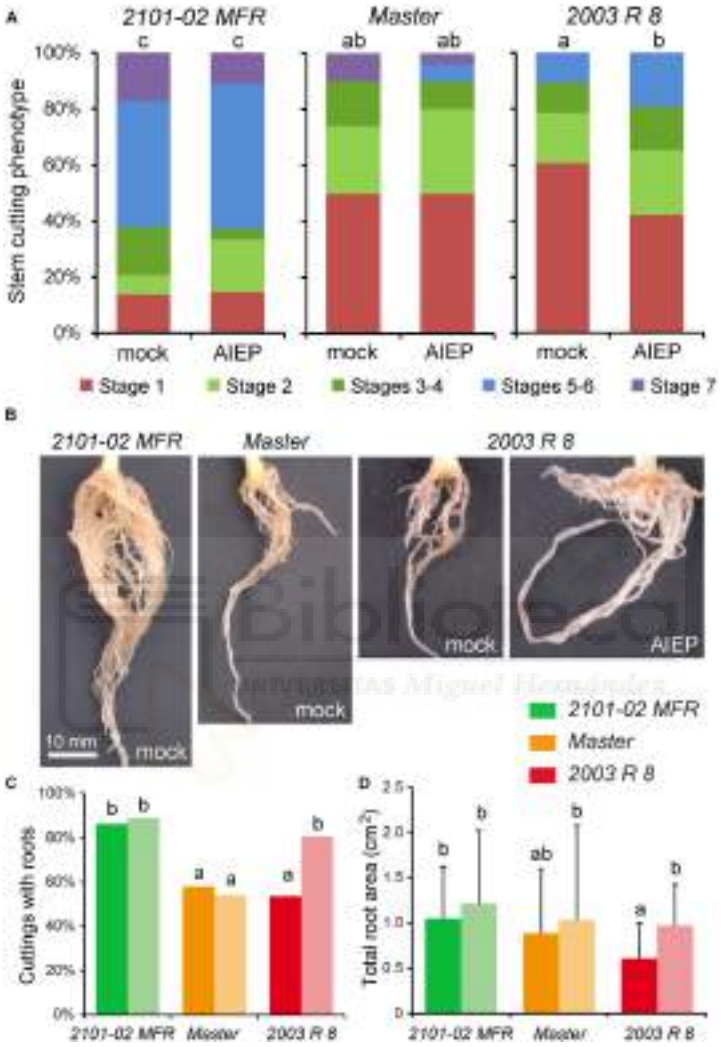

FIGURE 5 | Auxin homeostasis at the stem cutting base is required for AR formation. **(A)** Graphic representations of rooting stage values in different carnation cultivars and treatments (n = 50). **(B)** Representative images of adventitious rooting in the studied carnation cultivars at 29 days treated with GH3 inhibitor (10 μM AIEP) or with mock. **(C,D)** The percentage of cuttings with roots **(C)** and the area of the scanned root system **(D)** at 29 days in rooted stem cuttings (n = 50). Dark- and light-colored bars represent data from mock- or AIEP-treated samples, respectively. Different letters indicate significant differences ($P < 0.05$) over sample means (cultivar × treatment).

ROOT PRIMORDIUM 1 (*LRP1*; Smith and Fedoroff, 1995) (*Dca58211*) was expressed at higher levels in the stem cutting base of "2101–02 MFR" at 54 h, coinciding with cell cluster formation in this region (Villacorta-Martín et al., 2015). These results were consistent with the high amount of active IAA in the stem cutting base of "2101–02 MFR" at earlier time points during rooting (**Figure 4A**) that triggered AR formation.

Consistently with the high amount of *tZ* found in the stem cutting base of "2003 R 8" (**Supplementary Figure S4A**), the

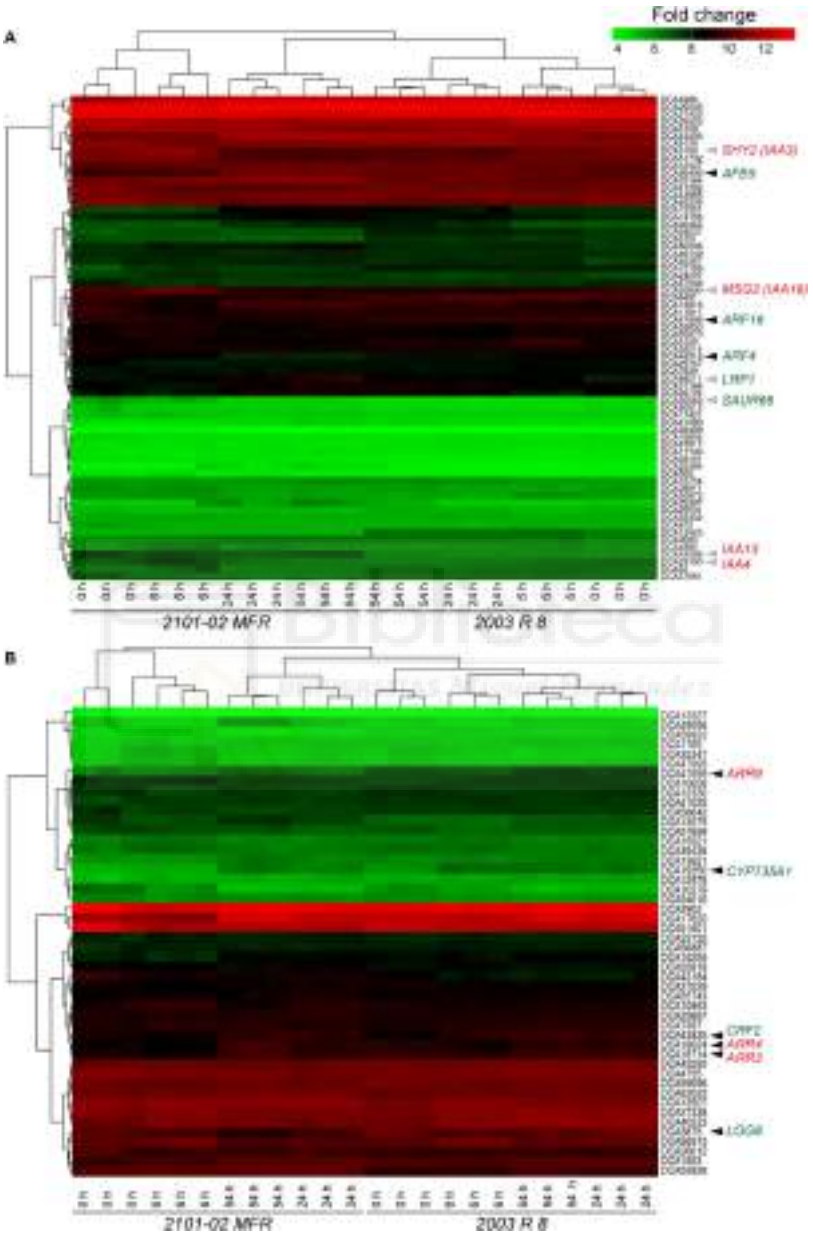

FIGURE 6 | Analysis of expression of transcripts related to auxin **(A)** and cytokinin (CK) **(B)** homeostasis during AR formation. Heat map drawing and clustering was done as described in the section "Materials and Methods". Arrowheads indicate those genes mentioned in the text with differential expression at defined time-points in *2101–02 MFR* (gray arrowheads) or "2003 R 8" (black arrowheads). Putative positive regulators are indicated in green, while negative regulators are shown in red.

expression levels of *Dca19350*, the putative ortholog encoding CYP735A1 that catalyzes an early step of *tZ* biosynthesis in Arabidopsis (Takei et al., 2004), were increased in "2003 R 8" compared with those in "2101–02 MFR", particularly during the first hours after planting (**Figure 6B**, and **Supplementary Figure S5A** and **Supplementary Table S2**). In addition, the expression of *Dca3875*, the closest carnation homolog to *LONELY GUY 8* (*LOG8*), which is also required for *tZ* biosynthesis (Kuroha et al., 2009), was also found at higher levels in the stem cutting base of "2003 R 8" (**Figure 6B** and **Supplementary Table S2**). Regarding the expression of other CK-related genes, carnation genes encoding some ARABIDOPSIS RESPONSE REGULATOR (ARR) proteins, such as *Dca18714*, *Dca18024*, and *Dca47559*, were expressed at high levels in the stem cutting base of "2003 R 8" shortly after planting, while in the good-rooting cultivar, "2101–02 MFR", their expression levels were initially low and increased much later after planting (**Figure 6B**, and **Supplementary Figure S5B** and **Supplementary Table S2**). In Arabidopsis, the expression of *CK RESPONSE FACTOR* (*CRF*) genes is rapidly induced by CKs (Rashotte et al., 2006). We found that *Dca43835*, putatively encoding CRF2, was expressed at higher levels in the stem cutting base of "2003 R 8" than in "2101–02 MFR", confirming higher CK signaling in the bad-rooting cultivar during early rooting (**Figure 6B**, and **Supplementary Figure S5C** and **Supplementary Table S2**).

DISCUSSION

We characterized the root system architecture of stem cuttings in two standard ("Master" and "2003 R 8") and one spray ("2101–02 MFR") carnation (*D. caryophyllus*) cultivars selected because of their contrasting rooting performance (Birlanga et al., 2015). We determined that the bad-rooting performance of "2003 R 8" was mostly caused by a severe delay in AR initiation compared to the other cultivars (Agulló-Antón et al., 2014; Villacorta-Martín et al., 2015). On the other hand, the highly developed root system of "2101–02 MFR" was caused by an early AR initiation and a sustained growth of its AR system.

Auxin is mainly produced at the tip of the leaf through the IPyA pathway in most species (Cheng et al., 2007; Yamamoto et al., 2007; Liu et al., 2014) and it is then channeled through PAT to the vasculature and into the root (Gao et al., 2008; Naramoto, 2017). The standard cultivars "Master" and "2003 R 8" showed increased production of IPyA compared to the spray cultivar ("2101–02 MFR"), due to their higher expression of *DcTAR2a* in the most distal region of the leaf, with less differentiated cells (Agulló-Antón et al., 2013). IPyA is converted to IAA in the distal region of the leaf where *DcYUC1* is highly expressed, as this is the rate-limiting step of auxin biosynthesis (Zhao, 2012). We found very low IAA levels in the proximal region of the leaf in all the studied cultivars, suggestive of IAA mobilization via the PAT system preventing its accumulation in the leaf. In Arabidopsis, PIN1 is mainly expressed at the stele region of the root and the treatment with low concentrations of auxin up-regulates *PIN1* gene expression and modifies its protein localization (Vieten et al., 2005; Sauer et al., 2006; Omelyanchuk et al., 2016). These results suggest that endogenous auxin could directly affect the directionality and intensity of its own transport. Similarly, higher auxin biosynthesis in the standard cultivars (as measured by the amount of the IPyA precursor) could up-regulate PIN1 expression in the distal region of the leaves which, in turn, will increase PAT in these two cultivars. We found higher expression levels of several auxin influx genes (*DcAUX1* and *DcLAX3*) and auxin efflux genes (*DcPIN1*, *DcABCB1*, and *DcABCB19*) in the leaves of the cultivars with higher IPyA (and thus IAA) levels. These results suggested that "Master" and "2003 R 8" transported IAA through the leaf more efficiently than "2101–02 MFR". Therefore, auxin was produced in the distal region of mature carnation leaves in all three cultivars at a different pace where it was quickly mobilized by PAT toward their proximal region (**Figure 7**). As a consequence, a gradient of IAA concentration along the leaf blade could be established, which was visualized by *DcIAA19* expression, used previously as a read-out of endogenous auxin levels (Villacorta-Martín et al., 2015).

We found that IAA transport through the stem was higher in "Master" and "2003 R 8" than in "2101–02 MFR", which mirrored the expression of their auxin transport genes in this tissue. Auxin transport inhibitors block PIN cycling between the plasma membrane and endosomal compartments (Geldner et al., 2001; Parry et al., 2001). Inhibition of PAT through the stem with NPA abolished AR formation in all three cultivars, while the auxin influx inhibitor 1-NOA strongly affected "Master" and "2003 R 8". These cultivar-specific responses to PAT inhibitors might be caused by the differential expression of auxin transport genes, which were much lower in the "2101–02 MFR". Indeed, the reduced rate of auxin biosynthesis in the leaves and the slower PAT in the stem cutting base of "2101–02 MFR" might contribute to the temporal delay and its lower IAA concentration found after harvesting compared to that of "Master". However, the contrasting rooting behavior of "Master" and "2003 R 8" could not be explained because of their differences in auxin biosynthesis in mature leaves or in their auxin transport rates through the stem. Exogenously added auxins enhanced AR formation in "Master" and they partially restored the bad-rooting behavior of "2003 R 8", indicating that both cultivars are similarly responsive to auxin.

Interestingly, despite the high auxin biosynthesis and transport rate in "2003 R 8", the localized auxin accumulation in the stem cutting base required for rooting was not observed, suggesting altered auxin homeostasis (i.e., auxin degradation) in the stem cutting base of "2003 R 8". The dynamic regulation of IAA oxidation by the DAO1 family of dioxygenases and of amino acid IAA conjugation by GH3 represents the major contribution to auxin homeostasis in Arabidopsis (Mellor et al., 2016; Porco et al., 2016). We found very low oxIAA levels in the stem cutting base of the studied cultivars which otherwise was not detected in leaves (Sánchez-García et al., 2018), indicating that IAA oxidation is not involved in the main regulatory pathway of IAA homeostasis in carnation. The expression of *DcDAO1* genes was constitutively low and remained unchanged during rooting. As oxIAA can be further metabolized by conjugation to glucose, one possibility is that glucosylation of oxIAA to 2-oxoindole-3-acetic acid glucose (oxIAA-Glc) by the UDP glucosyltransferase

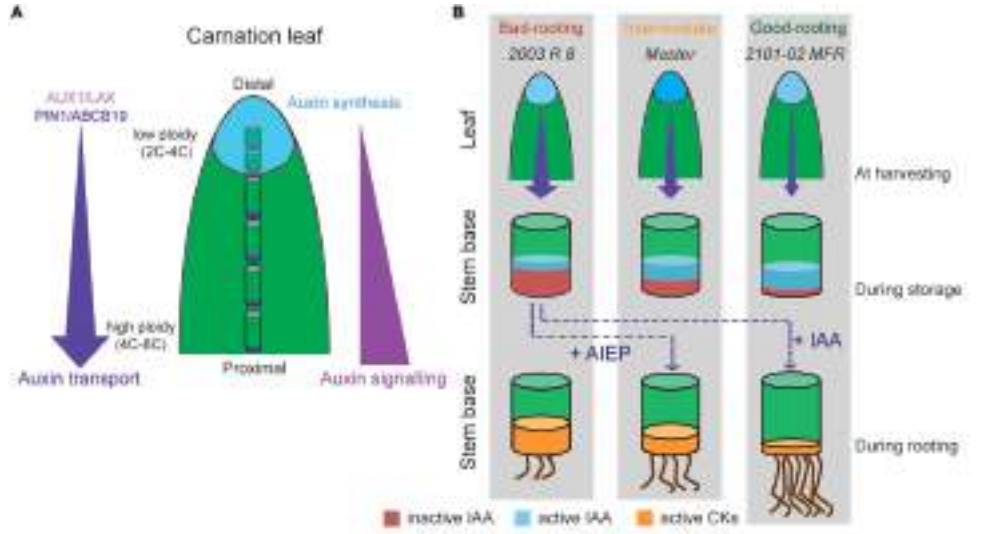

FIGURE 7 | An integrated model of AR formation in carnation stem cuttings. **(A)** Regulation of auxin homeostasis in stem cutting leaves. Auxin influx proteins (AUX1/LAXs) are depicted in pink; auxin efflux proteins (PIN1 and ABCB19) are shown in purple. Size and ploidy level of mesophyll cells varied between distal (small size and 2C–4C ploidy level) and proximal (large size and 4C–8C ploidy level) leaf regions. The site of auxin synthesis is depicted in light blue. **(B)** Differences in auxin homeostasis in selected carnation genotypes during rooting of stem cuttings. In the leaf diagrams, the size of the purple arrow indicates the magnitude of the PAT from the leaves and the blue intensity indicates the level of auxin synthesis. In the stem cutting base diagrams, the height of the colored cylinders (red, blue, yellow) indicates the amount of hormone. IAA levels were highest during storage and were quickly downregulated after planting and during rooting. Treatment with AIEP (a well-known inhibitor of GH3 enzymes) results in a higher auxin-to-CK ratio at planting time that enhanced rooting in "2003 R 8" cultivar. Exogenous IAA treatment also enhanced rooting in the "2003 R 8" cultivar.

UGT74D1 (Tanaka et al., 2014) reduced endogenous oxIAA levels. However, we could not detect oxIAA-Glc in the stem cutting base of these cultivars, despite of the high expression of DcUGT74D1 in this tissue (Sánchez-García et al., 2018), which confirmed the low relevance of the oxIAA pathway to explain varietal differences during rooting of carnation stem cuttings.

Several forms of auxin conjugates have been identified in plants, including IAA-sugar (i.e., IAA-Glucose and IAA-Glc) and IAA–amino acid conjugates (Ludwig-Müller, 2011). The conversion of IAA to IAA-Glc is catalyzed by the UDP glucosyltransferase UGT84B1, and its overexpression in Arabidopsis caused phenotypes compatible with auxin depletion, suggesting that IAA-Glc is an irreversible IAA catabolite rather than as an intermediate in the synthesis of other conjugates (Jackson et al., 2002). IAA-Glc was not detected either in leaves or in the stem cutting base of the studied cultivars, indicating that IAA-Glc conjugates might represent relatively minor components of the conjugate pool in carnation (Sánchez-García et al., 2018). The conjugation of IAA to amino acids, such as aspartic acid and glutamic acid, is catalyzed by a group of IAA–amido synthetases belonging to the family of GH3 proteins (Staswick et al., 2005). We found low levels of IAA-Asp both in the leaves and in basal region of the stem in cuttings harvested from the mother plants (Sánchez-García et al., 2018). Interestingly, IAA-Asp levels in the stem cutting base of "2003 R 8" progressively increased after planting and during rooting. On the other hand, endogenous IAA-Asp levels remained low and constant during rooting in "2101–02 MFR". Although the expression of *DcGH3.1* was strongly up-regulated in the stem cutting base of both cultivars during rooting, the highest expression in the stem cutting base of "2003 R 8" might increase its endogenous GH3 activity leading to the observed IAA reduction after harvesting and before planting.

Indole-3-acetic acid conjugated to aspartic acid is believed to be inactive (Ludwig-Müller, 2011); hence, high IAA-Asp might interfere with the build-up of the localized auxin response required for AR formation in the stem cutting base of "2003 R 8". Previous results in pea suggested that there are high levels of IAA inactivation in the base of mature cuttings compared with the juvenile ones, which might directly contribute for the observed decline in AR formation with age in this species (Rasmussen et al., 2015). To confirm our hypothesis that enhanced IAA-Asp conjugation in the stem cutting base reduced rooting of "2003 R 8", we applied AIEP, a known inhibitor of the GH3 family of enzymes that it has been shown to be effective *in vivo* (Böttcher et al., 2012). Treatment of stem cuttings with AIEP significantly improved rooting of "2003 R 8". The percentage of AIEP-treated cuttings with roots increased significantly only in

"2003 R 8" compared to the non-treated ones and without any effect on the other studied cultivars, indicating that the active IAA levels in the stem cutting base required for AR initiation were only limiting in the bad-rooting cultivar ("2003 R 8"). Hence, the delay in AR initiation of "2003 R 8" was fully rescued by chemically inhibiting GH3 activities, confirming that enhanced auxin homeostasis in the stem cutting base of "2003 R 8" was responsible for its bad-rooting performance. It might be possible that other bad-rooting cultivars could also accumulate IAA-Asp in the stem cutting base during storage and that AIEP treatment might improve adventitious rooting. Preliminary results indicate that other standard cultivars with poor rooting performance, such as "2441-7 R" (Birlanga et al., 2015), also responded to the AIEP treatment (M.S. Justamante and J.M. Pérez-Pérez, personal communication).

Several Aux/IAA genes were expressed at high levels in the stem cutting base of "2101–02 MFR" during early rooting. Due to most Aux/IAA genes are auxin-inducible (Overvoorde et al., 2005; Paponov et al., 2008), the Aux/IAA function is regulated by endogenous auxin at both protein stability and gene expression level (Pierre-Jerome et al., 2013). In Arabidopsis, several Aux/IAA gain-of-function mutants, such as *msg2/iaa19* (Tatematsu et al., 2004), *shy2/iaa3* (Tian et al., 2002), *bodenlos/iaa12* (Hamann et al., 2002), or *solitary root/indole-3-acetic acid14* (Fukaki et al., 2002), are auxin insensitive and are defective in LR formation, indicating that multiple Aux/IAA–ARF modules cooperatively regulate the developmental steps during LR formation (De Smet et al., 2010; Goh et al., 2012). Some of these Aux/IAA–ARF modules are also conserved during AR formation from whole leaves (Bustillo-Avendaño et al., 2017). Hence, the high expression levels of *DcIAA3*, *DcIAA13* (the closest ortholog of *BDL/IAA12*), and *DcIAA19* in the stem cutting base of the good-rooting cultivar might indicate low levels of these three repressors after PAT-induced auxin accumulation in the formative region of the stem. Conversely, lower IAA levels in the stem cutting base of the bad-rooting cultivar ("2003 R 8") might allow the DcIAA co-repressors to accumulate and hence inhibit rooting. Intriguingly, we found *DcAFB5* and some *DcARFs* were expressed at higher levels in the stem cutting base of "2003 R 8", which might indicate a compensatory mechanism to regulate high DcIAA activity. It is tempting to speculate that ARF dimerization in the stem cutting base of "2101–02 MFR" will thus activate the expression of specific targets involved in AR initiation more efficiently than in "2003 R 8", one of which might be *LRP1*, which is 1 of the 10 members of the *SHI* gene family (Kuusk et al., 2006). *LRP1* is induced by auxin and expressed in cells derived from the pericycle and appears to be active both in LR and AR formation (Welander et al., 2014).

We found that CK levels (*t*Z) in the stem cutting base of the bad-rooting cultivar ("2003 R 8") increased during rooting at higher levels than in the other studied cultivars, which was correlated with the higher expression of two *t*Z biosynthesis genes (Kiba et al., 2013), *DcCYP735A1* and *DcLOG8*. Notably, a negative role for CK in AR formation has been proposed as mutants defective in CK biosynthesis or perception displayed increased production of ARs whereas enhanced CK biosynthesis has the opposite effects (de Klerk et al., 2001; Werner et al., 2003; Riefler et al., 2006; Ramírez-Carvajal et al., 2009). In agreement with a negative role of CKs in AR formation, two ARR CK response genes, *DcARR3* and *DcARR9*, were significantly upregulated in the stem cutting base of "2003 R 8". ARR3 and ARR4 are type-A of response regulators (Hwang et al., 2012) that are quickly induced by CKs and that redundantly regulate branching patters in the shoot in response to nitrate availability (Müller et al., 2015). Recently, ammonium has been shown to improve adventitious rooting in leafy cuttings of *Petunia hybrida* (Hilo et al., 2017). Further investigations will clarify the role of *DcARR3* and *DcARR4* in nutrient-induced AR formation in carnation stem cuttings.

Our deep understanding of the physiological and molecular events leading to the specific developmental responses of AR formation in "2101–02 MFR" and "2003 R 8" cultivars will allow establishing a marker-assisted selection approach of DEGs to select for enhanced adventitious rooting traits during breeding and to limit production losses during vegetative propagation of elite lines.

AUTHOR CONTRIBUTIONS

MA and JMP-P were involved in the conceptualization and supervision. AC, AA, MA, and JMP-P performed the methodology. AC, ABS-G, AA, RG-B, MSJ, and SI were involved in the investigation. AC, MA, and JMP-P performed the formal analysis. JMP-P was involved in the writing of the original draft. AC, MA, and JMP-P were involved in the writing and review and editing of the manuscript. JMP-P provided the funding acquisition. AA, MA, and JMP-P collected resources for the study.

FUNDING

This work was supported by the Ministerio de Economía, Industria y Competitividad (MINECO) of Spain (Grant Nos. AGL2012-33610 and BIO2015-64255-R), and by Fonds Européen de Développement Régional (FEDER) Funds of the European Commission.

ACKNOWLEDGMENTS

We thank Emilio Á. Cano (Barberet & Blanc S.A., Puerto Lumbreras, Murcia, Spain) for plant material, Christine Böttcher (CSIRO Plant Industry, Glen Osmond, Australia) for providing the IAA–amido synthetase inhibitor, and Francisco Pérez-Alfocea (CEBAS-CSIC) for the use of the U-HPLC–MS Orbitrap equipment.

SUPPLEMENTARY MATERIAL

The Supplementary Material for this article can be found online at: https://www.frontiersin.org/articles/10.3389/fpls.2018.00566/full#supplementary-material

FIGURE S1 | Rooting stages in carnation stem cuttings grown in soil plugs. **(A)** Stacked histograms of rooting stages in a representative sample ($n = 50$) of stem cuttings growing in soil plugs for 20 or 27 days after planting. Letters indicate significant differences ($P < 0.05$) over samples (cultivar × time). **(B)** Representative soil plug images of stem cuttings rooting for 20 or 27 days.

FIGURE S2 | Real-time PCR quantification of the expression of selected transcripts related to auxin transport (auxin influx, **A,B**; auxin efflux, **C,E**) or auxin biosynthesis **(F)** in the stem cutting base during adventitious rooting. Bars indicate normalized expression levels ± standard deviation relative to the −23 h dataset in the "2101–02 MFR" cultivar. Letters indicate significant differences between samples ($P < 0.05$).

FIGURE S3 | Real-time PCR quantification of the expression of selected transcripts related to auxin transport (auxin influx, **A–B**; auxin efflux, **C–F**) in mature leaves of carnation stem cuttings at harvesting time. Bars indicate normalized expression levels ± standard deviation relative to the distal region of the leaf in the 'Master' cultivar. Letters indicate significant differences between samples ($P < 0.05$).

FIGURE S4 | Endogenous levels of other key hormones in the stem cutting base during adventitious rooting. **(A)** *trans*-zeatin (*tZ*), **(B)** the ethylene precursor 1-aminocyclopropane-1-carboxylic acid (ACC), and **(C)** abscisic acid (ABA). Average ± standard deviation values are shown. Asterisks indicate significant differences ($P < 0.05$) over time for a given treatment. H, harvesting; P, planting.

FIGURE S5 | Real-time PCR quantification of the expression of selected transcripts related to CK biosynthesis **(A)** or signaling **(B,C)** in the stem cutting base during adventitious rooting. Bars indicate normalized expression levels ± standard deviation relative to the −23 h dataset in the "2101–02 MFR" cultivar. Letters indicate significant differences between samples ($P < 0.05$).

TABLE S1 | Oligonucleotides used in this study.

TABLE S2 | RNA-seq data from carnation genes selected as putative auxin-responsive and CK-related genes.

REFERENCES

Acosta, M., Oliveros-Valenzuela, M. R., Nicolas, C., and Sanchez-Bravo, J. (2009). Rooting of carnation cuttings. The auxin signal. *Plant Signal. Behav.* 4, 234–236. doi: 10.4161/psb.4.3.7912

Agulló-Antón, M., Olmos, E., Pérez-Pérez, J. M., and Acosta, M. (2013). Evaluation of ploidy level and endoreduplication in carnation (*Dianthus* spp.). *Plant Sci.* 201–202, 1–11. doi: 10.1016/j.plantsci.2012.11.006

Agulló-Antón, M. A., Sánchez Bravo, J., Acosta, M., and Druege, U. (2011). Auxins or sugars: What makes the difference in the adventitious rooting of stored carnation cuttings? *J. Plant Growth Regul.* 30, 100–113. doi: 10.1007/s00344-010-9174-8

Agulló-Antón, M. Á., Ferrández-Ayela, A., Fernández-García, N., Nicolás, C., Albacete, A., Pérez-Alfocea, F., et al. (2014). Early steps of adventitious rooting: morphology, hormonal profiling and carbohydrate turnover in carnation stem cuttings. *Physiol. Plant.* 150, 446–462. doi: 10.1111/ppl.12114

Berardini, T. Z., Reiser, L., Li, D., Mezheritsky, Y., Muller, R., Strait, E., et al. (2015). The Arabidopsis information resource: making and mining the "gold standard" annotated reference plant genome. *Genesis* 53, 474–485. doi: 10.1002/dvg.22877

Birlanga, V., Villanova, J., Cano, A., Cano, E. A., Acosta, M., and Pérez-Pérez, J. M. (2015). Quantitative analysis of adventitious root growth phenotypes in carnation stem cuttings. *PLoS One* 10:e0133123. doi: 10.1371/journal.pone.0133123

Böttcher, C., Dennis, E. G., Booker, G. W., Polyak, S. W., Boss, P. K., and Davies, C. (2012). A novel tool for studying auxin-metabolism: the inhibition of grapevine indole-3-acetic acid-amido synthetases by a reaction intermediate analogue. *PLoS One* 7:e37632. doi: 10.1371/journal.pone.0037632

Bustillo-Avendaño, E., Ibáñez, S., Sanz, O., Sousa Barros, J. A., Gude, I., Perianez-Rodriguez, J., et al. (2017). Regulation of hormonal control, cell reprogramming and patterning during de novo root organogenesis. *Plant Physiol.* 176, 1709–1727. doi: 10.1104/pp.17.00980

Chacón, B., Ballester, R., Birlanga, V., Rolland-Lagan, A. G., and Pérez-Pérez, J. M. (2013). A quantitative framework for flower phenotyping in cultivated carnation (*Dianthus caryophyllus* L.). *PLoS One* 8:e82165. doi: 10.1371/journal.pone.0082165

Cheng, Y., Dai, X., and Zhao, Y. (2007). Auxin synthesized by the YUCCA flavin monooxygenases is essential for embryogenesis and leaf formation in *Arabidopsis*. *Plant Cell* 19, 2430–2439. doi: 10.1105/tpc.107.053009

de Klerk, G. J., Hanecakova, J., and Jasik, J. (2001). The role of cytokinins in rooting of stem slices cut from apple microcuttings. *Plant Biosyst.* 135, 79–84. doi: 10.1080/11263500112331350680

de Klerk, G. J., van der Krieken, W., and de Jong, J. C. (1999). Review the formation of adventitious roots: new concepts, new possibilities. *In Vitro Cell. Dev. Biol. Plant* 35, 189–199. doi: 10.1007/s11627-999-0076-z

De Smet, I., Lau, S., Voss, U., Vanneste, S., Benjamins, R., Rademacher, E. H., et al. (2010). Bimodular auxin response controls organogenesis in *Arabidopsis*. *Proc. Natl. Acad. Sci. U.S.A.* 107, 2705–2710. doi: 10.1073/pnas.0915001107

Díaz-Sala, C. (2014). Direct reprogramming of adult somatic cells toward adventitious root formation in forest tree species: the effect of the juvenile-adult transition. *Front. Plant Sci.* 5:310. doi: 10.3389/fpls.2014.00310

Druege, U., Franken, P., and Hajirezaei, M. R. (2016). Plant hormone homeostasis, signaling, and function during adventitious root formation in cuttings. *Front. Plant Sci.* 7:381. doi: 10.3389/fpls.2016.00381

Fukaki, H., Tameda, S., Masuda, H., and Tasaka, M. (2002). Lateral root formation is blocked by a gain-of-function mutation in the SOLITARY-ROOT/IAA14 gene of Arabidopsis. *Plant J.* 29, 153–168. doi: 10.1046/j.0960-7412.2001.01201.x

Gao, X., Nagawa, S., Wang, G., and Yang, Z. (2008). Cell polarity signaling: focus on polar auxin transport. *Mol. Plant* 1, 899–909. doi: 10.1093/mp/ssn069

Garrido, G., Cano, E. A., Acosta, M., and Sánchez-Bravo, J. (1998). Formation and growth of roots in carnation cuttings: influence of cold storage period and auxin treatment. *Sci. Hortic.* 74, 219–231. doi: 10.1016/S0304-4238(98)00078-8

Garrido, G., Cano, E. A., Arnao, M. B., Acosta, M., and Sánchez-Bravo, J. (1996). Influence of cold storage period and auxin treatment on the subsequent rooting of carnation cuttings. *Sci. Hortic.* 65, 73–84. doi: 10.1016/0304-4238(95)00860-8

Garrido, G., Guerrero, J. R., Cano, E. A., Acosta, M., and Sánchez-Bravo, J. (2002). Origin and basipetal transport of the IAA responsible for rooting of carnation cuttings. *Physiol. Plant.* 114, 303–312. doi: 10.1034/j.1399-3054.2002.1140217.x

Geldner, N., Friml, J., Stierhof, Y. D., Jürgens, G., and Palme, K. (2001). Auxin transport inhibitors block PIN1 cycling and vesicle trafficking. *Nature* 413, 425–428. doi: 10.1038/35096571

Goh, T., Kasahara, H., Mimura, T., Kamiya, Y., and Fukaki, H. (2012). Multiple AUX/IAA-ARF modules regulate lateral root formation: the role of *Arabidopsis* SHY2/IAA3-mediated auxin signalling. *Philos. Trans. R. Soc. B Biol. Sci.* 367, 1461–1468. doi: 10.1098/rstb.2011.0232

Großkinsky, D. K., Albacete, A., Jammer, A., Krbez, P., van der Graaff, E., Pfeifhofer, H., et al. (2014). A rapid phytohormone and phytoalexin screening method for physiological phenotyping. *Mol. Plant* 7, 1053–1056. doi: 10.1093/mp/ssu015

Guerrero, J. R., Garrido, G., Acosta, M., and Sánchez-Bravo, J. (1999). Influence of 2,3,5-triiodobenzoic acid and 1-N-naphthylphthalamic acid on indoleacetic acid transport in carnation cuttings: relationship with rooting. *J. Plant Growth Regul.* 18, 183–190. doi: 10.1007/PL00007068

Hamann, T., Benkova, E., Bäurle, I., Kientz, M., and Jürgens, G. (2002). The *Arabidopsis BODENLOS* gene encodes an auxin response protein inhibiting MONOPTEROS-mediated embryo patterning. *Genes Dev.* 16, 1610–1615. doi: 10.1101/gad.229402

Hilo, A., Shahinnia, F., Druege, U., Franken, P., Melzer, M., Rutten, T., et al. (2017). A specific role of iron in promoting meristematic cell division during adventitious root formation. *J. Exp. Bot.* 68, 4233–4247. doi: 10.1093/jxb/erx248

Hwang, I., Sheen, J., and Müller, B. (2012). Cytokinin signaling networks. *Annu. Rev. Plant Biol.* 63, 353–380. doi: 10.1146/annurev-arplant-042811-105503

Jackson, R. G., Kowalczyk, M., Li, Y., Higgins, G., Ross, J., Sandberg, G., et al. (2002). Over-expression of an *Arabidopsis* gene encoding a glucosyltransferase of indole-3-acetic acid: phenotypic characterisation of transgenic lines. *Plant J.* 32, 573–583. doi: 10.1046/j.1365-313X.2002.01445.x

Jawaharlal, M., Ganga, M., Padmadevi, K., Jegadeeswari, V., and Karthikeyan, S. (2009). *A technical Guide on Carnation*. Coimbatore: Tamil Nadu Agricultural University, 1–56.

Kiba, T., Takei, K., Kojima, M., and Sakakibara, H. (2013). Side-chain modification of cytokinins controls shoot growth in *Arabidopsis*. *Dev. Cell* 27, 452–461. doi: 10.1016/j.devcel.2013.10.004

Konieczny, R., Kepczynski, J., Pilarska, M., Cembrowska, D., Menzel, D., and Samaj, J. (2009). Cytokinin and ethylene affect auxin transport-dependent rhizogenesis in hypocotyls of common ice plant (*Mesembryanthemum crystallinum* L.). *J. Plant Growth Regul.* 28, 331–340. doi: 10.1007/s00344-009-9097-4

Kuroha, T., Tokunaga, H., Kojima, M., Ueda, N., Ishida, T., Nagawa, S., et al. (2009). Functional analyses of *LONELY GUY* cytokinin-activating enzymes reveal the importance of the direct activation pathway in *Arabidopsis*. *Plant Cell* 21, 3152–3169. doi: 10.1105/tpc.109.068676

Kuusk, S., Sohlberg, J. J., Magnus Eklund, D., and Sundberg, E. (2006). Functionally redundant *SHI* family genes regulate Arabidopsis gynoecium development in a dose-dependent manner. *Plant J.* 47, 99–111. doi: 10.1111/j.1365-313X.2006.02774.x

Lanková, M., Smith, R. S., Pesek, B., Kubes, M., Zazímalová, E., Petrásek, J., et al. (2010). Auxin influx inhibitors 1-NOA, 2-NOA, and CHPAA interfere with membrane dynamics in tobacco cells. *J. Exp. Bot.* 61, 3589–3598. doi: 10.1093/jxb/erq172

Lavy, M., and Estelle, M. (2016). Mechanisms of auxin signaling. *Development* 143, 3226–3229. doi: 10.1242/dev.131870

Liu, H., Xie, W. F., Zhang, L., Valpuesta, V., Ye, Z. W., Gao, Q. H., et al. (2014). Auxin biosynthesis by the *YUCCA6* flavin monooxygenase gene in woodland strawberry. *J. Integr. Plant Biol.* 56, 350–363. doi: 10.1111/jipb.12150

Livak, K. J., and Schmittgen, T. D. (2001). Analysis of relative gene expression data using real-time quantitative PCR and the $2^{-\Delta\Delta C_T}$ method. *Methods* 25, 402–408. doi: 10.1006/meth.2001.1262

Lu, Y., Xie, L., and Chen, J. (2012). A novel procedure for absolute real-time quantification of gene expression patterns. *Plant Methods* 8:9. doi: 10.1186/1746-4811-8-9

Ludwig-Müller, J. (2011). Auxin conjugates: their role for plant development and in the evolution of land plants. *J. Exp. Bot.* 62, 1757–1773. doi: 10.1093/jxb/erq412

Mano, Y., and Nemoto, K. (2012). The pathway of auxin biosynthesis in plants. *J. Exp. Bot.* 63, 2853–2872. doi: 10.1093/jxb/ers091

Mashiguchi, K., Tanaka, K., Sakai, T., Sugawara, S., Kawaide, H., Natsume, M., et al. (2011). The main auxin biosynthesis pathway in *Arabidopsis*. *Proc. Natl. Acad. Sci. U.S.A.* 108, 18512–18517. doi: 10.1073/pnas.1108434108

Mellor, N., Band, L. R., Pěnčik, A., Novák, O., Rashed, A., Holman, T., et al. (2016). Dynamic regulation of auxin oxidase and conjugating enzymes AtDAO1 and GH3 modulates auxin homeostasis. *Proc. Natl. Acad. Sci. U.S.A.* 113, 11022–11027. doi: 10.1073/pnas.1604458113

Müller, D., Waldie, T., Miyawaki, K., To, J. P., Melnyk, C. W., Kieber, J. J., et al. (2015). Cytokinin is required for escape but not release from auxin mediated apical dominance. *Plant J.* 82, 874–886. doi: 10.1111/tpj.12862

Naramoto, S. (2017). Polar transport in plants mediated by membrane transporters: focus on mechanisms of polar auxin transport. *Curr. Opin. Plant Biol.* 40, 8–14. doi: 10.1016/j.pbi.2017.06.012

Nicolás, J. I., Acosta, M., and Sánchez-Bravo, J. (2007). Variation in indole-3-acetic acid transport and its relationship with growth in etiolated lupin hypocotyls. *J. Plant Physiol.* 164, 851–860. doi: 10.1016/j.jplph.2006.06.005

Oliveros-Valenzuela, M. R., Reyes, D., Sánchez-Bravo, J., Acosta, M., and Nicolás, C. (2008). Isolation and characterization of a cDNA clone encoding an auxin influx carrier in carnation cuttings. Expression in different organs and cultivars and its relationship with cold storage. *Plant Physiol. Biochem.* 46, 1071–1076. doi: 10.1016/j.plaphy.2008.07.009

Omelyanchuk, N. A., Kovrizhnykh, V. V., Oshchepkova, E. A., Pasternak, T., Palme, K., and Mironova, V. V. (2016). A detailed expression map of the PIN1 auxin transporter in *Arabidopsis thaliana* root. *BMC Plant Biol.* 16(Suppl. 1):5. doi: 10.1186/s12870-015-0685-0

Overvoorde, P. J., Okushima, Y., Alonso, J. M., Chan, A., Chang, C., Ecker, J. R., et al. (2005). Functional genomic analysis of the AUXIN/INDOLE-3-ACETIC ACID gene family members in *Arabidopsis thaliana*. *Plant Cell* 17, 3282–3300. doi: 10.1105/tpc.105.036723

Paponov, I. A., Paponov, M., Teale, W., Menges, M., Chakrabortee, S., Murray, J. A., et al. (2008). Comprehensive transcriptome analysis of auxin responses in *Arabidopsis*. *Mol. Plant* 1, 321–337. doi: 10.1093/mp/ssm021

Parry, G., Delbarre, A., Marchant, A., Swarup, R., Napier, R., Perrot-Rechenmann, C., et al. (2001). Novel auxin transport inhibitors phenocopy the auxin influx carrier mutation aux1. *Plant J.* 25, 399–406. doi: 10.1046/j.1365-313x.2001.00970.x

Pencík, A., Simonovik, B., Petersson, S. V., Henyková, E., Simon, S., Greenham, K., et al. (2013). Regulation of auxin homeostasis and gradients in Arabidopsis roots through the formation of the indole-3-acetic acid catabolite 2-oxindole-3-acetic acid. *Plant Cell* 25, 3858–3870. doi: 10.1105/tpc.113.114421

Pierre-Jerome, E., Moss, B. L., and Nemhauser, J. L. (2013). Tuning the auxin transcriptional response. *J. Exp. Bot.* 64, 2557–2563. doi: 10.1093/jxb/ert100

Porco, S., Pěnčik, A., Rashed, A., Voß, U., Casanova-Sáez, R., Bishopp, A., et al. (2016). Dioxygenase-encoding *AtDAO1* gene controls IAA oxidation and homeostasis in *Arabidopsis*. *Proc. Natl. Acad. Sci. U.S.A.* 113, 11016–11021. doi: 10.1073/pnas.1604375113

Ramírez-Carvajal, G. A., Morse, A. M., Dervinis, C., and Davis, J. M. (2009). The cytokinin type-B response regulator PtRR13 is a negative regulator of adventitious root development in *Populus*. *Plant Physiol.* 150, 759–771. doi: 10.1104/pp.109.137505

Rashotte, A. M., Mason, M. G., Hutchison, C. E., Ferreira, F. J., Schaller, G. E., and Kieber, J. J. (2006). A subset of Arabidopsis AP2 transcription factors mediates cytokinin responses in concert with a two-component pathway. *Proc. Natl. Acad. Sci. U.S.A.* 103, 11081–11085. doi: 10.1073/pnas.0602038103

Rasmussen, A., Hosseini, S. A., Hajirezaei, M. R., Druege, U., and Geelen, D. (2015). Adventitious rooting declines with the vegetative to reproductive switch and involves a changed auxin homeostasis. *J. Exp. Bot.* 66, 1437–1452. doi: 10.1093/jxb/eru499

Riefler, M., Novak, O., Strnad, M., and Schmülling, T. (2006). *Arabidopsis* cytokinin receptor mutants reveal functions in shoot growth, leaf senescence, seed size, germination, root development, and cytokinin metabolism. *Plant Cell* 18, 40–54. doi: 10.1105/tpc.105.037796

Sánchez-García, A. B., Ibáñez, S., Cano, A., Acosta, M., and Pérez-Pérez, J. M. (2018). A comprehensive phylogeny of auxin homeostasis genes involved in adventitious root formation in carnation stem cuttings. *PLoS One* (in press). doi: 10.1371/journal.pone.0196663

Sauer, M., Balla, J., Luschnig, C., Wisniewska, J., Reinöhl, V., Friml, J., et al. (2006). Canalization of auxin flow by Aux/IAA-ARF-dependent feedback regulation of PIN polarity. *Genes Dev.* 20, 2902–2911. doi: 10.1101/gad.390806

Sheela, V. L. (2008). "Carnation," in *Flowers for Trade,* eds V. L. Sheela and M. N. Sheela (New Delhi: New India Publishing), 95–112.

Smith, D. L., and Fedoroff, N. V. (1995). *LRP1*, a gene expressed in lateral and adventitious root primordia of Arabidopsis. *Plant Cell* 7, 735–745. doi: 10.1105/tpc.7.6.735

Staswick, P. E., Serban, B., Rowe, M., Tiryaki, I., Maldonado, M. T., Maldonado, M. C., et al. (2005). Characterization of an Arabidopsis enzyme family that conjugates amino acids to indole-3-acetic acid. *Plant Cell* 17, 616–627. doi: 10.1105/tpc.104.026690

Takei, K., Yamaya, T., and Sakakibara, H. (2004). *Arabidopsis CYP735A1* and *CYP735A2* encode cytokinin hydroxylases that catalyze the biosynthesis of *trans*-Zeatin. *J. Biol. Chem.* 279, 41866–41872. doi: 10.1074/jbc.M406337200

Tanaka, K., Hayashi, K., Natsume, M., Kamiya, Y., Sakakibara, H., Kawaide, H., et al. (2014). UGT74D1 catalyzes the glucosylation of 2-oxindole-3-acetic acid in the auxin metabolic pathway in *Arabidopsis*. *Plant Cell Physiol.* 55, 218–228. doi: 10.1093/pcp/pct173

Tatematsu, K., Kumagai, S., Muto, H., Sato, A., Watahiki, M. K., Harper, R. M., et al. (2004). *MASSUGU2* encodes Aux/IAA19, an auxin-regulated protein that functions together with the transcriptional activator NPH4/ARF7 to regulate differential growth responses of hypocotyl and formation of lateral

roots in *Arabidopsis thaliana*. *Plant Cell* 16, 379–393. doi: 10.1105/tpc.018630

Tian, Q., Uhlir, N., and Reed, J. (2002). Arabidopsis SHY2/IAA3 inhibits auxin-regulated gene expression. *Plant Cell* 14, 301–319. doi: 10.1105/tpc.010283

Tivendale, N. D., Ross, J. J., and Cohen, J. D. (2014). The shifting paradigms of auxin biosynthesis. *Trends Plant Sci.* 19, 44–51. doi: 10.1016/j.tplants.2013.09.012

Van der Weij, H. G. (1932). Der mechanismus des wuchsstofftransportes. *Rec. Trav. Bot. Néerl.* 31, 810–857.

Vieten, A., Vanneste, S., Wisniewska, J., Benková, E., Benjamins, R., Beeckman, T., et al. (2005). Functional redundancy of PIN proteins is accompanied by auxin-dependent cross-regulation of PIN expression. *Development* 132, 4521–4531. doi: 10.1242/dev.02027

Villacorta-Martín, C., Sánchez-García, A. B., Villanova, J., Cano, A., van de Rhee, M., de Haan, J., et al. (2015). Gene expression profiling during adventitious root formation in carnation stem cuttings. *BMC Genomics* 16:789. doi: 10.1186/s12864-015-2003-5

Villanova, J., Cano, A., Albacete, A., López, A., Cano, E. Á, Acosta, M., et al. (2017). Multiple factors influence adventitious rooting in carnation (*Dianthus caryophyllus* L.) stem cuttings. *Plant Growth Regul.* 81, 511–521. doi: 10.1007/s10725-016-0228-1

Weijers, D., Benkova, E., Jäger, K. E., Schlereth, A., Hamann, T., Kientz, M., et al. (2005). Developmental specificity of auxin response by pairs of ARF and Aux/IAA transcriptional regulators. *EMBO J.* 24, 1874–1885. doi: 10.1038/sj.emboj.7600659

Welander, M., Geier, T., Smolka, A., Ahlman, A., Fan, J., and Zhu, L. H. (2014). Origin, timing, and gene expression profile of adventitious rooting in *Arabidopsis* hypocotyls and stems. *Am. J. Bot.* 101, 255–266. doi: 10.3732/ajb.1300258

Werner, T., Motyka, V., Laucou, V., Smets, R., Van Onckelen, H., and Schmulling, T. (2003). Cytokinin-deficient transgenic Arabidopsis plants show multiple developmental alterations indicating opposite functions of cytokinins in the regulation of shoot and root meristem activity. *Plant Cell* 15, 2532–2550. doi: 10.1105/tpc.014928

Won, C., Shen, X., Mashiguchi, K., Zheng, Z., Dai, X., Cheng, Y., et al. (2011). Conversion of tryptophan to indole-3-acetic acid by TRYPTOPHAN AMINOTRANSFERASES OF *ARABIDOPSIS* and YUCCAs in *Arabidopsis*. *Proc. Natl. Acad. Sci. U.S.A.* 108, 18518–18523. doi: 10.1073/pnas.1108436108

Yagi, M., Kosugi, S., Hirakawa, H., Ohmiya, A., Tanase, K., Harada, T., et al. (2014). Sequence analysis of the genome of carnation (*Dianthus caryophyllus* L.). *DNA Res.* 21, 231–241. doi: 10.1093/dnares/dst053

Yamamoto, Y., Kamiya, N., Morinaka, Y., Matsuoka, M., and Sazuka, T. (2007). Auxin biosynthesis by the YUCCA genes in rice. *Plant Physiol.* 143, 1362–1371. doi: 10.1104/pp.106.091561

Zhao, Y. (2010). Auxin biosynthesis and its role in plant development. *Annu. Rev. Plant Biol.* 61, 49–64. doi: 10.1146/annurev-arplant-042809-112308

Zhao, Y. (2012). Auxin biosynthesis: a simple two-step pathway converts tryptophan to indole-3-acetic acid in plants. *Mol. Plant* 5, 334–338. doi: 10.1093/mp/ssr104

Conflict of Interest Statement: The authors declare that the research was conducted in the absence of any commercial or financial relationships that could be construed as a potential conflict of interest.

Supplementary Figures:

Figure S1. Rooting stages in carnation stem cuttings grown in soil plugs.

Figure S2. Real-time PCR quantification of the expression of selected transcripts related to auxin transport (auxin influx, A, B; auxin efflux, C, E) or auxin biosynthesis (F) in the stem cutting base during adventitious rooting.

Figure S3. Real-time PCR quantification of the expression of selected transcripts related to auxin transport (auxin influx, A–B; auxin efflux, C–F) in mature leaves of carnation stem cuttings at harvesting time.

Figure S4. Endogenous levels of other key hormones in the stem cutting base during adventitious rooting.

Figure S5. Real-time PCR quantification of the expression of selected transcripts related to CK biosynthesis (A) or signaling (B, C) in the stem cutting base during adventitious rooting.

Supplementary Tables:

Table S1. Oligonucleotides used in this study.

Table S2. RNA-seq data from carnation genes selected as putative auxin-responsive and CK-related genes.

FIGURE S1

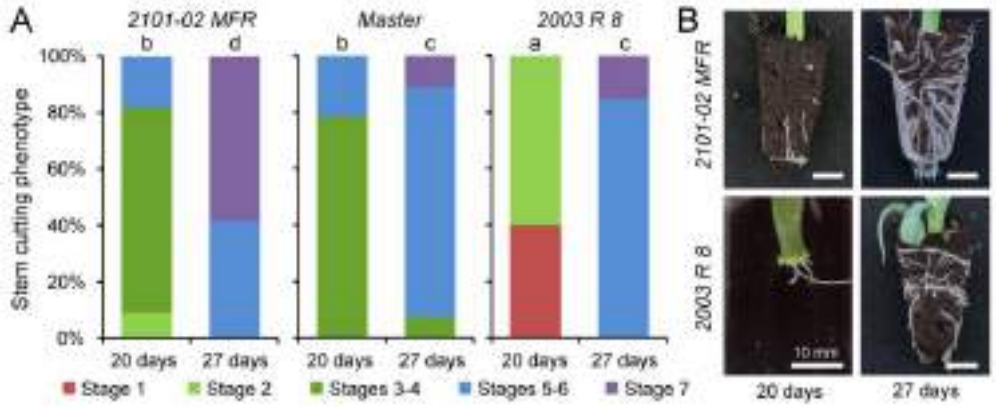

FIGURE S1 | Rooting stages in carnation stem cuttings grown in soil plugs. **(A)** Stacked histograms of rooting stages in a representative sample (n = 50) of stem cuttings growing in soil plugs for 20 or 27 days after planting. Letters indicate significant differences ($P < 0.05$) over samples (cultivar × time). **(B)** Representative soil plug images of stem cuttings rooting for 20 or 27 days.

FIGURE S2

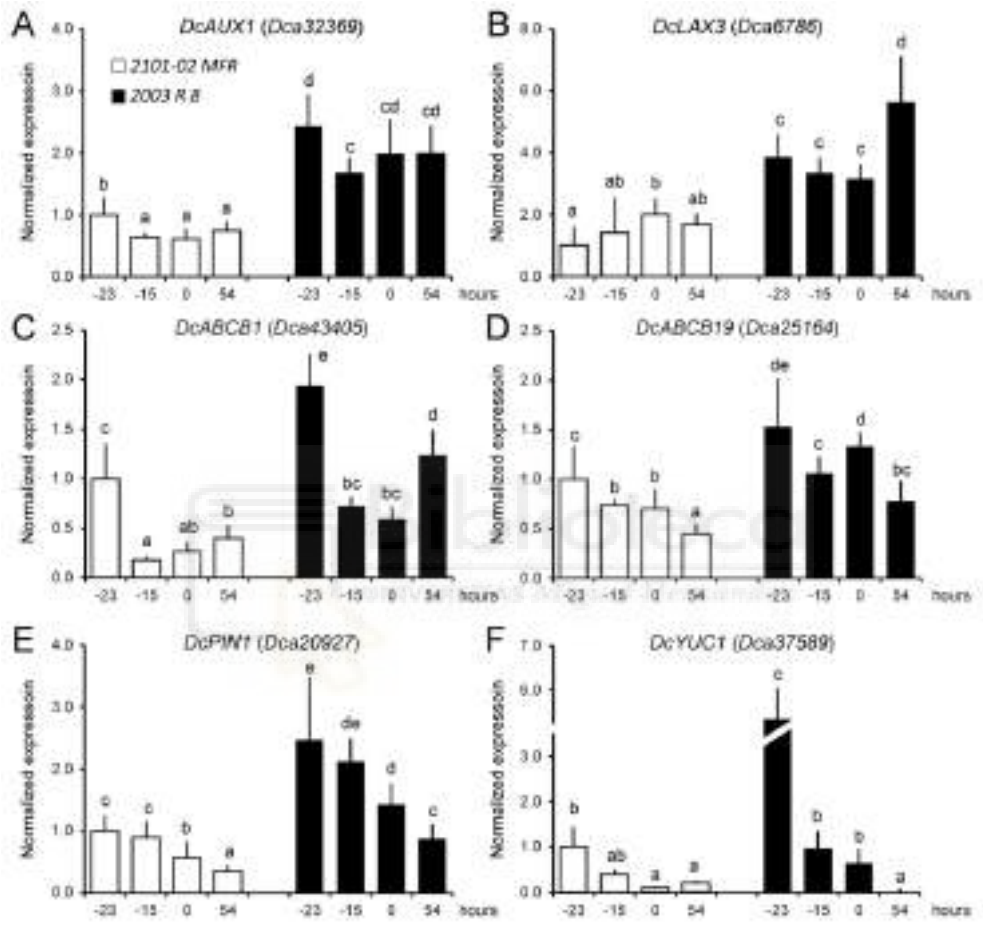

FIGURE S2 | Real-time PCR quantification of the expression of selected transcripts related to auxin transport (auxin influx, **A, B**; auxin efflux, **C, E**) or auxin biosynthesis **(F)** in the stem cutting base during adventitious rooting. Bars indicate normalized expression levels ± standard deviation relative to the -23 h dataset in the "*2101–02 MFR*" cultivar. Letters indicate significant differences between samples ($P < 0.05$).

FIGURE S3

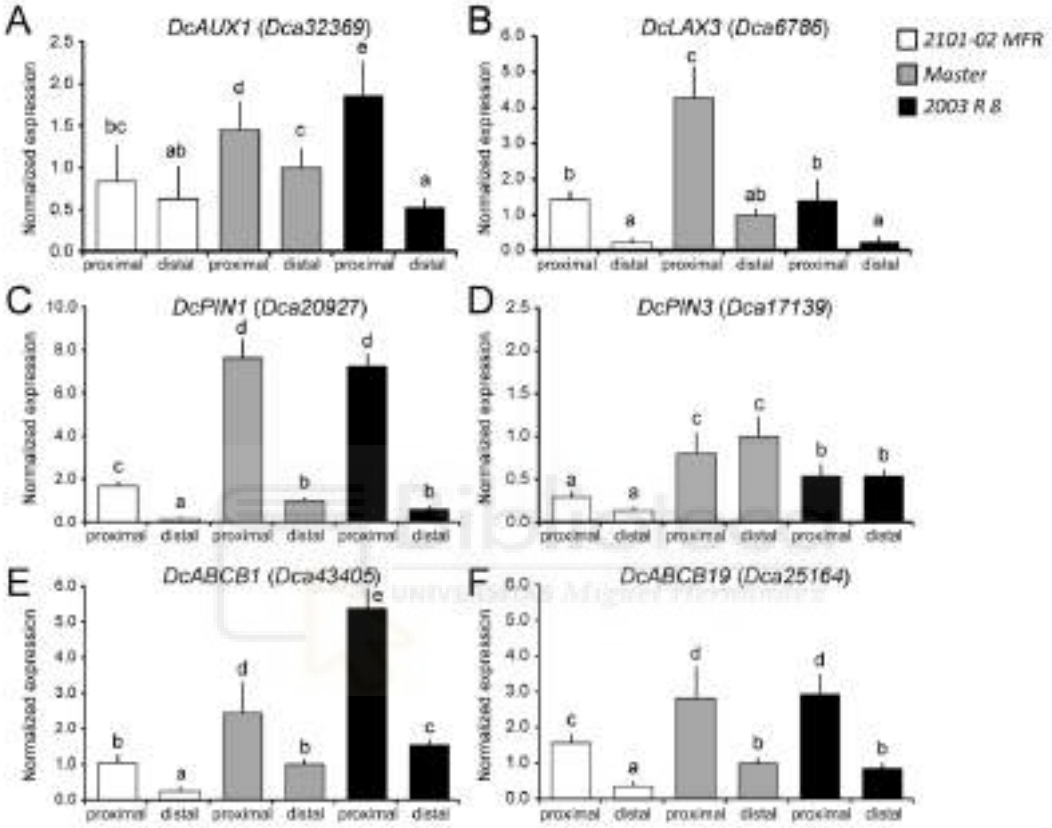

FIGURE S3 | Real-time PCR quantification of the expression of selected transcripts related to auxin transport (auxin influx, **A–B**; auxin efflux, **C–F**) in mature leaves of carnation stem cuttings at harvesting time. Bars indicate normalized expression levels ± standard deviation relative to the distal region of the leaf in the '*Master'* cultivar. Letters indicate significant differences between samples ($P < 0.05$).

FIGURE S4

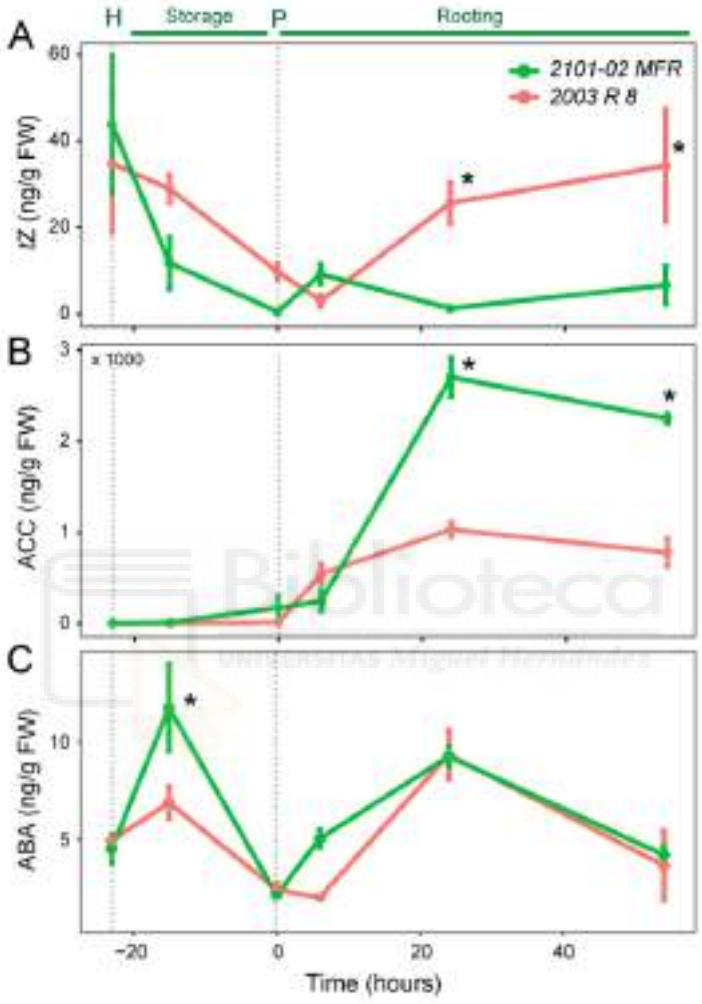

FIGURE S4 | Endogenous levels of other key hormones in the stem cutting base during adventitious rooting. **(A)** *trans*-zeatin (*t*Z), **(B)** the ethylene precursor 1-aminocyclo propane-1-carboxylic acid (ACC), and **(C)** abscisic acid (ABA). Average ± standard deviation values are shown. Asterisks indicate significant differences ($P < 0.05$) over time for a given treatment. H, harvesting; P, planting.

FIGURE S5

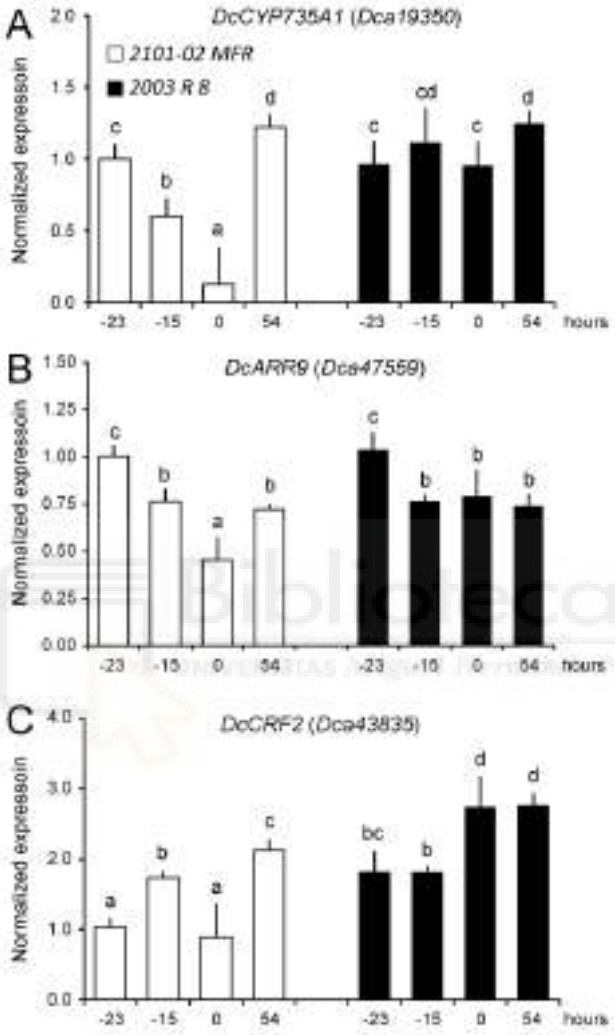

FIGURE S5 | Real-time PCR quantification of the expression of selected transcripts related to CK biosynthesis **(A)** or signaling **(B, C)** in the stem cutting base during adventitious rooting. Bars indicate normalized expression levels ± standard deviation relative to the -23 h dataset in the "*2101–02 MFR*" cultivar. Letters indicate significant differences between samples ($P < 0.05$).

Table S1. Oligonucleotides used in this study

Gene	Accession number	Oligonucleotide sequences (5'→3')		Product (bp)
DcABCB1	*Dca43405*	TGCCGGAAAAACCATAGCACTTG	CTAATAGAAGTTGTCCTTCAGTGG	107
DcABCB19	*Dca25164*	GTTCATGAAGTTTCCAAGTATGC	CCAGCATGCAATTTCTGCGTAG	87
DcARR9	*Dca47559*	TTCATTCCAAGTTACAGCAGTTG	ATTCACCTCTACTTCCTGCTG	130
DcAUX1	*Dca32369*	GTATGGTCCCAATAATCCGTCC	CGTACCTCATTAGTGTATTGTAC	119
DcCRF2	*Dca43835*	AGAAGTCGGGTCTTATGTG	ACTAGACCAACCCGAATAC	148
DcCYP735A1	*Dca19350*	TCTCGCTTTTACGGGAAGAG	ACCATTAGCCATAAGTAAACCAC	178
DcDAO1	*Dca2789*	TGCCGTTCCATGGAGCAATGGA	TGTGCTTCAATGACCATTTCTGGC	126
DcGH3.1	*Dca37575*	TTCCGAGTTCCTTACTAGTTCG	GAAGGCTGTACAATAGTTGACG	101
DcIAA19	*Dca30890*	GGTTGTCTTAGCTTAGAAGATGC	CATGACTCAACAAACAGGTTCC	128
DcLAX3	*Dca6786*	ACAAGCAATAAGCTGGATAACAG	TCGAAACCATGTCATTCAGTGG	127
DcPIN1	*Dca20927*	CTAGTCTGTTTCAGGTGGAATTTG	GCAATGCCATGAATAAACCAAGAC	118
DcPIN3	*Dca17139*	CGGCGAATCTAAAGGTGCTAG	CCAAGTTTGTTCAGTCGAATTG	114
DcTAR2a	*Dca35926*	TGCTGGGATGCGCATTGGTTG	GAAACACCAATGCTACTCAGCT	93
DcYUC1	*Dca37589*	TCCGTAACTCGGTGCATGTAC	GTGAGATTCGCGATTAAGAGCA	130
DcEF1α	*Dca3524*	CTCCACCACTGGAGGTTTTGAA	CTTGACGATTTCTTCGTACCTC	166

Artículo 3

Integration of phenotypic and hormone data during adventitious rooting in carnation (*Dianthus caryophyllus* L.) stem cuttings

María Salud Justamante[1], José Ramón Acosta-Motos[2,3], Antonio Cano[4], Joan Villanova[1], Virginia Birlanga[1], Alfonso Albacete[3], Emilio A. Cano[5], Manuel Acosta[4], José Manuel Pérez-Pérez[1]

[1] Instituto de Bioingeniería, Universidad Miguel Hernández, 03202 Elche, Spain

[2] Universidad Católica San Antonio de Murcia, Campus de los Jerónimos, 30107 Guadalupe, Spain

[3] CEBAS-CSIC, Campus Universitario de Espinardo, 30100 Murcia, Spain

[4] Departamento de Biología Vegetal, Universidad de Murcia, 30100 Murcia, Spain

[5] Dümmen Orange, 30890 Puerto Lumbreras, Spain

Plants (Basel) 2019; 8: 226

Published online 15 July 2019. doi: 10.3390/plants8070226

FI (2018): 2,623 (Q2; 59 de 228)

plants

MDPI

Article

Integration of Phenotype and Hormone Data during Adventitious Rooting in Carnation (*Dianthus caryophyllus* L.) Stem Cuttings

María Salud Justamante [1], José Ramón Acosta-Motos [2,3], Antonio Cano [4], Joan Villanova [1], Virginia Birlanga [1], Alfonso Albacete [3], Emilio Á. Cano [5], Manuel Acosta [4] and José Manuel Pérez-Pérez [1,*]

1 Instituto de Bioingeniería, Universidad Miguel Hernández, 03202 Elche, Spain
2 Universidad Católica San Antonio de Murcia, Campus de los Jerónimos, 30107 Guadalupe, Spain
3 CEBAS-CSIC, Campus Universitario de Espinardo, 30100 Murcia, Spain
4 Departamento de Biología Vegetal, Universidad de Murcia, 30100 Murcia, Spain
5 Dümmen Orange, 30890 Puerto Lumbreras, Spain
* Correspondence: jmperez@umh.es; Tel.: +34-96-665-8958

Received: 29 May 2019; Accepted: 12 July 2019; Published: 15 July 2019

Abstract: The rooting of stem cuttings is a highly efficient procedure for the vegetative propagation of ornamental plants. In cultivated carnations, an increased auxin level in the stem cutting base produced by active auxin transport from the leaves triggers adventitious root (AR) formation from the cambium. To provide additional insight into the physiological and genetic basis of this complex trait, we studied AR formation in a collection of 159 F_1 lines derived from a cross between two hybrid cultivars (*2003 R 8* and *2101-02 MFR*) showing contrasting rooting performances. In three different experiments, time-series for several stem and root architectural traits were quantified in detail in a subset of these double-cross hybrid lines displaying extreme rooting phenotypes and their parental genotypes. Our results indicate that the water content and area of the AR system directly contributed to the shoot water content and shoot growth. Moreover, morphometric data and rooting quality parameters were found to be associated with some stress-related metabolites such as 1-aminocyclopropane-1-carboxylic acid (ACC), the ethylene precursor, and the conjugated auxin indol-3-acetic acid-aspartic acid (IAA-Asp).

Keywords: vegetative plant propagation; hormone profiling; root architectural traits; stress-related hormones; ACC; IAA-Asp; water content; shoot growth

1. Introduction

In contrast to most root tissues, adventitious roots (ARs) arise from non-root cells in response to some abiotic stresses or after wounding [1,2]. AR formation in stem cuttings is required for the vegetative propagation of many horticultural and forestry plant species and depends on a large set of exogenous and endogenous factors [3].

Carnation (*Dianthus caryophyllus* L.) plants are vegetatively propagated from terminal stem cuttings that undergo adventitious rooting, a process which has a strong genetic dependency and which leads to production losses in certain commercial cultivars [4]. As a first step towards the identification of the molecular pathways involved in this process, a quantitative description of rooting performance was obtained from ten carnation cultivars displaying extreme and contrasting phenotypic values selected from a wide collection of commercial lines [5]. The bad rooting cultivars were characterized by one or several of the following features: a delay in AR initiation, a reduced number of AR primordia,

or a slow elongation rate of these ARs. In addition, genome-wide gene expression profiling and functional changes occurring in the stem cutting base during the early stages of adventitious rooting were further analyzed in two of these cultivars, *2003 R 8* and *2101-02 MFR*, which were selected because of their contrasting rooting performances [6]. Differences in rooting ability were caused by delayed activation of formative divisions from cambial-derived cells in the bad rooting cultivar (*2003 R 8*), a phenotype that could be rescued by exogenous auxin treatment [6]. Additional studies confirmed that the differential regulation of endogenous auxin homeostasis between these two carnation cultivars limited active auxin accumulation in formative cambial cells [7]. Despite the high auxin biosynthesis and transport rate in *2003 R 8*, the high expression of *GRETCHEN HAGEN3* (*GH3*) genes in the stem cutting base of this cultivar enhanced the conjugation of the active auxin indol-3-acetic acid (IAA) to amino acids, such as aspartic acid, which directly contributed to quick turnover of active auxin in the cambium [7].

To better understand the genetic basis of this complex trait, we studied AR formation in a collection of 33 selfed lines (from the *2101-02 MFR* cultivar) and 126 outcrossing lines from a cross between the *2003 R 8* and *2101-02 MFR* hybrid cultivars. Several morphological and physiological traits were quantified during rooting over different growing seasons in eight of these double-cross hybrid lines displaying extreme adventitious rooting phenotypes and their parental lines. Our understanding of the physiological and molecular events leading to the complex developmental response of AR formation in carnation stem cuttings will allow us to establish a marker-assisted selection approach to select for enhanced adventitious rooting traits during breeding of this economically important ornamental species.

2. Results

2.1. Phenotype Characterization of Parental Lines and the F_1 Population Under Study

2.1.1. Morphological Variation in *2003 R 8* and *2101-02 MFR* During Rooting

Cold-stored stem cuttings periodically collected between April and June from mature mother plants of *2003 R 8* and *2101-02 MFR* lines were sequentially planted (sowings B01 to B13) on a demarcated greenhouse plot between June and October (see Materials and Methods). We found a significant variation in the stem cutting size, estimated by the SA_13 trait, between sowings in both parental lines (Figure 1a and Supplementary Materials Figure S1). Indeed, *2003 R 8* stem cuttings in several consecutive sowings (B04 to B07) displayed higher SA_13 values than the average (16.30 ± 5.01 cm^2, n = 260) due to an increase in the average leaf width of those samples. On the other hand, the SA_13 values of *2101-02 MFR* were the lowest in B01 (7.74 ± 2.65 cm^2) and the highest in B09 (17.60 ± 4.52 cm^2), relative to the average SA_13 value throughout all sowings (11.5 ± 4.2 cm^2, n = 260). These results confirmed the morphological heterogeneity in *2003 R 8* and *2101-02 MFR* stem cuttings during the production process, which is known to be dependent on environmental and physiological factors at the production plot [8].

The average values of the rooting response at 20 days after planting (dap) in *2003 R 8* and *2101-02 MFR* were 53.8 ± 24.9% and 84.0 ± 12.1%, respectively, which is consistent with previous findings [5,8]. The rooting response at 20 dap (RR_20) in *2003 R 8* stem cuttings was highly heterogeneous among different sowings (Figure 1b, left panel), and the lowest RR_20 values (<20%) corresponded to B04 and B05. Conversely, *2101-02 MFR* displayed a uniform rooting response (>60%) throughout all sowings (Figure 1b, right panel). The average values of the root area at 20 dap (RA_20) are a good predictor of the adventitious rooting performance, allowing a direct comparison between genotypes and experimental conditions [5,8]. Quantification of the adventitious rooting of the *2003 R 8* stem cuttings in B04 to B06 sowings was unsuccessful (Figure 1c, left panel), due to their low rooting responses (see above). These sowings overlapped with the warmest summer period (between 8 July and 13 August), which was characterized by the highest air temperature (~37 °C) registered inside the greenhouse plot during the experiment. Hence, we discarded the *2003 R 8* samples grown in the

B04 to B06 sowings. The adventitious rooting performance in *2101-02 MFR*, estimated by RA_20, ranged three-fold, between 0.40 ± 0.24 cm^2 in B11 and 1.22 ± 0.55 cm^2 in B02, with an average value of 0.74 ± 0.43 cm^2 (n = 250; Figure 1c, right panel). As described previously [6], the bad rooting behavior of *2003 R 8* was mostly caused by a delay in AR initiation (low RR_20 values), which contributed to the significant differences (Least Significant Difference [LSD]; *p*-value < 0.05) in RA_20 between *2003 R 8* (0.63 ± 0.36 cm^2, n = 146; Figure 1d, left panel) and *2101-02 MFR* (0.74 ± 0.43 cm^2, n = 250; Figure 1d, right panel).

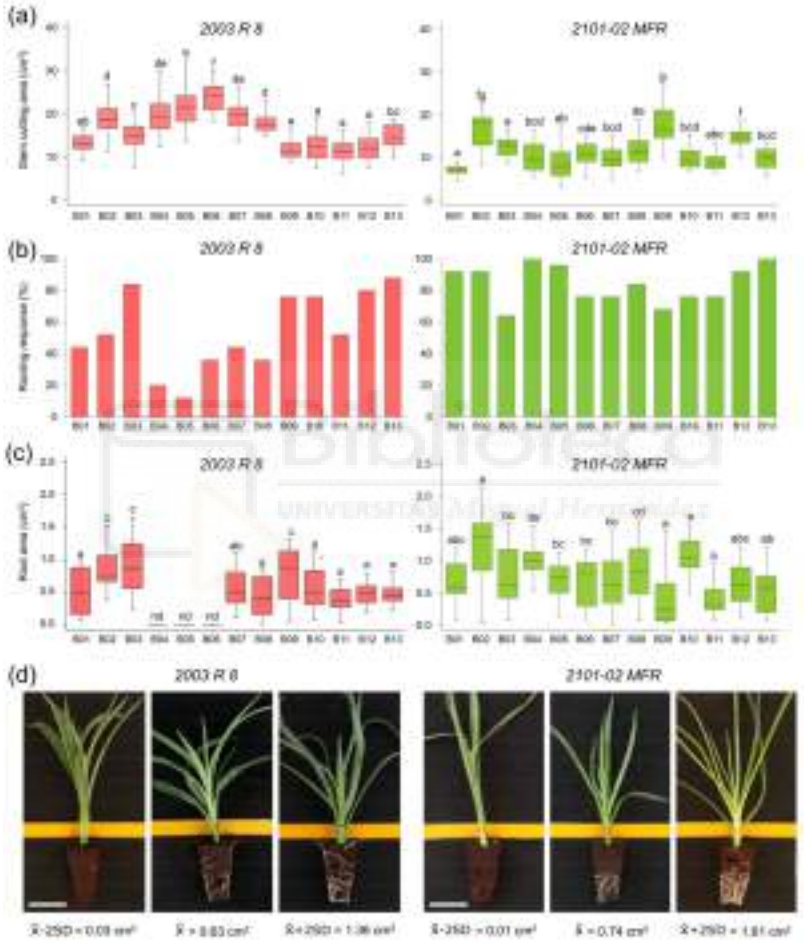

Figure 1. Quantitative description of the *2003 R 8* and *2101-02 MFR* parental lines among different batches. (**a**) The stem cutting area (cm^2) at 13 days after planting (dap), (**b**) rooting response (%) and (**c**) root area (cm^2) at 20 dap. The letters indicate significant differences between batches (Least Significant Difference [LSD]; *p*-value < 0.05). (**d**) Representative images of the phenotypic distribution of the root area (cm^2) at 20 dap in *2003 R 8* (left) and *2101-02 MFR* (right). Scale bar: 25 mm.

2.1.2. Morphological Variation of the Studied F_1 Population

We measured six shoot traits and seven root traits (Table 1) that significantly changed during the rooting experiment (13 and 20 dap) in a population of 159 F_1 lines obtained from a cross between *2003 R 8* and *2101-02 MFR* plants (see Materials and Methods). The average rooting response value in the

studied F_1 population at 20 dap (RR_20) was 74.6 ± 24.6%. The lowest rooting response values were found in *L107* (4%), *L240* (8%), and *L245* (8%), whereas twenty-nine F_1 lines displayed full rooting (100%; Figure 2a). We defined eight rooting stages (RS) representing the different adventitious rooting phenotypes observed in carnation stem cuttings [5]. The average RS value of the F_1 population ranged from 0.56 ± 1.3 (n = 25) in *L245* to 5.48 ± 1.1 (n = 25) in *L222* (Figure 2b).

Table 1. Selected shoot and root traits measured in the first and second experiments.

Studied Traits	Acronym	Measurement Mode [a]	Unit
Leaf number	LN_13	Human operator	>1
Average leaf section	ALS_13	Average Width[1]	mm
Cutting height	CH_13	Network Depth[1]	cm
Shoot area	SA_13, SA_20	Network Area[1]	cm^2
Shoot area increase	ΔSA	SA_20–SA_13	cm^2
Rooting response	RR_20	Human operator[2]	%
Rooting stage	RS_20	Human operator[2]	0 to 7
Maximum number of roots	MaxNR_20	Maximum number of roots[1]	>1
Average root diameter	ARD_20	Average root width[1]	mm
Root area	RA_20	Network area[1]	cm^2
Root convex area	RCA_20	Network convex area[1]	cm^2
Root perimeter	RP_20	Network perimeter[1]	cm

[a] 1: [9]; 2: [5].

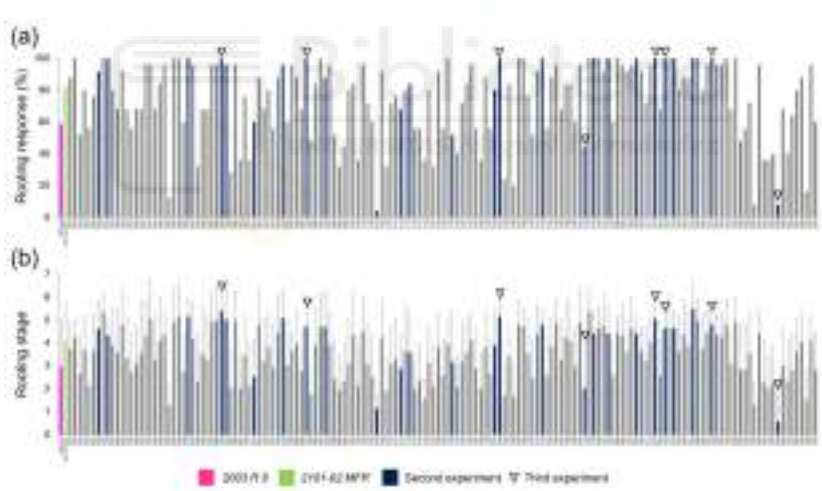

Figure 2. Quantitative description of some rooting parameters of the F_1 lines derived from a cross between *2003 R 8* and *2101-02 MFR*. (**a**) Rooting response (%) and (**b**) rooting stage of the studied lines in the first experiment (n = 159) at 20 dap. The blue bars indicate the lines selected for the second experiment (n = 26), and the arrowheads indicate the lines selected for the third experiment (n = 8).

We then performed a principal component analysis (PCA) with the remaining quantitative traits (see Materials and Methods). We found highly significant and positive correlations for traits related to the root system size (Supplementary Materials Figure S2a). Three principal components (PCs) accounted for 97.3% of the variation among the studied samples (Supplementary Materials Figure S2b). PC1 explained 65.3% of the variance and was positively dependent on the root thickness (estimated by ARD_20) but was negatively affected by the root convex area (RCA_20) and root number (MaxNR_20). PC2 and PC3 accounted for 24.4% and 7.6% of the variance, respectively. PC2 was explained by the root area (RA_20) and ARD_20, while PC3 was explained positively by RCA_20 and negatively by

MaxNR_20. To visualize the effects of PC1, PC2, and PC3 on the root system architecture, representative images are shown in Supplementary Materials Figure 2c, where the PC values varied by plus or minus two standard deviations (SDs) from the mean.

2.1.3. Transgressive Phenotypes in the Studied F_1 Population

Despite the *2101-02 MFR* ovaries being used as receptors for *2003 R 8* pollen, 33 F_1 lines were annotated as selfings based on microsatellite data (E.Á. Cano, personal communication). The remaining 126 F_1 lines were double-cross hybrids between *2003 R 8* and *2101-02 MFR*. We next studied the phenotype distribution of selected rooting traits (ARD_20, RA_20, and MaxNR_20) in the parental lines, as well as in selfing (n = 33 lines) and outcrossing (n = 126 lines) subpopulations.

We previously determined that the root diameter (ARD_20) was negatively correlated with the adventitious rooting performance in a small population of carnation genotypes [5]. In this study though, we did not find significant variation in ARD_20 values between parental lines (Figure 3a, left panel), despite their contrasting rooting behaviors [6]. We found high levels of best-parent heterosis for this trait, with a ~60% increase in values in either selfing or outcrossing F_1 subpopulations (Figure 3a, right panel and Supplementary Materials Table S1a). The highest ARD_20 values were found in the *L073* outcrossing line (0.84 ± 0.09 mm; n = 25), which corresponded to a 2.3-fold variation in the parental line and a 2.6-fold variation in the *L192* crossing line, with the lowest ARD_20 value (0.32 ± 0.07 mm; n = 25).

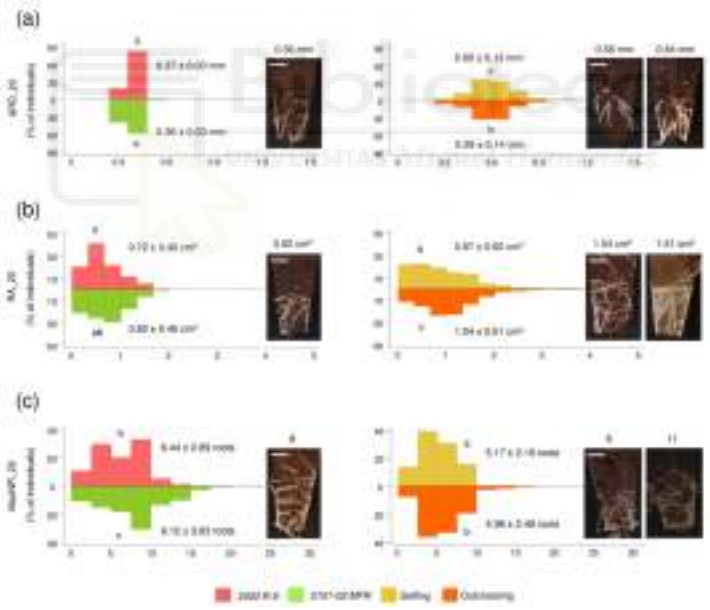

Figure 3. Examples of transgressive segregation observed in principal component analysis (PCA) relevant traits at 20 dap. (**a**) Average root width (ARD_20), (**b**) root area (RA_20), and (**c**) maximum number of roots (MaxNR_20) in the F_1 population grouped by selfing (yellow) and outcrossing (orange) lines compared with *2003 R 8* (red) and *2101-02 MFR* (green) parental lines. Representative images of the average values of the best-rooting parental line *2101-02 MFR* (left) and average (medium) and maximum (right) values in the outcrossing subpopulation are shown. Letters indicate significant differences between the population groups (LSD; p-value < 0.05). Scale bar: 10 mm.

Regarding the AR area at 20 dap (RA_20), we found a slight variation between *2003 R 8* (0.72 ± 0.40 cm^2; n = 175) and *2101-02 MFR* (0.82 ± 0.46 cm^2; n = 250), as well as between selfing

(0.87 ± 0.60, n = 825) and outcrossing (1.04 ± 0.61, n = 3150) subpopulations (Figure 3b). From these results, best-parent heterosis reached 0.3% and 22.0% in the selfing and outcrossing subpopulations, respectively (Supplementary Materials Table S1a). We observed a 1.3-fold variation in the maximum RA_20 value between *2101-02 MFR* and the outcrossing subpopulation (Figure 3b).

The root density in the soil plug was estimated by the MaxNR_20 trait, with statistically significant (LSD; p-value < 0.01) variation between *2003 R 8* (6.44 ± 2.89, n = 175) and *2101-02 MFR* (8.12 ± 3.83 cm^2; n = 250). Interestingly, MaxNR_20 displayed negative heterosis both in selfing and outcrossing subpopulations (Figure 3c and Supplementary Materials Table S1a), despite some individual lines (e.g., *L079* and *L062*) displaying higher average values than the *2101-02 MFR* parental line.

2.2. Study of a Reduced Panel of Double-Cross F_1 Hybrids

2.2.1. Selection of Double-Cross F_1 Hybrids and Heritability Estimation of the Studied Traits

Based on the results from the first experiment (see above), we selected 26 outcrossing lines displaying contrasting and severe rooting phenotypes (Figure 2a,b) to initiate the identification of the genetic determinants responsible for the rooting performance differences observed among carnation genotypes.

We found significant variation between the first and second experiments in the studied traits for most of the selected genotypes, which might indicate a strong environmental dependency of the studied traits that would make their further genetic dissection difficult. To reduce the environmental dependency on the studied traits, we discarded the F_1 outcrossing lines with significant differences (LSD; p-value < 0.05) in RA_20 values and with unavailable plant material at the rooting station (E.Á. Cano, personal communication). As a result, eight outcrossing lines (Supplementary Materials Figure S3a) were selected.

Heritability (H^2) results were estimated for these eight lines and compared to H^2 results obtained for the initial 26 outcrossing selected lines (see Materials and Methods). In all cases, the heritability values for the seven studied rooting traits increased when calculated for the eight selected lines. The heritability results had values ranging from 0.53 for the average root diameter at 20 dap (ARD_20) to 0.88 for the rooting stage at 20 dap (RS_20) (Supplementary Materials Figure S3b).

2.2.2. Rooting Performance of Double-Cross F_1 Hybrids

In the third experiment, we measured six shoot traits and nine root traits (Table 2) at planting times of 19, 29, and 40 dap (see Materials and Methods). Two of the studied F_1 lines, *L062* and *L162*, displayed higher rooting response values at 19 dap (RR_19) than the good rooting parental line *2101-02 MFR*, while only *L245* showed lower RR_19 values than the bad rooting *2003 R 8* genotype (Figure 4a). Four other lines displayed higher (*L087*, *L214*, and *L229*) or lower (*L192*) RR values than the good rooting and bad rooting parental genotypes, respectively, at the other measured times (29 and 40 dap) (Figure 4a). The studied lines were clustered in five groups for RA_40, where *L062* was characterized by a significant RA increase compared with the good rooting parental line (Figure 4b,c). Despite *L162*, *L214*, and *L216* displaying significantly higher RA values at 29 dap than *2101-02 MFR*, their growth rate was maintained afterwards (40 dap). On the contrary, *L245* showed slightly reduced root growth throughout the experiment (Figure 4b,c). Taken together, and as previously described [5,8], the rooting performance of carnation genotypes appears to be influenced by a combinatorial effect of the rooting response and subsequent root growth, which was represented by the contrasting rooting behavior of *L192* and *L062* (Figure 4c), with the former being moderately affected by the rooting stage but with reduced root growth as compared with the bad rooting *L245* line.

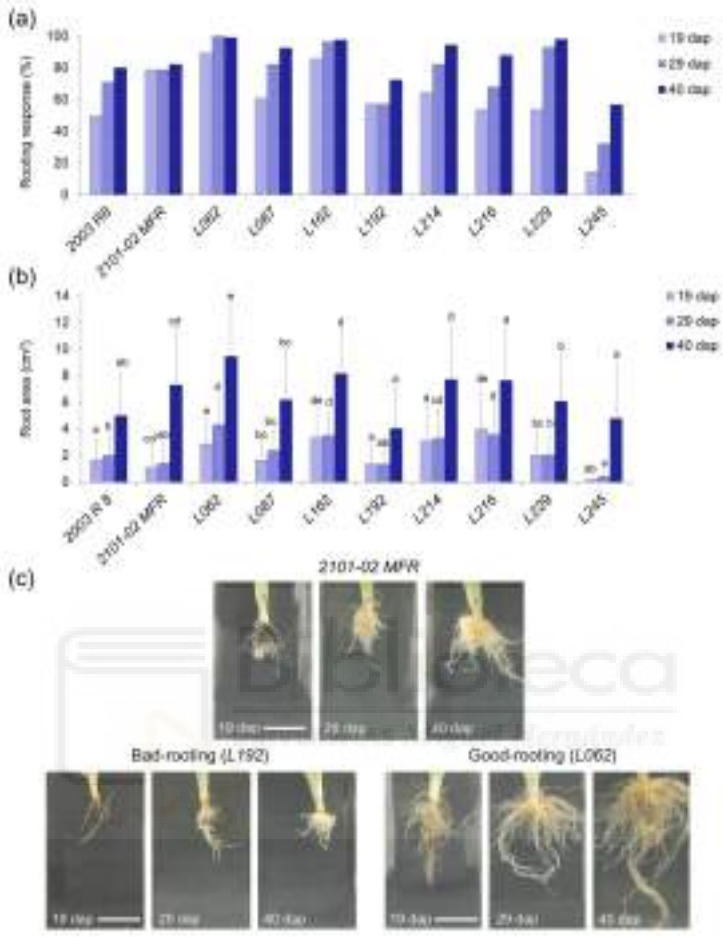

Figure 4. Adventitious rooting in the third experiment. (**a**) Rooting response measurements and (**b**) average root area (cm^2) values in the studied lines at 19, 29, and 40 dap. Letters indicate significant differences between samples (LSD; p-value < 0.05). (**c**) Representative images of the *2101-02 MFR* parental line (up) and two lines with contrasting adventitious rooting phenotypes: the *L192* bad rooting line (left down) and the *L062* good rooting line (right down). Scale bar: 25 mm.

Table 2. Selected shoot and root traits measured in the third experiment.

Shoot Traits	Acronym [a]	Measurement Mode [b]	Unit
Shoot fresh weight	SFW_0, SFW_40	Precision scale	g
Cutting length	CL_0	Digital caliper	cm
Shoot dry weight	SDW_40	Heater, high precision scale	mg
Shoot water content	SWC	SFW_40 − SDW_40	g
Shoot growth	SG	SFW_40 − SFW_0	g
Root fresh weight/root growth	RFW_40	Precision scale	g
Root dry weight	RDW_40	Heater, high precision scale	mg
Root water content	RWC	RFW_40 − RDW_40	g
Rooting response	RR	Human operator[1]	%
Average root diameter	ARD	Average root width[2]	mm
Root area	RA	Network area[2]	cm^2

Table 2. *Cont.*

Shoot Traits	Acronym [a]	Measurement Mode [b]	Unit
Root convex area	RCA	Network convex area^2	cm^2
Root depth	RD	Network depth^2	cm
Root length	RL	Network length^2	cm

[a] Measured at 19, 29, and 40 dap or as otherwise indicated. [b] 1: [5]; 2: [9].

2.2.3. Stem Cutting Ecophysiology of Double-Cross F_1 Hybrids

In the third experiment, we performed a series of analyses to determine whether physiological parameters of stem cuttings at planting time (SFW_0) correlated with the root area at the end of the experiment (RA_40). In addition, we determined whether the root area and its water content (RA and RWC) affected the shoot water content and its growth (SWC and SG) at the end of the experiment (Figure 5, Supplementary Materials Table S2). The correlation analysis between RA_40 and SFW_0 showed that the values of the root area at the end of the experiment could not be predicted from the initial shoot fresh weight (p-value > 0.05) and that there was no significant effect of the studied genotypes (Figure 5a and Supplementary Materials Table S2a). Conversely, positive and highly significant correlations (p-value < 0.001) indicated that the high water content of the root system (RWC) contributed to high water content values in the shoots (SWC) and to optimal shoot growth (SG) at the end of the experiment (Figure 5b,c, and Supplementary Materials Table S2b,c). In a similar way, additional correlation analyses between SWC and RA, SG and RWC, and RWC and RA were performed, and in most of the studied genotypes, the same highly-significant correlations were observed (p-value < 0.001) with large sample sizes in each genotype (Figures S4a–c, and Supplementary Materials Figures S2d–f).

Specifically, in the regression of SWC vs. RWC, genotypes with good rooting performances (green color) showed an average value in the RWC of 0.53 ± 0.35 g, which predicted an average value in the SWC of 2.22 ± 0.79 g. The genotypes with bad rooting performance (red color) presented comparatively lower average values than those of the good rooting ones, where 0.17 ± 0.14 g in the RWC predicted 1.62 ± 0.76 g in the SWC. Both parental lines *2101-02 MFR* (good rooting, blue color) and *2003 R 8* (bad rooting, pink color) showed lower values than selected lines with average values of 0.31 ± 0.22 and 0.12 ± 0.05 g in the RWC which equaled 1.76 ± 0.74 and 1.13 ± 0.40 g in the SWC, respectively (Figure 5b). Further, similar changes were also observed in the average RA values, as they could predict the values in SG (SG vs. RA_40 regression). Good rooting genotypes showed an average value in the RA_40 of 8.19 ± 3.90 cm^2 that predicted an average value in SG of 1.25 ± 0.74 g. The genotypes with bad rooting performance presented lower average values than the good rooting ones. Namely, a RA_40 value of 5.30 ± 3.60 cm^2 predicted a SG of 0.50 ± 0.95 g. The parental lines *2101-02 MFR* and *2003 R 8* showed lower values than the respective selected lines with average values of 7.38 ± 4.31 cm^2 and 4.98 ± 3.39 cm^2 in the RA_40, which predicted similar values in SG of 0.60 ± 0.70 g and 0.55 ± 0.61 g, respectively (Figure 5c).

2.2.4. Capturing Variation in Morphometric, Ecophysiological, and Adventitious Rooting Traits in Carnation Stem Cuttings

Through correlation analysis and PCA, we aimed to predict the rooting performance using a reduced number of the measured traits (see Materials and Methods). Three PCs accounted for 80.8% of the variation at 40 dap (Supplementary Materials Figure S5a). PC1 explained 48.9% of the variance and was strongly influenced by the root system size (e.g., RA_40, RL_40), while PC2 accounted for 21.7% of the variation and was positively influenced by shoot morphological and physiological parameters, such as SFW_0 and CL_0. PC3 explained 10.2% of the variation and was mostly influenced by the root diameter (ARD_40). Consistent with the high correlation found between most vegetative and rooting parameters (see above and Supplementary Materials Figure S5b), PC1 clearly clustered different vegetative and rooting traits. Figure 6a includes representative stem cutting images corresponding to

plus or minus two times the standard deviation for PC1 and PC3. To help visualize the relative effect of each trait on the rooting performance, we built a star and rays graph for the double cross F_1 hybrids studied, which were ordered based on their average RA_40 values (Figure 6b). In agreement with these results, *L192* and *L245* displayed lower rooting performances than their bad rooting parental line (*2003 R 8*), while *L162* and *L062* displayed higher rooting performances than their good rooting parental line (*2101-02 MFR*).

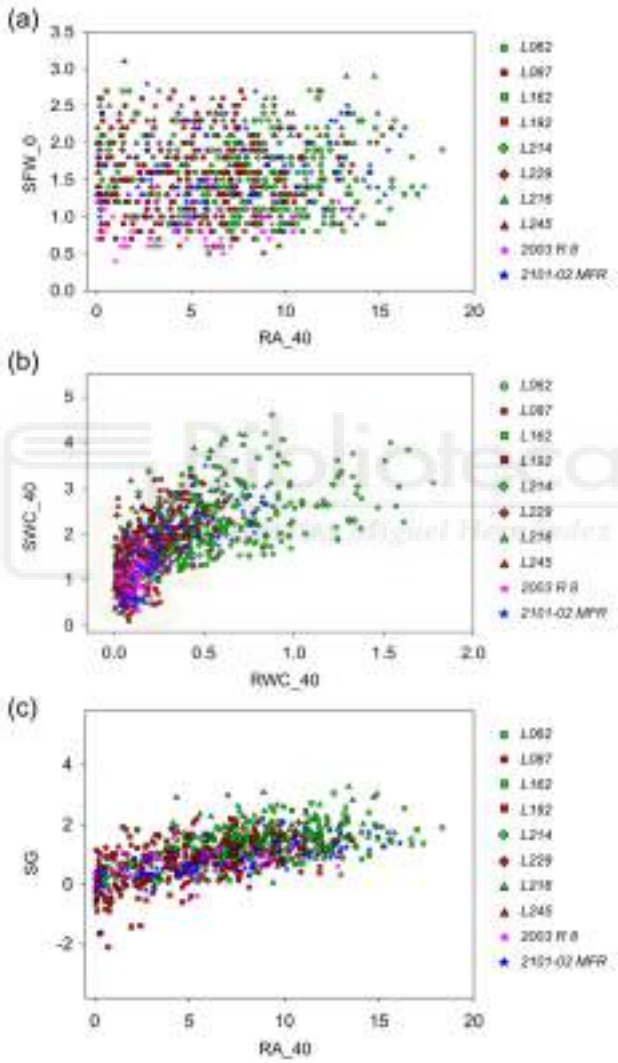

Figure 5. Parameter correlation observed in the third experiment for different physiological traits in the studied lines. Relationship between (**a**) the final root area (cm^2) and the initial shoot fresh weight (g), (**b**) the root water content (g) and the shoot water content (g) and (**c**) the root area (cm^2) and the final root growth. Each color and shape indicates one F_1 studied line (good rooting lines in green and bad rooting lines in red), including parental lines (stars).

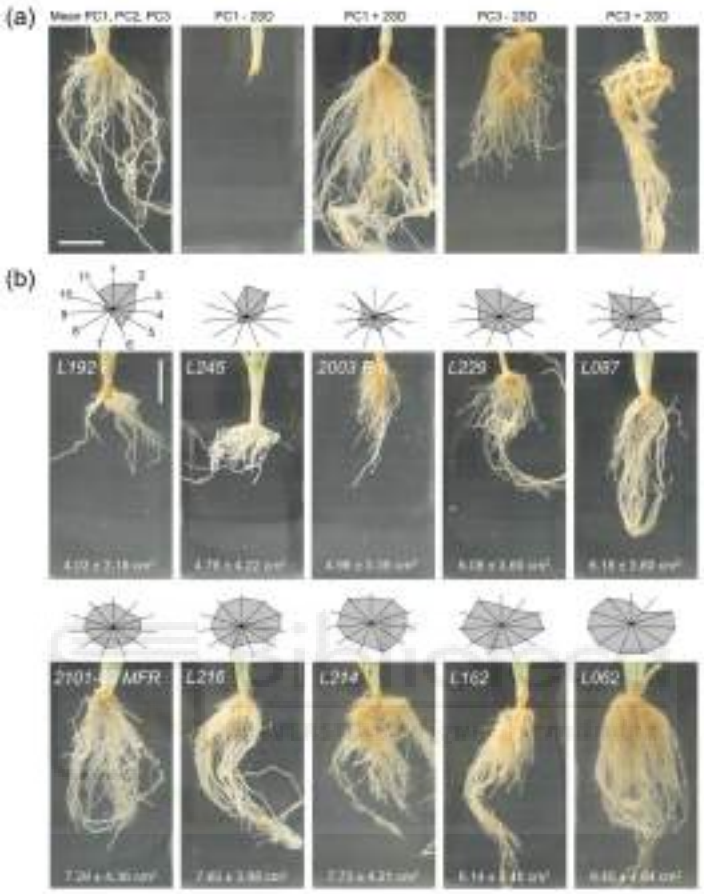

Figure 6. The double cross F_1 hybrid lines with extreme rooting phenotypes studied in the third experiment. (**a**) Representative images corresponding to plus or minus two times the standard deviation (+2 SD and −2 SD) for PC1 and PC3. (**b**) The stars and rays graphs highlight the differences between genotypes. Each axis represents one parameter, and its intersection with the polygon sides indicates the relative magnitude for that parameter: (1) shoot fresh weight at planting time, (2) cutting length at planting time, (3) shoot water content, (4) shoot growth, (5) root water content, (6) average root width, (7) root area, (8) root convex area, (9) root depth, (10) root length, and (11) rooting response. Parameters 3 to 11 were measured at 40 dap. Representative images for the studied F_1 lines are sorted by average root area values from the worst rooting line (*L192*) to the best rooting one (*L062*). Scale bar: 20 mm.

2.2.5. Hormonal Profiling in the Stem Cutting Base During the Rooting of Double-Cross F_1 Hybrids

We measured endogenous cytokinin (CK; *trans*-zeatin and zeatin riboside) levels in the stem cutting base during rooting. We found lower *trans*-zeatin levels in freshly harvested stem cuttings in all studied genotypes and these significantly increased after cold storage (Figure 7a). Compared to steady state levels, the average *trans*-zeatin level increased from 2.0-fold in *L245* to 6.1-fold in *2003 R 8* after cold storage. The *trans*-zeatin level was not significantly increased in the studied genotypes 24 h after planting. Together, we did not find any trend between CK levels and rooting performance in the double-cross F_1 hybrids studied (Figure 7a). However, we found a clear distinction between the *2003 R*

8 and *2101-02 MFR* parental genotypes, due to *2003 R 8* stem cuttings having doubled or quadrupled *trans*-zeatin levels at harvest and at planting time, respectively, as compared to those in *2101-02 MFR*.

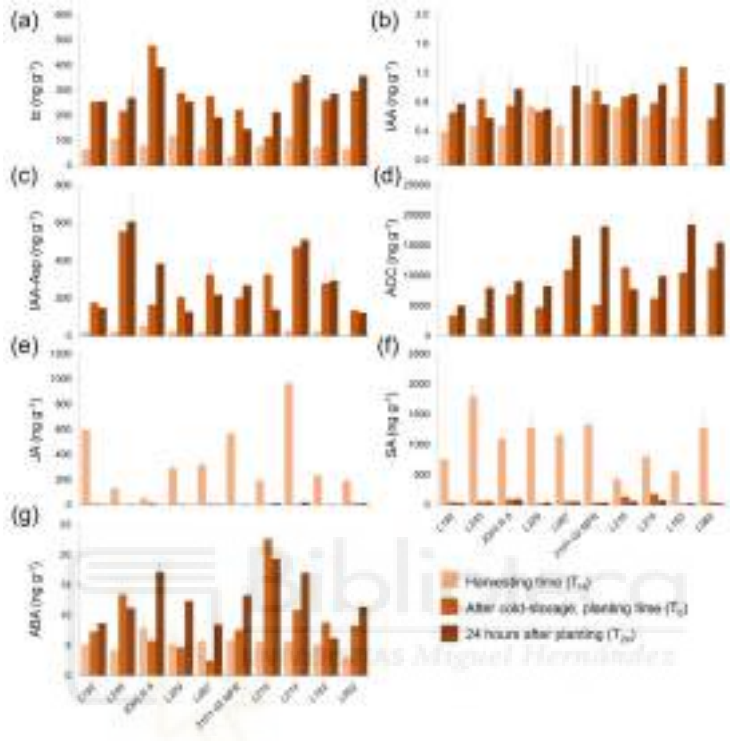

Figure 7. Hormonal profiling in selected lines for the third experiment. Bar charts at harvesting time (T_H), at planting time (T_0), and 24 hours after planting (T_{24}) for (**a**) *trans*-zeatin (*tZ*), (**b**) indole-3-acetic acid (IAA), (**c**) indole-3-acetyl-aspartate (IAA-Asp), (**d**) 1-aminocyclopropane-1-carboxylic acid (ACC), (**e**) jasmonic acid (JA), (**f**) salicylic acid (SA), and (**g**) abscisic acid (ABA).

We found low indole-3-acetic acid (IAA) levels in the stem cutting base of double-cross F_1 hybrids during the experiment, irrespective of their rooting performance (Figure 7b). Some inactive IAA conjugates, such as IAA-Asp, have previously been found at low levels at harvest time with a significant increase after cold storage [8]. In addition, the time course differences in IAA-Asp levels between the *2003 R 8* and *2101-02 MFR* lines might partially account for their contrasting rooting performances [7]. In agreement with our previous results, we found low IAA-Asp levels at harvest time and a significant increase after cold storage in all the studied genotypes (Figure 7c). Interestingly, contrasting IAA-Asp values were found in *L062* and *L245* throughout the experiment, which also corresponded to the best-rooting and worst-rooting double-cross F_1 hybrids studied (see above).

The level of 1-aminocyclopropane-1-carboxylic acid (ACC) in the stem cutting base is an indirect estimate of the ethylene concentration [10]. Confirming our previous results [8], low ACC levels were found in the freshly harvested stem cuttings of the studied genotypes, whereas ACC levels significantly increased during cold storage and were higher in the *2101-02 MFR* genotype compared with *2003 R 8* at the moment of planting (6802.67 and 11381.51 ng g^{-1}, respectively; Figure 7d). Interestingly, most bad rooting genotypes, such as *L192*, *L229,* and *L245*, displayed much lower ACC levels at planting time than those in the good rooting cultivars (*L062* or *L162*, Figure 7d), which suggests a positive correlation between rooting performance and endogenous ACC levels in the stem cutting

base at planting time in this species. Unusually, the *L087* line displayed high ACC levels at planting time and a bad rooting performance (Figure 7d). Jasmonic acid (JA) has been recently connected to a positive role in wound-induced adventitious rooting in several species through crosstalk with auxin and ethylene signals [11–13]. Thus, the JA level at harvesting time might be considered a direct read-out of the wound signal due to its quick turnover in carnation stem cuttings [8]. We did not find any clear correlation between the JA level at harvesting time (Figure 7e) and the rooting performance in carnation double-cross F_1 hybrids, as the highest JA-producers (*L192* and *L216*) displayed contrasting rooting phenotypes (Figure 6b). These results supported the hypothesis that the overall endogenous JA level is not critical for adventitious rooting in carnation stem cuttings. We also found significant variation in the endogenous SA level at harvesting time between the studied genotypes, which was reduced to the steady-state level during cold storage (Figure 7f). Despite this, we did not find any significant correlation between the endogenous SA level and the rooting performance; most of the bad rooting cultivars were characterized by a combination of low JA and high SA at harvest time, with the exception of the good rooting *L062* line. The highest ABA levels at harvest time were found in the *2003 R 8* parental line (7.86 ng g^{-1}; Figure 7g). In many cases, the endogenous ABA levels significantly increased during cold storage, except in *2003 R 8*, *L087*, and *L229*, and the highest fold-increase was observed in *2101-02 MFR*, followed by the bad rooting line *L245* (Figure 7g). These results indicate that endogenous ABA levels during early rooting are not directly correlated with the rooting performance in the double-cross F_1 hybrids studied, although they might contribute to stress adaptation during subsequent root growth.

3. Discussion

We previously reported that differences in the physiological status of *2003 R 8* and *2101-02 MFR* mother plants strongly contribute to successful adventitious rooting [8]. Our results confirm the morphological heterogeneity in stem cutting production and reveal high environmental dependence for *2003 R 8*, which also displayed a negative correlation between the leaf area at collection time and the rooting performance. Indeed, a large stem cutting area might directly contribute to significant water loss at planting time and before the newly produced adventitious root (AR) system is functional. A study performed in rice [14] identified the AR length as a useful marker for evaluating drought stress in different genotypes. Hence, carnation cultivars with a reduced stem cutting area and rapid AR production, such as *2101-02 MFR*, will handle water stress more efficiently than other genotypes.

Our F_1 population initially consisted of 114 selfed lines (from the *2101-02 MFR* cultivar) and 148 double-cross hybrid (i.e., outcrossing) lines derived from a cross between the *2003 R 8* and *2101-02 MFR* hybrid cultivars (E.Á. Cano, personal communication). We performed quantitative phenotyping of stem cutting morphology in a subset of these lines, which were selected based on breeding performance during stem cutting production. As a result, only 28.9% of the selfed lines (in contrast to 85.1% of outcrossing lines) were studied, which was in agreement with previous results of inbreeding depression in this species [15,16]. Adventitious rooting in soil plugs was studied as described previously [5], and transgressive segregation was found in both F_1 subpopulations for most of the studied traits. Interestingly, the AR area (RA_20) displayed high heterotic values in the outcrossing F_1 subpopulation as compared with the good rooting *2101-02 MFR* parental line, which suggests an additive effect of favorable alleles from both parental lines on AR growth and development. In a recent study in cucumber, a large F_2 population derived from two contrasting lines differing in the AR number during waterlogging stress was studied, and the genetic dissection of this quantitative trait has been initiated [17]. We also found high heterotic values for the AR diameter (ARD_20) in both F_1 subpopulations that deserve further investigation. In contrast, previous experiments reported low levels of heterosis in the primary root diameter in maize during early development [18].

To initiate the genetic dissection of AR development in this species, in a second experiment, we evaluated several AR traits in 26 outcrossing lines displaying contrasting heterotic values. We discarded most of these lines for further experiments due to strong genotype × environment (G × E) interactions or

unavailable plant material (E.Á. Cano, personal communication). We found higher heritability values on AR traits when considering only the selected lines that were environmentally stable. However, in some AR traits, heritability values were low (e.g., ARD_20), which might complicate subsequent genetic analyses. Some studies have initiated the genetic analysis of AR development in several species, such as teosinte [19], bean [20], rice [21], poplar [22], barley [23], and cucumber [17], with variable success. In the poplar study [22], despite moderate heritability for the AR number (H^2 = 0.27–0.34), the integration of genetic, genomic, and transcriptomic information allowed the identification of two quantitative trait loci (QTL) for this trait. Their results suggest that the difference in the AR numbers of two contrastingly distinct species, *Populus deltoides* and *Populus trichocarpa*, is driven by the difference in the expression of two genes in the IAA biosynthesis pathway, possibly the poplar homologues of *SUPERROOT2* (*SUR2*) and *TRYPTOPHAN SYNTHASE ALPHA CHAIN* (*TSA1*).

In a third experiment, we studied several physiological and adventitious rooting traits in a selected population of double-cross F_1 hybrids and their parental lines, *2003 R 8* and *2101-02 MFR*. For a complete visualization of their AR systems, we removed substrates at different times after planting (dap). At 40 dap, we identified three PCs associated with 80.8% of the variation. Traits related to the AR system size positively contributed to PC1 (48.9% of the observed variance), while shoot traits at planting time positively contributed to PC2 (21.7% of the variance). These results are in agreement with our previous observation that large stem cuttings displayed lower rooting performances [5], likely due to their higher drought stress sensitivity. Root system architecture traits, such as length, diameter, and area, determine root performance, enabling plants to acquire water and nutrients and thereby increase the replacement rate of their water loss [24]. Optimum root systems can support shoot growth and improve plant yield, since roots are the functional interface between plants and the soil [25]. An enlarged root system will penetrate into deeper layers of soil to acquire water and nutrients more efficiently [26]. Our study identified a key correlation between a large, functional root system (estimated by RA_40 and RWC) and proper water balance in the shoot, which is essential for shoot growth (SWC and SG, respectively). Interestingly, a significant amount of the observed variation was influenced by the root diameter, which greatly contributed to PC3 (10.2%). A recent study on wheat indicated that the root diameter plays an important role in phosphorus-deficiency tolerance, as it defines the volume of soil in contact with the roots [27]. In this and other species, the survival ability of individual roots increases with an increasing root diameter [28]. However, the effect of the root diameter on plant performance is controversial, as the increase in this trait has been shown to promote nutrient uptake due to increases in xylem and phloem tissues as the surface area increases [29], while seemingly relatively thinner roots might be more effective at absorbing soil phosphate. Therefore, an increased carnation AR root diameter might negatively contribute to limiting the nutrient uptake (i.e., phosphorus) during early AR development and thus restrict root growth. Our previous results with a limited number of carnation genotypes suggest that the root diameter is negatively correlated with the rooting performance [5]. Our current results show a low correlation between the AR diameter and AR system size traits. Consequently, it remains unclear whether the AR diameter increases or decreases the AR performance of carnation stem cuttings, and additional experiments will be required to determine whether the AR diameter should be included as a positive or negative trait during breeding.

In our study, the double-cross F_1 hybrids *L192* and *L245* displayed poor rooting performances as compared with the bad rooting *2003 R 8* parental line. However, significant differences were found in the JA, SA, and IAA-Asp levels in the stem cutting bases of *L192* and *L245* during the experiment. *L245* presented a lower rooting response and more retarded root growth than *L192*, which was correlated with the high SA/JA proportion at harvest time and the high IAA-Asp level during rooting in the *L245* line. Low levels of exogenously-applied SA promoted AR formation in mung bean (*Vigna radiata*) hypocotyl cuttings, but an increased SA concentration inhibited this process [30]. As in most species [31], adventitious rooting is also strongly influenced by auxin homeostasis in carnations [7], and one intriguing possibility is that unknown SA–JA–IAA crosstalk might play a regulatory role

in adventitious rooting. *L062* and *L162* displayed better rooting performance than the good rooting *2101-02 MFR* parental line. The ACC levels were quite high in these good rooting lines while their IAA-Asp levels were moderate. High levels of ACC after cold storage and during early rooting might reflect increased ethylene production after planting, which might contribute to enhanced adventitious rooting, as suggested previously [6]. In mung bean cuttings, exogenous ethylene application promoted AR formation, with a positive effect during AR initiation [32]. There is additional evidence of direct crosstalk between ethylene and auxin transport during AR formation [33,34], and further experiments are needed to elucidate if similar crosstalk is operating in carnation stem cuttings.

The rooting ability in carnation stem cuttings involves a multifactorial process that is regulated by different phytohormones, where endogenous auxin homeostasis and stress-related metabolites such as ethylene might play essential roles. Regulation of these hormonal pathways can establish the AR quality of each line and the improvement of some morphological and physiological traits involved in this process, as we have seen here. Further studies are necessary in order to improve the characterization of the studied cultivars and to determine the causative molecular basis. To this end, time series transcriptome analysis during AR formation in bulked samples from bad rooting (*2003 R 8*, *L192* and *L245*) and good rooting (*L062* and *L162*) F_1 hybrids will allow the identification of differentially regulated genes with alternative alleles that could be used to map some of the QTLs involved in the observed differences in adventitious rooting quality traits.

4. Materials and Methods

4.1. Plant Material, Growing Conditions, and Sample Collection

Carnation cultivars *2003 R 8* and *2101-02 MFR* with contrasting rooting phenotypes were obtained from Dümmen Orange (http://www.dummenorange.com). The studied population consisted of 159 F_1 lines derived from a cross between these parental cultivars, which included 33 selfed lines (from the *2101-02 MFR* cultivar) and 126 outcrossing lines. Mother plants from all of these lines and the two parental cultivars were grown in the same greenhouse and under environmental conditions at 37°34′50″N, 1°46′35″W and at an altitude of 395 m (Puerto Lumbreras, Murcia, Spain).

4.1.1. First and Second Experiments

For each genotype, commercial quality stem cuttings were pinched from several mature (>1 year old) mother plants by skilled operators every 15 days from 7 April to 30 July 2014. Stem cuttings were immediately wrapped in plastic bags and stored in a cold chamber at 5 ± 2 °C and 60% relative humidity in complete darkness. For each experiment, 20–25 stem cuttings from each genotype were randomly selected and individually planted, as described previously [5].

The first experiment was divided into 10 batches (B01 to B10), and the stem cuttings of different lines were planted from 17 June to 9 September 2014. Twenty-six outcrossing F_1 lines from the first experiment with contrasting rooting phenotypes were selected for the second experiment. This second experiment included three additional batches (B11 to B13), and stem cuttings were planted from 7 October to 29 October 2014. All stem cuttings were individually planted in moistened peat-perlite (90/10 *v/v*) substrate trays of truncated pyramid plugs (2.5 × 2.5 × 4.0 cm; 16 cm^3), as indicated above. Water, fertilizer, and adequate phytosanitary treatments were periodically applied [5,35].

4.1.2. Third Experiment

With the results obtained in the previous two experiments, eight F_1 outcrossing lines with extreme rooting phenotypes were selected based on the rooting stage and root area average values at 20 dap. Carnation stem cuttings from these selected lines and the parental lines were pinched from several mature mother plants by skilled operators from 23 January to 19 April 2017. Stem cuttings were wrapped in plastic bags and stored in a dark and cold chamber at 5 ± 2 °C.

A total of 106 cold-stored stem cuttings of each genotype were randomly selected and individually planted in moistened peat-perlite (50/50 *v/v*) substrate trays of truncated pyramid plugs (3.8 × 3.8 × 4.0 cm; 32 cm^3). Stem cuttings were grown from 11 May to 20 June 2017 in a single batch (B14), on a gothic-arch greenhouse at 38°16′43′′ N, 0°41′15′′ W at an altitude of 96 m (Elche, Spain) under environmental conditions and with periodic sprinkler irrigation.

At planting time (0 dap), the stem cutting length and fresh weight were measured in each sample. At the end of the experiment (40 dap), fresh weights were separately measured for shoot and root tissue in each sample. For dry weight measurements, shoot and root tissues were dehydrated for three days in a stove at 80 °C (J.P. Selecta S.A., Barcelona, Spain) and weighed on a high precision scale (PCE Instruments, Spain).

For hormone analysis, three replicates of each genotype, each consisting of 12 (T_0 and T_{24}) or 25 (T_H) stem cutting bases (about 4 mm long), were collected at three different times: (T_H) when stem cuttings were collected from the mother plants, (T_0) at planting time (0 dap), and (T_{24}) 24 hours after planting (1 dap). Samples were immediately frozen in liquid nitrogen and stored at −80 °C.

4.2. Picture and Image Processing

4.2.1. Image Collection

For the first and second experiments, stem cutting pictures were taken from one side of the soil plug at 13 dap (n = 20 stem cuttings) and 20 dap (n = 25 stem cuttings). Pictures were taken using a Canon 60D camera with a Canon EF-S 17-85 mm f/4-5.6 IS USM lens with a resolution of 5184 × 3466 pixels.

Pictures of 28 randomly selected stem cuttings from the third experiment were taken from one side of the soil plug at 19 and 29 dap. The soil plug was carefully removed at 40 dap by washing it with high-pressure tap water, and the entire root system was imaged after transferring it to a water bath (n = 106 stem cuttings). Pictures were taken using a Canon EOS camera with a Canon EF-S 18–55 mm lens and a resolution of 4272 × 2848 pixels.

To minimize variations due to sunlight quality during the day, a portable photographic bench was used, and all the pictures were taken at the greenhouse between 11 a.m. and 1 p.m. These pictures were saved as an RGB color image in jpeg format. All original pictures are available upon request.

4.2.2. Image Processing

In each picture, stem and root tissue were separated by using the Multiple Image Processor plug-in of ImageJ (https://imagej.net/) and batch-imported into GiA Roots software [9]. After scale calibration and grayscale conversion (RGB to gray simple conversion option), stem cutting images were segmented using the Global Thresholding method, and soil plugs and root images were segmented using the Double Adaptive Thresholding method (Supplementary Materials Figure S1). Eventually, thresholds were manually adjusted in some batches to maximize object identification (stem or roots) depending on the image brightness or darkness level. In the third experiment, a defined region in each image (1000 × 1100 pixels) containing the rooting region was used for image segmentation with the GiA Roots software, as described above.

All root system architectural traits and shoot traits measured by GiA Roots were initially selected and were computed directly from the image mask or from the skeleton of the image mask, as described elsewhere [9]. After batch-processing, raw measurements were exported to Excel spreadsheets for data analysis. Other parameters were visually quantified (leaf number, rooting stage, and rooting response) or calculated from previous parameters (e.g., shoot area increase). Measurements of selected traits (Table 1) in the first and second experiment are shown in Supplementary Materials Table S3 for all F_1 studied lines. In the third experiment, the following additional parameters were also measured: fresh weight and length of stem cuttings measured at planting time (0 dap) and shoot fresh weight, shoot

dry weight, shoot water content, shoot growth, root fresh weight, root dry weight, and root water content measured at 40 dap (Table 2 and Supplementary Materials Table S4).

4.3. Statistical Analyses

Statistical analyses of the data and descriptors (mean, SD, maximum and minimum, and correlation values) were estimated with StatGraphics Centurion XV software (StatPoint Technologies, United States). Data outliers were identified based on aberrant standard deviation values and were excluded for posterior analyses, as described elsewhere [36]. One-sample Kolmogorov–Smirnov tests were performed to analyze the goodness-of-fit between the distribution of the data and a theoretical normal distribution. Non-parametric tests and data transformation ($y = \frac{1}{x}; y = x^2; y = log_2(x); y = \sqrt{x}$) were applied when needed. To reduce the number of studied traits, we performed multiple correlation tests. To compare the data for a given variable, we performed multiple testing analyses with the ANOVA F-test or the Fisher's LSD methods. Significant differences were defined as a 5% level of significance (p-value < 0.05), unless otherwise indicated. To establish the level of correlation between different morphometric parameters, multiple correlation tests were carried out for selected parameters at different times for all experiments. PCA was performed to check the best-fitting parameter combination in each case at the end of the parameter selection protocol. Star and ray graphs showing differences between selected cultivars in the third experiment were constructed using the Multivariate visualization option and Star and ray chart option in StatGraphics Centurion XV software, comparing average values for all studied traits.

For the statistical analysis of stem cutting ecophysiology traits, nonparametric Kruskall–Wallis tests were assayed. SigmaPlot v12.0 (Systat Software Inc., San José CA, USA) was used for correlation studies and graphical representation.

4.3.1. Estimation of Heterosis in Selfing and Outcrossing F_1 Populations

Heterosis (H) percentage values were calculated for each studied trait in the first experiment for selfing and outcrossing populations, as described elsewhere [37], and expressed as an increase or decrease of F_1 hybrid values over mid-parent (relative heterosis, *MP*) or better parent (*BP*) values. Heterosis was calculated as indicated below:

$$H(BP) = \left(\frac{F1 - BP}{BP}\right)x\,100$$

$$H(MP) = \left(\frac{F1 - MP}{MP}\right)x\,100$$

where F1 represents the mean performance of F_1, BP represents the average better-parent performance, and MP represents the average mid-parental value.

4.3.2. Estimation of Broad-Sense Heritability in Selected Lines

We estimated the broad-sense heritability (H^2) of measured traits in selected lines of the third experiment by means of a multifactorial ANOVA, as described elsewhere [38]. The data values for these selected lines in the first and second experiments allowed us to compare their behaviors in two different environments (e). Heritability was calculated as indicated below:

$$H^2 = \frac{\sigma^2 G}{\sigma^2 G + \left(\frac{\sigma^2 GE}{e}\right) + \frac{\sigma^2 E}{re}}$$

where $\sigma^2 G = \frac{MS_G}{re}$; $\sigma^2 GE = \frac{MS_{GE} - MS_E}{r}$; $\sigma^2 E = MS_E$, r represents the number of replicates or individuals per experiment, e represents the number of environments or experiments, MS_G represents the mean square of the genotype, MS_{GE} represents the mean square of the interaction between the genotype and the experiment, and MS_E represents the mean square error.

4.4. Phytohormone Extraction and Analysis

Indole-3-acetic acid (IAA), IAA-aspartate conjugate (IAA-Asp), *trans*-zeatin (*tZ*), salicylic acid (SA), jasmonic acid (JA), abscisic acid (ABA), and the ethylene precursor 1-aminocyclopropane-1-carboxylic acid (ACC) were analyzed in accordance with Reference [39] with some modifications. Cold stored samples were freeze-dried in liquid nitrogen and ground with a pestle into a coarse powder. Powdered samples were homogenized in 0.5 mL of cold (−20 °C) extraction mixture of methanol/water (80/20, *v/v*). Solids were separated by centrifugation (20,000 g, 15 min) and re-extracted for 30 min at 4 °C in an additional 0.5 mL of the same extraction solution. Pooled supernatants were passed through Sep-Pak Plus †C18 cartridges (SepPak Plus, Waters, USA) to remove interfering lipids and part of the plant pigment. They were evaporated at 40 °C under vacuum either to near dryness or until the organic solvent was removed. The residue was dissolved in 1 mL of methanol/water (20/80, *v/v*) solution using an ultrasonic bath. The dissolved samples were filtered through 13 mm diameter Millex filters with nylon membrane (0.22 μm pore size, Millipore, Bedford, MA, USA).

Ten microliters of filtrated extract was injected into a U-HPLC-MS system consisting of an Accela Series U-HPLC (ThermoFisher Scientific, Waltham, MA, USA) coupled to an Exactive mass spectrometer (ThermoFisher Scientific, Waltham, MA, USA) using a heated electrospray ionization (HESI) interface. Mass spectra were obtained using Xcalibur software, version 2.2 (ThermoFisher Scientific, Waltham, MA, USA). For quantification of the plant hormones, calibration curves were constructed for each analyzed component (1, 10, 50, and 100 μg L^{-1}) and corrected for 10 μg L^{-1} deuterated internal standards. Recovery percentages ranged between 92% and 95%. The raw data for phytohormone extraction are shown in Supplementary Materials Table S5.

5. Conclusions

Vegetative propagation of elite carnation genotypes depends on successful rooting of their stem cuttings. AR formation is a complex developmental process that is strongly influenced by exogenous and endogenous factors. We found a striking variation in rooting performance in a selected F_1 population derived from a cross between *2003 R 8* and *2101-02 MFR*, which could be used to breed carnation cultivars with enhanced rooting ability to increase production under challenging environmental conditions, such as drought. The leaf water content of the mother plants could be measured in vivo with terahertz spectroscopy technology [40], and this information could be used to predict the adventitious rooting performance of different carnation genotypes. Additional analyses are necessary in order to verify the usefulness of this new technique and its possible implementation in the vegetative mass-production of highly valued ornamental species.

Supplementary Materials: The following are available online at http://www.mdpi.com/2223-7747/8/7/226/s1: Figure S1: Image analysis of carnation stem cuttings; Figure S2: Descriptive traits of the double-cross F1 lines studied in the first experiment; Figure S3: Descriptive traits of the double-cross F1 lines studied in the third experiment; Figure S4: Parameter correlation for different physiological traits in the third experiment; Figure S5: Descriptive traits of the double-cross F1 lines studied in the third experiment. Table S1: Heterosis values for the F1 subpopulations studied; Table S2: Correlation analyses among different physiological traits in the third experiment; Table S3: Raw data for selected parameters in the first and second experiments; Table S4: Raw data for selected parameters in the third experiment; Table S5: Raw data for phytohormones measured.

Author Contributions: Conceptualization, J.M.P.-P., E.A.C., M.A.; methodology, J.M.P.-P.; validation, J.M.P.-P, M.S.J; formal analysis, J.M.P.-P, M.S.J.; hormonal analysis, A.C., A.A.; experiment performance, J.V., V,B.; investigation, J.M.P.-P., M.S.J. and J.R.A.; resources, J.M.P.-P, E.A.C.; data curation, M.S.J. and J.R.A.; writing—original draft preparation, J.M.P.-P., M.S.J. and J.R.A.; writing—review and editing, J.M.P.-P., M.S.J. and J.R.A.; supervision J.M.P.-P.; project administration, M.A., J.M.P.-P., E.A.C.; funding acquisition, J.M.P.-P., E.A.C.

Funding: This research was funded by the Ministerio de Economía, Industria y Competitividad (MINECO) of Spain (grants no. AGL2012-33610 and BIO2015-64255-R), by the Center for the Development of Industrial Technology (CARNOMICS Eurostars-EUREKA Project E! 6384), and by the European Regional Development Fund (ERDF) of the European Commission.

Acknowledgments: We would like to thank Dümmen Orange for providing plant material and research facilities.

Conflicts of Interest: The authors declare no conflict of interest.

References

1. Bellini, C.; Pacurar, D.I.; Perrone, I. Adventitious roots and lateral roots: Similarities and differences. *Annu. Rev. Plant Biol.* **2014**, *65*, 639–666. [CrossRef] [PubMed]
2. Steffens, B.; Rasmussen, A. The physiology of adventitious roots. *Plant Physiol.* **2016**, *170*, 603–617. [CrossRef] [PubMed]
3. Druege, U.; Hilo, A.; Pérez-Pérez, J.M.; Koplotek, Y.; Acosta, M.; Shahinnia, F.; Zerche, S.; Franken, P.; Hajirezaei, M.R. Molecular and physiological control of adventitious rooting in cuttings: Phytohormone action meets resource allocation. *Ann. Bot.* **2019**, *123*, 929–949. [CrossRef] [PubMed]
4. Garrido, G.; Arnao, M.B.; Acosta, M.; Sánchez-Bravo, J. Polar transport of indole-3-acetic acid in relation to rooting in carnation cuttings: Influence of cold storage duration and cultivar. *Biol. Plant.* **2003**, *47*, 481–485. [CrossRef]
5. Birlanga, V.; Villanova, J.; Cano, A.; Cano, E.A.; Acosta, M.; Pérez-Pérez, J.M. Quantitative analysis of adventitious root growth phenotypes in carnation stem cuttings. *PLoS ONE* **2015**, *10*, e0133123. [CrossRef] [PubMed]
6. Villacorta-Martín, C.; Sánchez-García, A.B.; Villanova, J.; Cano, A.; van de Rhee, M.; de Haan, J.; Acosta, M.; Passarinho, P.; Pérez-Pérez, J.M. Gene expression profiling during adventitious root formation in carnation stem cuttings. *BMC Genom.* **2015**, *16*, 789–806. [CrossRef] [PubMed]
7. Cano, A.; Sánchez-García, A.B.; Albacete, A.; González-Bayón, R.; Justamante, M.S.; Ibáñez, S.; Acosta, M.; Pérez-Pérez, J.M. Enhanced conjugation of auxin by GH3 enzymes leads to poor adventitious rooting in carnation stem cuttings. *Front. Plant Sci.* **2018**, *9*, 566. [CrossRef]
8. Villanova, J.; Cano, A.; Albacete, A.; López, A.; Cano, E.Á.; Acosta, M.; Pérez-Pérez, J.M. Multiple factors influence adventitious rooting in carnation (*Dianthus caryophyllus* L.) stem cuttings. *Plant Growth Regul.* **2017**, *81*, 511–521. [CrossRef]
9. Galkovskyi, T.; Mileyko, Y.; Bucksch, A.; Moore, B.; Symonova, O.; Price, C.A.; Topp, C.N.; Iyer-Pascuzzi, A.S.; Zurek, P.R.; Fang, S.; et al. GiA Roots: Software for the high throughput analysis of plant root system architecture. *BMC Plant Biol.* **2012**, *12*, 116. [CrossRef]
10. Agulló-Antón, M.Á.; Ferrández-Ayela, A.; Fernández-García, N.; Nicolás, C.; Albacete, A.; Pérez-Alfocea, F.; Sánchez-Bravo, J.; Pérez-Pérez, J.M.; Acosta, M. Early steps of adventitious rooting: Morphology, hormonal profiling and carbohydrate turnover in carnation stem cuttings. *Physiol. Plant.* **2014**, *150*, 446–462. [CrossRef]
11. Lischweski, S.; Muchow, A.; Guthörl, D.; Hause, B. Jasmonates act positively in adventitious root formation in petunia cuttings. *BMC Plant Biol.* **2015**, *15*, 229. [CrossRef] [PubMed]
12. Fattorini, L.; Hause, B.; Gutierrez, L.; Veloccia, A.; Della Rovere, F.; Piacentini, D.; Falasca, G.; Altamura, M.M. Jasmonate promotes auxin-induced adventitious rooting in dark-grown *Arabidopsis thaliana* seedlings and stem thin cell layers by a cross-talk with ethylene signalling and a modulation of xylogenesis. *BMC Plant Biol.* **2018**, *18*, 182. [CrossRef] [PubMed]
13. Zhang, G.; Zhao, F.; Chen, L.; Pan, Y.; Sun, L.; Bao, N.; Zhang, T.; Cui, C.X.; Qiu, Z.; Zhang, Y.; et al. Jasmonate-mediated wound signalling promotes plant regeneration. *Nat. Plants* **2019**, *5*, 491–497. [CrossRef] [PubMed]
14. Zheng, B.; Yang, L.; Mao, C.; Huang, Y.; Wu, P. Comparison of QTLs for rice seedling morphology under different water supply conditions. *J. Genet. Genom.* **2008**, *35*, 473–484. [CrossRef]
15. Sato, S.; Katoh, N.; Yoshida, H.; Iwai, S.; Hagimori, M. Production of doubled haploid plants of carnation (*Dianthus caryophyllus* L.) by pseudofertilized ovule culture. *Sci. Hortic.* **2000**, *83*, 301–310. [CrossRef]
16. Onozaki, T. Breeding of carnations (*Dianthus caryophyllus* L.) for long vase life. *Breed. Sci.* **2018**, *68*, 3–13. [CrossRef]
17. Xu, X.; Ji, J.; Xu, Q.; Qi, X.; Weng, Y.; Chen, X. The major-effect quantitative trait locus CsARN6.1 encodes an AAA ATPase domain-containing protein that is associated with waterlogging stress tolerance by promoting adventitious root formation. *Plant J.* **2018**, *93*, 917–930. [CrossRef]
18. Hoecker, N.; Keller, B.; Piepho, H.P.; Hochholdinger, F. Manifestation of heterosis during early maize (*Zea mays* L.) root development. *Theor. Appl. Genet.* **2006**, *112*, 421–429. [CrossRef]
19. Mano, Y.; Muraki, M.; Fujimori, M.; Takamizo, T.; Kindiger, B. Identification of QTL controlling adventitious root formation during flooding conditions in teosinte (*Zea mays* ssp. huehuetenangensis) seedlings. *Euphytica* **2005**, *142*, 33–42. [CrossRef]

20. Ochoa, I.E.; Blair, M.W.; Lynch, J.P. QTL analysis of adventitious root formation in common bean under contrasting phosphorus availability. *Crop Sci.* **2006**, *46*, 1609–1621. [CrossRef]
21. Horii, H.; Nemoto, K.; Miyamoto, N.; Harada, J. Quantitative trait loci for adventitious and lateral roots in rice. *Plant Breed.* **2006**, *125*, 198–200. [CrossRef]
22. Ribeiro, C.L.; Silva, C.M.; Drost, D.R.; Novaes, E.; Novaes, C.R.; Dervinis, C.; Kirst, M. Integration of genetic, genomic and transcriptomic information identifies putative regulators of adventitious root formation in *Populus*. *BMC Plant Biol.* **2016**, *16*, 66. [CrossRef] [PubMed]
23. Guo, J.; Chen, G.; Zhang, X.; Li, T.; Yu, H.; Liu, C. Quantitative trait locus analysis of adventitious and lateral root morphology of barley grown at low and high P. *Funct. Plant Biol.* **2018**, *45*, 957–967. [CrossRef]
24. Dodd, I.C.; Puértolas, J.; Huber, K.; Pérez-Pérez, J.G.; Wright, H.R.; Blackwell, M.S. The importance of soil drying and re-wetting in crop phytohormonal and nutritional responses to deficit irrigation. *J. Exp. Bot.* **2015**, *66*, 2239–2252. [CrossRef] [PubMed]
25. Faget, M.; Nagel, K.A.; Walter, A.; Herrera, J.M.; Jahnke, S.; Schurr, U.; Temperton, V.M. Root–root interactions: Extending our perspective to be more inclusive of the range of theories in ecology and agriculture using in-vivo analyses. *Ann. Bot.* **2013**, *112*, 253–266. [CrossRef]
26. Franco, J.A.; Bañón, S.; Vicente, M.J.; Miralles, J.; Martínez-Sánchez, J.J. Root development in horticultural plants grown under abiotic stress conditions—A review. *J. Hortic. Sci. Biotechnol.* **2011**, *86*, 543–556. [CrossRef]
27. Wu, F.; Yang, X.; Wang, Z.; Deng, M.; Ma, J.; Chen, G.; Wei, Y.; Liu, Y. Identification of major quantitative trait loci for root diameter in synthetic hexaploid wheat under phosphorus-deficient conditions. *J. Appl. Genet.* **2017**, *58*, 437–447. [CrossRef]
28. Qiu, X.Q.; Gao, Y.; Huang, L.; Li, X.Q.; Sun, J.S.; Duan, A.W. Temporal and spatial distribution of root morphology of winter wheat. *Sci. Agric. Sin.* **2013**, *46*, 2211–2219.
29. Zhao, C.; Craig, J.C.; Petzold, H.E.; Dickerman, A.W.; Beers, E.P. The xylem and phloem transcriptomes from secondary tissues of the Arabidopsis root-hypocotyl. *Plant Physiol.* **2005**, *138*, 803–818. [CrossRef]
30. Yang, W.; Zhu, C.; Ma, X.; Li, G.; Gan, L.; Ng, D.; Xia, K. Hydrogen peroxide is a second messenger in the salicylic acid-triggered adventitious rooting process in mung bean seedlings. *PLoS ONE* **2013**, *8*, e84580. [CrossRef]
31. Pacurar, D.I.; Perrone, I.; Bellini, C. Auxin is a central player in the hormone cross-talks that control adventitious rooting. *Physiol. Plant.* **2014**, *151*, 83–96. [CrossRef] [PubMed]
32. De Klerk, G.J.; Hanecakova, J. Ethylene and rooting of mung bean cuttings. The role of auxin induced ethylene synthesis and phase-dependent effects. *Plant Growth Regul.* **2008**, *56*, 203. [CrossRef]
33. Veloccia, A.; Fattorini, L.; Della Rovere, F.; Sofo, A.; D'angeli, S.; Betti, C.; Falasca, G.; Altamura, M.M. Ethylene and auxin interaction in the control of adventitious rooting in *Arabidopsis thaliana*. *J. Exp. Bot.* **2016**, *67*, 6445–6458. [CrossRef] [PubMed]
34. Negi, S.; Sukumar, P.; Liu, X.; Cohen, J.D.; Muday, G.K. Genetic dissection of the role of ethylene in regulating auxin-dependent lateral and adventitious root formation in tomato. *Plant J.* **2010**, *61*, 3–15. [CrossRef] [PubMed]
35. Jawaharlal, M.; Ganga, M.; Padmadevi, K.; Jegadeeswari, V.; Karthikeyan, S. *A Technical Guide on Carnation*; Tamil Nadu Agricultural University: Coimbatore, India, 2009; pp. 1–56.
36. Aguinis, H.; Gottfredson, R.K.; Joo, H. Best-practice recommendations for defining, identifying, and handling outliers. *Organ. Res. Methods* **2013**, *16*, 270–301. [CrossRef]
37. Zeleke, H. Heterosis and combining ability for grain yield and yield component traits of maize in eastern Ethiopia. *Sci. Technol. Arts Res. J.* **2015**, *4*, 32–37. [CrossRef]
38. Lynch, M.; Walsh, B. *Genetics and Analysis of Quantitative Traits*; Sinauer: Sunderland, MA, USA, 1998; Volume 1, pp. 535–557.
39. Albacete, A.; Ghanem, M.E.; Martínez-Andújar, C.; Acosta, M.; Sánchez-Bravo, J.; Martínez, V.; Lutts, S.; Dodd, I.C.; Pérez-Alfocea, F. Hormonal changes in relation to biomass partitioning and shoot growth impairment in salinized tomato (*Solanum lycopersicum* L.) plants. *J. Exp. Bot.* **2008**, *59*, 4119–4131. [CrossRef]
40. Gente, R.; Koch, M. Monitoring leaf water content with THz and sub-THz waves. *Plant Methods* **2015**, *11*, 15. [CrossRef]

Supplementary Figures:

Figure S1. Image analysis of carnation stem cuttings.

Figure S2. Descriptive traits of the double-cross F_1 lines studied in the first experiment.

Figure S3. Descriptive traits of the double-cross F_1 lines studied in the third experiment.

Figure S4. Parameter correlation for different physiological traits in the third experiment.

Figure S5. Descriptive traits of the double-cross F_1 lines studied in the third experiment.

Supplementary Tables:

Supplementary Table S1. Heterosis values for the F_1 subpopulations studied. Heterosis (H) percentages estimated for F_1 subpopulations for the studied traits compared with the best-rooting parental line (BP, *2101-02 MFR*) or both parental lines (MP).

Supplementary Table S2. Correlation analyses among different physiological traits in the third experiment. Interaction between shoot and root traits was estimated by (a) shoot fresh weigth and root area, (b) shoot water content and root water content, (c) shoot growth and root area, (d) shoot water content and root area and (e) shoot growth and root water content. For each correlation, R^2 values, r values (Pearson correlation coefficient) and p-values are shown for each genotype. ns = not significant.

Supplementary Table S3. Raw data for selected parameters in the first and second experiments.

Supplementary Table S4. Raw data for selected parameters in the third experiment.

Supplementary Table S5. Raw data for phytohormones measured.

Figure S1

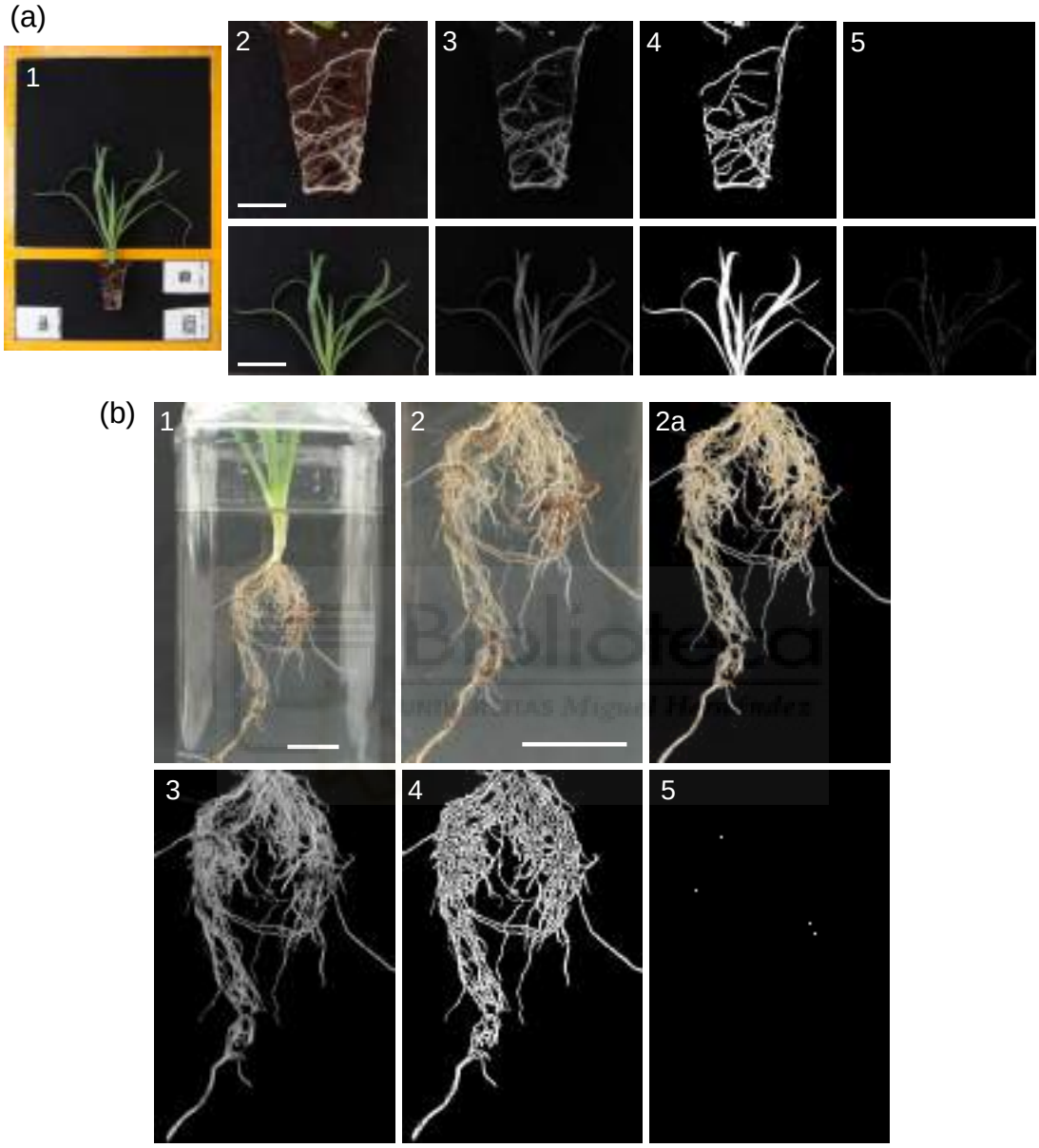

Figure S1. Image analysis of carnation stem cuttings. (**a**) Pictures obtained in the first and second experiment (soil plug and the vegetative part), where 1) is the original picture, 2) cropped pictures, 3) grey scale converted images, 4) thresholded images and 5) skeletonized images. Scale bars: 10 mm (roots) and 35 mm (shoots). (**b**) Pictures obtained in the third experiment on the whole root system, with and additional step of image processing (2a) to remove background noise. Scale bars: 20 mm.

Figure S2

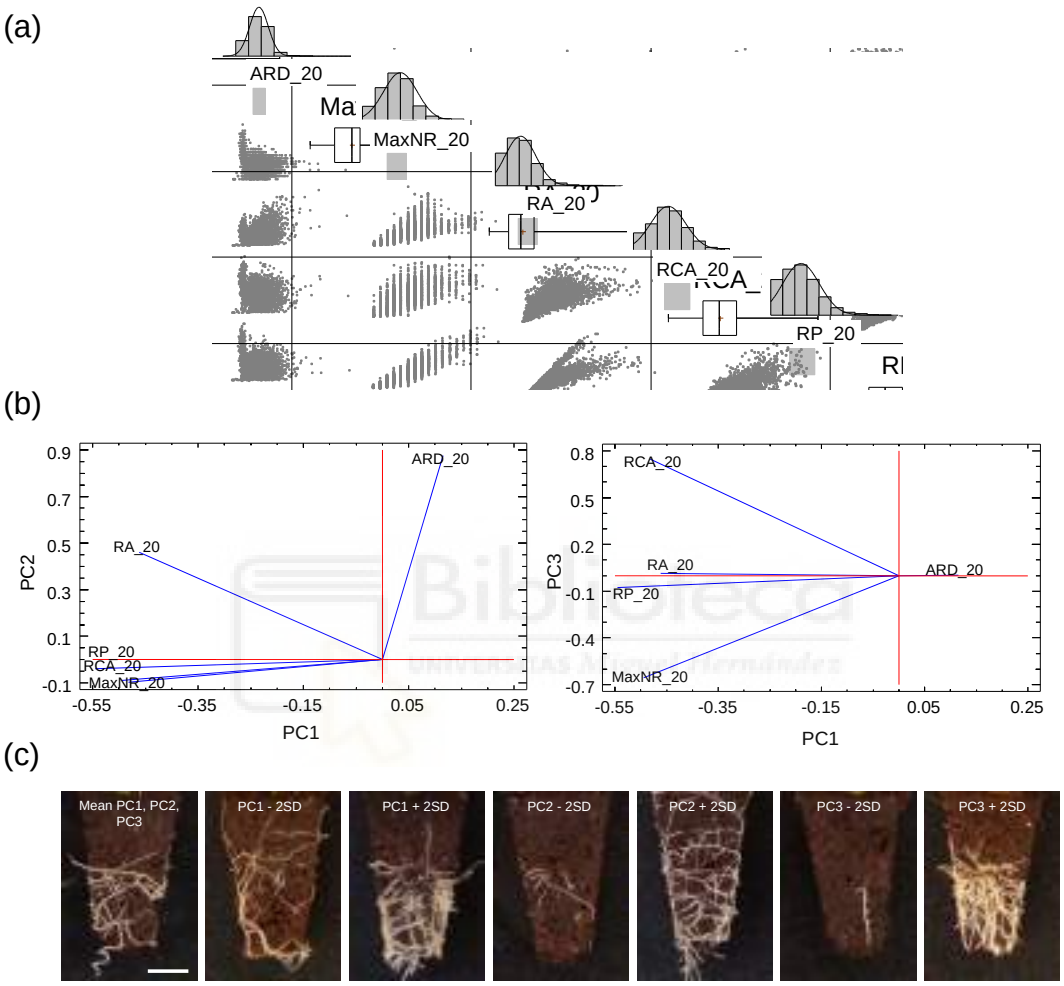

Figure S2. Descriptive traits of the double-cross F_1 lines studied in the first experiment. (**a**) Scatter plots of rooting parameters from the first experiment. (**b**) Principal component analysis (PCA) of selected root traits at 20 dap and representation of PC1, PC2 and PC3 in a tridimensional space. (**c**) Representative images corresponding to plus or minus two times the standard deviation (+2SD and −2SD) for each PC. Scale bar: 10 mm.

Figure S3

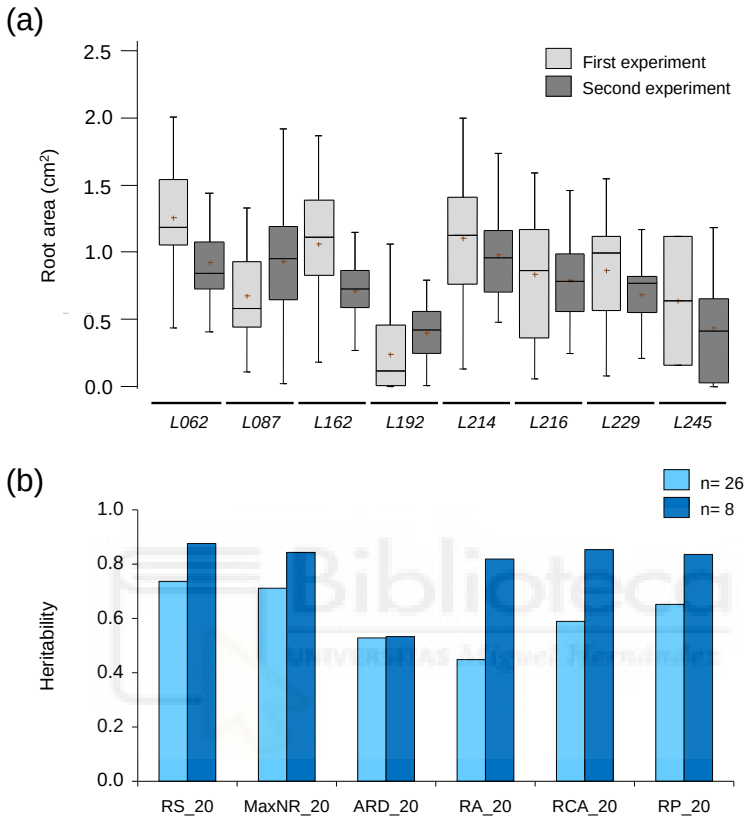

Figure S3. Descriptive traits of the double-cross F_1 lines studied in the third experiment. (**a**) Average root area (cm^2) values in the first and the second experiment for selected F_1 lines. (**b**) Heritability estimates of some rooting parameters on selected lines in the second experiment (n=26) (light blue bars) and for lines selected for the third experiment (n=8) (dark blue bars).

Figure S4

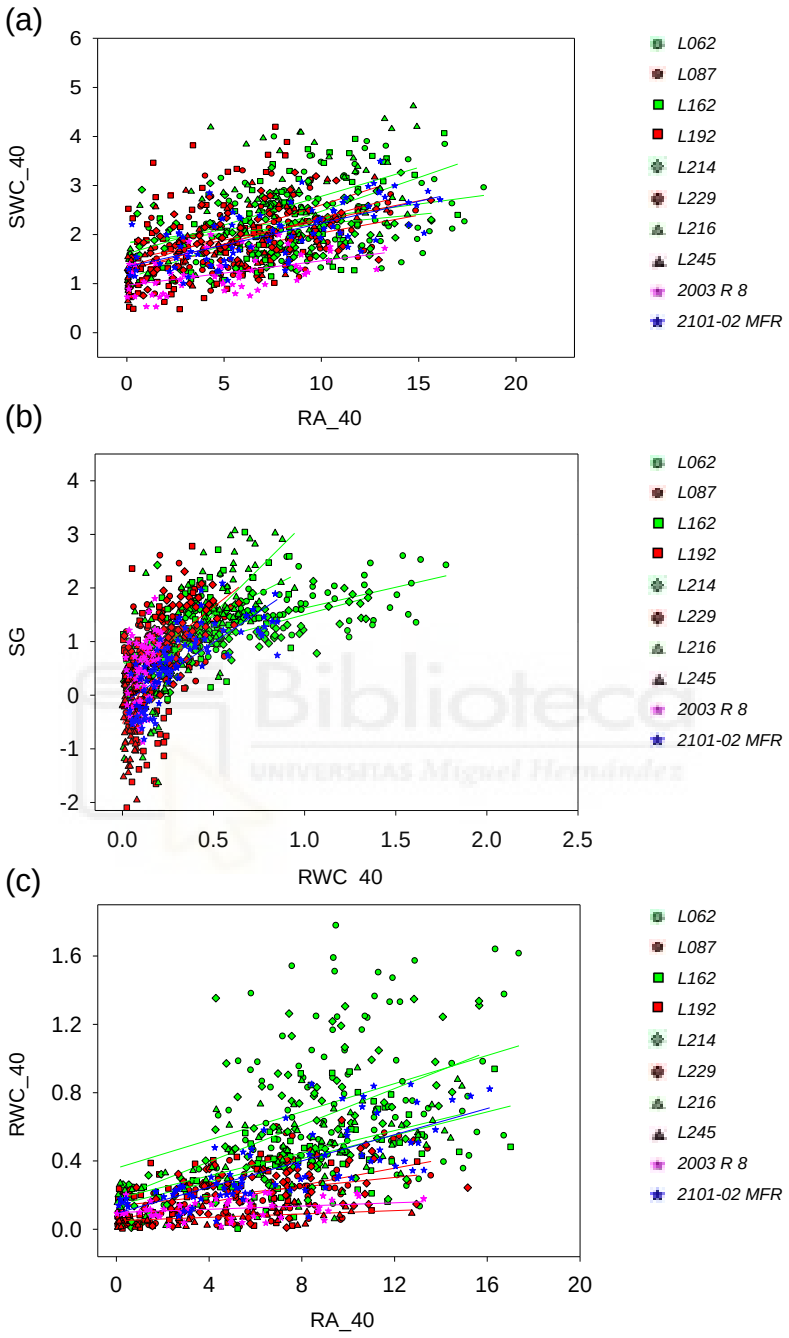

Figure S4. Parameter correlation for different physiological traits in the third experiment. Relationship between (**a**) final root area (cm^2) and shoot water content (g), (**b**) root water content (g) and shoot growth (g) and (**c**) root area (cm^2) and root water content (g). Each color and shape indicates one each F_1 studied line (good-rooting lines in green and bad-rooting lines in red), including parental lines (stars).

Figure S5

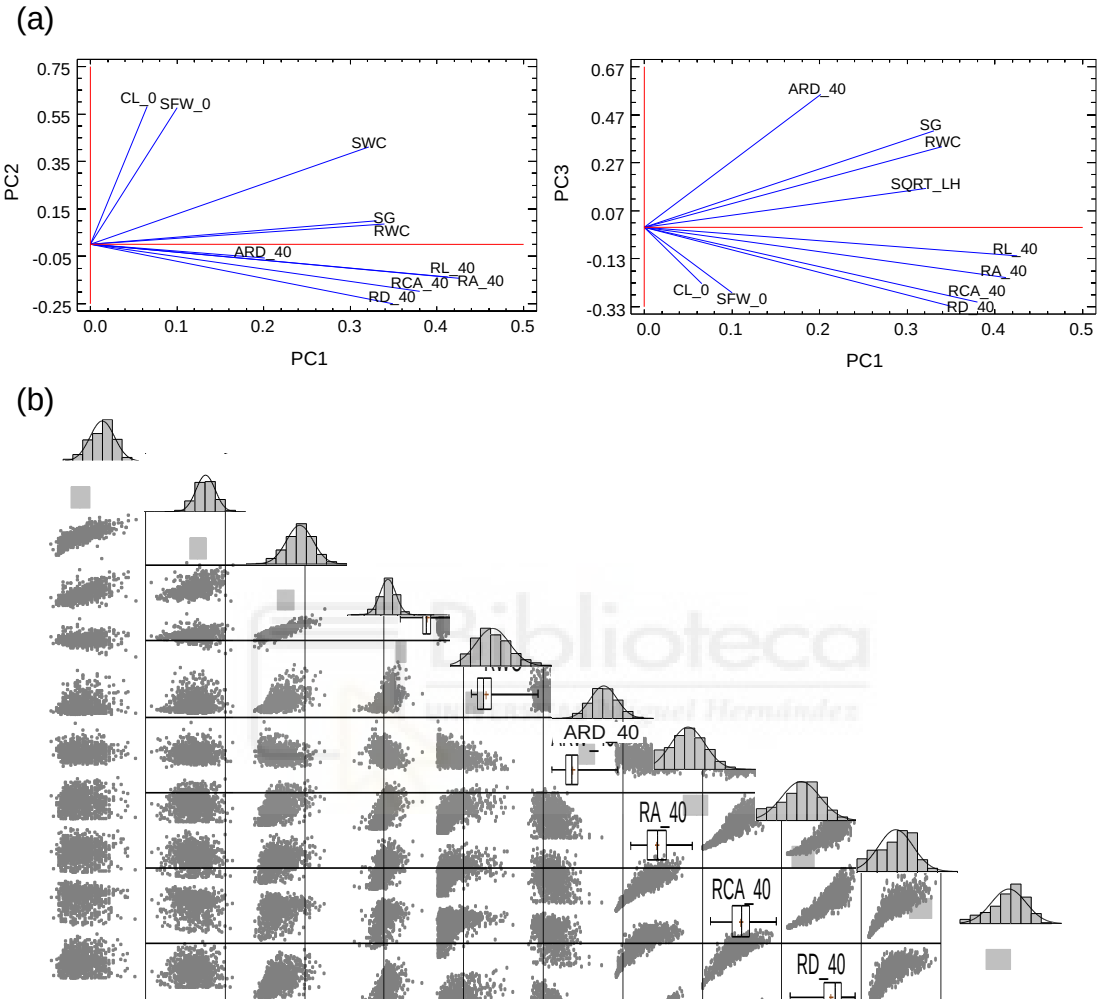

Figure S5. Descriptive traits of the double-cross F_1 lines studied in the third experiment. (**a**) Principal component analysis (PCA) of selected root traits at different times in the third experiment and representation of PC1, PC2 and PC3 in a tridimensional space. (**b**) Scatter plots of rooting parameters from the third experiment.

Supplementary Table S1. Heterosis values for the F_1 subpopulations studied. Heterosis (H) percentages estimated for F_1 subpopulations for the studied traits compared with the best-rooting parental line (BP, *2101-02 MFR*) or both parental lines (MP).

	Selfing F_1 lines		**Crossing F_1 lines**	
Trait	**H (BP) (%)**	**H (MP) (%)**	**H (BP) (%)**	**H (MP) (%)**
LN_13	-0.8	-3.7	-0.3	-3.2
ALS_13	62.5	36.8	93.2	62.6
CH_13	-4.6	-6.0	3.5	1.9
SA_13	14.8	-1.5	42.1	21.9
SA_20	-5.8	-9.1	16.2	12.2
ΔSA	-70.6	-53.1	-65.1	-44.2
RR_20	-17.8	-4.1	-7.2	8.2
RS_20	-22.4	-9.4	-11.7	3.1
MaxNR_20	-38.5	-31.3	-29.3	-21.1
ARD_20	66.8	63.5	63.1	60.0
RA_20	0.3	6.6	22.0	29.7
RCA_20	-41.6	-45.6	-19.0	-24.6
RP_20	-45.4	-41.1	-28.6	-23.0

Supplementary Table S2. Correlation analyses among different physiological traits in the third experiment. Interaction between shoot and root traits was estimated by (**a**) shoot fresh weigth and root area, (**b**) shoot water content and root water content, (**c**) shoot growth and root area, (**d**) shoot water content and root area and (**e**) shoot growth and root water content. For each correlation, R^2 values, r values (Pearson correlation coefficient) and p-values are shown for each genotype. ns = not significant.

(**a**)

Genotypes	**RA_40 vs SWF_0**
L062 (n = 102)	R^2 = 0.003; r = 0.05; p > 0.05 n.s
L087 (n = 97)	R^2 = 0.0001; r = 0.01; p > 0.05 n.s
L162 (n = 82)	R^2 = 0.04; r = 0.20; p > 0.05 n.s
L192 (n = 74)	R^2 = 0.0004; r = 0.02; p > 0.05 n.s
L214 (n=94)	R^2 = 0.03; r = 0.17; p > 0.05 n.s
L216 (n=92)	R^2 = 0.004; r = 0.06; p > 0.05 n.s
L229 (n=92)	R^2 = 0.006; r = 0.08; p > 0.05 n.s
L245 (n=59)	R^2 = 0.04; r = 0.20; p > 0.05 n.s
2003 R8 (n=53)	R^2 = 0.02; r = -0.14; p > 0.05 n.s
2101-02 MFR (n=86)	R^2 = 0.004; r = 0.06; p > 0.05 n.s

(**b**)

Genotypes	**SWC vs RWC**
L062 (n = 98)	R^2 = 0.37; r = 0.61; p < 0.001***
L087 (n = 88)	R^2 = 0.25; r = 0.50; p < 0.001***
L162 (n = 78)	R^2 = 0.35; r = 0.59; p < 0.001***
L192 (n = 69)	R^2 = 0.29; r = 0.54; p < 0.001***
L214 (n=98)	R^2 = 0.21; r = 0.46; p < 0.001***
L216 (n=98)	R^2 = 0.51; r = 0.71 ;p < 0.001***
L229 (n=86)	R^2 = 0.34; r = 0.58;p < 0.001***
L245 (n=83)	R^2 = 0.18; r = 0.42;p < 0.001***
2003 R8 (n=61)	R^2 = 0.12; r = 0.35;p < 0.01**
2101-02 MFR (n=98)	R^2 = 0.54; r = 0.73;p < 0.001***

(**c**)

Genotypes	SG vs RA_40
L062 (n =98)	R^2 = 0.16; r = 0.40; p < 0.001***
L087 (n = 93)	R^2 = 0.23; r = 0.48; p < 0.001***
L162 (n =79)	R^2 = 0.30; r = 0.55; p < 0.001***
L192 (n = 70)	R^2 = 0.22; r = 0.47; p < 0.001***
L214 (n=92)	R^2 = 0.36; r = 0.60; p < 0.001***
L216 (n=93)	R^2 = 0.41; r = 0.64; p < 0.001***
L229 (n=89)	R^2 = 0.39; r = 0.62; p < 0.001***
L245 (n=53)	R^2 = 0.49; r = 0.70; p < 0.001***
2003 R8 (n=56)	R^2 = 0.19; r = 0.44; p < 0.001***
2101-02 MFR (n=81)	R^2 = 0.56; r = 0.75; p < 0.001***

(**d**)

Genotypes	SWC vs RA_40
L062 (n = 101)	R^2 = 0.10; r = 0.32; p < 0.001***
L087 (n = 95)	R^2 = 0.20; r = 0.45; p < 0.001***
L162 (n = 82)	R^2 = 0.33; r = 0.57; p < 0.001***
L192 (n = 75)	R^2 = 0.19; r = 0.44; p < 0.001***
L214 (n=95)	R^2 = 0.11; r = 0.33; p < 0.001***
L216 (n=93)	R^2 = 0.30; r = 0.55; p < 0.001***
L229 (n=94)	R^2 = 0.27; r = 0.52; p < 0.001***
L245 (n=58)	R^2 = 0.43; r = 0.66; p < 0.001***
2003 R 8 (n=55)	R^2 = 0.20; r = 0.45; p < 0.001***
2101-02 MFR (n=84)	R^2 = 0.45; r = 0.67; p < 0.001***

(**e**)

Genotypes	SG vs RWC
L062 (n = 94)	R^2 = 0.42; r = 0.67; p < 0.001***
L087 (n = 90)	R^2 = 0.20; r = 0.45; p < 0.001***
L162 (n = 80)	R^2 = 0.30; r = 0.55; p < 0.001***
L192 (n = 72)	R^2 = 0.16; r = 0.40; p < 0.001***
L214 (n=95)	R^2 = 0.40; r= 0.63; p < 0.001***
L216 (n=99)	R^2 = 0.53; r = 0.73; p < 0.001***
L229 (n=87)	R^2 = 0.42; r = 0.65; p < 0.001***
L245 (n=82)	R^2 = 0.11; r = 0.34; p < 0.01**
2003 R 8 (n=61)	R^2 = 0.16; r = 0.40 p < 0.001***
2101-02 MFR (n=95)	R^2 = 0.58; r = 0.76; p < 0.001***

(**f**)

Genotypes	RWC vs RA_40
L062 (n = 99)	R^2 = 0.14; r = 0.37; p < 0.001***
L087 (n =88)	R^2 = 0.35; r = 0.59; p < 0.001***
L162 (n = 81)	R^2 = 0.29; r = 0.54; p < 0.001***
L192 (n = 52)	R^2 = 0.12; r = 0.35; p < 0.01**
L214 (n=93)	R^2 = 0.35; r= 0.59; p < 0.001***
L216 (n=87)	R^2 = 0.35; r = 0.59; p < 0.001***
L229 (n=86)	R^2 = 0.42; r = 0.65; p < 0.001***
L245 (n=46)	R^2 = 0.17; r = 0.41; p < 0.01***
2003 R 8 (n=48)	R^2 = 0.08; r = 0.28 p < 0.05*
2101-02 MFR (n=95)	R^2 = 0.53; r = 0.73; p < 0.001***

Artículo 4

Vegetative propagation of argan tree (*Argania spinosa* (L.) Skeels) using *in vitro* germinated seeds and stem cuttings

María Salud Justamante, Sergio Ibáñez, Joan Villanova, José Manuel Pérez-Pérez

Instituto de Bioingeniería, Universidad Miguel Hernández, 03202 Elche, Spain

Scientia Horticulturae 2017; 225: 81

Published online 7 July 2017. doi: 10.1016/j.scienta.2017.06.066

FI (2017): 1,760 (Q1; 8 de 37)

Vegetative propagation of argan tree (*Argania spinosa* (L.) Skeels) using *in vitro* germinated seeds and stem cuttings

María Salud Justamante[1], Sergio Ibáñez[1], Joan Villanova[1,2], José Manuel Pérez-Pérez[1,*]

[1]Instituto de Bioingeniería, Universidad Miguel Hernández, Elche, Spain.

[2]Current address: Timac Agro España S.A., Orcoyen, Navarra, Spain.

Mailing address: Instituto de Bioingeniería, Universidad Miguel Hernández, 03202 Elche, Alicante, Spain

*Corresponding author: José Manuel Pérez-Pérez (jmperez@umh.es; tel. +34 966658958; arolab.edu.umh.es)

Published in:

Justamante, M.S., Ibáñez, S., Villanova, J., Pérez-Pérez, J.M. (2017). Vegetative propagation of argan tree (*Argania spinosa* (L.) Skeels) using *in vitro* germinated seeds and stem cuttings. *Sci Hort* **221**: 81.

Word number (including references): 4776 Character number: 27307

Figures: 6 Supporting Information: 1

HIGHLIGHTS

- We developed a novel protocol for *in vitro* micropropagation of argan plantlets
- Higher rooting percentages in hardwood lignified cuttings were obtained
- Efficient production of clonally identical argan plants have been achieved

ABSTRACT

In vitro culture and rooting of stem cuttings can be used for vegetative propagation of plant material. Argan trees (*Argania spinosa* (L.) Skeels) are endemic to semi-desert areas of South-western Morocco, where they cover more than 8,000 km2 and have important socio-economic and environmental impacts. Seed germination was improved by culturing *in vitro* isolated kernels on Murashige and Skoog (MS) axenic medium with 1.0 mg/L gibberellic acid (GA_3). Newly *in vitro*-produced seedlings were then transferred to MS medium containing 0.5 mg/L thidiazuron (TDZ) and 1.0 mg/L GA_3 to promote shoot development. The microcuttings produced were rooted using MS medium supplemented with two synthetic auxins, 1-naphthaleneacetic acid (NAA) and indole-3-butyric acid (IBA), at 1.0 mg/L each. The rooted microcuttings were then transplanted to soil and acclimated in a greenhouse environment. In addition, hardwood stem cuttings collected from adult argan trees were rooted by using a combination of IBA and NAA.

GRAPHICAL ABSTRACT

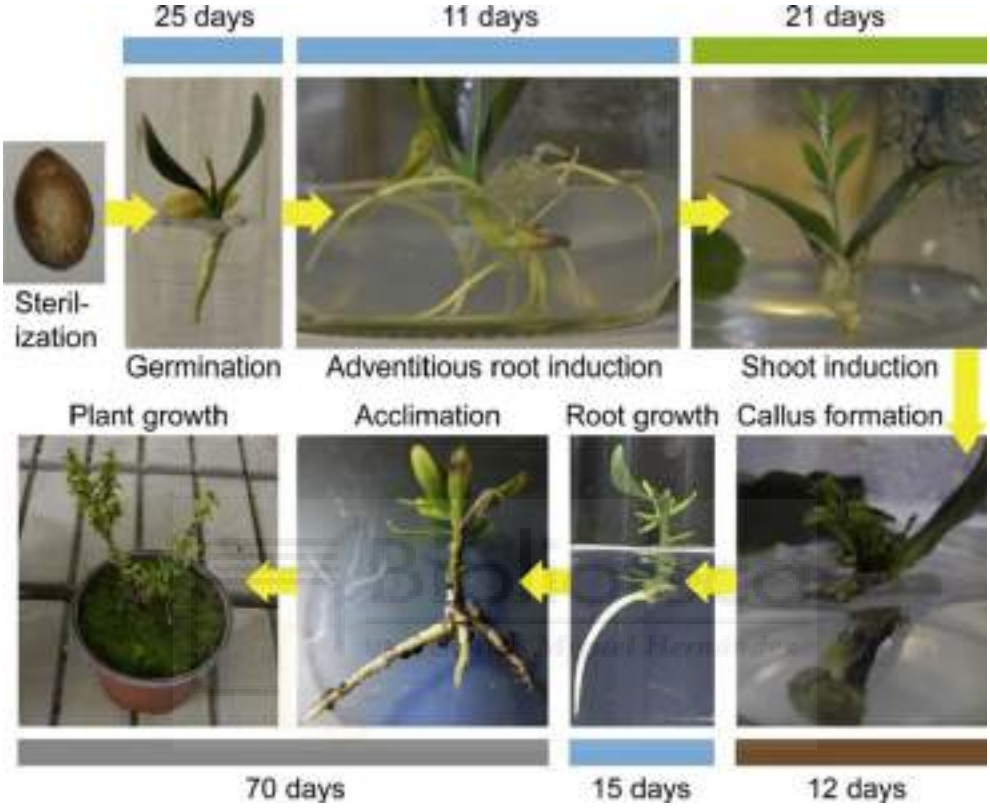

The steps used in this work are indicated. Colored rectangles indicate the different growing media (blue: 1.0 mg/L GA_3-supplemented medium, green: 0.5 mg/L TDZ-supplemented medium, brown: 1.0 mg/L of both NAA- and IBA-supplemented medium, grey: soil substrate) and the duration of the treatment.

ABBREVIATIONS

GA_3: gibberellic acid

IBA: indole-3-butyric acid

MS: Murashige and Skoog

NAA: 1-naphthaleneacetic acid

PPFD: photosynthetic photon flux density

TDZ: thidiazuron

KEYWORDS

Micropropagation; Germination; Rooting; Gibberellins; Auxins

1. INTRODUCTION

Argan trees (*Argania spinosa* (L.) Skeels) are important forest species which can grow up to 8-10 meters high and are resistant to drought and heat. They belong to the Sapotaceae family and are endemic to semi-desert areas of South-western Morocco, where they occupy more than 8,000 km^2 on a wide range of altitude, from sea level to 1,500 m (Msanda et al. 2005; Charrouf and Guillaume 2009; Bani-Aameur and Ferradous 2001; Mateille et al. 2015). Argan oil is a highly valued product due to its nutritional, medicinal and cosmetic properties (Charrouf and Guillaume 1999; Charrouf and Guillaume 2008; Charrouf et al. 2008), and argan trees have been traditionally used in Berber culture for feeding livestock and for oil production (Charrouf et al. 2002; Charrouf and Guillaume 2009). Besides its remarkable socio-economic role, this species also plays important environmental performance: their deep-root system facilitates nutrient and water uptakes from poor and dry soils.

Projected climate change during this century will result in warmer temperatures and altered rainfall patterns, which will threaten many native plant species (Thuiller et al. 2005; García et al. 2014). Argan tree forests are particularly sensitive to climate change, and during the twentieth century, their area has been reduced by half due to, among other factors, over-exploitation of the trees by the local population (Charrouf and Guillaume 2008; Lybbert et al. 2011). Based on the role of argan roots in restoring soil fertility and retaining water moisture, the planting of argan trees in regions susceptible to desertification might reduce land degradation (Ait Aabd et al. 2011; Zohra et al. 2014), and this species is anticipated to ecologically replace other drought-sensitive oil-producing plants, such as olive trees, in Northern latitudes if global temperatures continue to rise.

In natural conditions, multiplication of argan plants is limited because they are slow-growing trees with low seed production (Charrouf and Guillaume 2008). Propagation of argan plants from seeds is challenging

and commercially inefficient because of heterogeneity in seed size, seed viability and seed dormancy, which are strongly genotype-dependent (Nouaim et al. 2002; Alouani and Bani-Aameur 2004; Al-Menaie et al. 2007; Miloudi and Belkhodja 2009). Both seed germination and the earliest stages of seedling development are crucial for the establishment of viable argan plantlets, which are strongly influenced by specific environmental conditions, such as light intensity, temperature and soil moisture (Alouani and Bani-Aameur 2004; Al-Menaie et al. 2007; Miloudi and Belkhodja 2009; Benaouf et al. 2016). In addition, the hard shells of argan seeds difficult their germination in native conditions, limiting its natural turnover. Although studies have established that argan trees can be vegetatively propagated by various nursery and *in vitro* techniques (Nouaim et al. 2002; Bellefontaine et al. 2010; Ferradous et al. 2011), lignified stem cuttings collected from mature trees are still difficult to root. Rooting argan cuttings could be improved by using softwood cuttings and axenic conditions (Nouaim et al. 2002). *In vitro* culture is a useful technique for the mass production of recalcitrant oil-producing trees (Mangal et al. These techniques have a great potential for argan micropropagation because they minimize environmental influence on germination and further seedling growth (Bousselmame et al. 2001; Nouaim et al. 2002; Martínez-Gómez et al. 2007). *In vitro* germination of argan seeds has been tested previously in different types of media and treatments with varying success (Martínez-Gómez et al. 2007).

Adventitious rooting of argan stem cuttings has proved to be difficult, but the improvement of this technique becomes an essential target for preservation of this endangered species. With this study we aim to develop a new procedure for the micropropagation of argan trees from *in vitro* isolated kernels, and to improve adventitious rooting from mature, hardwood, stem cuttings.

2. MATERIALS AND METHODS

2.1 Plant material and growth conditions

In this work we used 250 mature argan fruits collected in October 2015 from three different argan trees of nearly 120 year-old and growing in an abandoned field at 38°23´16´´ N, 0°27´46´´ W and 45 m altitude (San Vicente del Raspeig, Spain) (Figure 1A-B). Several young branches of approximately one year old and 70 cm in length were collected from these trees in March 2016 and they were used for adventitious rooting (Figure 1C). Randomly collected argan fruits were dried at 45°C in an oven for 14-21 days and the soft parts of their pericarp were removed. Clean argan nuts were stored for two to four weeks at 4°C in the dark. Nuts between 0.5 and 2.5 g fresh weight and between 12 and 28 mm length were chosen for our studies (Figure 1D). *In vitro* produced seedlings were kept in a growth chamber at 22±2°C and 70% relative humidity with a 16 h light / 8h dark photoperiod and a photosynthetic photon flux density (PPFD) of 50μmol m^{-2} s^{-1}. For plantlet acclimation (March-September 2016), we used a gothic-arch greenhouse at 38°16´43´´ N, 0°41´15´´ W and 96 m altitude (Elche, Spain).

2.2 Seed sterilization

The cold-stored argan nuts were washed with a 50% dilution of commercial bleach for 20 min with occasional stirring, followed by three 10-min washes with sterile distilled water under laminar flow hood (Telstar AH-100, Telstar Technologies, S.L.). Argan kernels were isolated by cracking the woody endocarp with a disinfected hammer, and they were surface-sterilized using 50% dilution of commercial bleach for 8 min, followed by four washes with distilled sterile water for 5 min each under laminar flow hood.

2.3 Plant culture media

Using sterile forceps, disinfected argan kernels were individually placed in sterile glass tubes (30 mm diameter × 200 mm length; Fisher Scientific, ref. 11892353) containing 35 mL of different plant culture media assayed. The Murashige and Skoog (MS) plant culture medium was prepared with 2.15 g/L MS basal salt medium (Duchefa, ref. M0221), 30 g/L sucrose, 2 mL/L of 500× Gamborg B5 Vitamin Mixture (Duchefa, ref. G0415), 0.5 g/L 2-(N-morpholino)ethanesulfonic acid (MES; Duchefa, ref. M1503), 4 g/L gelrite (Duchefa, ref. G1101) and 90 µg/mL cefotaxime sodium (Fisher Scientific, ref. BP29511), adjusted to pH 5.7 with 1 M KOH. Sterile 500 mL-glass bottles with 85 mL of MS plant culture medium supplemented with different concentrations of growth regulators were used, as indicated next. These were prepared by adding gibberellic acid (GA_3; Duchefa, ref. G0907), thidiazuron (TDZ; Duchefa, ref. T0916), indole-3-butyric acid (IBA; Duchefa, ref. I0902) or 1-naphthaleneacetic acid (NAA; Duchefa, ref. N0903) to autoclaved MS plant culture medium (20 min at 121°C) that was maintained at 55°C on a water bath. All growth regulators were dissolved in absolute ethanol and 0.22 m pore size-filtered before use.

2.4 *In vitro* culture and plantlet acclimation

Germinated argan kernels were kept in 1.0 mg/L GA_3-supplemented MS medium up to 25 days to allow primary root growth, cotyledon unfolding and leaf initiation (germination medium). To induce secondary root formation, approximately 5 mm of the primary root apex was excised with a sterile scalpel. Seedlings were transferred to glass bottles containing fresh germination medium. After 12 days, these seedlings were transferred to new bottles of germination medium with or without 0.5 mg/L thidiazuron (TDZ) to induce shoot growth. Microcuttings with 2-3 leaves and 15-25 mm-long were removed from *in vitro* elongated shoots and transferred to glass bottles with MS plant culture medium supplemented with 0.0, 0.1 or 1.0 mg/L of

both 1-naphthaleneacetic acid (NAA) and indole-3-butyric acid (IBA) for callus induction. To induce adventitious root development, we transferred the explants grown for 20 days in high auxin-supplemented medium to new glass bottles containing (1) MS medium, (2) MS medium with 1.0 mg/L GA_3, or (3) MS medium with 1.0 mg/L NAA and IBA. Rooted microcuttings were transferred to 150 mL pots with an equivalent volume of peat-perlite mix covered with plastic glasses to avoid dehydration. For the following 4 weeks, argan plantlets were grown under controlled environmental conditions in the growth chamber with periodic subirrigation with a balanced NPK nutrient solution containing 5% N (nitrogen), 5% P_2O_5 (water-soluble phosphate) and 5% K_2O (water-soluble potassium) (Abono Universal 1L Comercial Química Massó, S.A.).

2.5 Adventitious rooting in hardwood cuttings

For adventitious rooting, 120 hardwood nodal cuttings of 6-8 cm in length and with 3-5 leaves each were obtained from several previously collected apical argan tree branches. Nodal cuttings were obtained with a 50° oblique angle at their proximal side and an orthogonal angle at their distal side. Leaves and thorns close to the proximal side of the cuttings were removed. Before transplanting the nodal cuttings to soil, 2-3 cm of their proximal region were submerged into liquid MS medium without auxin (mock pre-treatment, M_) or into liquid MS supplemented with 1 mg/L IBA and 2 mg/L NAA (auxin pre-treatment, A_) for 18 h at 12°C in the dark.

Once in the greenhouse, the cuttings from each pre-treatment (mock or auxin) were separated into two batches: _M (mock treatment) and _A (auxin treatment). In the mock treatment (MM and AM), nodal cuttings were dipped into powder chalk. In the auxin treatment (MA and AA), the cut stems were dipped into a commercial powder mixture of 0.4% w/w IBA and 0.4% w/w NAA before planting. According to this experimental layout, four different conditions were assayed: (1) pre-treatment and treatment

without auxins (MM), (2) pre-treatment with auxins and treatment without auxins (AM), (3) pre-treatment without auxins and treatment with auxins (MA), and (4) pre-treatment and treatment with auxins (AA). In each condition, between 34 and 84 cuttings were then individually planted in 42-rounded-plug (5 cm diameter × 4 cm deep) trays in a water-saturated 1:1 mixture of perlite and peat. Stem cuttings were grown from March to June 2016 under the environmental conditions of the greenhouse, with periodic sprinkler irrigation (5 minutes every 4 hours).

2.6 Statistical analyses

Descriptive statistics such as mean, standard deviation, maximum and minimum were calculated by using the StatGraphics Centurion XV (http://www.statgraphics.com/). The differences between groups were analysed by t test ($P<0.05$) when two groups were compared. We performed multiple testing analyses using the ANOVA F-test or the Fisher's least significant difference. Nonparametric tests were used when necessary. For more than two groups, the data were analysed using the Kruskal-Wallis test ($P<0.05$).

3. RESULTS

3.1 *In vitro* culture of argan seedlings

3.1.1 Germination of argan seeds

Individual argan kernels were incubated in transparent glass tubes filled with semi-solid MS media at increasing GA_3 levels (Figure 2A; n=90). The number of kernels showing elongating primary roots longer than 5 mm were measured every 5 days, and used to estimate germination percentages (Figure 2B). Compared with the non-supplemented MS medium (n=30), GA_3-supplemented media (even at 0.1 mg/L) (n=60) significantly improved seed germination rates (Figure 2B), thus average seed dormancy of argan kernels was reduced to 20.7±7 days compared with 25.6±4.5 days of their average seed dormancy in the non-supplemented medium. This germination procedure was highly efficient, allowing up to 86% germination percentage at 30 days on MS medium supplemented with 1.0 mg/L GA_3. All germinated seedlings were free of fungal and bacterial contamination.

3.1.2 Secondary rooting and shoot growth

Secondary root formation from *in vitro* germinated argan kernels was observed at low frequency in the germination medium (10% of the kernels with 1 lateral root; n=30). We induced secondary root formation by primary root apex excision. Between 5 and 11 days afterwards, secondary roots longer than 5 mm appeared in 40.9% of the seedlings (n=30), with an average number of 4.9±3.6 secondary roots per seedling 21 days after transfer. Once secondary roots were developed, plantlets were transferred to TDZ-supplemented medium. After 21 days on these conditions, shoot elongation was observed in 80% of the samples (Figure 3A-C; n=30), while only 20% of the samples grown on non-supplemented germination medium displayed shoot elongation (n=30).

3.1.3 In vitro *organogenesis*

Microcuttings excised from these *in vitro* elongated shoots were transferred to MS plant culture medium supplemented with and without 1.0 mg/L of both NAA and IBA. After 30 days on this medium, we observed profuse callus formation in the proximal end of the microcuttings exclusively on the NAA- plus IBA-supplemented medium (Figure 4B). A higher percentage of callus formation (>90%; n=36) was found for the microcuttings after 20 days on NAA- plus IBA-supplemented medium (Figure 4A). Next, all of these microcuttings were transferred to glass bottles containing: (1) MS plant culture medium, (2) germination medium with 1.0 mg/L GA_3, or (3) MS plant culture medium with 1.0 mg/L of both NAA plus IBA, and the percentages of rooted microcuttings were studied at different times (Figure 4C). Adventitious roots came out from pre-existing calli near the proximal end of the microcutting as early as 4 days after transfer them to MS plant culture medium (1) or to germination medium (2), and rooting percentage reached 100% of the explants after 15 days on these two media (n=24). Adventitious roots from the germination medium (2) were significantly longer than those from non-supplemented MS medium (1) (Figure 4D). On the other hand, adventitious root growth was inhibited in the MS medium with 1.0 mg/L of both NAA and IBA (3).

3.1.3 Acclimation of in vitro *produced seedlings*

Rooted microcuttings were acclimated during 4 weeks at the growth chamber (Figure 5A). At the end of the acclimation period, the argan plantlets had developed a functional root system and new lateral shoots had been produced from the leaf axils or thorn axils (Figure 5B). These plantlets were then transferred to larger pots and maintained under the environmental conditions of the greenhouse with occasional watering with nutrient solution. After 4 months, all the transplanted rooted microcuttings (n=16) had survived (Figure 5C).

3.2 *Ex vitro* adventitious rooting of hardwood stem cuttings

In an attempt to improve adventitious rooting from mature lignified stem cuttings, we devised an assay using four conditions (see Materials and Methods). Average stem cutting length was 89.9±13.3 mm, with non-significant length differences between the four experiments (Figure 6A). After three months, we scored the presence of callus formation at the proximal tip of the stem cutting, as well as the number of adventitious roots and the number of green leaves per stem cutting. In two experiments, MM and AM, no callus was formed, the stem cuttings completely defoliated, and lacked adventitious rooting. Callus and adventitious root formation were more efficiently induced in MA than AA experiment (Figure 6B-C). In addition, adventitious rooting was observed at a lower percentage (14.2%) in the AA treatment (N=42) than in the MA treatment (42.8%) (n=42).

4. DISCUSSION

In this work, we developed and tested a detailed protocol for efficient in *vitro* micropropagation of argan trees (*Argania spinosa* (L.) Skeels). Argan kernels are protected from dehydration and herbivore damage by a woody shell; hence, their germination in natural conditions might be influenced by environmental factors allowing shell cracking, such as extreme temperatures (Al-Menaie et al. 2007). Long dormancy and asynchronous germination can also contribute to the low percentage of argan seed germination in natural populations (30%) and thus to the low turnover in this species (Bani-Aameur and Alouani 1999). In some studies (Nouaim et al. 2002; Alouani and Bani-Aameur 2003; Alouani and Bani-Aameur 2004), the combination of cold-storage of argan fruits, seed scarification (shell removal by means of physical or chemical procedures), and gibberellin-supplemented germination medium significantly improved the germination efficiency in this species up to 80%. Fungicide application to the germination medium reduced fungal contamination of the argan kernels, although it significantly delayed seed germination (Al-Menaie et al. 2007). By using a harsh sterilization protocol and a defined germination media supplemented with 1.0 mg/L GA_3, it is possible to reduce seed dormancy and synchronize germination under axenic conditions, as we observed in this study.

We found that profuse rooted argan seedlings could be obtained from field-collected argan fruits in a high percentage (86%) in only 36 days. Germinated argan kernels kept in TDZ-containing growth medium produced new lateral shoots after excision of the main stem, which enabled continuous microcutting production. Additionally, the rooted microcuttings obtained from *in vitro* germinated kernels could be used as mother plant stocks for vegetative micropropagation of selected individuals. By using this new protocol, we estimated that in a period of 5-6 months, approximately 40 to 50 rooted argan microcuttings (primary microcuttings) could be obtained from a single germinated kernel. Each of these primary microcuttings could

be used as a starting explant to produce secondary microcuttings; therefore, from a single individual (one germinated kernel) it might be possible to obtain 1,600-2,000 *in vitro* rooted plantlets after one year. In our conditions, acclimation of *in vitro*-produced argan microcuttings in a growth chamber with controlled environmental conditions (photoperiod, light intensity, day/night temperature, relative humidity and nutrient solution) provided high survival rates when transferred to the greenhouse (>90%).

Argan trees have an important horticultural role due to its contribution to the local economy of drought-threatened areas. Previous studies regarding the phenotypic and genetic structure of argan tree populations from their natural distribution range revealed that the highest diversity was found within individuals of the same population (Bani-Aameur 2004; Majourhat et al. 2008; Mouhaddab et al. 2015). Genetic clustering, using molecular marker information (Majourhat et al. 2008; Mouhaddab et al. 2015), was consistent with a model of high genetic differentiation of argan populations, which might be explained by limited gene flow among populations due to its scattered distribution and limited pollen and seed dispersal. These results revealed that characterization of argan tree accessions based on morphological traits might not represent the genetic diversity of this species, and this needs to be considered when building core collections of argan germplasm (Majourhat et al. 2008). Improvement of *in vitro* propagation techniques represent a fundamental step towards *ex-situ* conservation of selected germplasm.

Rooting of hardwood lignified stem cuttings has proven to be difficult and strongly genotype-dependent which difficult its application for commercial production of elite cultivars in this species (Nouaim et al. 2002; Ferradous et al. 2011). In contrast, when softwood cuttings were used with exogenously applied auxins, higher rooting percentages were obtained (Nouaim et al. 2002). We achieved an important rooting percentage in hardwood lignified cuttings by using a combination of IBA and NAA, and

these results demonstrate a cost-effective procedure for clonal propagation of highly productive individuals, which will help to overcome the shortcomings of the current propagation methods of this species. Combined with the selection of high-yield argan cultivars, our procedure will enable the efficient production of clonally identical argan plants of defined genotypes on a relatively large scale.

ACKNOWLEDGEMENTS

We are indebted to José David Celdrán for preliminary work and for sharing unpublished data. We specially thank two anonymous reviewers whose comments and suggestions helped improve and clarify this manuscript. Our work was supported by the Ministerio de Economía y Competitividad (MINECO) of Spain (grant no. BIO2015-64255-R); and by FEDER Funds of the European Commission. J.V. was supported by a grant from the Center of the Development of Industrial Technology (CARNOMICS Eurostars-EUREKA Project E!).

REFERENCES

Ait Aabd, N., El Ayadi, F., Msanda, F., El Mousadik, A., (2011). Evaluation of agromorphological variability of argan tree under different environmental conditions in Morocco: Implication for selection. International Journal of Biodiversity and Conservation. 3(3), 73-82.

Al-Menaie, H. S., Bhat, N. R., El-Nil, M. A., Al-Dosery, S. M., Al-Shatti, A. A., Gamalin, P.,& Suresh, N. (2007). Seed germination of Argan (*Argania spinosa* L.). American-Eurasian Journal of Scientific Research. 2(1),01-04.

Alouani, M., and Bani-Aameur, F., (2003). Effect of light on germination of Argan (*Argania spinosa* (L.) Skeels) seeds. Acta Botanica Gallica. 150(1), 59-64.

Alouani, M., and Bani-Aameur, F., (2004). Argan (*Argania spinosa* (L.) Skeels) seed germination under nursery conditions: Effect of cold storage, gibberellic acid and mother-tree genotype. Annals of Forest Science. 61(2), 191-194.

Bani-Aameur, F., and Alouani, M., (1999). Viabilité et dormance des semences d'arganier (*Argania spinosa* (L.) Skeels). Ecologia Mediterranea. 25, 75-86.

Bani-Aameur, F., & Ferradous, A., (2001). Fruits and stone variability in three argan (*Argania spinosa* (L.) Skeels) populations. Forest Genetics, 8(1), 39-43.

Bani-Aameur, F., (2004). Morphological diversity of argan (*Argania spinosa* (L.) Skeels) populations in Morocco. Forest Genetics, 11(3/4), 311.

Bellefontaine, R., Ferradous, A., Alifriqui, M., Monteuuis, O., (2010). Multiplication végétative de l'arganier, *Argania spinosa*, au Maroc: le projet John Goelet. Bois et Fôrets des Tropiques. 304, 47-59.

Benaouf, Z., Souidi, Z., Arabi, Z., (2016). Propagation of Argan (*Argania spinosa* (L.) Skeels) by seeds: Effects of temperature and soaking on seed germination of two taxa in Algeria. International Journal of Ecological Economics and Statistics. 37(1), 31-42.

Bousselmame, F., Kenny, L., Chlyah, H., (2001). Optimisation des conditions de culture pour l'enracinement *in vitro* de l'arganier (*Argania spinosa* L.). Life Sciences. 324(11), 995-1000.

Charrouf, Z., and Guillaume, D., (1999). Ethnoeconomical, ethnomedical, and phytochemical study of *Argania spinosa* (L.) Skeels. Journal of Ethnopharmacology. 67(1), 7–14.

Charrouf, Z., and Guillaume, D., (2008). Argan oil: Occurrence, composition and impact on human health. European Journal of Lipid Science and Technology. 110(7), 632-636.

Charrouf, Z., Harhar, H., Gharby, S., Guillaume, D., (2008). Enhancing the value of argan oil is the best mean to sustain the argan grove economy and biodiversity, so far. Oilseeds & Fats Crops and Lipids. 15(4), 269-271.

Charrouf, Z., and Guillaume, D., (2009). Sustainable development in Northern Africa: The Argan forest case. Sustainability. 1(4), 1012-1022.

Ferradous, A., Alifriqui, M., Bellefontaine, R., (2011). Optimisation des techniques de bouturage sous mist chez l'arganier. Actes du Premier Congrès International de l´Arganier. 135-144.

García, R.A., Cabeza, M., Rahbek, C., Araújo, M.B., (2014). Multiple dimensions of climate change and their implications for biodiversity. Science. 344(6183), 1247579.

Lybbert, T.J., Aboudrare, A., Chaloud, D., Magnan, N., Nash, M., (2011). Booming markets for Moroccan argan oil appear to benefit some rural households while threatening the endemic argan forest. Proceedings of the National Academy of Sciences. 108(34), 13963-13968.

Majourhat, K., Jabbar, Y., Hafidi, A., & Martínez-Gómez, P., (2008). Molecular characterization and genetic relationships among most common identified morphotypes of critically endangered rare Moroccan species *Argania spinosa* (Sapotaceae) using RAPD and SSR markers. Annals of Forest Science, 65(8), 1.

Mangal, M., Sharma, D., Sharma, M., Kumar, S., (2014). *In vitro* regeneration in olive (Olea europaea L.) cv, 'Frontio' from nodal segments. Indian Journal of Experimental Biology. 52, 912-916.

Martínez-Gómez, P., Majourhat, K., Zeinalabedini, M., Erogul, D., Khayam-Nekoui, M., Grigorian, V., Hafidi, A., Piqueras, A., Gradziel, T.M., (2007). Use of biotechnology for preserving rare fruit germplasm. Bioremediation, Biodiversity and Bioavailability. 1(1), 31-40.

Mateille, T., Tavoillot, J., Martiny, B., Dmowska, E., Winiszewska, G., Ferji, Z., ... & El Mousadik, A., (2016). Aridity or low temperatures: What affects the diversity of plant-parasitic nematode communities in the Moroccan argan relic forest? Applied Soil Ecology, 101, 64-71.

Miloudi, A., and Belkhodja, M., (2009). The contribution to the research of the germination conditions of argan seeds (*Argania spinosa* L. Skeels): The particular study of the water pre-soaking duration and the harvest year of seeds effects on the germination. European Journal of Scientific Research. 25(3), 376-383.

Mouhaddab, J., Naima, A. I. T., Achtak, H., Msanda, F., Zahidi, A., Filali-Maltouf, A., ... & El Mousadik, A., (2015). Patterns of Genetic Diversity and Structure at Fine Scale of an Endangered Moroccan Endemic Tree. Notulae Botanicae Horti Agrobotanici Cluj-Napoca, 43(2),528.

Msanda, F., El Aboudi, A., Peltier, J.P., (2005). Biodiversity and biogeography of Moroccan argan tree communities. Cahiers Agricultures. 14(4),357-364.

Nouaim, R., Mangin, G., Breuil, M.C., Chaussod, R., (2002). The argan tree (*Argania spinosa*) in Morocco: Propagation by seeds, cuttings and *in-vitro* techniques. Agroforestry Systems. 54,71-81.

Thuiller, W., Lavorel, S., Araujo, M.B., Sykes, M.T., Prentice, I.C., (2005). Climate change threats to plant diversity in Europe. Proceedings of the National Academy of Sciences of the United States of America. 102(23), 8245-8250.

Zohra, B., Ali, M., Moulay, B., (2014). Germination tests of seeds of argan tree (*Argania spinosa* (L.) skeels) of two sources (Tindouf and Mostaganem) in the semi-arid western Algerian. African Journal of Plant Science. 8(6), 260-270.

FIGURES

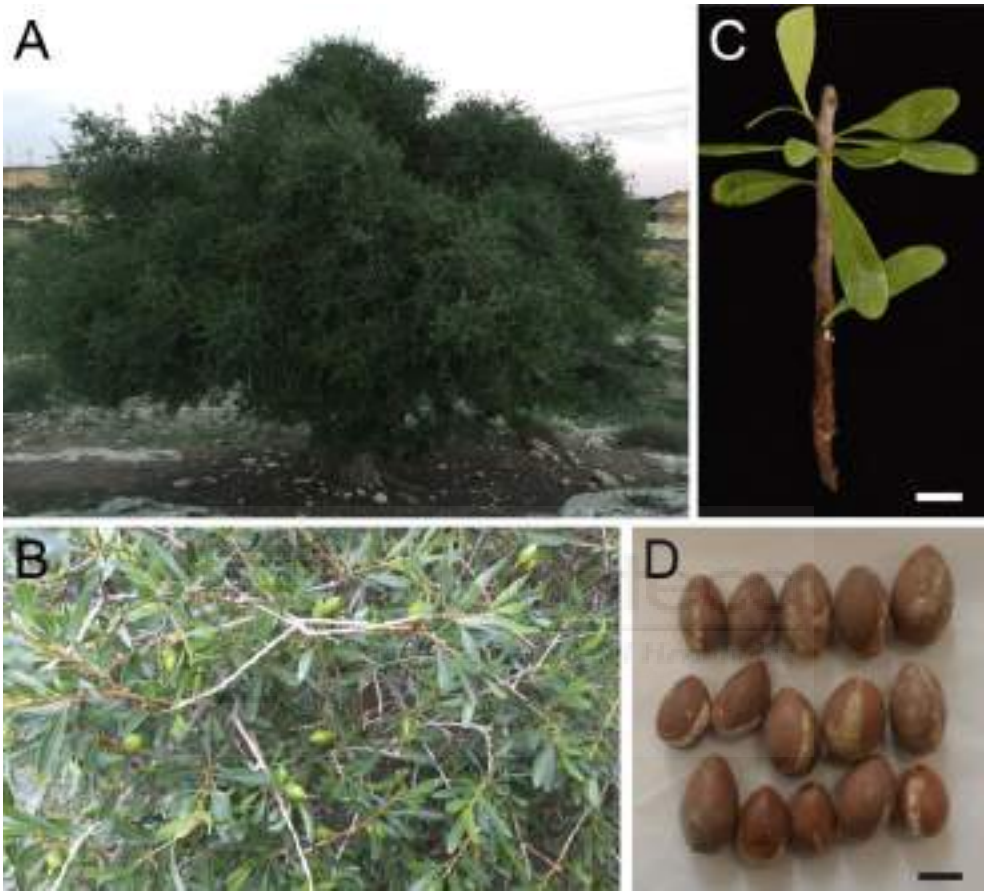

Figure 1. Plant material used in this work. (A) Mature adult argan tree (*Argania spinosa* (L.) Skeels) bearing immature fruits (B). (C) Nodal stem cutting used for the *ex vitro* rooting experiments. (D) Mature disinfected argan nuts used for the initiation of *in vitro* culture. Note their size and shape heterogeneity. Images A and B were taken in spring 2016. Scale bars: 10 mm.

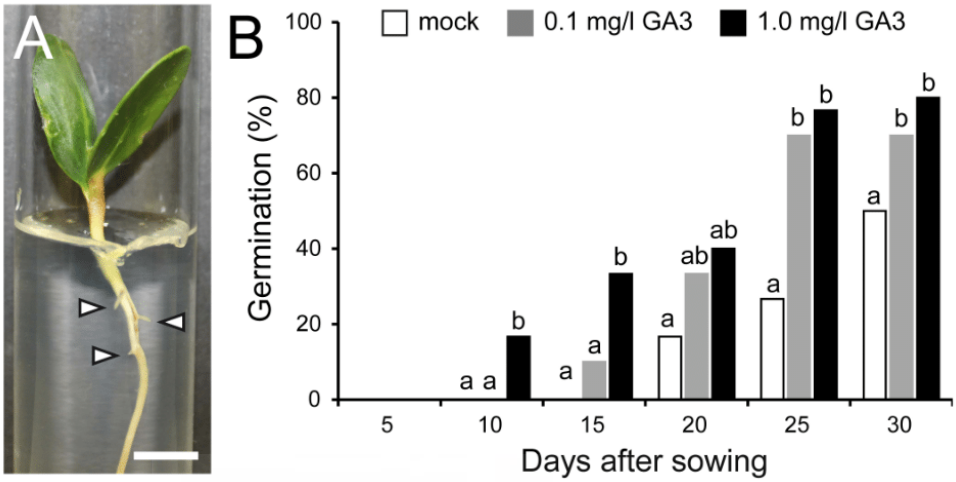

Figure 2. *In vitro* culture of argan kernels. (A) An argan kernel cultivated *in vitro* for 25 days. Arrowheads indicate young lateral roots. Scale bar: 10 mm. (B) Germination rates were measured from 30 kernels for each treatment. Letters distinguish significant differences ($P<0.05$) between treatments for the same numbers of days after sowing.

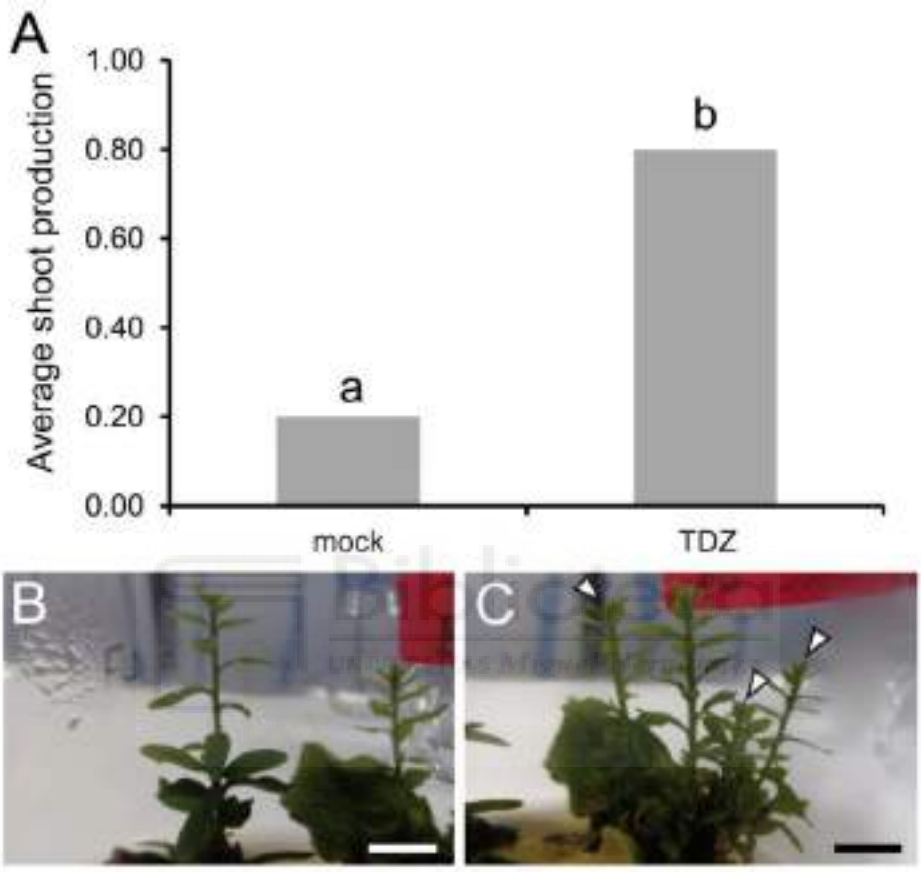

Figure 3. Shoot induction of *in vitro* cultured argan seedlings. (A) Average shoot production in microcuttings after 21 days of culture on MS medium containing 0 (mock) or 0.5 mg/L TDZ. Letters distinguish significant differences ($P<0.05$) between treatments for the same numbers of days after sowing. (B,C) Microcuttings grown for 21 days in media supplemented with mock (B) or TDZ (C). Arrowheads indicate newly produced lateral shoots. Scale bars: 10 mm.

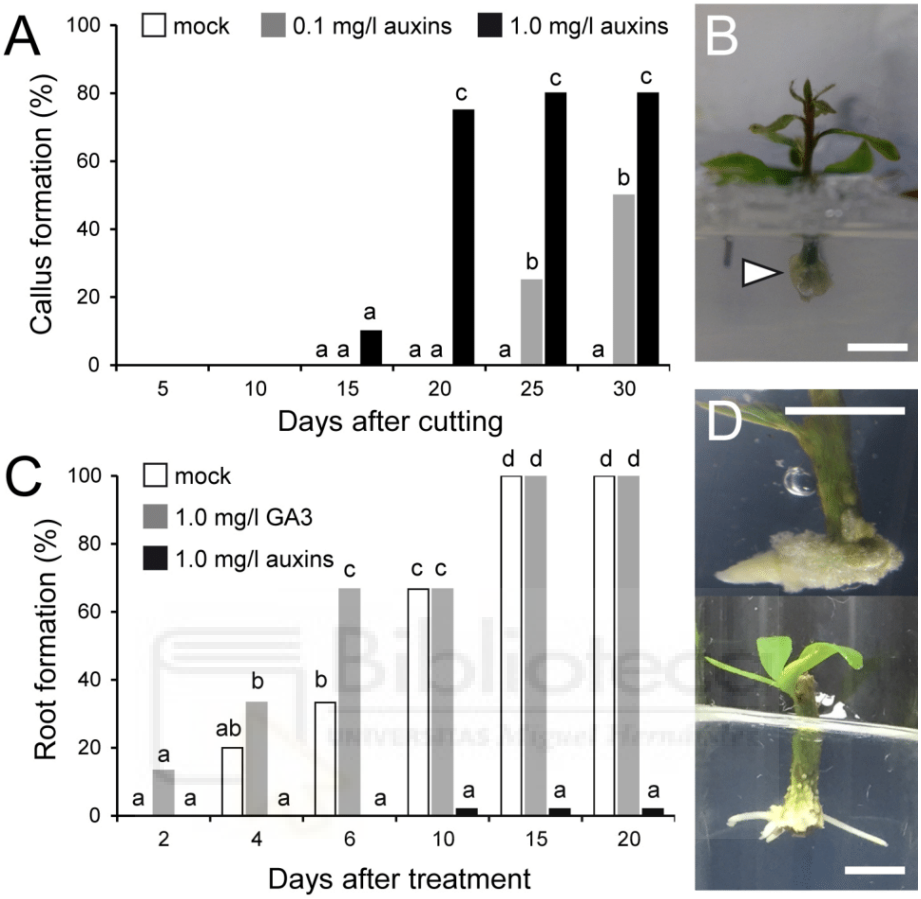

Figure 4. *In vitro* adventitious rooting of argan cuttings. (A) Callus formation was scored on 36 microcuttings for each treatment. 1.0 mg/L of both NAA and IBA were used at different concentrations. (B) An argan microcutting grown *in vitro* for 30 days that displays callus formation at the wound region (white arrowhead). (C) Percentage of root formation after transferring stem cuttings from the previous experiment to media supplemented with hormones. (D) Images of microcuttings grown on 1.0 mg/L GA_3 at 4 (top) and 20 (bottom) days after treatment. Letters distinguish significant differences ($P<0.05$) between treatments for the same numbers of days after sowing. Scale bars: 5 mm.

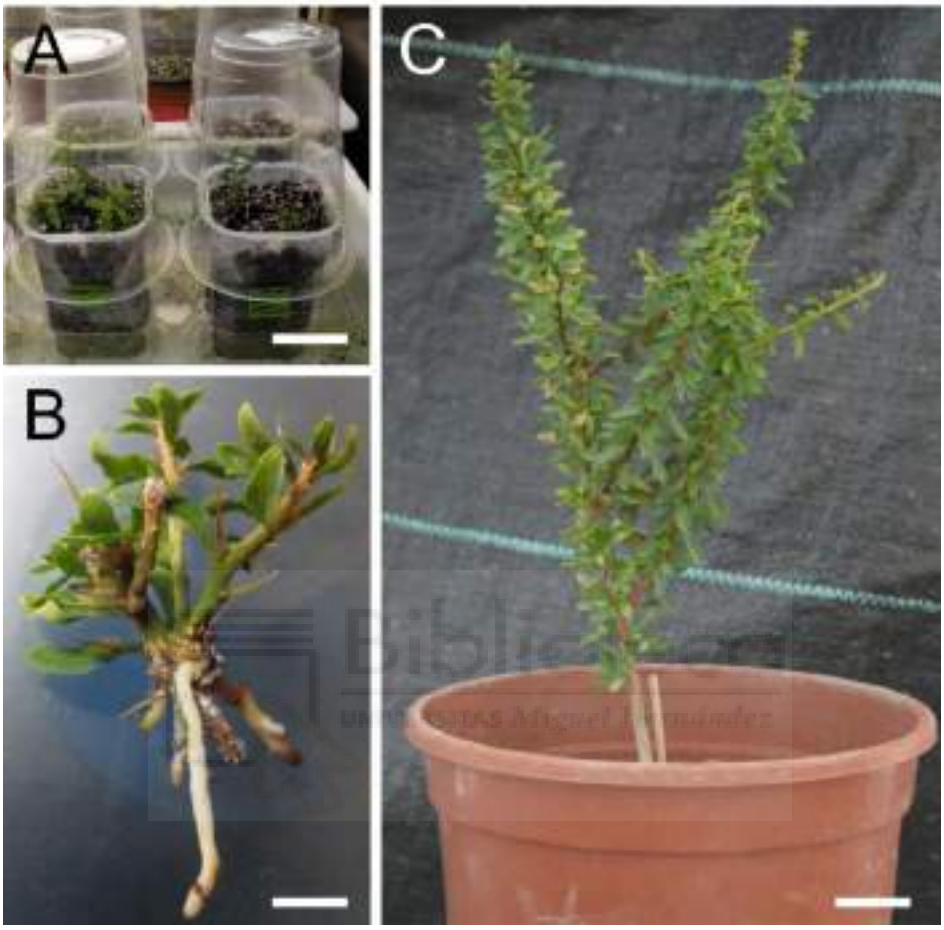

Figure 5. Acclimation of *in vitro*-produced argan tree microcuttings. (A) Acclimation of *in vitro* rooted argan tree microcuttings in controlled environment. (B) A two-month-old argan tree microcutting showing profuse adventitious root development. (C) Rooted argan tree microcutting after six months in greenhouse. Scale bars: 5 mm (B) and 15 mm (A, C).

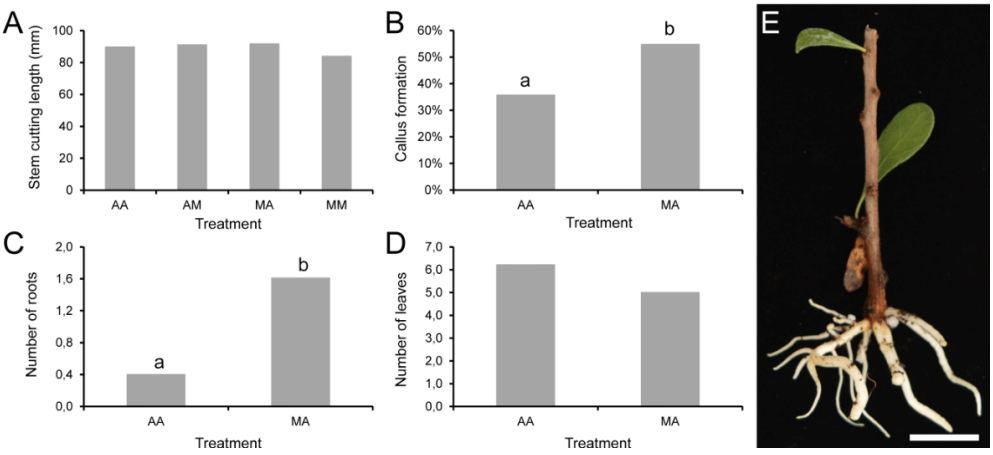

Figure 6. Adventitious rooting from mature argan tree stem cuttings. (A) Stem cutting length in the different experiments (AA: pre-treatment and treatment with auxin; AM: pre-treatment with auxin and treatment with mock; MA: pre-treatment with mock and treatment with auxin; MM: pre-treatment and treatment with mock). (B) Percentage of callus formation and (C) average number of adventitious roots in the stem cutting base two months after transplanting to soil. (D) Average number of green leaves in rooted stem cuttings at the end of the experiment. Data represent the average of a minimum of 25 samples. Letters distinguish significant differences ($P<0.05$) between treatments for the same numbers of days after sowing. (E) A rooted argan tree stem cutting after five months in the greenhouse. Scale bar: 5 mm.

Anexo

Comunicaciones a congresos

XXI Reunión de la Sociedad Española de Fisiología Vegetal, Toledo, junio 2015

Sánchez-García AB, Villanova J, Ruiz-Cano H, Ibáñez S, **Justamante MS**, Pérez-Pérez JM. Novel gene functions required for adventitious root development. Comunicación oral, presentada por AB Sánchez-García.

Plant Organ Growth Symposium 2017, Elche (Alicante), marzo 2017

Justamante MS, Ibáñez S, Pérez-Pérez JM. A genome-wide association study identifies new loci for root formation after wounding. Presentación de Póster.

XXII Reunión de la Sociedad Española de Fisiología Vegetal, Barcelona, junio 2017

Justamante MS, Cano A, Villanova J, López A, Cano EA, Acosta M, Pérez-Pérez JM. Integration of phenotypic, metabolomic and genetic data to identify novel regulators of adventitious root development in carnation cuttings. Presentación de poster y comunicación oral, presentada por **MS Justamante**.

XIV Reunión de Biología Molecular de Plantas, Salamanca, julio 2018

Justamante MS, Villanova J, Cano A, Cano EA, Acosta M, Pérez-Pérez JM. Hormonal crosstalk regulates adventitious root formation in diverse carnation genotypes. Presentación de Póster.

XIV Reunión de Biología Molecular de Plantas, Salamanca, julio 2018

Ibáñez S, **Justamante MS**, Ruiz-Cano H, Fernández-López MA, Micol JL, Pérez-Pérez JM. Novel regulators of *de novo* root organogenesis in *Arabidopsis thaliana*. Presentación de Póster.

International Symposium BAICTBMD and UPSC, Beijing, agosto 2018

Justamante MS, Villanova J, Cano A, Cano EA, Acosta M, Pérez-Pérez JM. Integration of phenotypic, metabolomic and genetic data to identify novel regulators of adventitious root development in carnation. Comunicación oral, presentada por JM Pérez-Pérez.

Fitohormonas. Metabolismo y modo de acción, Valencia, diciembre 2018

Acosta-Motos JR, **Justamante MS**, Villanova J, Birlanga V, Cano A, Cano EA, Acosta M, Pérez-Pérez JM. Integration of phenotypic, metabolomic and genetic data to identify novel regulators of adventitious root development in carnation. Comunicación oral, presentada por JR Acosta-Motos.

Novel gene functions required for adventitious root development

Ana Belén Sánchez-García, Joan Villanova, Helena Ruiz, Sergio Ibáñez, María Salud Justamante, José Manuel Pérez-Pérez
Instituto de Bioingeniería, Universidad Miguel Hernández, Avda. de la Universidad s/n, 03202 Elche, Spain
ana.sanchezg@umh.es

Adventitious roots (ARs) are ectopic roots that arise either naturally or in response to stressful environmental conditions from various plant tissues, such as stems and leaves; they may also be induced by mechanical damage or following *in vitro* tissue culture regeneration. The formation of ARs is a complex genetic process regulated by both environmental and endogenous factors, among which the plant hormone auxin plays a central role (Bellini et al. 2014).

By combining physiological, genetic, and histological techniques, we intend to identify the molecular networks that participate in the formation of ARs of the model plant *Arabidopsis thaliana*. In the basic side, our results will contribute to determine whether the genetic circuitries of *de novo* root formation are conserved among species, as well as to shed some light on the molecular basis of the hormonal crosstalk observed during plant regeneration. In the applied side, the molecular tools and the protocols developed in our group will help either to the optimization or to the design of new strategies aimed to increase the success rate in the vegetative propagation of tissue-culture recalcitrant plant species and cultivars.

To identify additional gene functions required for AR development we are screening the *Arabidopsis thaliana* unimutant collection with a visible leaf phenotype (Wilson-Sánchez et al. 2014). We will present our preliminary results on a series of novel AR formation mutants that suggest a prominent role for protein biosynthesis in the regulation of pre-meristematic cell formation during *de novo* organogenesis.

Bellini et al. (2014). Annu. Rev. Plant Biol., 65: 639-66

Wilson-Sánchez et al. (2014). Plant J., 79: 878-91

Work funded by Eurostars-EUREKA (CARNOMICS E!6834) and MINECO/FEDER (AGL2012-33610)

Novel gene functions required for adventitious root development

Ana Belén Sánchez-García

Toledo, 17/06/2015

De novo root organogenesis

- Adventitious roots (ARs) are ectopic roots that arise either naturally or in response to stressful environmental conditions from various plant tissues, such as stems and leaves

- Most of the commercially-grown ornamental plants are vegetatively propagated through shoot tissue culture where insufficient rooting limits their commercial scale-up

A model to study *de novo* root organogenesis

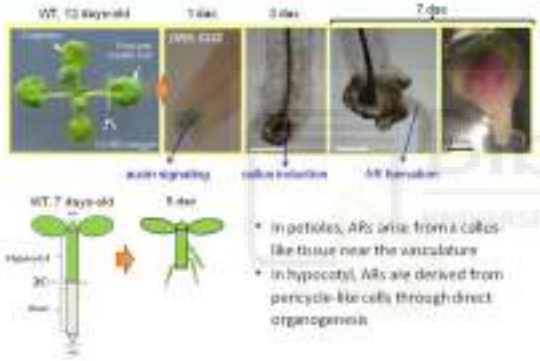

- In petioles, ARs arise from a callus like tissue near the vasculature
- In hypocotyl, ARs are derived from pericycle-like cells through direct organogenesis

Auxin plays a central role in AR formation

- Auxin accumulation and polar transport are essential for AR formation
- Exogenous auxin induces adventitious rooting in many species

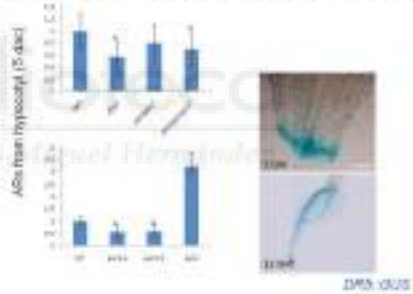

Cytokinin (CK) signaling is required for AR formation

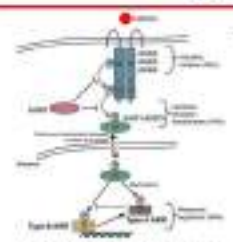

- CKs have been shown to negatively impact on AR formation

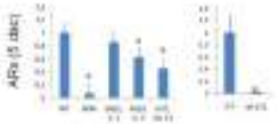

- Formative cell divisions require CK signaling
- CK response precedes (and is required for) callus formation

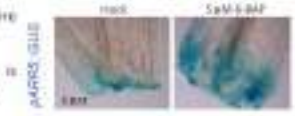

Novel functions involved in AR formation

PhenoLeaf

- A collection of 413 confirmed Salk Unimutant lines displaying aberrant leaf phenotypes was chosen (Wilson-Sánchez et al. 2014)
- Expression data during regeneration was retrieved from the *eFP browser*
- T-DNA lines from 110 genes were randomly selected from seven expression clusters (C0-C6)

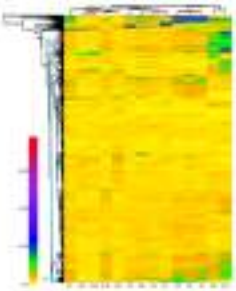

Novel functions involved in AR formation

- We identified 33 mutants with altered numbers of ARs from the wounded hypocotyl
  - 22 with a lower AR number than the WT
  - 11 with a higher AR number than the WT

Mutants affected in chromatin remodeling are deficient in AR formation

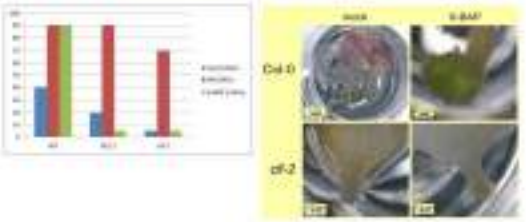

- Some mutants affected in chromatin remodeling display reduced number of ARs due to defective cytokinin-induced callus formation

Conclusions

- Our results suggest a positive crosstalk between auxin transport and cytokinin signaling during early formative stages (*i.e.* callus formation)
- Furthermore, AR from wounded tissues involves two processes that could be independently dissected by using genetics: (1) timing of AR initiation after wounding, and (2) the production rate of new AR
- In addition, we found a positive correlation between the number of lateral roots and adventitious roots after wounding which implies the existence of common regulatory mechanisms
- Finally, some mutants affected in chromatin remodeling display reduced number of ARs due to defective cytokinin-induced callus formation

www.arolab.es

PLANT KBBE

A genome-wide association study identifies new loci for root formation after wounding

Justamante, M.S., Ibáñez, S., and Pérez-Pérez, J.M.

Instituto de Bioingeniería, Universidad Miguel Hernández de Elche, Avda. de la Universidad s/n, 03202 Elche, Spain.

We are interested to contribute to the identification of some of the genetic determinants involved in *de novo* organ formation after wounding using *Arabidopsis thaliana* as a model organism. We have analyzed lateral and adventitious root formation in response to wounding on a collection of 120 natural accessions of Arabidopsis. Genome-wide association studies have been performed to identify some of the genomic regions that may be involved in the phenotypic variation for some of the studied traits.

We found statistically significant associations between the number of lateral roots after wounding and several polymorphic markers at the coding region of some genes on chromosomes 1, 3 and 5. Likewise we have found some markers associated with lateral root density and with the timing of lateral root primordial initiation. However, we found no significant association between the number of adventitious roots and the studied molecular markers. Our results suggest some specificity in the genetic mechanisms that regulate the formation of lateral and adventitious roots after wounding. Subsequent studies will allow us to confirm whether the polymorphisms identified contribute to the phenotypic differences observed in the studied accessions.

Work funded by MINECO/FEDER (AGL2012-33610 and BIO2015-64255).

A genome-wide association study identifies new loci for root formation after wounding

María Salud Justamante, ***José Manuel Pérez-Pérez***

Instituto de Bioingeniería, Universidad Miguel Hernández, Avda. de la Universidad s/n, 03202 Elche, Spain
mjustamante@umh.es

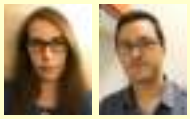

Introduction

We are interested in contributing to the identification of some of the genetic determinants involved in *de novo* organ formation using *Arabidopsis thaliana* as a model organism[1].

Results

We studied lateral and adventitious root formation in a collection of 120 wild *Arabidopsis thaliana* accessions[2] after primary root decapitation. Average data were obtained for parameters such as root number, root density or main root length. Through the GWAPP online application tool, which contained information up to 250,000 SNP markers, several GWAS (Genome-Wide Association Study) analyses were performed to look for statistically significant polymorphisms associated to the different traits under study. We have identified a missense mutation in a gene encoding a vesicle trafficking protein highly conserved in eukaryotes in those accessions with an increase in the number of lateral roots after decapitation. Another polymorphism linked to an Aux/IAA repressor has been correlated with lateral root densities after decapitation. Subsequent studies will allow us to confirm whether the polymorphisms identified contribute to the phenotypic differences observed in the studied accessions.

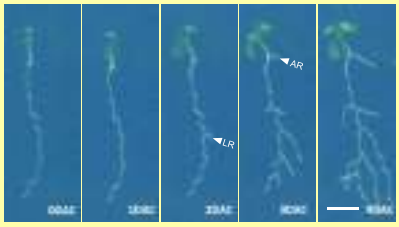

Figure 1.- Root development in Col-0 seedlings after primary root decapitation. Representative example of a Col-0 seedling where lateral (LR) and adventitious (AR) root formation are observed along several days after cutting (DAC). Scale bar: 4 mm.

Figure 2.- Natural variation in some of the studied traits. (A) Number of lateral roots and (B) number of adventitious roots at 4 DAC after primary root decapitation. Eight accession with contrasting phenotypes were highlighted (red: lower values, orange: higher values). Col-0 (green) was used as a reference accession.

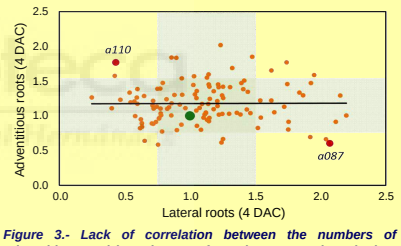

Figure 3.- Lack of correlation between the numbers of adventitious and lateral roots after primary root decapitation. Grey rectangles represent the mean values ± 1 SD in the studied population. Col-0 values are shown in green and two of the accessions with extreme phenotypes are shown in red.

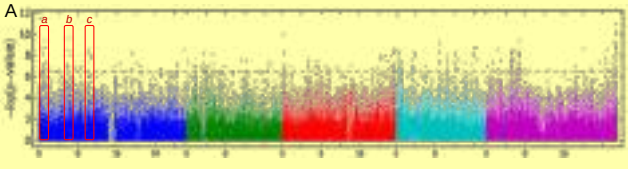

Accession	Location	Phenotypic values	*a*	*b*	*c*
a110	Spain	0.432	C	**C**	A
a111	Spain	1.927	C	**G**	A
a055	Russia	0.598	C	**C**	A
a033	Russia	1.032	C	**G**	C

Figure 4.- GWAS for the number of lateral roots. (A) *Manhattan plot* for the number of lateral roots at 4 DAC with the genomic regions of chromosome 1 (blue) that were analyzed in more detail. (B) Graphical representation of the phenotypic values of the studied lines according to their genotype for the *a* marker. (C) Haplotype for some of the geographically-close lines with extreme phenotypes. Note the marker *b*, with different haplotypes for lines of the same location and displaying contrasting phenotypic values.

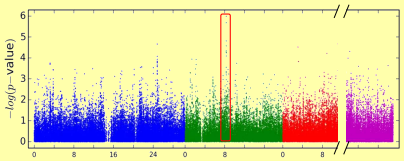

Figure 5.- GWAS for the number of adventitious roots. *Manhattan plot* for the number of adventitious roots at 4 DAC. We found two linked polymorphisms in the intergenic region between *At2g19130* and *At2g19146*, although not statistically significant due to the low phenotypic variation of the studied trait.

Conclusion

Through GWAS, we have identified a number of significant polymorphisms in chromosomes 1, 3 and 5 that might explain some of the variation found in root formation after wounding in a collection of wild accessions.

Our results highlighted new regulators of lateral and adventitious root formation in Arabidopsis.

References

1.- Lamesch *et al.* (2012). *Nucleic Acids Res*, 40: 202

2.- Alonso-Blanco *et al.* (2009). *Plant Cell*, 21: 1877

Acknowledgements
Work in the laboratory of J.M.P.-P. is funded by FEDER/MINECO grants (AGL2012-33610 and BIO2015-64255-R).

FV 2017 BARCELONA SPAIN 26-29 DE JUNIO
FISIOLOGÍA VEGETAL
XXII REUNIÓN DE LA SOCIEDAD ESPAÑOLA DE FISIOLOGÍA VEGETAL | XV SPANISH PORTUGUESE CONGRESS OF PLANT PHYSIOLOGY

ROOM: SALA CAPRI+ MEDES

SESSION 10. APPLIED PLANT PHYSIOLOGY AND MOLECULAR BREEDING

C0085 INTEGRATION OF PHENOTYPIC, METABOLOMIC AND GENETIC DATA TO IDENTIFY NOVEL REGULATORS OF ADVENTITIOUS ROOT DEVELOPMENT IN CARNATION CUTTINGS

María Salud Justamante Clemente[1], *Antonio Cano*[2], *Joan Villanova*[3], *Alfonso López*[4], *Emilio A. Cano*[4], *Manuel Acosta*[2], *José Manuel Pérez-Pérez*[3]

[1]*Universidad Miguel Hernández de Elche (Alicante) España*
[2]*Departamento de Biología Vegetal (Fisiología Vegetal), Universidad de Murcia (Murcia) España*
[3]*Instituto de Bioingeniería, Universidad Miguel Hernández de Elche (Elche) España*
[4]*Barberet & Blanc (Murcia) España*

1 Resumen

The rooting of stem cuttings is a common vegetative propagation practice in many ornamental plants. In cultivated carnation, adventitious root (AR) formation in the base of the cuttings is triggered by an endogenous auxin peak built-up by an active auxin transport from the leaves. To provide fundamental insights into the genetic basis of this complex trait, we studied AR formation in a collection of 194 lines derived from a cross between two hybrid cultivars, *2102-01 MFR* and *2003 R 8*, showing contrasting rooting performance[1, 2]. Time-series for several root architectural traits were quantified in sixteen of these lines displaying extreme rooting phenotypes, which were significantly correlated with the metabolomic profiles of the stem cuttings at harvesting time. Selective transcriptome profiling will allow us to identify a collection of candidate SNPs linked to rooting performance traits that might be used to establish a novel marker-assisted selection approach in this species for improved adventitious rooting.

References:
[1]Villanova *et al*. (2017) *Plant Growth Regul.* **81**:511
[2]Birlanga *et al*. (2015) *PLOS ONE* **10**: e0133123

Work funded by MINECO/FEDER (AGL2012-33610 and BIO2015-64255-R)

arolab

Integration of phenotypic, metabolomic and genetic data to identify novel regulators of adventitious root development in carnation cuttings

P-0085

Justamante MS, Cano A, Villanova J, López A, Cano EA, Acosta MA, Pérez-Pérez JM

Barcelona, 28/06/2017

FV 2017

Dissecting AR formation

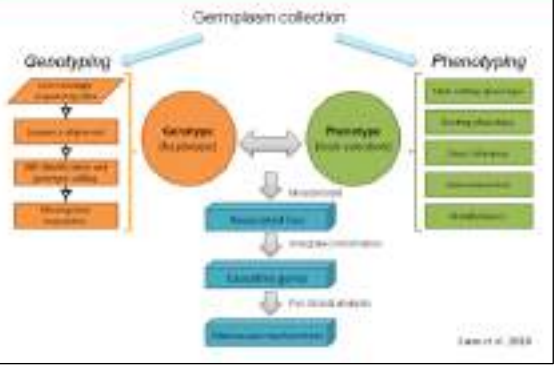

Adventitious rooting in carnation

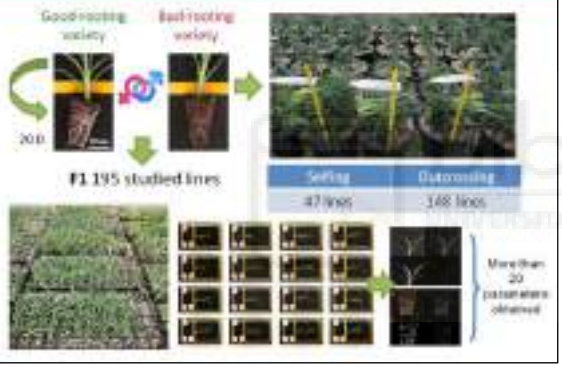

Variability on selected rooting traits

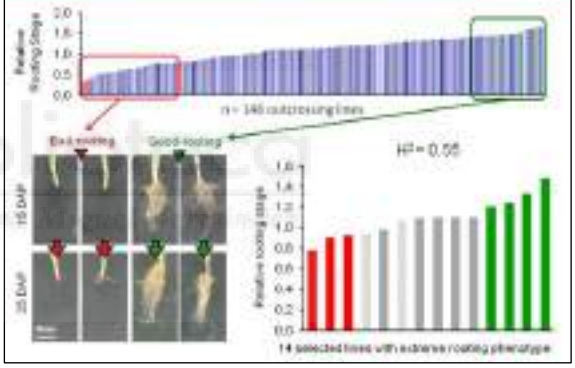

Adventitious rooting in carnation

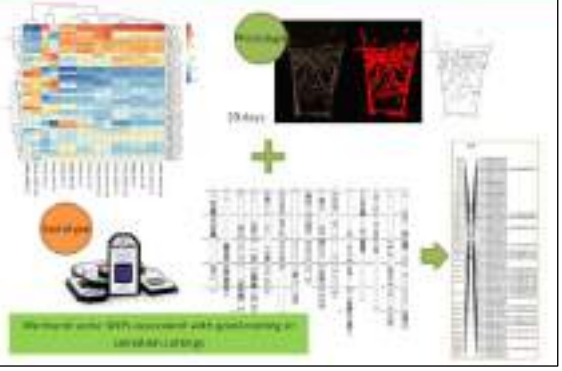

Integration of phenotypic, metabolomic and genetic data to identify novel regulators of adventitious root development in carnation cuttings

María Salud Justamante[1], *Antonio Cano*[2], *Joan Villanova*[1], *Alfonso López*[3], *Emilio A. Cano*[3], *Manuel Acosta*[2], ***José Manuel Pérez-Pérez***[1]

[1] Instituto de Bioingeniería, Universidad Miguel Hernández, Avda. de la Universidad s/n, 03202 Elche, Spain
[2] Departamento de Fisiología Vegetal, Universidad de Murcia (Murcia), Spain
[3] Barberet & Blanc (Murcia), Spain
mjustamante@umh.es

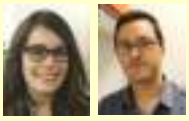

Introduction

The rooting of stem cuttings is a common vegetative propagation practice in many ornamental plants. In cultivated carnation, adventitious root (AR) formation in the base of the cuttings is triggered by an endogenous auxin peak built-up by an active auxin transport from the leaves.

Results

To provide fundamental insights into the genetic basis of this complex trait, we studied AR formation in a collection of 194 lines derived from a cross between two hybrid cultivars, *2101−02 MFR* and *2003 R 8*, showing contrasting rooting performane[1,2]. Time-series for several root architectural traits were quantified in 14 of these lines displaying extreme rooting phenotypes, which were significantly correlated with the metabolomic profiles of the stem cuttings at harvesting time.

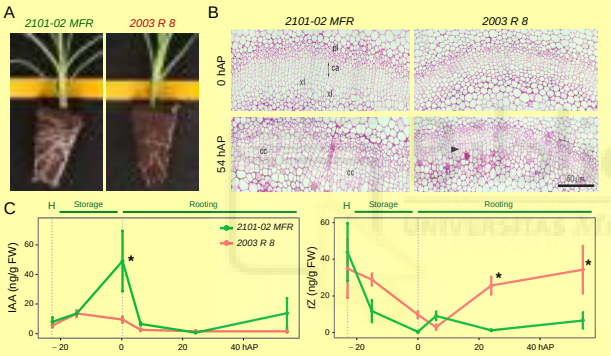

Figure 1.- Characterization of parent lines. (A) Cultivar-dependent adventitious rooting in carnation stem cuttings (green, good rooting; red, bad rooting). (B) Light micrographs from cross-sections of stem cutting basal regions at 0 and 54 h after planting (hAP). Black arrowhead indicates periclinal cell divisions in the cambium (ca); cc, cell clusters; pl: phloem; Xl, xylem. (C) Endogenous levels of some key hormones in the stem cutting base during adventitious rooting. Indole-3-acetic acid (IAA) (left) and *trans*-zeatin (*tZ*) (rigth). Average values ± a standard deviation values are shown. Asterisks indicate significant differences (P<0.05) over time for a given treatment. H: harvest.

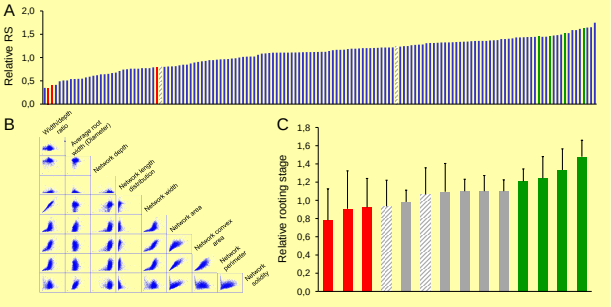

Figure 3.- Variability on selected rooting traits. (A) Rooting stage (RS) at 20 days after planting (DAP) referenced to parent lines. (B) Correlation between most descriptive rooting parameters identified by principal component analysis (PCA). (C) Rooting stage of selected lines with extreme rooting values for most of the parameters studied referenced to parent lines. Red bars, bad-rooting cultivars; green bars, good-rooting cultivars; stripped bars, parent lines.

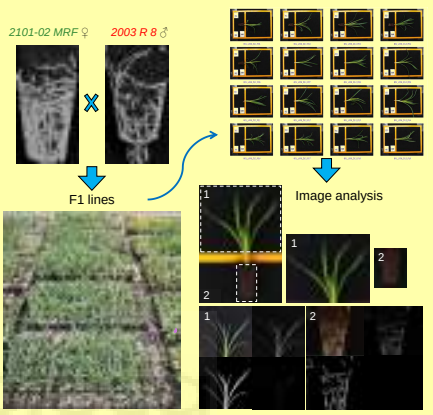

Figure 2.- Experimental design. 194 F1 lines were obtained from a crossing between *2101-02 MFR* and *2003 R 8*. Stem cuttings from these lines were periodically collected and cold-stored before being planted in the rooting station. Image processing, analysis and data collection of several root and shoot traits were obtained after rooting for 27 days.

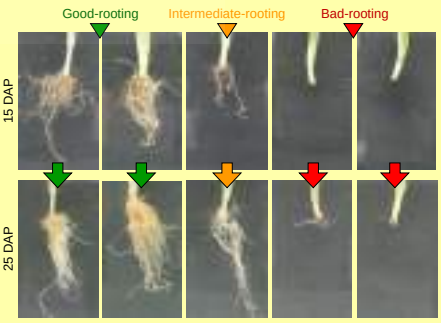

Figure 4.- Analysis of selected cultivars. 12 F1 lines showing extreme rooting phenotypes and the parent lines were further studied. Root architecture parameters were measured at different stages during rooting. Tissue samples were frozen for metabolomic and gene expression analyses.

Conclusion

Selective transcriptome profiling will allow us to identify a collection of candidate SNPs linked to rooting performance traits that might be used to establish a novel marker-assisted selection approach in this species for improved adventitious rooting.

References

1.- Villanova *et al*. (2017) *Plant Growth Regul* **81**:511

2.- Birlanga *et al*. (2015) *PLOS ONE* **10**: e0133123

Acknowledgements
Work in the laboratory of J.M.P.-P. (AGL2012-33610 and BIO2015-64255-R) is financed by the Ministry of Economy and Competitiveness (MINECO) and by FEDER funds of the EC - "A way to build Europe"

S-II. Póster 11

HORMONAL CROSSTALK REGULATES ADVENTITIOUS ROOT FORMATION IN DIVERSE CARNATION GENOTYPES

María Salud Justamante[1], Joan Villanova[1], Antonio Cano[2], Emilio A. Cano[3], Manuel Acosta[2], José Manuel Pérez-Pérez[1]

[1]Instituto de Bioingeniería, Universidad Miguel Hernández, Elche, Spain, [2]Departamento de Fisiología Vegetal, Universidad de Murcia, Spain, [3]Dümmen Orange, Murcia, Spain.

Corresponding author: José Manuel Pérez-Pérez (jmperez@umh.es)

Adventitious rooting of stem cuttings is an essential process needed for vegetative propagation in many ornamental plants. In cultivated carnation, adventitious roots (ARs) are formed in the base of the cuttings in response to a localized auxin gradient. Differences in biosynthesis, transport and conjugation of auxin levels in the stem cutting base during the first hours after excision accounts for the differences observed in AR formation between cultivars with contrasting rooting efficiencies (Cano *et al*. 2018). To better understand the genetic basis of this complex trait, we studied AR formation in 177 lines derived from a cross between two hybrid cultivars with contrasting rooting performance (Birlanga *et al.* 2015). Several architectural traits were quantified in fourteen of these lines displaying extreme AR phenotypes. Combining hormonal and phenotypic results with selective transcriptome profiling will allow us to identify a collection of candidate SNPs linked to adventitious rooting performance, which will be used to establish a novel marker-assisted selection approach to improve adventitious rooting in this species.

Birlanga, V., et al. (2015) PLOS ONE 10: e0133123
Cano et al. (2018). Front Plant Sci doi: 10.3389/fpls.2018.00566

Work in the laboratory of J.M.P.-P. (AGL2012-33610 and BIO2015-64255-R) is funded by the Ministry of Economy and Competitiveness and by FEDER funds of the EC - "A way to build Europe“.

Hormonal crosstalk regulates adventitious root formation in diverse carnation genotypes

María Salud Justamante[1], Joan Villanova[1], Antonio Cano[2], Emilio A. Cano[3], José Ramón Acosta-Motos[2], Manuel Acosta[2],
José Manuel Pérez-Pérez[1]

[1] Instituto de Bioingeniería, Universidad Miguel Hernández, Avda. de la Universidad s/n, 03202 Elche, Spain
[2] Departamento de Fisiología Vegetal, Universidad de Murcia, Murcia, Spain
[3] Dümmen Orange, Puerto Lumbreras, Murcia, Spain
jmperez@umh.es


Introduction

Adventitious rooting of stem cuttings is an essential process needed for vegetative propagation in many ornamental plants. In cultivated carnation, adventitious roots (ARs) are formed in the base of the cuttings in response to a localized auxin gradient.

Results

To better understand the genetic basis of this complex trait, we studied AR formation in 177 lines derived from a cross between two hybrid cultivars with contrasting rooting performance[1]. Differences in biosynthesis, transport and conjugation of auxin levels in the stem cutting base during the first hours after excision accounts for the differences observed in AR formation between parental lines[2]. Several architectural traits were quantified in fourteen of the studied lines displaying extreme AR phenotypes at selected time points.

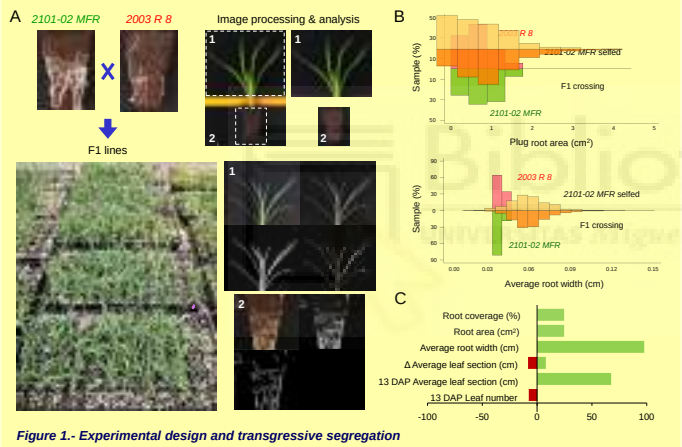

Figure 1.- Experimental design and transgressive segregation

(A) 177 F1 lines were obtained from a crossing between *2101-02 MFR* and *2003 R 8 cultivars*. Image processing, analysis and data collection of several root and shoot traits were obtained after rooting for 13 and 20 days after planting (DAP). (B) Transgressive segregation observed in some relevant rooting parameters at 20 DAP for F1 crossing and *2101-02 MFR* selfed populations. (C) Percentage values for transgressive segregation in the studied parameters.

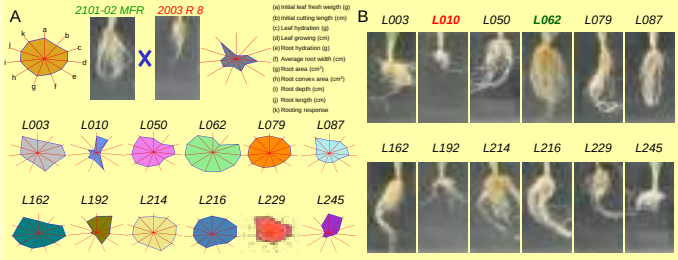

Figure 3.- Variability on selected rooting traits

12 F1 lines showing extreme rooting phenotypes and the parental lines were studied. (A) Stars and rays graphs showing differences between cultivars. Each axis (red) represents one parameter, and its intersection with the blue line indicates the relative magnitude for that parameter. (B) Representative images for each cultivar. According to the different analyses performed, best-rooting cultivar was *L062* and the worst-rooting one was *L010*.

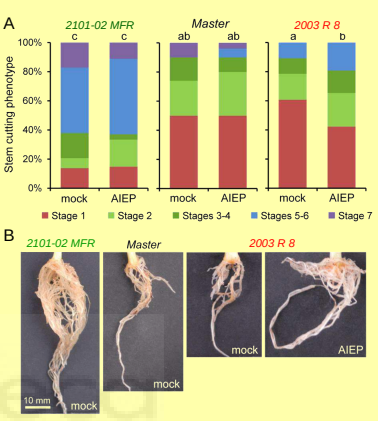

Figure 2.- Auxin homeostasis at the stem cutting base is required for adventitious rooting

(A) Graphic representations of rooting stage values in different carnation cultivars and treatments. Letters indicate significant differences (P<0.05) over sample means (cultivar × treatment). (B) Representative images of adventitious rooting in the studied carnation cultivars at 29 DAP treated with the GH3 inhibitor (10 µM AIEP) or with mock (DMSO).

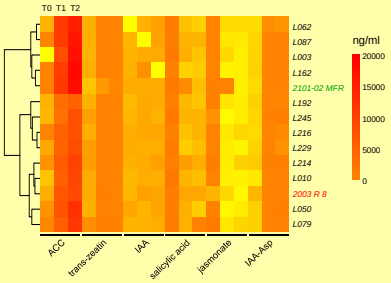

Figure 4.- Hormonal profiling for selected lines

A heat map representation for the most relevant metabolites was performed to study differences between selected cultivars. ACC, jasmonate and salicilic acid seemed to contribute to the differences in adventitious rooting between cultivars.

Conclusion

Combining hormonal and phenotypic results with selective transcriptome profiling will allow us to identify a collection of candidate SNPs linked to adventitious rooting performance, that might be used to establish a novel marker-assisted selection approach to improve adventitious rooting in this species.

References

1.- Birlanga *et al.* (2015) *PLOS ONE* **10**: e0133123
2.- Cano *et al.* (2018) *Front Plant Sci* **9**: 566

Acknowledgements
Work in the laboratory of J.M.P.-P. (AGL2012-33610 and BIO2015-64255-R) is financed by the Ministry of Economy and Competitiveness (MINECO) and by FEDER funds of the EC - "A way to build Europe". We thank Alfonso Albacete (CEBAS-CSIC) for hormone profiling. M.S. Justamante has been awarded a SEFV travel grant.

S-IV. Póster 31

NOVEL REGULATORS OF *DE NOVO* ROOT ORGANOGENESIS IN *Arabidopsis thaliana*

Sergio Ibáñez[1], María Salud Justamante[1], Helena Ruiz-Cano[1], María Ángeles Fernández-López[1,2], José Luis Micol[1], José Manuel Pérez-Pérez[1]

[1]Instituto de Bioingeniería, Universidad Miguel Hernández, Elche, Spain, [2]Instituto de Biología Molecular y Celular de Plantas, UPV–CSIC, Valencia, Spain.

Corresponding author: José Manuel Pérez-Pérez (jmperez@umh.es)

Lateral roots (LRs) and adventitious roots (ARs) are formed *de novo* during post-embryonic development, in processes that are highly dependent on environmental inputs (Bellini *et al*., 2014). Wound-induced *de novo* root organogenesis is a suitable model to study regeneration in plants, as it includes local hormone signalling, cell proliferation, founder cell specification and patterning (Bustillo-Avendaño *et al*., 2018). We searched for genes involved in *de novo* root formation by means of two complementary approaches. First, we screened 139 T-DNA homozygous lines from the PhenoLeaf collection (Wilson-Sánchez *et al*., 2014) and 23 of them (16.5%) showed altered *de novo* root organogenesis. Gene products related to vesicle trafficking and ABA signalling, among others, were confirmed to modulate AR formation. We performed a genome-wide association study on a collection of 120 natural accessions to identify additional regulators of *de novo* root organogenesis. We found statistically significant associations between several LR traits after root tip excision and non-synonymous SNPs in the coding region of eight genes in chromosomes 1, 3, 4 and 5. Interestingly, we found some overlap in the developmental pathways identified by the different approaches, indicating that wound-induced LRs and ARs might share molecular regulators.

Bellini, C., et al. (2014). Annu Rev Plant Biol 65: 639-666 Bustillo-Avendaño, E., et al. (2018). Plant Physiol 176: 1709-1727
Wilson-Sánchez, D., et al. (2014). Plant J 75: 878-891

Work in the laboratory of J.M.P-P is funded by the Ministry of Science and Innovation (AGL2012-33610 and BIO2015-64255-R).

Novel regulators of *de novo* root organogenesis in *Arabidopsis thaliana*

Sergio Ibáñez[1], María Salud Justamante[1], Helena Ruiz-Cano[1], María Ángeles Fernández-López[1,2], José Luis Micol[1],
José Manuel Pérez-Pérez[1]

[1]Instituto de Bioingeniería, Universidad Miguel Hernández, Elche, Spain
[2]Instituto de Biología Molecular y Celular de Plantas, UPV–CSIC, Valencia, Spain
s.ibanez@umh.es

Introduction

We are interested in contributing to the identification of some of the genetic determinants involved in *de novo* organ formation using *Arabidopsis thaliana* as a model organism[1].

Results

We studied lateral and adventitious root formation in a collection of 120 wild *Arabidopsis thaliana* accessions[2] after primary root decapitation. Average data were obtained for parameters such as root number, root density or main root length. Through the GWAPP online application tool, which contained information up to 250,000 SNP markers, several GWAS (Genome-Wide Association Study) analyses were performed to look for statistically significant polymorphisms associated to the different traits under study. We have identified a missense mutation in a gene encoding a vesicle trafficking protein highly conserved in eukaryotes in those accessions with an increase in the number of lateral roots after decapitation. Another polymorphism linked to an Aux/IAA repressor has been correlated with lateral root densities after decapitation. Subsequent studies will allow us to confirm whether the polymorphisms identified contribute to the phenotypic differences observed in the studied accessions.

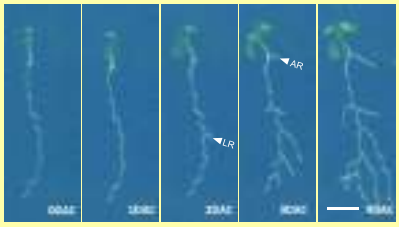

Figure 1.- Root development in Col-0 seedlings after primary root decapitation. Representative example of a Col-0 seedling where lateral (LR) and adventitious (AR) root formation are observed along several days after cutting (DAC). Scale bar: 4 mm.

Figure 2.- Natural variation in some of the studied traits. (A) Number of lateral roots and (B) number of adventitious roots at 4 DAC after primary root decapitation. Eight accession with contrasting phenotypes were highlighted (red: lower values, orange: higher values). Col-0 (green) was used as a reference accession.

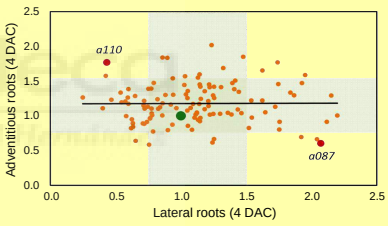

Figure 3.- Lack of correlation between the numbers of adventitious and lateral roots after primary root decapitation. Grey rectangles represent the mean values ± 1 SD in the studied population. Col-0 values are shown in green and two of the accessions with extreme phenotypes are shown in red.

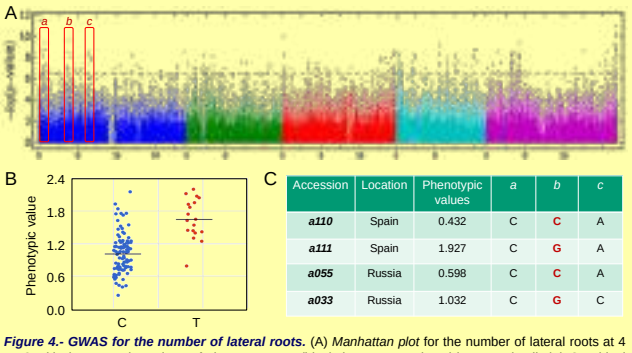

Accession	Location	Phenotypic values	*a*	*b*	*c*
a110	Spain	0.432	C	**C**	A
a111	Spain	1.927	C	**G**	A
a055	Russia	0.598	C	**C**	A
a033	Russia	1.032	C	**G**	C

Figure 4.- GWAS for the number of lateral roots. (A) *Manhattan plot* for the number of lateral roots at 4 DAC with the genomic regions of chromosome 1 (blue) that were analyzed in more detail. (B) Graphical representation of the phenotypic values of the studied lines according to their genotype for the *a* marker. (C) Haplotype for some of the geographically-close lines with extreme phenotypes. Note the marker *b*, with different haplotypes for lines of the same location and displaying contrasting phenotypic values.

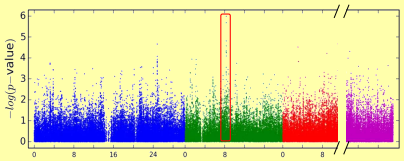

Figure 5.- GWAS for the number of adventitious roots. *Manhattan plot* for the number of adventitious roots at 4 DAC. We found two linked polymorphisms in the intergenic region between *At2g19130* and *At2g19146*, although not statistically significant due to the low phenotypic variation of the studied trait.

Conclusion

Through GWAS, we have identified a number of significant polymorphisms in chromosomes 1, 3 and 5 that might explain some of the variation found in root formation after wounding in a collection of wild accessions.

Our results highlighted new regulators of lateral and adventitious root formation in Arabidopsis.

References

1.- Lamesch *et al.* (2012). *Nucleic Acids Res*, 40: 202

2.- Alonso-Blanco *et al.* (2009). *Plant Cell*, 21: 1877

Acknowledgements
Work in the laboratory of J.M.P.-P. (AGL2012-33610 and BIO2015-64255-R) is financed by the Ministry of Economy and Competitiveness (MINECO) and by FEDER funds of the EC - "A way to build Europe"

Integration of phenotypic, metabolomic and genetic data to identify novel regulators of adventitious root development in carnation

María Salud Justamante[1], Joan Villanova[1], Antonio Cano[2], Emilio A. Cano[3], Manuel Acosta[2], José Manuel Pérez-Pérez[1]

[1]Instituto de Bioingeniería, Universidad Miguel Hernández, Elche, Spain, [2]Departamento de Fisiología Vegetal, Universidad de Murcia, Spain, [3]Dümmen Orange, Murcia, Spain.

Corresponding author: José Manuel Pérez-Pérez (jmperez@umh.es)

Adventitious rooting of stem cuttings is an essential process needed for vegetative propagation in many ornamental plants. In cultivated carnation, adventitious roots (ARs) are formed in the base of the cuttings in response to a localized auxin gradient. Differences in biosynthesis, transport and conjugation of auxin levels in the stem cutting base during the first hours after excision accounts for the differences observed in AR formation between cultivars with contrasting rooting efficiencies (Cano *et al*. 2018). To better understand the genetic basis of this complex trait, we studied AR formation in 177 lines derived from a cross between two hybrid cultivars with contrasting rooting performance (Birlanga *et al.* 2015). Several architectural traits were quantified in fourteen of these lines displaying extreme AR phenotypes. Combining hormonal and phenotypic results with selective transcriptome profiling will allow us to identify a collection of candidate SNPs linked to adventitious rooting performance, which will be used to establish a novel marker-assisted selection approach to improve adventitious rooting in this species.

Birlanga, V., et al. (2015) PLOS ONE 10: e0133123
Cano et al. (2018). Front Plant Sci doi: 10.3389/fpls.2018.00566

Work in the laboratory of J.M.P.-P. (AGL2012-33610 and BIO2015-64255-R) is funded by the Ministry of Economy and Competitiveness and by FEDER funds of the EC - "A way to build Europe“.

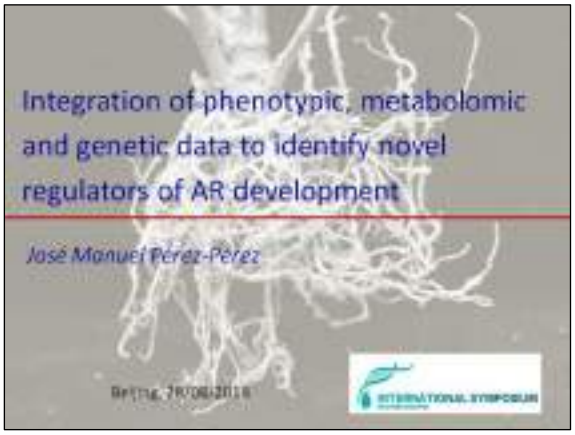
Integration of phenotypic, metabolomic and genetic data to identify novel regulators of AR development
José Manuel Pérez-Pérez

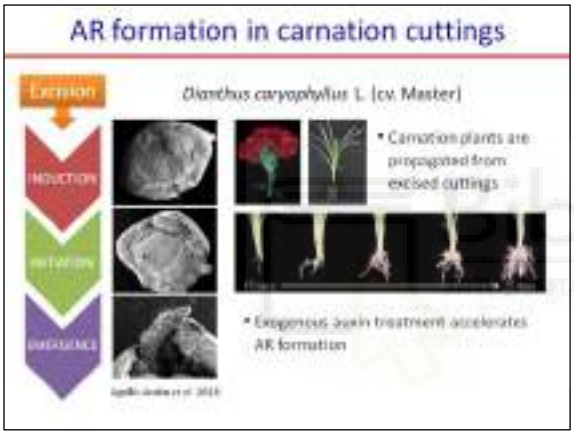
AR formation in carnation cuttings
Excision
Dianthus caryophyllus L. (cv. Master)
INDUCTION
INITIATION
EMERGENCE
• Carnation plants are propagated from excised cuttings
• Exogenous auxin treatment accelerates AR formation

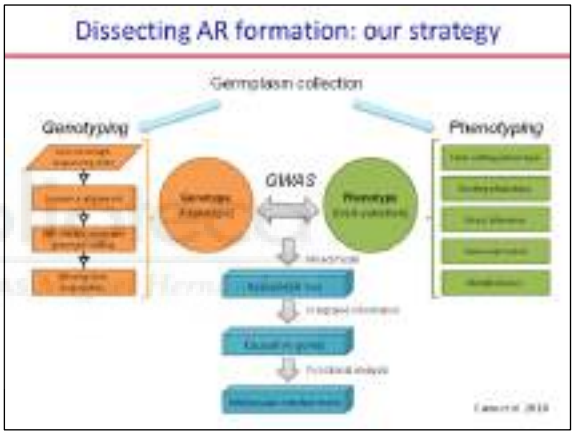
Dissecting AR formation: our strategy
Germplasm collection
Genotyping
Phenotyping
GWAS

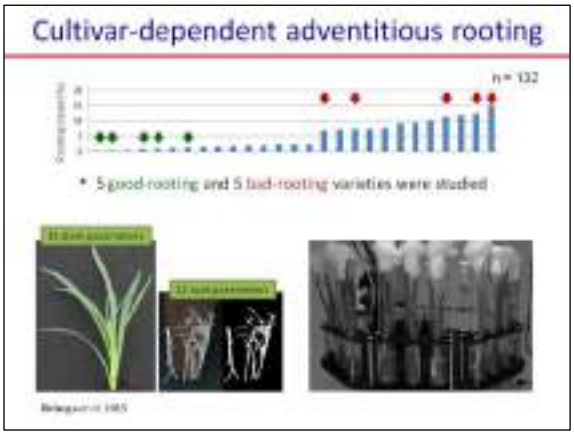
Cultivar-dependent adventitious rooting
n= 132
• 5 good-rooting and 5 bad-rooting varieties were studied

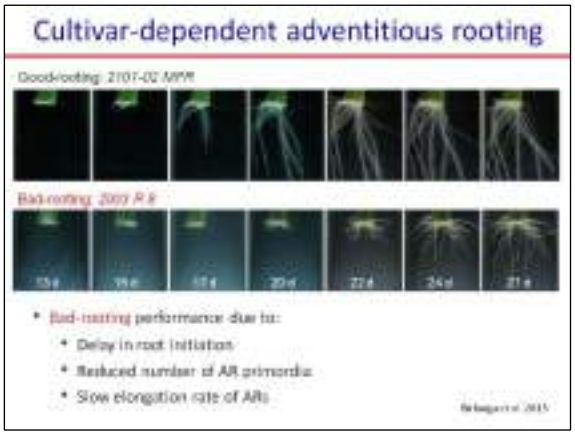
Cultivar-dependent adventitious rooting
Good-rooting: 2107-02 MPR
Bad-rooting: 2003 P 8
• Bad-rooting performance due to:
• Delay in root initiation
• Reduced number of AR primordia
• Slow elongation rate of ARs

Histological analyses of AR formation

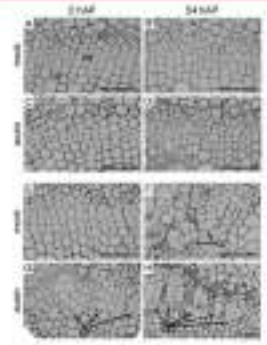

- *2003 R 8*
  - Local activation of cell divisions in the cambial ring at 54 hAP
  - Auxin treatment: activation of cell divisions in the cambial ring at 6 hAP
- *2101-02 MFR*
  - Later time points: clusters of meristematic cells (cc)
  - Auxin treatment: cell clusters became apparent already at 0 hAP

Expression profiling during AR formation

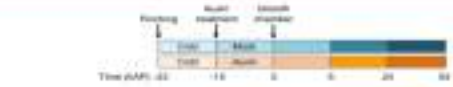

- A large proportion of genes were differentially expressed during AR formation

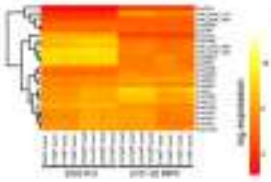

- Genes encoding mitotic cyclins showed a peak of expression between 24 hAP and 54 hAP (*2101-02 MFR*) and moderately respond to the auxin treatment (*2003 R 8*)

General Results

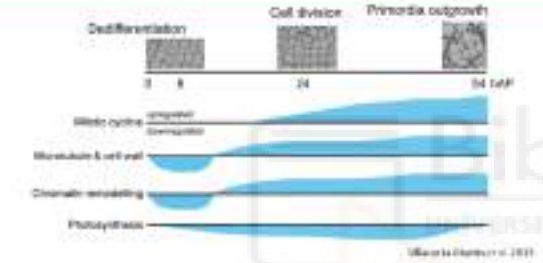

- A transient endogenous auxin peak during the first hours after excision was correlated with formative divisions in some cells along the cambial ring leading to the new root primordia

Morphogenetic hormones during AR formation

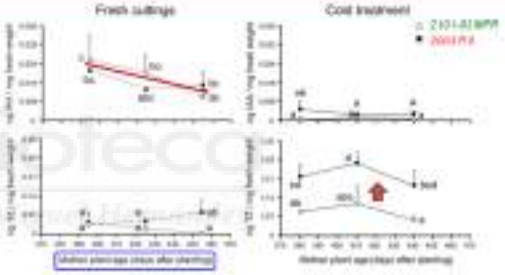

- Cold-storage of cuttings alters endogenous CK-to-auxin ratios in the stem cutting base, which is strongly genotype- and age-dependent

Morphogenetic hormones during AR formation

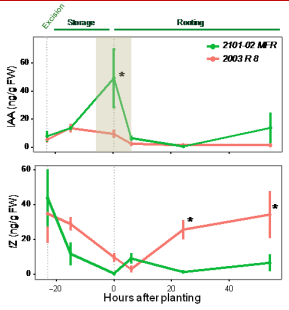

Stem cutting base

- High endogenous IAA levels in the good-rooting cultivar at earlier time points, which were quickly downregulated up to steady-state levels
- *trans*-zeatin (*tZ*) levels are quickly downregulated. In the bad-rooting cultivar, *tZ* levels steadily increased across the time-course

IAA/tZ ratio might be used to predict rooting performance

Cano *et al.* 2018

Auxin is produced in mature leaves

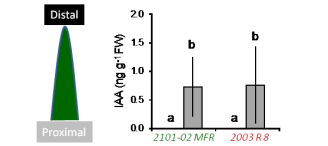

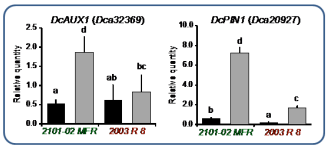

- IAA is mainly produced in the distal region of mature leaves and is actively transported onto the proximal region in both cultivars

Cano *et al.* 2018

PAT is required for AR formation

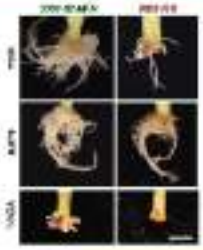

- Exogenous auxin treatment enhances AR formation in the **bad-rooting** cultivar

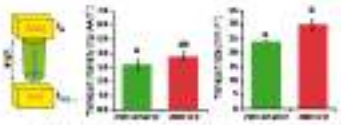

- PAT inhibition prevents AR formation in both cultivars

Differences in PAT between contrasting cultivars do not account for AR differences

Auxin degradation in the cutting base

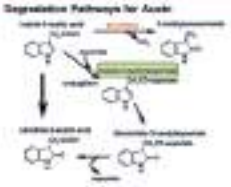

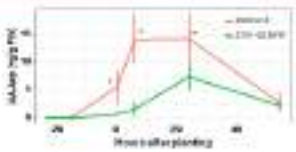

- Compounds derived from both decarboxylative and non-decarboxylative catabolism of IAA were identified

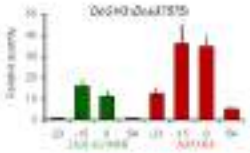

Auxin degradation in the cutting base

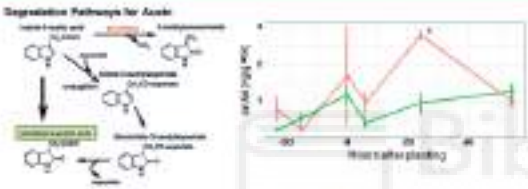

- The main regulation of active IAA levels in carnation stem cuttings was through their conjugation with aspartic acid

The bad-rooting cultivar has higher auxin catabolism, which results in less active IAA

Auxin inactivation regulates AR formation

- We treated freshly harvested stem cuttings with 10 µM AIEP, a known inhibitor of GH3 activities

GH3-mediated IAA-Asp accumulation negatively affects adventitious rooting in 2003/F.8

GRN of auxin response

- We searched for DEGs encoding known players of the auxin signaling pathway

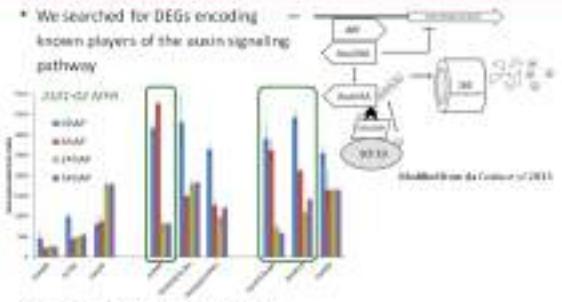

- Gene expression dynamics suggest conserved Aux/IAA-ARF modules for AR initiation

Genetic dissection of adventitious rooting in carnation stem cuttings

164 lines were studied

From selfings	From crossings
33 lines	131 lines

20 days

Transgressive segregation in rooting parameters

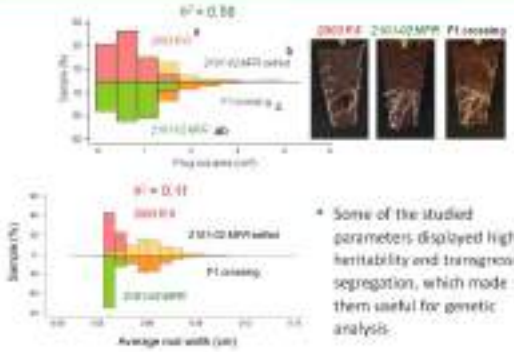

* Some of the studied parameters displayed high heritability and transgressive segregation, which made them useful for genetic analysis

GWAS of adventitious rooting in stem cuttings

164 lines ~ 24.000 eSNPs ⟺ Rooting parameters

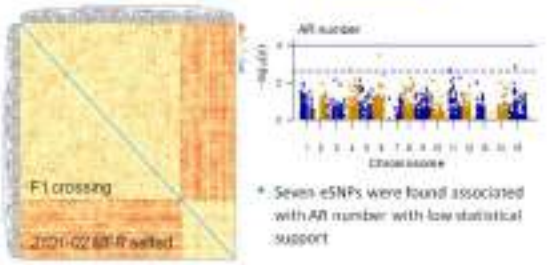

* Seven eSNPs were found associated with AR number with low statistical support

GRN of adventitious rooting in carnation

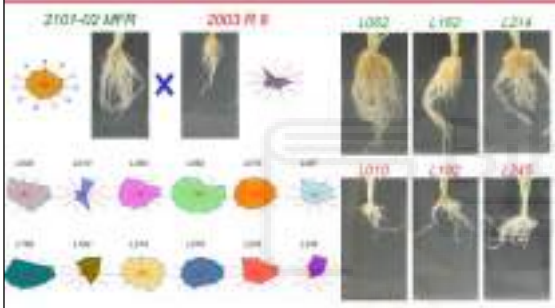

* 12 F1 lines with extreme rooting phenotypes were selected for hormone and gene profiling studies

GRN of adventitious rooting in carnation

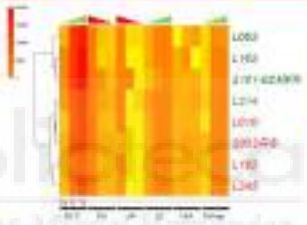

Selective transcriptome profiling

Combining hormonal and phenotypic results with selective transcriptome profiling will allow us to identify a collection of candidate eSNPs linked to AR performance, that might be used to establish a novel marker-assisted selection approach to improve adventitious rooting in carnation

GRN of adventitious rooting

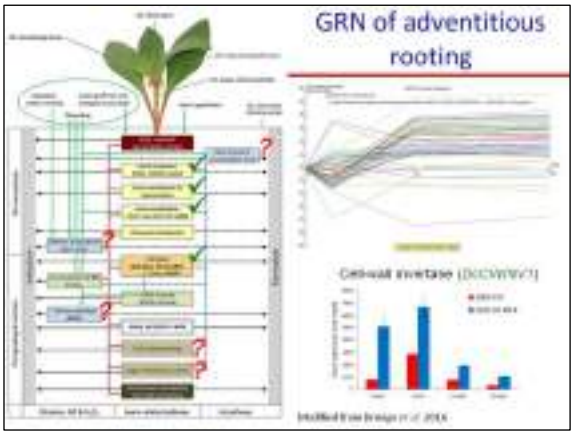

arolab.edu.umh.es

José Manuel Pérez-Pérez
Virginia Estrada Manzo
Rebeca González Bayón
Sergio Ibáñez
Marta Sabal Justavante
Ana Belén Sánchez

Prof Manuel Acedo
Dr. Antonio Cano
Department of Plant Biology
University of Murcia, Spain

CSIC

Barberet Blanc

Integration of phenotypic, metabolomic and genetic data to identify novel regulators of adventitious root development in carnation

José Ramón Acosta-Motos[1,2], María Salud Justamante[1], Joan Villanova[1], Virginia Birlanga[1], Antonio Cano3, Emilio A. Cano[4], Manuel Acosta[3], José Manuel Pérez-Pérez[1]

1 *Instituto de Bioingeniería, Universidad Miguel Hernández, Elche, Spain,*
2 *Universidad Católica San Antonio de Murcia, Campus de los Jerónimos, Guadalupe, Spain,* ***3*** *Departamento de Fisiología Vegetal, Universidad de Murcia, Spain,* ***4*** *Dümmen Orange, Murcia, Spain.*
Corresponding author: José Manuel Pérez-Pérez (jmperez@umh.es)

Adventitious rooting of stem cuttings is an essential process needed for vegetative propagation in many ornamental plants. In cultivated carnation, adventitious roots (ARs) are formed in the base of the cuttings in response to a localized auxin gradient. Differences in biosynthesis, transport and conjugation of auxin levels in the stem cutting base during the first hours after excision accounts for the differences observed in AR formation between cultivars with contrasting rooting efficiencies (Cano et al. 2018). To better understand the genetic basis of this complex trait, we studied AR formation in 177 lines derived from a cross between two hybrid cultivars with contrasting rooting performance (Birlanga et al. 2015). Several architectural traits were quantified in fourteen of these lines displaying extreme AR phenotypes. Combining hormonal and phenotypic results with selective transcriptome profiling will allow us to identify a collection of candidate SNPs linked to adventitious rooting performance, which will be used to establish a novel marker-assisted selection approach to improve adventitious rooting in this species.

Birlanga, V., et al. (2015) PLOS ONE 10: e0133123
Cano et al. (2018). Front Plant Sci 9: 566

Work in the laboratory of J.M.P.-P. (AGL2012-33610 and BIO2015-64255-R) is funded by the Ministry of Economy and Competitiveness and by European Regional Development Fund (ERDF) of the EC - "A way to build Europe“.

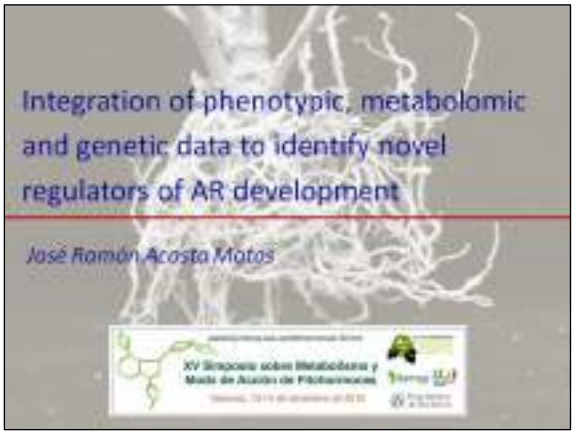
Integration of phenotypic, metabolomic and genetic data to identify novel regulators of AR development
José Ramón Acosta Motos

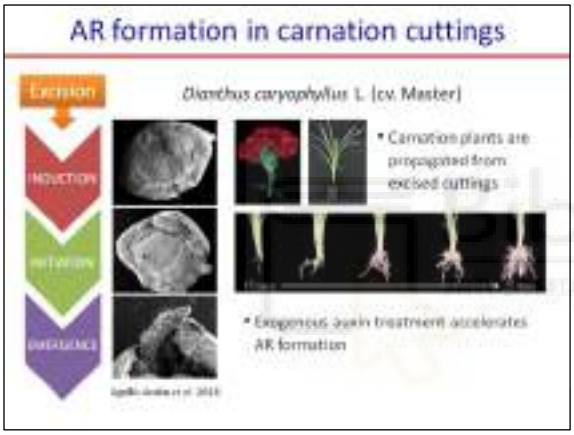
AR formation in carnation cuttings
Excision
Dianthus caryophyllus L. (cv. Master)
INDUCTION
INITIATION
EMERGENCE
• Carnation plants are propagated from excised cuttings
• Exogenous auxin treatment accelerates AR formation

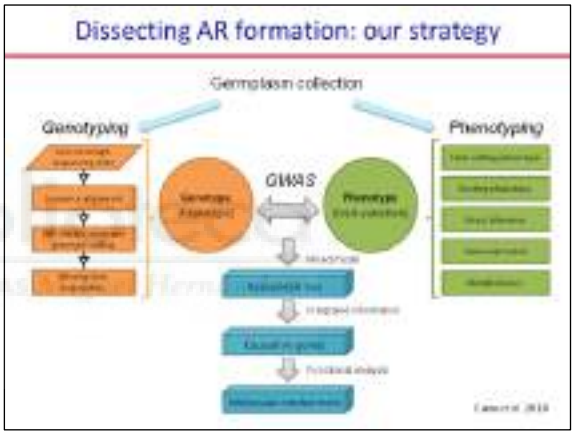
Dissecting AR formation: our strategy
Germplasm collection
Genotyping
Phenotyping
GWAS

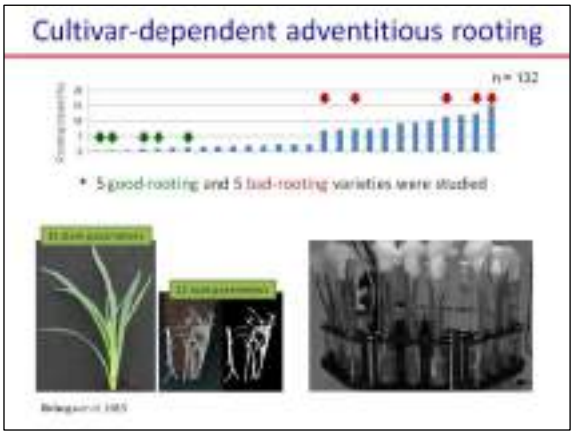
Cultivar-dependent adventitious rooting
n= 132
• 5 good-rooting and 5 bad-rooting varieties were studied

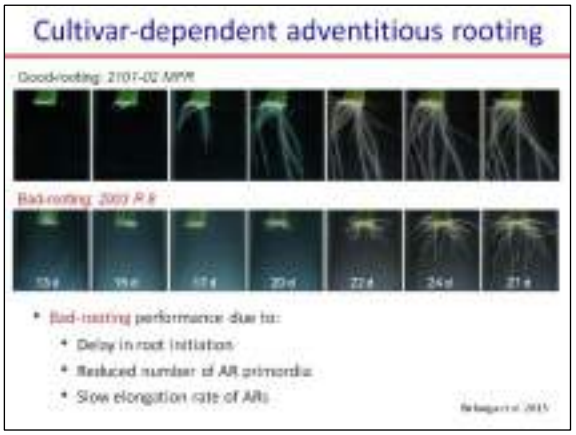
Cultivar-dependent adventitious rooting
Good-rooting: 2107-02 MPR
Bad-rooting: 2003 P 8
• Bad-rooting performance due to:
• Delay in root initiation
• Reduced number of AR primordia
• Slow elongation rate of ARs

Histological analyses of AR formation

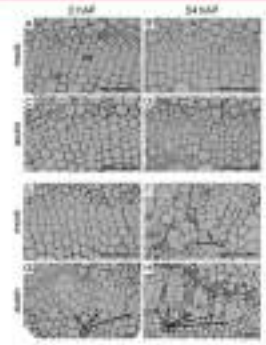

- *2003 R 8*
  - Local activation of cell divisions in the cambial ring at 54 hAP
  - Auxin treatment: activation of cell divisions in the cambial ring at 6 hAP
- *2101-02 MFR*
  - Later time points: clusters of meristematic cells (cc)
  - Auxin treatment: cell clusters became apparent already at 0 hAP

Expression profiling during AR formation

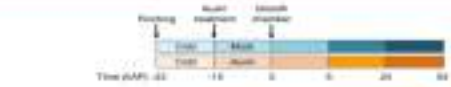

- A large proportion of genes were differentially expressed during AR formation

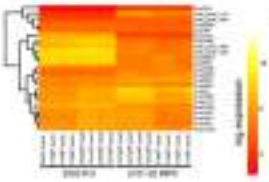

- Genes encoding mitotic cyclins showed a peak of expression between 24 hAP and 54 hAP (*2101-02 MFR*) and moderately respond to the auxin treatment (*2003 R 8*)

General Results

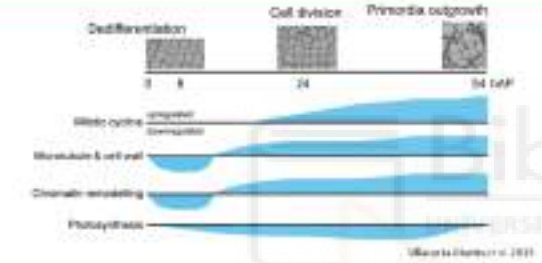

- A transient endogenous auxin peak during the first hours after excision was correlated with formative divisions in some cells along the cambial ring leading to the new root primordia

Morphogenetic hormones during AR formation

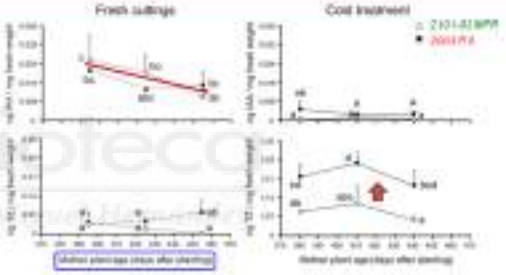

- Cold-storage of cuttings alters endogenous CK-to-auxin ratios in the stem cutting base, which is strongly genotype- and age-dependent

Morphogenetic hormones during AR formation

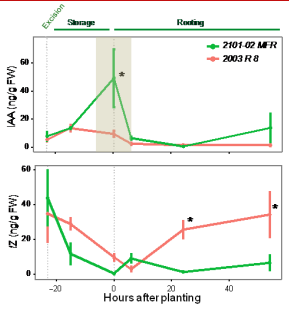

Stem cutting base

- High endogenous IAA levels in the good-rooting cultivar at earlier time points, which were quickly downregulated up to steady-state levels
- *trans*-zeatin (*tZ*) levels are quickly downregulated. In the bad-rooting cultivar, *tZ* levels steadily increased across the time-course

IAA/tZ ratio might be used to predict rooting performance

Cano *et al.* 2018

Auxin is produced in mature leaves

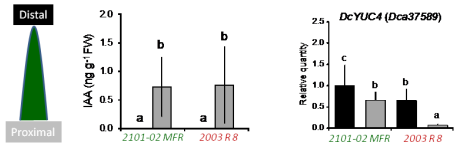

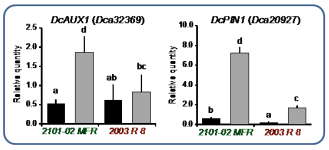

- IAA is mainly produced in the distal region of mature leaves and is actively transported onto the proximal region in both cultivars

Cano *et al.* 2018

PAT is required for AR formation

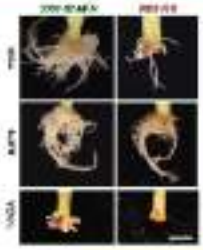

- Exogenous auxin treatment enhances AR formation in the bad-rooting cultivar

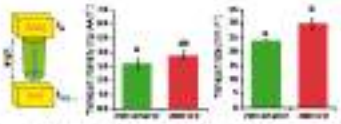

- PAT inhibition prevents AR formation in both cultivars

Differences in PAT between contrasting cultivars do not account for AR differences

Auxin degradation in the cutting base

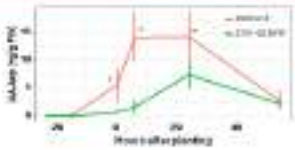

- Compounds derived from both decarboxylative and non-decarboxylative catabolism of IAA were identified

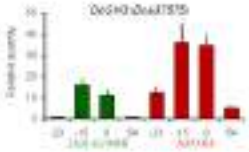

Auxin degradation in the cutting base

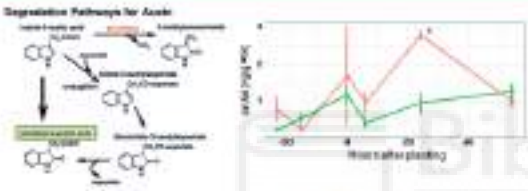

- The main regulation of active IAA levels in carnation stem cuttings was through their conjugation with aspartic acid

The bad-rooting cultivar has higher auxin catabolism, which results in less active IAA

Auxin inactivation regulates AR formation

- We treated freshly harvested stem cuttings with 10 µM AIEP, a known inhibitor of GH3 activities

GH3-mediated IAA-Asp accumulation negatively affects adventitious rooting in 2003/F.8

GRN of auxin response

- We searched for DEGs encoding known players of the auxin signaling pathway

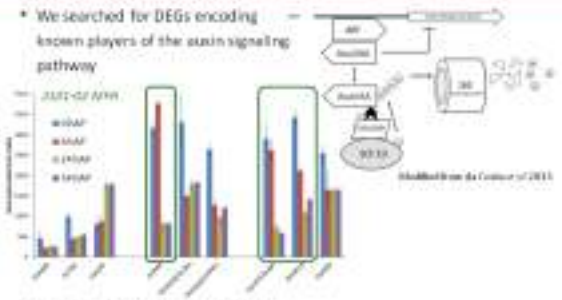

- Gene expression dynamics suggest conserved Aux/IAA-ARF modules for AR initiation

Genetic dissection of adventitious rooting in carnation stem cuttings

164 lines were studied

From selfings	From crossings
33 lines	131 lines

Transgressive segregation in rooting parameters

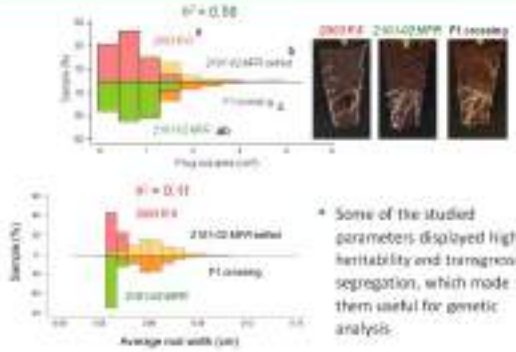

* Some of the studied parameters displayed high heritability and transgressive segregation, which made them useful for genetic analysis

GWAS of adventitious rooting in stem cuttings

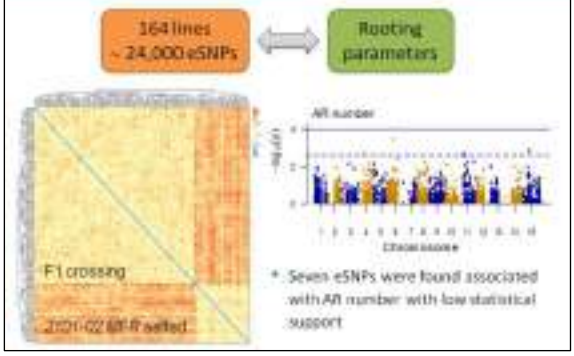

* Seven eSNPs were found associated with AR number with low statistical support

GRN of adventitious rooting in carnation

* 12 F1 lines with extreme rooting phenotypes were selected for hormone and gene profiling studies

GRN of adventitious rooting in carnation

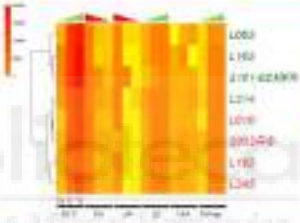

Selective transcriptome profiling

Combining hormonal and phenotypic results with selective transcriptome profiling will allow us to identify a collection of candidate eSNPs linked to AR performance, that might be used to establish a novel marker-assisted selection approach to improve adventitious rooting in carnation

GRN of adventitious rooting

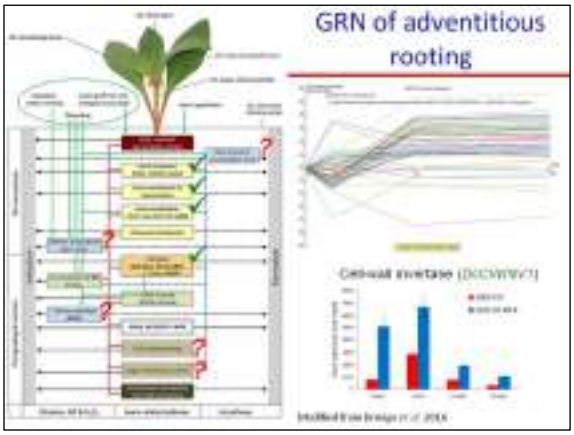

arolab.edu.umh.es

José Manuel Pérez-Pérez
Virginia Estrada Manzo
Rebeca González Bayón
Sergio Ibáñez
María Salud Justamante
Ana Belén Sánchez

Prof Manuel Acedo
Dr. Antonio Cano
Department of Plant Biology
University of Murcia, Spain

CSIC

Barberet Blanc

En esta Tesis se propone el estudio a nivel genético, morfológico y hormonal de la formación de raíces *de novo* en la crucífera modelo *Arabidopsis thaliana* (L.) Heynh, y en dos especies de interés agronómico en la región mediterránea: el clavel cultivado (*Dianthus caryophyllus* L.) y el argán (*Argania spinosa* [L.] Skeels).

Nuestros resultados en Arabidopsis indican que existen asociaciones significativas entre los cambios en la arquitectura radicular en respuesta a herida y 19 regiones genómicas concretas. Hemos encontrado una interacción epistática entre los SNPs de la región codificante del gen *KUP5* (*K⁺ UPTAKE TRANSPORTER 5*), cuyo producto participa en la asimilación del potasio, y del gen At5g19710, que codifica una proteína fosfotransferasa, lo que apuntaría a una relación funcional entre ambos procesos y la formación de raíces en respuesta a herida.

Hemos llevado a cabo un análisis detallado de la formación de raíces adventicias a partir de esquejes de clavel cultivado en una colección de 159 líneas F_1 derivadas del cruzamiento entre dos variedades comerciales, *2101-02 MFR* y *2003 R 8*, que difieren de forma significativa en su capacidad de enraizamiento adventicio. Además, este estudio ha proporcionado evidencias moleculares de que la baja capacidad de enraizamiento adventicio en los esquejes de la estirpe *2003 R 8* se debe a una inactivación temprana de la auxina activa (el ácido indolacético) en la base del esqueje, a través de su conjugación con ácido aspártico mediada por enzimas de la familia GRETCHEN HAGEN 3.

Finalmente, se ha desarrollado una metodología eficaz para la micropropagación del argán a partir de semillas germinadas *in vitro*, además de un protocolo que ha permitido incrementar considerablemente la formación de raíces adventicias en esquejes lignificados obtenidos a partir de plantas adultas.

UNIVERSITAS Miguel Hernández